

A Mathematical Introduction to Robotic Manipulation

Richard M. Murray
California Institute of Technology

Zexiang Li
Hong Kong University of Science and Technology
and
HIT Shenzhen Graduate School

S. Shankar Sastry
University of California, Berkeley

PREPRINT

Not to be distributed without permission of the authors

14 February 2005 (final)

©2005, Richard M. Murray, Zexiang Li, and S. Shankar Sastry

All rights reserved

This manuscript is for review purposes only and may not be reproduced, in whole or in part, in any form, without written consent from the authors.

To RuthAnne (RMM)

To Jianghua (ZXL)

In memory of my father (SSS)

Contents

Contentsvii Prefacexi Acknowledgementsxv

2	Rigid Body Motion	1
1	Rigid Body Transformations	2
2	Rotational Motion in \mathbb{R}^3	6
2.1	Properties of rotation matrices	6
2.2	Exponential coordinates for rotation	11
2.3	Other representations	17
3	Rigid Motion in \mathbb{R}^3	24
3.1	Homogeneous representation	27
3.2	Exponential coordinates for rigid motion and twists	31
3.3	Screws: a geometric description of twists	39
4	Velocity of a Rigid Body	47
4.1	Rotational velocity	47
4.2	Rigid body velocity	50
4.3	Velocity of a screw motion	55
4.4	Coordinate transformations	56
5	Wrenches and Reciprocal Screws	59
5.1	Wrenches	60
5.2	Screw coordinates for a wrench	64
5.3	Reciprocal screws	66

6	Constrained Rigid Motions	70
6.1	Subgroup Motions	71
6.2	Submanifold Motions	77
7	Summary	82
8	Bibliography	85
9	Exercises	86
3	Manipulator Kinematics	97
1	Introduction	97
2	Forward Kinematics	99
2.1	Problem statement	99
2.2	The product of exponentials (POE) formula	102
2.3	Parameterization of manipulators via twists	109
2.4	Manipulator workspace	114
3	Inverse Kinematics	118
3.1	A planar example	119
3.2	Paden-Kahan subproblems	121
3.3	Solving inverse kinematics using subproblems	127
4	The Manipulator Jacobian	135
4.1	End-effector velocity	135
4.2	End-effector forces	142
4.3	Singularities	145
4.4	Manipulability	151
5	Redundant and Parallel Manipulators	153
5.1	Redundant manipulators	153
5.2	Parallel manipulators	157
5.3	Four-bar linkage	160
5.4	Stewart platform	165

6	Summary	171
7	Bibliography	173
8	Exercises	175
4	Robot Dynamics and Control	189
1	Introduction	189
2	Lagrange's Equations	191
2.1	Basic formulation	191
2.2	Inertial properties of rigid bodies	196
2.3	Example: Dynamics of a two-link planar robot	200
2.4	Newton-Euler equations for a rigid body	201
3	Dynamics of Open-Chain Manipulators	205
3.1	The Lagrangian for an open-chain robot	205
3.2	Equations of motion for an open-chain manipulator	207
3.3	Robot dynamics and the product of exponentials formula	213
4	Lyapunov Stability Theory	218
4.1	Basic definitions	218
4.2	The direct method of Lyapunov	222
4.3	The indirect method of Lyapunov	225
4.4	Examples	227
4.5	Lasalle's invariance principle	230
5	Position Control and Trajectory Tracking	233
5.1	Problem description	233
5.2	Computed torque	234
5.3	PD control	237
5.4	Workspace control	240
6	Control of Constrained Manipulators	246
6.1	Dynamics of constrained systems	246

6.2	Control of constrained manipulators	248
6.3	Example: A planar manipulator moving in a slot	250
7	Summary	254
8	Bibliography	255
9	Exercises	257
	Bibliography	261

Preface

In the last two decades, there has been a tremendous surge of activity in robotics, both at in terms of research and in terms of capturing the imagination of the general public as to its seemingly endless and diverse possibilities. This period has been accompanied by a technological maturation of robots as well, from the simple pick and place and painting and welding robots, to more sophisticated assembly robots for inserting integrated circuit chips onto printed circuit boards, to mobile carts for parts handling and delivery. Several areas of robotic automation have now become “standard” on the factory floor and, as of the writing of this book, the field is on the verge of a new explosion to areas of growth involving hazardous environments, minimally invasive surgery, and micro electro-mechanical mechanisms.

Concurrent with the growth in robotics in the last two decades has been the development of courses at most major research universities on various aspects of robotics. These courses are taught at both the undergraduate and graduate levels in computer science, electrical and mechanical engineering, and mathematics departments, with different emphases depending on the background of the students. A number of excellent textbooks have grown out of these courses, covering various topics in kinematics, dynamics, control, sensing, and planning for robot manipulators.

Given the state of maturity of the subject and the vast diversity of students who study this material, we felt the need for a book which presents a slightly more

abstract (mathematical) formulation of the kinematics, dynamics, and control of robot manipulators. The current book is an attempt to provide this formulation not just for a single robot but also for multifingered robot hands, involving multiple cooperating robots. It grew from our efforts to teach a course to a hybrid audience of electrical engineers who did not know much about mechanisms, computer scientists who did not know about control theory, mechanical engineers who were suspicious of involved explanations of the kinematics and dynamics of garden variety open kinematic chains, and mathematicians who were curious, but did not have the time to build up lengthy prerequisites before beginning a study of robotics.

It is our premise that abstraction saves time in the long run, in return for an initial investment of effort and patience in learning some mathematics. The selection of topics—from kinematics and dynamics of single robots, to grasping and manipulation of objects by multifingered robot hands, to nonholonomic motion planning—represents an evolution from the more basic concepts to the frontiers of the research in the field. It represents what we have used in several versions of the course which have been taught between 1990 and 1993 at the University of California, Berkeley, the Courant Institute of Mathematical Sciences of New York University, the California Institute of Technology, and the Hong Kong University of Science and Technology (HKUST). We have also presented parts of this material in short courses at the Università di Roma, the Center for Artificial Intelligence and Robotics, Bangalore, India, and the National Taiwan University, Taipei, Taiwan.

The material collected here is suitable for advanced courses in robotics consisting of seniors or first- and second-year graduate students. At a senior level, we cover Chapters 1–4 in a twelve week period, augmenting the course with some discussion of technological and planning issues, as well as a laboratory. The laboratory consists of experiments involving on-line path planning and control of a few industrial robots, and the use of a simulation environment for off-line programming of robots. In courses stressing kinematic issues, we often replace material from Chapter 4 (Robot

Dynamics) with selected topics from Chapter 5 (Multifingered Hand Kinematics). We have also covered Chapters 5–8 in a ten week period at the graduate level, in a course augmented with other advanced topics in manipulation or mobile robots.

The prerequisites that we assume are a good course in linear algebra at the undergraduate level and some familiarity with signals and systems. A course on control at the undergraduate level is helpful, but not strictly necessary for following the material. Some amount of mathematical maturity is also desirable, although the student who can master the concepts in Chapter 2 should have no difficulty with the remainder of the book.

We have provided a fair number of exercises after Chapters 2–8 to help students understand some new material and review their understanding of the chapter. A toolkit of programs written in Mathematica for solving the problems of Chapters 2 and 3 (and to some extent Chapter 5) have been developed and are described in Appendix B. We have studiously avoided numerical exercises in this book: when we have taught the course, we have adapted numerical exercises from measurements of robots or other “real” systems available in the laboratories. These vary from one time to the next and add an element of topicality to the course.

The one large topic in robotic manipulation that we have not covered in this book is the question of motion planning and collision avoidance for robots. In our classroom presentations we have always covered some aspects of motion planning for robots for the sake of completeness. For graduate classes, we can recommend the recent book of Latombe on motion planning as a supplement in this regard. Another omission from this book is sensing for robotics. In order to do justice to this material in our respective schools, we have always had computer vision, tactile sensing, and other related topics, such as signal processing, covered in separate courses.

The contents of our book have been chosen from the point of view that they will remain foundational over the next several years in the face of many new technological innovations and new vistas in robotics. We have tried to give a snapshot of some of

these vistas in Chapter 9. In reading this book, we hope that the reader will feel the same excitement that we do about the technological and social prospects for the field of robotics and the elegance of the underlying theory.

Richard Murray

Berkeley, August 1993

Zexiang Li

Shankar Sastry

Acknowledgments

It is a great pleasure to acknowledge the people who have collaborated with one or more of us in the research contained in this book. A great deal of the material in Chapters 2 and 3 is based on the Ph.D. dissertation of Bradley Paden, now at the University of California, Santa Barbara. The research on multifingered robot hands, on which Chapters 5 and 6 are founded, was done in collaboration with Ping Hsu, now at San Jose State University; Arlene Cole, now at AT&T Bell Laboratories; John Hauser, now at the University of Colorado, Boulder; Curtis Deno, now at Intermedics, Inc. in Houston; and Kristofer Pister, now at the University of California, Los Angeles. In the area of nonholonomic motion planning, we have enjoyed collaborating with Jean-Paul Laumond of LAAS in Toulouse, France; Paul Jacobs, now at Qualcomm, Inc. in San Diego; Greg Walsh, Dawn Tilbury, and Linda Bushnell at the University of California, Berkeley; Richard Montgomery of the University of California, Santa Cruz; Leonid Gurvits of Siemens Research, Princeton; and Chris Fernandez at New York University.

The heart of the approach in Chapters 2 and 3 of this book is a derivation of robot kinematics using the product of exponentials formalism introduced by Roger Brockett of Harvard University. For this and manifold other contributions by him and his students to the topics in kinematics, rolling contact, and nonholonomic control, it is our pleasure to acknowledge his enthusiasm and encouragement by example. In a broader sense, the stamp of the approach that he has pioneered in

nonlinear control theory is present throughout this book.

We fondly remember the seminar given at Berkeley in 1983 by P. S. Krishnaprasad of the University of Maryland, where he attempted to convince us of the beauty of the product of exponentials formula, and the numerous stimulating conversations with him, Jerry Marsden of Berkeley, and Tony Bloch of Ohio State University on the many beautiful connections between classical mechanics and modern mathematics and control theory. Another such seminar which stimulated our interest was one on multifingered robot hands and cooperating robots given at Berkeley in 1987 by Yoshi Nakamura, now of the University of Tokyo. We have also enjoyed discussing kinematics, optimal control, and redundant mechanisms with John Baillieul of Boston University; Jeff Kerr, now of Zebra Robotics; Mark Cutkosky of Stanford University and Robert Howe, now of Harvard University; Dan Koditschek, now of the University of Michigan; Mark Spong of the University of Illinois at Urbana-Champaign; and Joel Burdick and Elon Rimon at the California Institute of Technology. Conversations with Hector Sussmann of Rutgers University and Gerardo Lafferiere of Portland State University on nonholonomic motion planning have been extremely stimulating as well.

Our colleagues have provided both emotional and technical support to us at various levels of development of this material: John Canny, Charles Desoer, David Dornfeld, Ronald Fearing, Roberto Horowitz, Jitendra Malik, and “Tomi” Tomizuka at Berkeley; Jaiwei Hong, Bud Mishra, Jack Schwartz, James Demmel, and Paul Wright at New York University; Joel Burdick and Pietro Perona at Caltech; Peter Cheung, Ruey-Wen Liu, and Matthew Yuen at HKUST; Robyn Owens at the University of West Australia; Georges Giralt at LAAS in Toulouse, France; Dorotheè Normand Cyrot at the LSS in Paris, France; Alberto Isidori, Marica Di Benedetto, Alessandro De Luca, and ‘Nando’ Nicoló at the Università di Roma; Sanjoy Mitter and Anita Flynn at MIT; Antonio Bicchi at the Università di Pisa; M. Vidyasagar at the Center for Artificial Intelligence and Robotics in Bangalore, India; Li-Chen

Fu of the National Taiwan University, Taipei, Taiwan; and T.-J. Tarn of Washington University. Finally, we are grateful to Mark Spong, Kevin Dowling, and Dalila Argez for their help with the photographs.

Our research has been generously supported by the National Science Foundation under grant numbers DMC 84-51129, IRI 90-14490, and IRI 90-03986, nurtured especially by Howard Moraff, the Army Research Office under grant DAAL88-K-0372 monitored by Jagdish Chandra, IBM, the AT&T Foundation, the GE Foundation, and HKUST under grant DAG 92/93 EG23. Our home institutions at UC Berkeley, the California Institute of Technology, and the Hong Kong University of Science and Technology have been exemplarily supportive of our efforts, providing the resources to help us to grow programs where there were none. We owe a special debt of gratitude in this regard to Karl Pister, Dean of Engineering at Berkeley until 1990.

The manuscript was classroom tested in various versions by James Clark at Harvard, John Canny, Curtis Deno and Matthew Berkemeier at Berkeley, and Joel Burdick at Caltech, in addition to the three of us. Their comments have been invaluable to us in revising the early drafts. We appreciate the detailed and thoughtful reviews by Greg Chirikjian of Johns Hopkins, and Michael McCarthy and Frank Park of the University of California, Irvine.

In addition, many students suffering early versions of this course have contributed to debugging the text. They include L. Bushnell, N. Getz, J.-P. Tennant, D. Tilbury, G. Walsh, and J. Wendlandt at Berkeley; R. Behnken, S. Kelly, A. Lewis, S. Sur, and M. van Nieuwstadt at Caltech; and A. Lee and J. Au of the Hong Kong University of Science and Technology. Sudipto Sur at Caltech helped develop a Mathematica package for screw calculus which forms the heart of the software described in Appendix B. We are ultimately indebted to these and the unnamed others for the inspiration to write this book.

Finally, on a personal note, we would like to thank our families for their support and encouragement during this endeavor.

Chapter 2

Rigid Body Motion

A rigid motion of an object is a motion which preserves distance between points. The study of robot kinematics, dynamics, and control has at its heart the study of the motion of rigid objects. In this chapter, we provide a description of rigid body motion using the tools of linear algebra and screw theory.

The elements of screw theory can be traced to the work of Chasles and Poinsot in the early 1800s. Chasles [10] proved that a rigid body can be moved from any one position to any other by a movement consisting of rotation about a straight line followed by translation parallel to that line. This motion is what we refer to in this book as a *screw motion*. The infinitesimal version of a screw motion is called a *twist* and it provides a description of the instantaneous velocity of a rigid body in terms of its linear and angular components. Screws and twists play a central role in our formulation of the kinematics of robot mechanisms.

The second major result upon which screw theory is founded concerns the representation of forces acting on rigid bodies. Poinsot [56] is credited with the discovery that any system of forces acting on a rigid body can be replaced by a single force applied along a line, combined with a torque about that same line. Such a force is referred to as a *wrench*. Wrenches are dual to twists, so that many of the theorems which apply to twists can be extended to wrenches.

Ball, R. S.
homogeneous
coordinates
matrix
exponential
screw the-
ory!advantages
of
rigid body
transformations
coordinate
frame

Using the theorems of Chasles and Poincot as a starting point, Sir Robert S. Ball developed a complete theory of screws which he published in 1900 [3]. In this chapter, we present a more modern treatment of the theory of screws based on linear algebra and matrix groups. The fundamental tools are the use of homogeneous coordinates to represent rigid motions and the matrix exponential, which maps a twist into the corresponding screw motion. In order to keep the mathematical prerequisites to a minimum, we build up this theory assuming only a good knowledge of basic linear algebra. A more abstract version, using the tools of matrix Lie groups and Lie algebras, can be found in Appendix A.

There are two main advantages to using screws, twists, and wrenches for describing rigid body kinematics. The first is that they allow a global description of rigid body motion which does not suffer from singularities due to the use of local coordinates. Such singularities are inevitable when one chooses to represent rotation via Euler angles, for example. The second advantage is that screw theory provides a very geometric description of rigid motion which greatly simplifies the analysis of mechanisms. We will make extensive use of the geometry of screws throughout the book, and particularly in the next chapter when we study the kinematics and singularities of mechanisms.

1 Rigid Body Transformations

The motion of a particle moving in Euclidean space is described by giving the location of the particle at each instant of time, relative to an inertial Cartesian coordinate frame. Specifically, we choose a set of three orthonormal axes and specify the particle's location using the triple $(x, y, z) \in \mathbb{R}^3$, where each coordinate gives the projection of the particle's location onto the corresponding axis. A trajectory of the particle is represented by the parameterized curve $p(t) = (x(t), y(t), z(t)) \in \mathbb{R}^3$.

In robotics, we are frequently interested not in the motion of individual parti-

cles, but in the collective motion of a set of particles, such as the link of a robot manipulator. To this end, we loosely define a perfectly rigid body as a completely “undistortable” body. More formally, a *rigid body* is a collection of particles such that the distance between any two particles remains fixed, regardless of any motions of the body or forces exerted on the body. Thus, if p and q are any two points on a rigid body then, as the body moves, p and q must satisfy

$$\|p(t) - q(t)\| = \|p(0) - q(0)\| = \text{constant}.$$

A *rigid motion* of an object is a continuous movement of the particles in the object such that the distance between any two particles remains fixed at all times. The net movement of a rigid body from one location to another via a rigid motion is called a *rigid displacement*. In general, a rigid displacement may consist of both translation and rotation of the object.

Given an object described as a subset O of \mathbb{R}^3 , a rigid motion of an object is represented by a continuous family of mappings $g(t) : O \rightarrow \mathbb{R}^3$ which describe how individual points in the body move as a function of time, relative to some fixed Cartesian coordinate frame. That is, if we move an object along a continuous path, $g(t)$ maps the initial coordinates of a point on the body to the coordinates of that same point at time t . A rigid displacement is represented by a single mapping $g : O \rightarrow \mathbb{R}^3$ which maps the coordinates of points in the rigid body from their initial to final configurations.

Given two points $p, q \in O$, the *vector* $v \in \mathbb{R}^3$ connecting p to q is defined to be the directed line segment going from p to q . In coordinates this is given by $v = q - p$ with $p, q \in \mathbb{R}^3$. Though both points and vectors are represented by 3-tuples of numbers, they are conceptually quite different. A vector has a direction and a magnitude. (By the magnitude of a vector, we will mean its Euclidean norm, i.e., $\sqrt{v_1^2 + v_2^2 + v_3^2}$.) It is, however, not attached to the body, since there may be other pairs of points on the body, for instance r and s with $q - p = s - r$, for which the same vector v also

rigid bodies
rigid body mo-
tion!definition
of
rigid
displacement
displacement,
rigid
vectors
vectors!points@vers
points
points!vectors@vers
vectors

rigid body
transforma-
tions!actions
on points and
vectors

connects r to s . A vector is sometimes called a *free vector* to indicate that it can be positioned anywhere in space without changing its meaning.

vectors!rigid
transformation
of

The action of a rigid transformation on points induces an action on vectors in a natural way. If we let $g : O \rightarrow \mathbb{R}^3$ represent a rigid displacement, then vectors transform according to

cross prod-
uct!preservation
by rigid body
transformations

$$g_*(v) = g(q) - g(p).$$

rigid body
transforma-
tions!formal
definition

Note that the right-hand side is the difference of two points and is hence also a vector.

Since distances between points on a rigid body are not altered by rigid motions, a necessary condition for a mapping $g : O \rightarrow \mathbb{R}^3$ to describe a rigid motion is that distances be preserved by the mapping. However, this condition is not sufficient since it allows internal reflections, which are not physically realizable. That is, a mapping might preserve distance but not preserve orientation. For example, the mapping $(x, y, z) \mapsto (x, y, -z)$ preserves distances but reflects points in the body about the xy plane. To eliminate this possibility, we require that the cross product between vectors in the body also be preserved. We will collect these requirements to define a *rigid body transformation* as a mapping from \mathbb{R}^3 to \mathbb{R}^3 which represents a rigid motion:

Definition 2.1. Rigid body transformation

A mapping $g : \mathbb{R}^3 \rightarrow \mathbb{R}^3$ is a *rigid body transformation* if it satisfies the following properties:

1. Length is preserved: $\|g(p) - g(q)\| = \|p - q\|$ for all points $p, q \in \mathbb{R}^3$.
2. The cross product is preserved: $g_*(v \times w) = g_*(v) \times g_*(w)$ for all vectors $v, w \in \mathbb{R}^3$.

There are some interesting consequences of this definition. The first is that the inner product is preserved by rigid body transformations. One way to show this is

to use the *polarization identity*,

$$v_1^T v_2 = \frac{1}{4}(\|v_1 + v_2\|^2 - \|v_1 - v_2\|^2),$$

and the fact that

$$\|v_1 + v_2\| = \|g_*(v_1) + g_*(v_2)\| \quad \|v_1 - v_2\| = \|g_*(v_1) - g_*(v_2)\|$$

to conclude that for any two vectors v_1, v_2 ,

$$v_1^T v_2 = g_*(v_1)^T g_*(v_2).$$

In particular, orthogonal vectors are transformed to orthogonal vectors. Coupled with the fact that rigid body transformations also preserve the cross product (property 2 of the definition above), we see that rigid body transformations take orthonormal coordinate frames to orthonormal coordinate frames.

The fact that the distance between points and cross product between vectors is fixed does not mean that it is inadmissible for particles in a rigid body to move relative to each other, but rather that they can rotate but not translate with respect to each other. Thus, to keep track of the motion of a rigid body, we need to keep track of the motion of any one particle on the rigid body and the rotation of the body about this point. In order to do this, we represent the *configuration* of a rigid body by attaching a Cartesian coordinate frame to some point on the rigid body and keeping track of the motion of this body coordinate frame relative to a fixed frame. The motion of the individual particles in the body can then be retrieved from the motion of the body frame and the motion of the point of attachment of the frame to the body. We shall require that all coordinate frames be *right-handed*: given three orthonormal vectors $\mathbf{x}, \mathbf{y}, \mathbf{z} \in \mathbb{R}^3$ which define a coordinate frame, they must satisfy $\mathbf{z} = \mathbf{x} \times \mathbf{y}$.

Since a rigid body transformation $g : \mathbb{R}^3 \rightarrow \mathbb{R}^3$ preserves the cross product, right-handed coordinate frames are transformed to right-handed coordinate frames.

configuration of
a rigid body
rigid body mo-
tion!representatio
using
body-fixed
frame
body frame
right-handed
coordinate
frame

rigid body transformations—) The action of a rigid transformation g on the body frame describes how the body frame rotates as a consequence of the rigid motion. More precisely, if we describe the rotational motion—(configuration of a rigid body by the right-handed frame given by the vectors v_1, v_2, v_3 attached to a point p , then the configuration of the rigid body after the rigid body transformation g is given by the right-handed frame of vectors $g_*(v_1), g_*(v_2), g_*(v_3)$ attached to the point $g(p)$.

rotation!representation using rotation matrices
body frame
rotation matrices
rotation matrices!properties of—(

The remainder of this chapter is devoted to establishing more detailed properties, characterizations, and representations of rigid body transformations and providing the necessary mathematical preliminaries used in the remainder of the book.

2 Rotational Motion in \mathbb{R}^3

We begin the study of rigid body motion by considering, at the outset, only the rotational motion of an object. We describe the orientation of the body by giving the relative orientation between a coordinate frame attached to the body and a fixed or inertial coordinate frame. From now on, all coordinate frames will be right-handed unless stated otherwise. Let A be the inertial frame, B the body frame, and $\mathbf{x}_{ab}, \mathbf{y}_{ab}, \mathbf{z}_{ab} \in \mathbb{R}^3$ the coordinates of the principal axes of B relative to A (see Figure 2.1). Stacking these coordinate vectors next to each other, we define a 3×3 matrix:

$$R_{ab} = \begin{bmatrix} \mathbf{x}_{ab} & \mathbf{y}_{ab} & \mathbf{z}_{ab} \end{bmatrix}.$$

We call a matrix constructed in this manner a *rotation matrix*: every rotation of the object relative to the ground corresponds to a matrix of this form.

2.1 Properties of rotation matrices

A rotation matrix has two key properties that follow from its construction. Let $R \in \mathbb{R}^{3 \times 3}$ be a rotation matrix and $r_1, r_2, r_3 \in \mathbb{R}^3$ be its columns. Since the columns

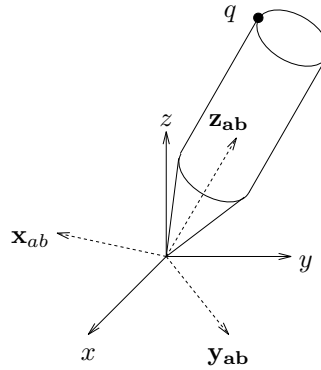

 $SO(3)$

Figure 2.1: Rotation of a rigid object about a point. The dotted coordinate frame is attached to the rotating rigid body.

of R are mutually orthonormal, it follows that

$$r_i^T r_j = \begin{cases} 0, & \text{if } i \neq j \\ 1, & \text{if } i = j. \end{cases}$$

As conditions on the matrix R , these properties can be written as

$$RR^T = R^T R = I. \quad (2.1)$$

From this it follows that

$$\det R = \pm 1.$$

To determine the sign of the determinant of R , we recall from linear algebra that

$$\det R = r_1^T (r_2 \times r_3).$$

Since the coordinate frame is right-handed, we have that $r_2 \times r_3 = r_1$ so that $\det R = r_1^T r_1 = 1$. Thus, coordinate frames corresponding to right-handed frames are represented by orthogonal matrices with determinant 1. The set of all 3×3 matrices which satisfy these two properties is denoted $SO(3)$. The notation SO abbreviates *special orthogonal*. Special refers to the fact that $\det R = +1$ rather than ± 1 .

group!definition
group!rotations@of
rotations

More generally, we may define the space of rotation matrices in $\mathbb{R}^{n \times n}$ by

$$SO(n) = \{R \in \mathbb{R}^{n \times n} : RR^T = I, \det R = +1\}. \quad (2.2)$$

We will be primarily interested in $n = 3$, although the $n = 2$ case (planar rotations) will also prove useful and is explored in the exercises.

$SO(3) \subset \mathbb{R}^{3 \times 3}$ is a *group* under the operation of matrix multiplication. A set G together with a binary operation \circ defined on elements of G is called a group if it satisfies the following axioms:

1. *Closure*: If $g_1, g_2 \in G$, then $g_1 \circ g_2 \in G$.
2. *Identity*: There exists an identity element, e , such that $g \circ e = e \circ g = g$ for every $g \in G$.
3. *Inverse*: For each $g \in G$, there exists a (unique) inverse, $g^{-1} \in G$, such that $g \circ g^{-1} = g^{-1} \circ g = e$.
4. *Associativity*: If $g_1, g_2, g_3 \in G$, then $(g_1 \circ g_2) \circ g_3 = g_1 \circ (g_2 \circ g_3)$.

In the instance of $SO(3)$, note that

1. If $R_1, R_2 \in SO(3)$, then $R_1 R_2 \in SO(3)$ since

$$\begin{aligned} R_1 R_2 (R_1 R_2)^T &= R_1 R_2 R_2^T R_1^T = R_1 R_1^T = I \\ \det(R_1 R_2) &= \det(R_1) \det(R_2) = +1. \end{aligned}$$

2. The identity matrix is the identity element.
3. By equation (2.1) it follows that the inverse of $R \in SO(3)$ is $R^T \in SO(3)$.
4. The associativity of the group operation follows from the associativity of matrix multiplication; that is, $(R_1 R_2) R_3 = R_1 (R_2 R_3)$.

Thus, $SO(3)$ is a group using the identity matrix I as the identity element and matrix multiplication as the group operation. We refer to $SO(3)$ as the *rotation group* of \mathbb{R}^3 .

rotation group
configuration
space
rotation matri-
ces!actions on
points and
vectors
points!rotational
transformation
of
vectors!rotational
transformation
of

Every configuration of a rigid body that is free to rotate relative to a fixed frame can be identified with a unique $R \in SO(3)$. Under this identification, the rotation group $SO(3)$ is referred to as the *configuration space* of the system and a trajectory of the system is a curve $R(t) \in SO(3)$ for $t \in [0, T]$. More generally, we shall call a set Q a configuration space for a system if every element $x \in Q$ corresponds to a valid configuration of the system and each configuration of the system can be identified with a unique element of Q .

A rotation matrix $R \in SO(3)$ also serves as a transformation, taking coordinates of a point from one frame to another. Consider the point q shown in Figure 2.1. Let $q_b = (x_b, y_b, z_b)$ be the coordinates of q relative to frame B . The coordinates of q relative to frame A can be computed as follows: since $x_b, y_b, z_b \in \mathbb{R}$ are projections of q onto the coordinate axes of B , which, in turn, have coordinates $\mathbf{x}_{ab}, \mathbf{y}_{ab}, \mathbf{z}_{ab} \in \mathbb{R}^3$ with respect to A , the coordinates of q relative to frame A are given by

$$q_a = \mathbf{x}_{ab}\mathbf{x}_b + \mathbf{y}_{ab}\mathbf{y}_b + \mathbf{z}_{ab}\mathbf{z}_b.$$

This can be rewritten as

$$q_a = \begin{bmatrix} \mathbf{x}_{ab} & \mathbf{y}_{ab} & \mathbf{z}_{ab} \end{bmatrix} \begin{bmatrix} x_b \\ y_b \\ z_b \end{bmatrix} = R_{ab}q_b.$$

In other words, R_{ab} , when considered as a map from \mathbb{R}^3 to \mathbb{R}^3 , rotates the coordinates of a point from frame B to frame A .

The action of a rotation matrix on a point can be used to define the action of the rotation matrix on a vector. Let v_b be a vector in the frame B defined as $v_b = q_b - p_b$. Then,

$$R_{ab}(v_b) := R_{ab}q_b - R_{ab}p_b = q_a - p_a = v_a.$$

rotational motion!composition rule

Since matrix multiplication is linear, it may be verified that if $v_b = q_b - p_b = s_b - r_b$ then we still have that

cross product!matrix representation

$$R_{ab}s_b - R_{ab}r_b = R_{ab}q_b - R_{ab}p_b = v_a$$

skew-symmetric

matrices!representing or representing cross product

and hence the action of R_{ab} on a vector is well defined.

Rotation matrices can be combined to form new rotation matrices using matrix multiplication. If a frame C has orientation R_{bc} relative to a frame B , and B has orientation R_{ab} relative to another frame A , then the orientation of C relative to A is given by

$$R_{ac} = R_{ab}R_{bc}. \quad (2.3)$$

R_{ac} , when considered as a map from \mathbb{R}^3 to \mathbb{R}^3 , rotates the coordinates of a point from frame C to frame A by first rotating from C to B and then from B to A . Equation (2.3) is the *composition rule* for rotations.

A rotation matrix represents a rigid body transformation in the sense of the definition of the previous section. This is to say, it preserves distance and orientation. We prove this using some algebraic properties of the cross product operation between two vectors. Recall that the cross product between two vectors $a, b \in \mathbb{R}^3$ is defined as

$$a \times b = \begin{bmatrix} a_2b_3 - a_3b_2 \\ a_3b_1 - a_1b_3 \\ a_1b_2 - a_2b_1 \end{bmatrix}.$$

Since the cross product by a is a linear operator, $b \mapsto a \times b$ may be represented using a matrix. Defining

$$(a)^\wedge = \begin{bmatrix} 0 & -a_3 & a_2 \\ a_3 & 0 & -a_1 \\ -a_2 & a_1 & 0 \end{bmatrix}, \quad (2.4)$$

we can write

$$a \times b = (a)^\wedge b. \quad (2.5)$$

We will often use the notation \hat{a} as a replacement for $(a)^\wedge$.

Lemma 2.1. *Given $R \in SO(3)$ and $v, w \in \mathbb{R}^3$, the following properties hold:*

$$R(v \times w) = (Rv) \times (Rw) \quad (2.6)$$

$$R(w)^\wedge R^T = (Rw)^\wedge. \quad (2.7)$$

The first property in the lemma asserts that rotation by the matrix R commutes with the cross product operation; that is, the rotation of the cross product of two vectors is the cross product of the rotation of each of the vectors by R . The second property has an interpretation in terms of rotation of an instantaneous axis of rotation, which will become clear shortly. For now, we will merely use it as an algebraic fact. The proof of the lemma is by calculation.

Proposition 2.2. Rotations are rigid body transformations

A rotation $R \in SO(3)$ is a rigid body transformation; that is,

1. R preserves distance: $\|Rq - Rp\| = \|q - p\|$ for all $q, p \in \mathbb{R}^3$.
2. R preserves orientation: $R(v \times w) = Rv \times Rw$ for all $v, w \in \mathbb{R}^3$.

Proof. Property 1 can be verified by direct calculation:

$$\begin{aligned} \|Rq - Rp\|^2 &= (R(q - p))^T (R(q - p)) = (q - p)^T R^T R (q - p) \\ &= (q - p)^T (q - p) = \|q - p\|^2. \end{aligned}$$

Property 2 follows from equation (2.6). □

2.2 Exponential coordinates for rotation

A common motion encountered in robotics is the rotation of a body about a given axis by some amount. For example, we might wish to describe the rotation of the link of a robot about a fixed axis, as shown in Figure 2.2. Let $\omega \in \mathbb{R}^3$ be a unit vector which specifies the direction of rotation and let $\theta \in \mathbb{R}$ be the angle of rotation

rotational motion
fixed about
a fixed axis
matrix
exponential
skew-symmetric
matrices

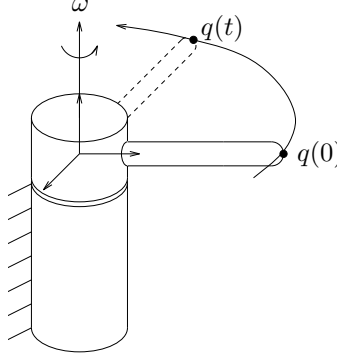


Figure 2.2: Tip point trajectory generated by rotation about the ω -axis.

in radians. Since every rotation of the object corresponds to some $R \in SO(3)$, we would like to write R as a function of ω and θ .

To motivate our derivation, consider the velocity of a point q attached to the rotating body. If we rotate the body at *constant* unit velocity about the axis ω , the velocity of the point, \dot{q} , may be written as

$$\dot{q}(t) = \omega \times q(t) = \hat{\omega}q(t). \quad (2.8)$$

This is a time-invariant linear differential equation which may be integrated to give

$$q(t) = e^{\hat{\omega}t}q(0),$$

where $q(0)$ is the initial ($t = 0$) position of the point and $e^{\hat{\omega}t}$ is the matrix exponential

$$e^{\hat{\omega}t} = I + \hat{\omega}t + \frac{(\hat{\omega}t)^2}{2!} + \frac{(\hat{\omega}t)^3}{3!} + \dots$$

It follows that if we rotate about the axis ω at unit velocity for θ units of time, then the net rotation is given by

$$R(\omega, \theta) = e^{\hat{\omega}\theta}. \quad (2.9)$$

From its definition, it is easy to see that the matrix $\hat{\omega}$ is a skew-symmetric matrix, i.e., it satisfies $\hat{\omega}^T = -\hat{\omega}$. The vector space of all 3×3 skew matrices is denoted $so(3)$ and more generally the space of $n \times n$ skew-symmetric matrices is

$$so(n) = \{S \in \mathbb{R}^{n \times n} | S^T = -S\}. \quad (2.10)$$

(The reason for the notation $so(n)$ will become clear shortly.) As with $SO(n)$, the cases we are interested in are $n = 2$ and $n = 3$. We concentrate on $n = 3$ here and explore $n = 2$ in the exercises.

The set $so(3) \subset \mathbb{R}^{3 \times 3}$ is a vector space over the reals. Thus, the sum of two elements of $so(3)$ is an element of $so(3)$ and the scalar multiple of any element of $so(3)$ is an element of $so(3)$. Furthermore, we can identify $so(3)$ with \mathbb{R}^3 using the relationship (2.4) and the fact $(v + w)^\wedge = \hat{v} + \hat{w}$.

It will be convenient to represent a skew-symmetric matrix as the product of a unit skew-symmetric matrix and a real number, i.e., for $\omega \in \mathbb{R}^3$, let $\omega = \frac{\omega}{\|\omega\|} \|\omega\|$. Given a matrix $\hat{\omega} \in so(3)$, $\|\omega\| = 1$, and a real number $\theta \in \mathbb{R}_+$, we write the exponential of $\hat{\omega}\theta$ as

$$\exp(\hat{\omega}\theta) = e^{\hat{\omega}\theta} = I + \theta\hat{\omega} + \frac{\theta^2}{2!}\hat{\omega}^2 + \frac{\theta^3}{3!}\hat{\omega}^3 + \dots \quad (2.11)$$

Equation (2.11) is an infinite series and, hence, not useful from a computational standpoint. To obtain a closed-form expression for $\exp(\hat{\omega}\theta)$, we make use of the following formulas for powers of \hat{a} , which are verified by direct calculation.

Lemma 2.3. *Given $\hat{a} \in so(3)$, the following relations hold:*

$$\hat{a}^2 = aa^T - \|a\|^2 I \quad (2.12)$$

$$\hat{a}^3 = -\|a\|^2 \hat{a} \quad (2.13)$$

and higher powers of \hat{a} can be calculated recursively.

Rodrigues' formula
 exponential map for rotations—
 rotational motion! fixed about a fixed axis

Utilizing this lemma with $a = \omega\theta$, $\|\omega\| = 1$, equation (2.11) becomes

$$e^{\hat{\omega}\theta} = I + \left(\theta - \frac{\theta^3}{3!} + \frac{\theta^5}{5!} - \cdots \right) \hat{\omega} + \left(\frac{\theta^2}{2!} - \frac{\theta^4}{4!} + \frac{\theta^6}{6!} - \cdots \right) \hat{\omega}^2$$

and hence

$$e^{\hat{\omega}\theta} = I + \hat{\omega} \sin \theta + \hat{\omega}^2 (1 - \cos \theta) \quad (2.14)$$

This formula, commonly referred to as *Rodrigues' formula* [60], gives an efficient method for computing $\exp(\hat{\omega}\theta)$. When $\|\omega\| \neq 1$, it may be verified (see Exercise 13) that

$$e^{\hat{\omega}\theta} = I + \frac{\hat{\omega}}{\|\omega\|} \sin(\|\omega\|\theta) + \frac{\hat{\omega}^2}{\|\omega\|^2} (1 - \cos(\|\omega\|\theta)).$$

We now verify that $\exp(\hat{\omega}\theta)$ is indeed a rotation matrix.

Proposition 2.4. Exponentials of skew-symmetric matrices are orthogonal

Given a skew-symmetric matrix $\hat{\omega} \in so(3)$ and $\theta \in \mathbb{R}$,

$$e^{\hat{\omega}\theta} \in SO(3).$$

Proof. Defining $R := \exp(\hat{\omega}\theta)$, we must verify that $R^T R = I$ and $\det R = +1$. To verify the first property, we have the following chain of equalities, which can be checked using equation (2.14),

$$\left[e^{\hat{\omega}\theta} \right]^{-1} = e^{-\hat{\omega}\theta} = e^{\hat{\omega}^T \theta} = \left[e^{\hat{\omega}\theta} \right]^T.$$

Thus $R^{-1} = R^T$ and consequently $R^T R = I$ as desired. From this, it follows that $\det R = \pm 1$. Using the continuity of the determinant as a function of the entries of a matrix, combined with continuity of the exponential map and the fact that $\det \exp(0) = 1$, we conclude that $\det R = +1$. \square

Proposition 2.4 asserts that the exponential map transforms skew-symmetric matrices into orthogonal matrices. Geometrically, the skew-symmetric matrix corresponds to an axis of rotation (via the mapping $\omega \mapsto \hat{\omega}$) and the exponential map

generates the rotation corresponding to rotation about the axis by a specified amount θ . This relationship between skew-symmetric matrices and orthogonal matrices explains, in part, the notation $so(3)$. We will now show that *every* rotation matrix can be represented as the matrix exponential of some skew-symmetric matrix; that is, the map $\exp : so(3) \rightarrow SO(3)$ is surjective (onto).

Proposition 2.5. The exponential map is surjective onto $SO(3)$

Given $R \in SO(3)$, there exists $\omega\theta \in \mathbb{R}^3$, $\|\omega\| = 1$ and $\theta \in \mathbb{R}_+$ such that $R = \exp(\widehat{\omega}\theta)$, and the exponential map has an inverse denoted by

$$\log : SO(3) \rightarrow so(3) : R \mapsto \log R = \widehat{\omega\theta}.$$

Proof. The proof is constructive. We equate terms of R and $\exp(\widehat{\omega}\theta)$ and solve the corresponding equations. By way of notation, we have the rotation matrix R to be

$$R = \begin{bmatrix} r_{11} & r_{12} & r_{13} \\ r_{21} & r_{22} & r_{23} \\ r_{31} & r_{32} & r_{33} \end{bmatrix}. \quad (2.15)$$

Defining $v_\theta = 1 - \cos \theta$, $c_\theta = \cos \theta$, and $s_\theta = \sin \theta$, write equation (2.14) as

$$\begin{aligned} e^{\widehat{\omega}\theta} &= I + \widehat{\omega} \sin \theta + \widehat{\omega}^2 (1 - \cos \theta) \\ &= \begin{bmatrix} 1 - v_\theta(\omega_2^2 + \omega_3^2) & \omega_1\omega_2v_\theta - \omega_3s_\theta & \omega_1\omega_3v_\theta + \omega_2s_\theta \\ \omega_1\omega_2v_\theta + \omega_3s_\theta & 1 - v_\theta(\omega_1^2 + \omega_3^2) & \omega_2\omega_3v_\theta - \omega_1s_\theta \\ \omega_1\omega_3v_\theta - \omega_2s_\theta & \omega_2\omega_3v_\theta + \omega_1s_\theta & 1 - v_\theta(\omega_1^2 + \omega_2^2) \end{bmatrix} \\ &= \begin{bmatrix} \omega_1^2v_\theta + c_\theta & \omega_1\omega_2v_\theta - \omega_3s_\theta & \omega_1\omega_3v_\theta + \omega_2s_\theta \\ \omega_1\omega_2v_\theta + \omega_3s_\theta & \omega_2^2v_\theta + c_\theta & \omega_2\omega_3v_\theta - \omega_1s_\theta \\ \omega_1\omega_3v_\theta - \omega_2s_\theta & \omega_2\omega_3v_\theta + \omega_1s_\theta & \omega_3^2v_\theta + c_\theta \end{bmatrix}. \end{aligned} \quad (2.16)$$

Now, equating (2.15) with (2.16), we see that

$$\text{trace}(R) = r_{11} + r_{22} + r_{33} = 1 + 2 \cos \theta.$$

To verify that this equation has a solution, we recall that the trace of R is equal to the sum of its eigenvalues. Since R preserves lengths and $\det R = +1$, its

eigenvalues of a rotation matrix
 rotation matrices!eigenvalues of
 exponential coordinates@for rotation
 rotational motion!exponential coordinates

eigenvalues have magnitude 1 and occur in complex conjugate pairs (see Exercise 3). It follows that $-1 \leq \text{trace}(R) \leq 3$. If $\text{trace}(R) = 3$, then $R = I$, and $\omega\theta = 0$. If $\text{trace}(R) = -1$. Let v be the unit eigenvector of R corresponding to the eigenvalue 1. Then, $\omega\theta = \pm\pi v$. If $-1 < \text{trace}(R) < 3$, by restricting θ to $(0, \pi)$, we have

$$\theta = \cos^{-1} \left(\frac{\text{trace}(R) - 1}{2} \right). \quad (2.17)$$

Equating the off-diagonal terms of R and $\exp(\hat{\omega}\theta)$, we get

$$r_{32} - r_{23} = 2\omega_1 s_\theta$$

$$r_{13} - r_{31} = 2\omega_2 s_\theta$$

$$r_{21} - r_{12} = 2\omega_3 s_\theta.$$

Thus,

$$\omega = \frac{1}{2s_\theta} \begin{bmatrix} r_{32} - r_{23} \\ r_{13} - r_{31} \\ r_{21} - r_{12} \end{bmatrix}. \quad (2.18)$$

In skew-symmetric notation, we have

$$\hat{\omega}\theta := \log R = \frac{\theta}{2s_\theta} (R - R^T). \quad (2.19)$$

Note that if $\omega\theta$ is a solution, then $\omega(\theta + 2\pi n)$, $n = 1, 2, \dots$ are also solutions. In other words, the exponential map is a many-to-one map from \mathbb{R}^3 onto $SO(3)$.

□

The components of the vector $\omega\theta \in \mathbb{R}^3$ given by equations (2.17) and (2.18) are called the *exponential coordinates* for R . These coordinates provide a *natural parameterization* of $SO(3)$ about a neighborhood of the identity. This neighborhood covers all of $SO(3)$ except for a "thin" set. Geometrically, $SO(3)$ can be pictured as a three-dimensional solid ball of radius π , centered at the origin. This representation is unique when restricted to the interior of the solid ball, whereas antipodal points

on the boundary of the solid ball represent the same physical rotation and should be identified [53].

Considering $\omega \in \mathbb{R}^3$ to be an axis of rotation with unit magnitude and $\theta \in \mathbb{R}$ to be an angle, Propositions 2.4 and 2.5 combine to give the following classic theorem.

Theorem 2.6 (Euler [20]). *Any orientation $R \in SO(3)$ is equivalent to a rotation about a fixed axis $\omega \in \mathbb{R}^3$ through an angle $\theta \in [0, \pi)$.*

This method of representing a rotation is also known as the *equivalent axis representation*. The exponential coordinates are an example of what is known as the *canonical coordinates of the first kind*. In general, let $(\hat{\omega}_1, \hat{\omega}_2, \hat{\omega}_3)$ be a basis of $so(3)$, i.e., $(\omega_1, \omega_2, \omega_3)$ forms a linearly independent set in \mathbb{R}^3 , and define a map from \mathbb{R}^3 to $SO(3)$ as

$$\alpha : (\alpha_1, \alpha_2, \alpha_3) \mapsto \exp(\alpha_1 \hat{\omega}_1 + \alpha_2 \hat{\omega}_2 + \alpha_3 \hat{\omega}_3). \quad (2.20)$$

The coordinates $(\alpha_1, \alpha_2, \alpha_3)$ are called the *canonical coordinates of the first kind* relative to the basis $(\hat{\omega}_1, \hat{\omega}_2, \hat{\omega}_3)$. In the special case that $\omega_1 = \mathbf{x} = (1, 0, 0)^T$, $\omega_2 = \mathbf{y} = (0, 1, 0)^T$ and $\omega_3 = \mathbf{z} = (0, 0, 1)^T$, we recover the exponential coordinates.

2.3 Other representations

Other coordinates for the rotation group also exist and are briefly described below and in the exercises. We emphasize the connection of these other representations with the exponential coordinates presented above; more classical treatments of these representations can be found in standard kinematics texts such as Goldstein [22] and Craig [13].

XYZ Fixed angles

One method of describing the orientation of a coordinate frame B relative to another coordinate frame A is as follows: start with frame B coincident with frame A . First,

Euler's theorem
rotational mo-
tion!equivalent
axis
representation
equivalent axis
representation
rotational mo-
tion!parameteriza-
singularities
exponential
coordi-
nates!rotation@fo
rotation—)
rotational mo-
tion!exponential
coordinates—)
Euler angles
rotational
motion!Euler
angle
representation

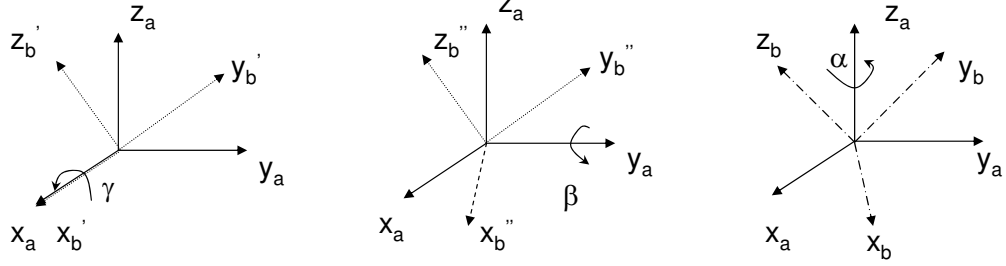


Figure 2.3: XYZ fixed angles. Rotations are performed in the order of $R_{\mathbf{x}}(\gamma), R_{\mathbf{y}}(\beta), R_{\mathbf{z}}(\alpha)$

rotate the B frame about the x -axis of frame A by an angle γ , then rotate about the y -axis of frame A by an angle β , and finally rotate about the z -axis of frame A by an angle α (see Figure 2.3). This yields a net orientation $R_{ab}(\gamma, \beta, \alpha)$ and the triple of angles (γ, β, α) is used to represent the rotation. Note that each of the three rotations takes place about an axis in the fixed reference frame A . We will call this convention for specifying an orientation *XYZ fixed angles*.

To derive the final orientation of frame B , we define the following elementary rotations about the x -, y - and z -axes:

$$R_{\mathbf{x}}(\phi) := e^{\widehat{\mathbf{x}}\phi} = \begin{bmatrix} 1 & 0 & 0 \\ 0 & \cos \phi & -\sin \phi \\ 0 & \sin \phi & \cos \phi \end{bmatrix},$$

$$R_{\mathbf{y}}(\beta) := e^{\widehat{\mathbf{y}}\beta} = \begin{bmatrix} \cos \beta & 0 & \sin \beta \\ 0 & 1 & 0 \\ -\sin \beta & 0 & \cos \beta \end{bmatrix},$$

and

$$R_{\mathbf{z}}(\alpha) := e^{\widehat{\mathbf{z}}\alpha} = \begin{bmatrix} \cos \alpha & -\sin \alpha & 0 \\ \sin \alpha & \cos \alpha & 0 \\ 0 & 0 & 1 \end{bmatrix}.$$

Using the definition of the rotation matrix, it is straightforward to see that the

equivalent rotation matrix $R_{ab}(\gamma, \beta, \alpha)$ is given by

atan2

$$\begin{aligned}
 R_{ab} &= R_{\mathbf{z}}(\alpha)R_{\mathbf{y}}(\beta)R_{\mathbf{x}}(\gamma) \\
 &= \begin{bmatrix} c_\alpha c_\beta & c_\alpha s_\beta s_\gamma - s_\alpha c_\gamma & c_\alpha s_\beta c_\gamma + s_\alpha s_\gamma \\ s_\alpha c_\beta & s_\alpha s_\beta s_\gamma + c_\alpha c_\gamma & s_\alpha s_\beta c_\gamma - c_\alpha s_\gamma \\ -s_\beta & c_\beta s_\gamma & c_\beta c_\gamma \end{bmatrix} \quad (2.21)
 \end{aligned}$$

where c_α, s_α are abbreviations for $\cos \alpha$ and $\sin \alpha$, respectively, and similarly for the other terms.

It is clear that any matrix of the form in equation (2.21) is an orthogonal matrix (since it is a composition of elementary rotations). As in the case of the exponential map, the converse question of whether the map from $(\gamma, \beta, \alpha) \rightarrow SO(3)$ is surjective is an important one. The answer to this question is affirmative: given a rotation $R \in SO(3)$, the angle coordinates can be computed by solving equation (2.21) for γ, β , and α . First, taking the square root of the sum of the squares of r_{11} and r_{21} , we can compute $\cos \beta$. Then, we can solve for β with the arc tangent of $-r_{31}$ over the computed cosine. Then, as long as $\cos \beta \neq 0$, we can solve for α and γ from the remaining entries of (2.21).

In summary,

$$\begin{aligned}
 \beta &= \text{atan2}(-r_{31}, \sqrt{r_{11}^2 + r_{21}^2}) \\
 \alpha &= \text{atan2}(r_{21}/c_\beta, r_{11}/c_\beta) \\
 \gamma &= \text{atan2}(r_{32}/c_\beta, -r_{33}/c_\beta),
 \end{aligned} \quad (2.22)$$

where $\text{atan2}(y, x)$ computes $\tan^{-1}(y/x)$ but uses the sign of both x and y to determine the quadrant in which the resulting angle lies.

Although a second solution exists, by using the positive square root in the formula for β , we always compute the single solution for which $-90^\circ \leq \beta \leq 90^\circ$. This defines a one-to-one mapping from the angle coordinates to the set of rotation matrices. If $\beta = \pm 90^\circ$ (so that $c_\beta = 0$), only the sum or the difference of α and γ can be computed. One possible convention is to choose $\alpha = 0$, and $\gamma = \pm \text{atan2}(r_{12}, r_{22})$.

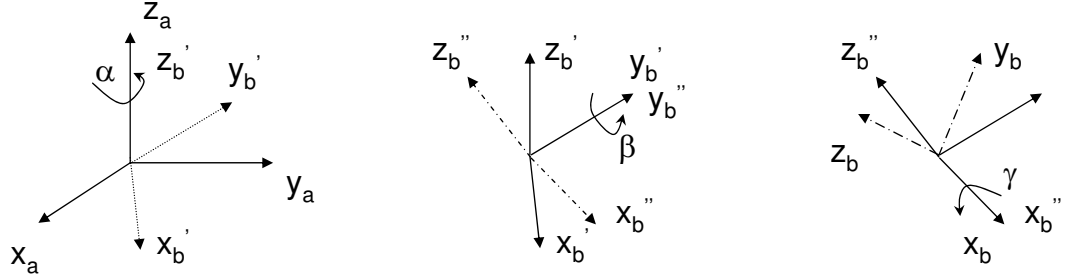


Figure 2.4: ZYX Euler angles

ZYX Euler angles

Another possible description of a frame B is as follows: Start with the frame coincident with frame A. Rotate B first about the z -axis of frame B by an angle α , then about the (new) y -axis of frame B by an angle β , and finally about the (once again, new) x -axis of frame B by an angle γ (see Figure 2.4). In this representation, each rotation is performed about an axis of the moving frame B rather than one of the fixed reference frame A. Such sets of three rotations are called *Euler angles*. Note that each rotation takes place about an axis whose location depends upon the preceding rotations. We will call this representation *ZYX Euler angles*, or sometimes the *roll*, *pitch*, and *yaw* angles.

Interpreting a rotation matrix as a rigid transformation leads to the following result for the rotation matrix of B relative to A

$$R_{ab} = R_{\mathbf{z}}(\alpha)R_{\mathbf{y}}(\beta)R_{\mathbf{x}}(\gamma) \quad (2.23)$$

which is exactly the same as that obtained for the same three rotations taken in the opposite order about fixed axes. Because (2.23) is the equivalent to (2.21), there is no need to repeat the solution for extracting the ZYX Euler angles from a rotation matrix.

ZYZ Euler angles

In a similar manner, we can define the ZYZ Euler angles (α, β, γ) as three successive rotations about the principal axes of the moving frame. The resulting rotation matrix in terms of these angle coordinates is given by

$$\begin{aligned} R_{ab} &= R_{\mathbf{z}}(\alpha)R_{\mathbf{y}}(\beta)R_{\mathbf{z}}(\gamma) \\ &= \begin{bmatrix} c_\alpha c_\beta c_\gamma - s_\alpha s_\gamma & -c_\alpha c_\beta s_\gamma - s_\alpha c_\gamma & c_\alpha s_\beta \\ s_\alpha c_\beta c_\gamma + c_\alpha s_\gamma & -s_\alpha c_\beta s_\gamma + c_\alpha c_\gamma & s_\alpha s_\beta \\ -s_\beta c_\gamma & s_\beta s_\gamma & c_\beta \end{bmatrix} \end{aligned} \quad (2.24)$$

The solution for extracting the ZYZ Euler angles from a rotation matrix is, for $\sin \beta \neq 0$,

$$\begin{aligned} \beta &= \text{atan2}(\sqrt{r_{31}^2 + r_{32}^2}, r_{33}) \\ \alpha &= \text{atan2}(r_{23}/s_\beta, r_{13}/s_\beta) \\ \gamma &= \text{atan2}(r_{32}/s_\beta, -r_{31}/s_\beta). \end{aligned} \quad (2.25)$$

We obtain a single solution for $0 \leq \beta \leq 180^\circ$. If $\beta = 0$ or 180° , the solution of (2.25) degenerates. In these cases, only the sum or the difference of α and γ may be computed.

Other angle-set conventions

The XYZ fixed angles, and the ZYX and ZYZ Euler angles are examples of a set of 24 conventions, known as the *angle-set conventions*, that have traditionally been used for specifying orientation. Of these 24, 12 conventions are for fixed angle sets, and 12 are for Euler-angle sets. Because of the duality of fixed angle sets with Euler-angle sets, there are really only 12 unique parameterizations of a rotation matrix by using successive rotations about principal axes.

In general, let $(\hat{\omega}_1, \hat{\omega}_2, \hat{\omega}_3)$ be a basis of $so(3)$, and define the mapping from \mathbb{R}^3

quaternions—(to $SO(3)$
rotational mo-
tion!quaternion
representation

$$\beta : (\beta_1, \beta_2, \beta_3) \mapsto \exp(\beta_1 \hat{\omega}_1) \exp(\beta_2 \hat{\omega}_2) \exp(\beta_3 \hat{\omega}_3). \quad (2.26)$$

The coordinates $(\beta_1, \beta_2, \beta_3)$ are referred to as the *canonical coordinates of the second kind*, relative to the basis $(\hat{\omega}_1, \hat{\omega}_2, \hat{\omega}_3)$ and in a neighborhood of the identity. In the special case that $\omega_1 = \mathbf{z}$, $\omega_2 = \mathbf{y}$, and $\omega_3 = \mathbf{x}$, we recover the ZYX Euler angles or the XYZ fixed angles. It is not difficult to see that the ZYZ Euler angle parameterization is singular at the identity configuration and so are the other five angle-set conventions. Hence, only 6 angle-set conventions give legitimate parameterizations of the rotation group around the identity. It is a fundamental topological fact that singularities can never be eliminated in any 3-dimensional representation of $SO(3)$. For example, the ZYX Euler angle parameterization is singular when $\beta = \pi/2$. This situation is similar to that of attempting to find a global coordinate chart on a sphere, which is doomed to failure.

To conclude, it is useful to know that the exponential map is not commutative, i.e., for $\hat{\omega}_1, \hat{\omega}_2 \in \mathfrak{so}(3)$,

$$e^{\hat{\omega}_1} e^{\hat{\omega}_2} \neq e^{\hat{\omega}_2} e^{\hat{\omega}_1} \neq e^{\hat{\omega}_1 + \hat{\omega}_2}$$

unless $\hat{\omega}_1 \hat{\omega}_2 = \hat{\omega}_2 \hat{\omega}_1$. The difference between $\hat{\omega}_1 \hat{\omega}_2$ and $\hat{\omega}_2 \hat{\omega}_1$ is called the Lie bracket on $\mathfrak{so}(3)$, denoted by

$$[\hat{\omega}_1, \hat{\omega}_2] = \hat{\omega}_1 \hat{\omega}_2 - \hat{\omega}_2 \hat{\omega}_1. \quad (2.27)$$

The linear structure of $\mathfrak{so}(3)$ together with the Lie bracket form what is known as the Lie algebra of the (Lie) group $SO(3)$ (see Appendix A for more detailed treatment).

Quaternions

Quaternions generalize complex numbers and can be used to represent rotations in much the same way as complex numbers on the unit circle can be used to represent

planar rotations. Unlike Euler angles, quaternions give a global parameterization of unit quaternions $SO(3)$, at the cost of using four numbers instead of three to represent a rotation.

Formally, a quaternion is a vector quantity of the form

$$Q = q_0 + q_1 \mathbf{i} + q_2 \mathbf{j} + q_3 \mathbf{k} \quad \mathbf{q}_i \in \mathbb{R}, \mathbf{i} = \mathbf{0}, \dots, \mathbf{3},$$

where q_0 is the *scalar* component of Q and $\vec{q} = (q_1, q_2, q_3)$ is the *vector* component. A convenient shorthand notation is $Q = (q_0, \vec{q})$ with $q_0 \in \mathbb{R}$, $\vec{q} \in \mathbb{R}^3$. The set of quaternions \mathbb{Q} is a 4-dimensional vector space over the reals and forms a group with respect to quaternion multiplication, denoted “ \cdot ”. Multiplication is distributive and associative, but *not* commutative; it satisfies the relations

$$a\mathbf{i} = \mathbf{i}a \quad a\mathbf{j} = \mathbf{j}a \quad a\mathbf{k} = \mathbf{k}a \quad a \in \mathbb{R}$$

$$\mathbf{i} \cdot \mathbf{i} = \mathbf{j} \cdot \mathbf{j} = \mathbf{k} \cdot \mathbf{k} = \mathbf{i} \cdot \mathbf{j} \cdot \mathbf{k} = -1$$

$$\mathbf{i} \cdot \mathbf{j} = -\mathbf{j} \cdot \mathbf{i} = \mathbf{k} \quad \mathbf{j} \cdot \mathbf{k} = -\mathbf{k} \cdot \mathbf{j} = \mathbf{i} \quad \mathbf{k} \cdot \mathbf{i} = -\mathbf{i} \cdot \mathbf{k} = \mathbf{j}$$

The *conjugate* of a quaternion $Q = (q_0, \vec{q})$ is given by $Q^* = (q_0, -\vec{q})$ and the magnitude of a quaternion satisfies

$$\|Q\|^2 = Q \cdot Q^* = q_0^2 + q_1^2 + q_2^2 + q_3^2.$$

It is straightforward to verify that the inverse of a quaternion is $Q^{-1} = Q^* / \|Q\|^2$ and that $Q = (1, 0)$ is the identity element for quaternion multiplication.

The product between two quaternions has a simple form in terms of the inner and cross products between vectors in \mathbb{R}^3 . Let $Q = (q_0, \vec{q})$ and $P = (p_0, \vec{p})$ be quaternions, where $q_0, p_0 \in \mathbb{R}$ are the scalar parts of Q and P and \vec{q}, \vec{p} are the vector parts. It can be shown algebraically that the product of two quaternions satisfies:

$$Q \cdot P = (q_0 p_0 - \vec{q} \cdot \vec{p}, q_0 \vec{p} + p_0 \vec{q} + \vec{q} \times \vec{p}).$$

In most applications, this formula eliminates the need to make direct use of the multiplicative relations given above.

quaternions—)
 rotational
 motion—)
 rigid body
 motion—(

The *unit quaternions* are the subset of all $Q \in \mathbb{Q}$ such that $\|Q\| = 1$. The unit quaternions also form a group with respect to quaternion multiplication (Exercise 6). Given a rotation matrix $R = \exp(\hat{\omega}\theta)$, we define the associated unit quaternion as

$$Q = (\cos(\theta/2), \omega \sin(\theta/2)),$$

where $\omega \in \mathbb{R}^3$ represents the unit axis of rotation and $\theta \in \mathbb{R}$ represents the angle of rotation. A detailed calculation shows that if Q_{ab} represents a rotation between frame A and frame B , and Q_{bc} represents a rotation between frames B and C , then the rotation between A and C is given by the quaternion

$$Q_{ac} = Q_{ab} \cdot Q_{bc}.$$

Thus, the group operation on unit quaternions directly corresponds to the group operation for rotations. Given a unit quaternion $Q = (q_0, \vec{q})$, we can extract the corresponding rotation by setting

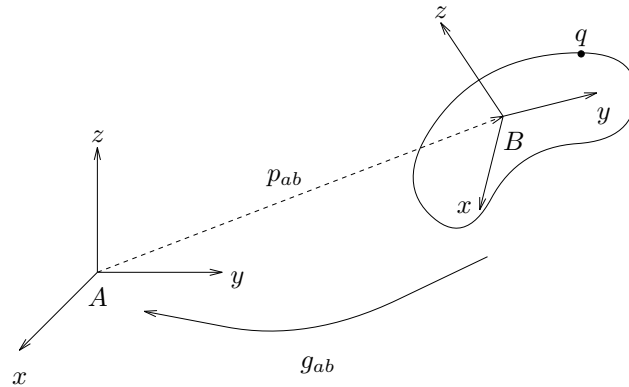
$$\theta = 2 \cos^{-1} q_0 \quad \omega = \begin{cases} \frac{\vec{q}}{\sin(\theta/2)} & \text{if } \theta \neq 0, \\ 0 & \text{otherwise,} \end{cases}$$

and $R = \exp(\hat{\omega}\theta)$.

Since the group structure for quaternions directly corresponds to that of rotations, quaternions provide an efficient representation for rotations which do not suffer from singularities. Their properties are explored more fully in the exercises.

3 Rigid Motion in \mathbb{R}^3

Recall from Section 1 that a rigid motion is one that preserves the distance between points and the angle between vectors. We represent rigid motions by using rigid body transformations to describe the instantaneous position and orientation of a body coordinate frame relative to an inertial frame. This representation relies on the



translational
motion
rigid body mo-
tion!representatio
using
\$“SE(3)”\$

Figure 2.5: Coordinate frames for specifying rigid motions.

fact that rigid body transformations map right-handed, orthonormal frames to right-handed, orthonormal frames, thus preserving distance and angles. In this book we refer to all transformations between coordinate frames as rigid body transformations (or just rigid transformations), whether or not a rigid body is explicitly present.

In general, rigid motions consist of rotation and translation. In the preceding section, we discussed representations of pure rotational motion. The procedure for representing pure translational motion is very simple: choose a (any) point in the body and keep track of the coordinates of the point relative to some known frame. This gives a curve $p(t) \in \mathbb{R}^3, t \in [0, T]$, for a trajectory of the entire rigid body.

The representation of general rigid body motion, involving both translation and rotation, is more involved. We describe the position and orientation of a coordinate frame B attached to the body relative to an inertial frame A (see Figure 2.5). Let $p_{ab} \in \mathbb{R}^3$ be the position vector of the origin of frame B from the origin of frame A , and $R_{ab} \in SO(3)$ the orientation of frame B , relative to frame A . A configuration of the system consists of the pair (p_{ab}, R_{ab}) , and the configuration space of the system is the product space of \mathbb{R}^3 with $SO(3)$, which shall be denoted as $SE(3)$ (for special

configuration space Euclidean group):

$SE(3)$

rigid body transformations on points and vectors

points rigid transformation of

$$SE(3) = \{(p, R) : p \in \mathbb{R}^3, R \in SO(3)\} = \mathbb{R}^3 \times SO(3). \quad (2.28)$$

We defer the proof of the fact that $SE(3)$ is a group to the next subsection. As in the case of $SO(3)$, there is a generalization to n dimensions,

$$SE(n) := \mathbb{R}^n \times SO(n).$$

Analogous to the rotational case, an element $(p, R) \in SE(3)$ serves as both a specification of the configuration of a rigid body and a transformation taking the coordinates of a point from one frame to another. More precisely, let $q_a, q_b \in \mathbb{R}^3$ be the coordinates of a point q relative to frames A and B , respectively. Given q_b , we can find q_a by a transformation of coordinates:

$$q_a = p_{ab} + R_{ab}q_b \quad (2.29)$$

where $g_{ab} = (p_{ab}, R_{ab}) \in SE(3)$ is the specification of the configuration of the B frame relative to the A frame. By an abuse of notation, we write $g(q)$ to denote the action of a rigid transformation on a point,

$$g(q) = p + Rq,$$

so that $q_a = g_{ab}(q_b)$.

The action of a rigid transformation $g = (p, R)$ on a vector $v = s - r$ is defined by the following formula:

$$g_*(v) := g(s) - g(r) = R(s - r) = Rv.$$

Thus, a vector is transformed by rotation.

3.1 Homogeneous representation

The transformation of points and vectors by rigid transformations has a simple representation in terms of matrices and vectors in \mathbb{R}^4 . We begin by adopting some notation. We append 1 to the coordinates of a point to yield a vector in \mathbb{R}^4 ,

$$\bar{q} = \begin{bmatrix} q_1 \\ q_2 \\ q_3 \\ 1 \end{bmatrix}.$$

These are called the *homogeneous coordinates* of the point q . Thus, the origin has the form

$$\bar{O} = \begin{bmatrix} 0 \\ 0 \\ 0 \\ 1 \end{bmatrix}.$$

Vectors, which are the difference of points, then have the form

$$\bar{v} = \begin{bmatrix} v_1 \\ v_2 \\ v_3 \\ 0 \end{bmatrix}.$$

Note that the form of the vector is different from that of a point. The 0 and 1 in the fourth component of vectors and points, respectively, will remind us of the difference between points and vectors and enforce a few rules of syntax:

1. Sums and differences of vectors are vectors.
2. The sum of a vector and a point is a point.
3. The difference between two points is a vector.
4. The sum of two points is meaningless.

The transformation $q_a = g_{ab}(q_b)$ given in equation (2.29) is an *affine* transformation. Using the preceding notation for points, we may represent it in *linear* form by writing it as

$$\bar{q}_a = \begin{bmatrix} q_a \\ 1 \end{bmatrix} = \begin{bmatrix} R_{ab} & p_{ab} \\ 0 & 1 \end{bmatrix} \begin{bmatrix} q_b \\ 1 \end{bmatrix} =: \bar{g}_{ab} \bar{q}_b.$$

homogeneous
coordinates—(
homogeneous
coordinates!points@for
points and
vectors
homogeneous
coordinates
homogeneous
coordinates!points@for
points and
vectors
points!vectors@vers
vectors
vectors!points@vers
points
rigid body
transforma-
tions!actions
on points and
vectors
points!rigid
transformation
of

homogeneous
coordi-
nates!rigid@for
rigid body
transformations

The 4×4 matrix \bar{g}_{ab} is called the *homogeneous representation* of $g_{ab} \in SE(3)$. In general, if $g = (p, R) \in SE(3)$, then

rigid body
transforma-
tions!homogeneous
representation

$$\bar{g} = \begin{bmatrix} R & p \\ 0 & 1 \end{bmatrix}. \quad (2.30)$$

perspective
transformations

The price to be paid for the convenience of having a homogeneous or linear representation of the rigid body motion is the increase in the dimension of the quantities involved from 3 to 4.

rigid body
transforma-
tions!composition
rule

group!of rigid
body
transformations

The last row of the matrix of equation (2.30) appears to be “extra baggage” as well. However, in the graphics literature, the number 1 is frequently replaced by a scalar constant which is either greater than 1 to represent dilation or less than 1 to represent contraction. Also, the row vector of zeros in the last row may be replaced by some other row vector to provide “perspective transformations.” In both these instances, of course, the transformation represented by the augmented matrix no longer corresponds to a rigid displacement.

rigid body
transforma-
tions!group
properties

Rigid body transformations can be composed to form new rigid body transformations. Let $g_{bc} \in SE(3)$ be the configuration of a frame C relative to a frame B , and g_{ab} the configuration of frame B relative to another frame A . Then, using equation (2.30), the configuration of C relative to frame A is given by

$$\bar{g}_{ac} = \bar{g}_{ab} \bar{g}_{bc} = \begin{bmatrix} R_{ab}R_{bc} & R_{ab}p_{bc} + p_{ab} \\ 0 & 1 \end{bmatrix}. \quad (2.31)$$

Equation (2.31) defines the *composition rule* for rigid body transformations to be the standard matrix multiplication. Using the homogeneous representation, it may be verified that the set of rigid transformations is a group; that is:

1. If $g_1, g_2 \in SE(3)$, then $g_1 g_2 \in SE(3)$.
2. The 4×4 identity element, I , is in $SE(3)$.

3. If $g \in SE(3)$, then the inverse of \bar{g} is determined by straightforward matrix inversion to be:

$$\bar{g}^{-1} = \begin{bmatrix} R^T & -R^T p \\ 0 & 1 \end{bmatrix} \in SE(3)$$

so that $g^{-1} = (-R^T p, R^T)$.

rigid body transformations! actions on points and vectors
vectors! rigid transformation of

4. The composition rule for rigid body transformations is associative.

Using the homogeneous representation for a vector $v = s - r$, we obtain the representation for a rigid body transformation of v by multiplying the homogeneous representations of v by the homogeneous representation of g ,

$$\bar{g}_* \bar{v} = \bar{g}(\bar{s}) - \bar{g}(\bar{r}) = \begin{bmatrix} R & p \\ 0 & 1 \end{bmatrix} \begin{bmatrix} v_1 \\ v_2 \\ v_3 \\ 0 \end{bmatrix}.$$

Note that by defining the homogeneous representation of a vector to have a zero in the bottom row, we are able to once again use matrix multiplication to represent the action of a rigid transformation, this time on a vector instead of a point. For notational simplicity, in what follows we will confuse homogeneous representations and the abstract representation of points, vectors, and rigid body transformations. Thus, we will write gq and gv instead of $\bar{g}\bar{q}$ and $\bar{g}_*\bar{v}$.

The next proposition establishes that elements of $SE(3)$ are indeed rigid body transformations; namely, that they preserve angles between vectors and distances between points.

Proposition 2.7. Elements of $SE(3)$ represent rigid motions

Any $g \in SE(3)$ is a rigid body transformation:

1. g preserves distance between points:

$$\|gq - gp\| = \|q - p\| \quad \text{for all points } q, p \in \mathbb{R}^3.$$

2. g preserves orientation between vectors:

$$g_*(v \times w) = g_*v \times g_*w \quad \text{for all vectors } v, w \in \mathbb{R}^3.$$

rotation about a
line

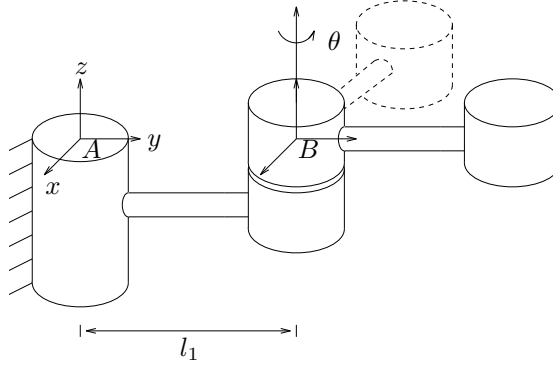


Figure 2.6: Rigid body motion generated by rotation about a fixed axis.

Proof. The proofs follow directly from the corresponding proofs for rotation matrices:

$$\|gq_1 - gq_2\| = \|Rq_1 - Rq_2\| = \|q_1 - q_2\|$$

$$g_*v \times g_*w = Rv \times Rw = R(v \times w).$$

□

Example 2.1. Rotation about a line

Consider the motion of a rigid body rotated about a line in the z direction, through the point $(0, l_1, 0) \in \mathbb{R}^3$, as shown in Figure 2.6. If we let θ denote the amount of rotation, then the orientation of coordinate frame B with respect to A is

$$R_{ab} = \begin{bmatrix} \cos \theta & -\sin \theta & 0 \\ \sin \theta & \cos \theta & 0 \\ 0 & 0 & 1 \end{bmatrix}.$$

The coordinates for the origin of frame B are

$$p_{ab} = \begin{bmatrix} 0 \\ l_1 \\ 0 \end{bmatrix},$$

again relative to frame A . The homogeneous representation of the configuration of the rigid body is given by

$$g_{ab}(\theta) = \begin{bmatrix} \cos \theta & -\sin \theta & 0 & 0 \\ \sin \theta & \cos \theta & 0 & l_1 \\ 0 & 0 & 1 & 0 \\ 0 & 0 & 0 & 1 \end{bmatrix}.$$

Note that when the angle $\theta = 0$, $g_{ab}(0)$ gives that the relative displacement between the two frames is a pure translation along the y -axis.

3.2 Exponential coordinates for rigid motion and twists

The notion of the exponential mapping introduced in Section 2 for $SO(3)$ can be generalized to the Euclidean group, $SE(3)$. We will make extensive use of this representation in the sequel since it allows an elegant, rigorous, and geometric treatment of spatial rigid body motion. We begin by presenting a pair of motivational examples and then present a formal set of definitions.

Consider the simple example of a one-link robot as shown in Figure 2.7a, where the axis of rotation is $\omega \in \mathbb{R}^3$, $\|\omega\| = 1$, and $q \in \mathbb{R}^3$ is a point on the axis. Assuming that the link rotates with unit velocity, then the velocity of the tip point, $p(t)$, is

$$\dot{p}(t) = \omega \times (p(t) - q). \quad (2.32)$$

This equation can be conveniently converted into homogeneous coordinates by defining the 4×4 matrix $\hat{\xi}$ to be

$$\hat{\xi} = \begin{bmatrix} \hat{\omega} & v \\ 0 & 0 \end{bmatrix}, \quad (2.33)$$

with $v = -\omega \times q$. Equation (2.32) can then be rewritten with an extra row appended to it as

$$\begin{bmatrix} \dot{p} \\ 0 \end{bmatrix} = \begin{bmatrix} \hat{\omega} & -\omega \times q \\ 0 & 0 \end{bmatrix} \begin{bmatrix} p \\ 1 \end{bmatrix} = \hat{\xi} \begin{bmatrix} p \\ 1 \end{bmatrix} \implies \dot{\bar{p}} = \hat{\xi} \bar{p}.$$

homogeneous
coordinates—
exponential co-
ordinates!rigid
motion@for
rigid
motion—(

matrix
exponential
prismatic joint

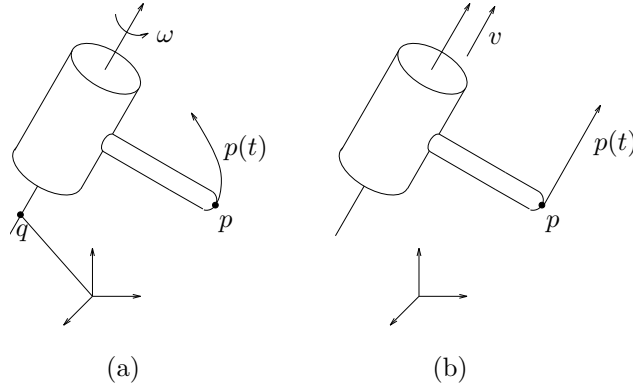


Figure 2.7: (a) A revolute joint and (b) a prismatic joint.

The solution of the differential equation is given by

$$\bar{p}(t) = e^{\hat{\xi}t} \bar{p}(0),$$

where $e^{\hat{\xi}t}$ is the matrix exponential of the 4×4 matrix $\hat{\xi}t$, defined (as usual) by

$$e^{\hat{\xi}t} = I + \hat{\xi}t + \frac{(\hat{\xi}t)^2}{2!} + \frac{(\hat{\xi}t)^3}{3!} + \dots$$

The scalar t is the total amount of rotation (since we are rotating with unit velocity). $\exp(\hat{\xi}t)$ is a mapping from the initial location of a point to its location after rotating t radians.

In a similar manner, we can represent the transformation due to translational motion as the exponential of a 4×4 matrix. The velocity of a point attached to a prismatic joint moving with unit velocity (see Figure 2.7b) is

$$\dot{p}(t) = v. \quad (2.34)$$

Again, the solution of equation (2.34) can be written as $\exp(\hat{\xi}t)\bar{p}(0)$, where t is the total amount of translation and

$$\hat{\xi} = \begin{bmatrix} 0 & v \\ 0 & 0 \end{bmatrix}. \quad (2.35)$$

The 4×4 matrix $\hat{\xi}$ given in equations (2.33) and (2.35) is the generalization of the skew-symmetric matrix $\hat{\omega} \in so(3)$. Analogous to the definition of $so(3)$, we define

$$se(3) := \{(v, \hat{\omega}) : v \in \mathbb{R}^3, \hat{\omega} \in so(3)\}. \quad (2.36)$$

In homogeneous coordinates, we write an element $\hat{\xi} \in se(3)$ as

$$\hat{\xi} = \begin{bmatrix} \hat{\omega} & v \\ 0 & 0 \end{bmatrix} \in \mathbb{R}^{4 \times 4}.$$

An element of $se(3)$ is referred to as a *twist*, or a (infinitesimal) generator of the Euclidean group. We define the \vee (vee) operator to extract the 6-dimensional vector which parameterizes a twist,

$$\begin{bmatrix} \hat{\omega} & v \\ 0 & 0 \end{bmatrix}^{\vee} = \begin{bmatrix} v \\ \omega \end{bmatrix}, \quad (2.37)$$

and call $\xi := (v, \omega)$ the *twist coordinates* of $\hat{\xi}$. The inverse operator, \wedge (wedge), forms a matrix in $se(3)$ out of a given vector in \mathbb{R}^6 :

$$\begin{bmatrix} v \\ \omega \end{bmatrix}^{\wedge} = \begin{bmatrix} \hat{\omega} & v \\ 0 & 0 \end{bmatrix}. \quad (2.38)$$

Thus, $\xi \in \mathbb{R}^6$ represents the twist coordinates for the twist $\hat{\xi} \in se(3)$; this parallels our notation for skew-symmetric matrices.

Proposition 2.8. Exponential map from $se(3)$ to $SE(3)$

Given $\hat{\xi} \in se(3)$ and $\theta \in \mathbb{R}$, the exponential of $\hat{\xi}\theta$ is an element of $SE(3)$, i.e.,

$$e^{\hat{\xi}\theta} \in SE(3).$$

Proof. The proof is by explicit calculation. In the course of the proof, we will obtain a formula for $\exp(\hat{\xi}\theta)$. Write $\hat{\xi}$ as

$$\hat{\xi} = \begin{bmatrix} \hat{\omega} & v \\ 0 & 0 \end{bmatrix}.$$

$se(3)$ is the definition of twist coordinates exponential map for rigid body transformations

Case 1 ($\omega = 0$). If $\omega = 0$, then a straightforward calculation shows that

$$\hat{\xi}^2 = \hat{\xi}^3 = \hat{\xi}^4 = \dots = 0$$

so that $\exp(\hat{\xi}\theta) = I + \hat{\xi}\theta$ and hence

$$\boxed{e^{\hat{\xi}\theta} = \begin{bmatrix} I & v\theta \\ 0 & 1 \end{bmatrix} \quad \omega = 0} \quad (2.39)$$

which is in $SE(3)$ as desired.

Case 2 ($\omega \neq 0$). Assume $\|\omega\| = 1$, by appropriate scaling of θ if necessary, and define a rigid transformation g by

$$g = \begin{bmatrix} I & \omega \times v \\ 0 & 1 \end{bmatrix}. \quad (2.40)$$

Now, using the calculation of Lemma 2.3, with $\|\omega\| = 1$, we have

$$\begin{aligned} \hat{\xi}' &= g^{-1}\hat{\xi}g \\ &= \begin{bmatrix} I & -\omega \times v \\ 0 & 1 \end{bmatrix} \begin{bmatrix} \hat{\omega} & v \\ 0 & 0 \end{bmatrix} \begin{bmatrix} I & \omega \times v \\ 0 & 1 \end{bmatrix} \\ &= \begin{bmatrix} \hat{\omega} & \omega\omega^T v \\ 0 & 0 \end{bmatrix} = \begin{bmatrix} \hat{\omega} & h\omega \\ 0 & 0 \end{bmatrix}, \end{aligned} \quad (2.41)$$

where $h := \omega^T v$. Using the following identity (see Exercise 9),

$$e^{\hat{\xi}\theta} = e^{g(\hat{\xi}')g^{-1}} = g e^{\hat{\xi}'\theta} g^{-1}, \quad (2.42)$$

it suffices to calculate $\exp(\hat{\xi}'\theta)$. This simplifies the calculation since it may be verified (using $\hat{\omega}\omega = \omega \times \omega = 0$) that

$$(\hat{\xi}')^2 = \begin{bmatrix} \hat{\omega}^2 & 0 \\ 0 & 0 \end{bmatrix}, \quad (\hat{\xi}')^3 = \begin{bmatrix} \hat{\omega}^3 & 0 \\ 0 & 0 \end{bmatrix}, \quad \dots$$

Hence,

$$e^{\hat{\xi}'\theta} = \begin{bmatrix} e^{\hat{\omega}\theta} & h\omega\theta \\ 0 & 1 \end{bmatrix},$$

and using equation (2.42) it follows that

$$e^{\hat{\xi}\theta} = \begin{bmatrix} e^{\hat{\omega}\theta} & (I - e^{\hat{\omega}\theta})(\omega \times v) + \omega\omega^T v\theta \\ 0 & 1 \end{bmatrix} \quad \omega \neq 0 \quad (2.43)$$

which is an element of $SE(3)$.

The transformation $g = \exp(\hat{\xi}\theta)$ is slightly different than the rigid transformations that we have encountered previously. We interpret it not as mapping points from one coordinate frame to another, but rather as mapping points from their initial coordinates, $p(0) \in \mathbb{R}^3$, to their coordinates after the rigid motion is applied:

$$p(\theta) = e^{\hat{\xi}\theta} p(0).$$

In this equation, both $p(0)$ and $p(\theta)$ are specified with respect to a *single* reference frame. Similarly, if we let $g_{ab}(0)$ represent the initial configuration of a rigid body relative to a frame A , then the final configuration, still with respect to A , is given by

$$g_{ab}(\theta) = e^{\hat{\xi}\theta} g_{ab}(0). \quad (2.44)$$

Thus, the exponential map for a twist gives the *relative* motion of a rigid body. This interpretation of the exponential of a twist as a mapping from initial to final configurations will be especially important as we study the kinematics of robot mechanisms in the next chapter.

Our primary interest is to use the exponential map as a representation for rigid motion, and hence we must show that every rigid transformation can be written as the exponential of some twist. The following proposition asserts that this is always possible and gives a constructive procedure for finding the twist which generates a given rigid transformation.

exponential map as relative transformation relative motion, representation using the exponential map
 □ exponential map surjectivity onto $SE(3)$

exponential co-
ordinates rigid
motion for
rigid motion

Proposition 2.9. Surjectivity of the exponential map onto $SE(3)$

Given $g \in SE(3)$, there exists $\hat{\xi} \in se(3)$ and $\theta \in \mathbb{R}$ such that $g = \exp(\hat{\xi}\theta)$, and the exponential map has an inverse denoted by

$$\log : SE(3) \rightarrow se(3) : g \mapsto \log g = \hat{\xi}\theta.$$

Proof. (Constructive). Let $g = (p, R)$ with $R \in SO(3)$, $p \in \mathbb{R}^3$. We ignore the trivial case $(p, R) = (0, I)$ which is solved with $\hat{\xi}\theta = 0$.

Case 1 ($R = I$). If there is no rotational motion, set

$$\hat{\xi} = \begin{bmatrix} 0 & p \\ 0 & 0 \end{bmatrix} \quad \theta = \|p\|.$$

Equation (2.39) verifies that $\exp(\hat{\xi}\theta) = (p, I) = g$.

Case 2 ($R \neq I$). To find $\xi = (v, \omega)$, we equate $\exp(\hat{\xi}\theta)$ and g and solve for v, ω . Using equation (2.43):

$$e^{\hat{\xi}\theta} = \begin{bmatrix} e^{\hat{\omega}\theta} & (I - e^{\hat{\omega}\theta})(\omega \times v) + \omega\omega^T v\theta \\ 0 & 1 \end{bmatrix}.$$

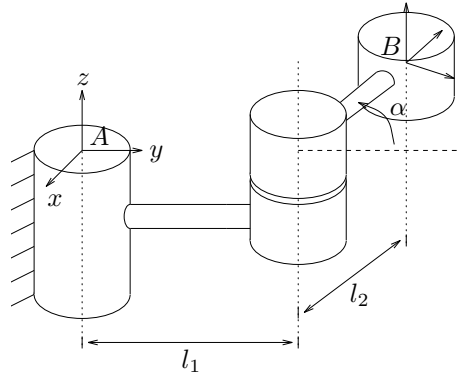
ω and θ are obtained by solving the rotation equation $\exp(\hat{\omega}\theta) = R$, as in Proposition 2.5 of the previous section. This leaves the equation

$$(I - e^{\hat{\omega}\theta})(\omega \times v) + \omega\omega^T v\theta = p, \quad (2.45)$$

which must be solved for v . It suffices to show that the matrix

$$A = (I - e^{\hat{\omega}\theta})\hat{\omega} + \omega\omega^T\theta$$

is nonsingular for all $\theta \in (0, \pi)$. This follows from the fact that the two matrices which comprise A have mutually orthogonal null spaces when $\theta \neq 0$ (and $R \neq I$). Hence, $Av = 0 \iff v = 0$. See Exercise 10 for more details. \square



rotation about a
line!
twist
coordinates

Figure 2.8: Rigid body displacement generated by rotation about a fixed axis.

In light of Proposition 2.9, every rigid transformation g can be written as the exponential of some twist $\hat{\xi}\theta \in se(3)$. We call the vector $\xi\theta \in \mathbb{R}^6$ the *exponential coordinates* for the rigid transformation g . Note that, as in the case of rotations, the mapping $\exp : se(3) \rightarrow SE(3)$ is many-to-one since the choice of ω and θ for solving the rotational component of the motion is not unique. This does not present great difficulties since for most applications we are given the twist as part of the problem and we wish to find the corresponding rigid motion.

Example 2.2. Twist coordinates for rotation about a line

Consider the rigid displacement generated by rotating about a fixed axis in space, as shown in Figure 2.8. The configuration of the B frame is given by

$$g_{ab} = \begin{bmatrix} \cos \alpha & -\sin \alpha & 0 & -l_2 \sin \alpha \\ \sin \alpha & \cos \alpha & 0 & l_1 + l_2 \cos \alpha \\ 0 & 0 & 1 & 0 \\ 0 & 0 & 0 & 1 \end{bmatrix}.$$

We wish to calculate the twist coordinates corresponding to the configuration of the frame B relative to frame A .

To compute the twist which generates g_{ab} , we follow the proof of Proposition 2.9, assuming $\alpha \neq 0$ (so that $R \neq I$). The axis $\omega \in \mathbb{R}^3$ and angle $\theta \in \mathbb{R}$ which satisfy

exponential
map! as
relative
transformation

$\exp(\hat{\omega}\theta) = R_{ab}$ are

$$\omega = \begin{bmatrix} 0 \\ 0 \\ 1 \end{bmatrix} \quad \theta = \alpha,$$

since we are rotating about the z -axis. To find v , we must solve

$$\left[\left(I - e^{\hat{\omega}\theta} \right) \hat{\omega} + \omega \omega^T \theta \right] v = p_{ab}.$$

Using the fact that $\theta = \alpha$ and expanding the left-hand side, this equation becomes

$$\begin{bmatrix} \sin \alpha & \cos \alpha - 1 & 0 \\ 1 - \cos \alpha & \sin \alpha & 0 \\ 0 & 0 & \alpha \end{bmatrix} v = \begin{bmatrix} -l_2 \sin \alpha \\ l_1 + l_2 \cos \alpha \\ 0 \end{bmatrix}.$$

The solution is given by

$$v = \begin{bmatrix} \frac{\sin \alpha}{2(1 - \cos \alpha)} & \frac{1}{2} & 0 \\ -\frac{1}{2} & \frac{\sin \alpha}{2(1 - \cos \alpha)} & 0 \\ 0 & 0 & \frac{1}{\alpha} \end{bmatrix} \begin{bmatrix} -l_2 \sin \alpha \\ l_1 + l_2 \cos \alpha \\ 0 \end{bmatrix} = \begin{bmatrix} \frac{l_1 - l_2}{2} \\ \frac{(l_1 + l_2) \sin \alpha}{2(1 - \cos \alpha)} \\ 0 \end{bmatrix}.$$

Thus, the twist coordinates for g_{ab} are

$$\xi = \begin{bmatrix} \frac{l_1 - l_2}{2} \\ \frac{(l_1 + l_2) \sin \alpha}{2(1 - \cos \alpha)} \\ 0 \\ 0 \\ 0 \\ 1 \end{bmatrix} \quad \theta = \alpha \neq 0.$$

This solution may be unexpected, considering that the motion was generated by a pure rotation about an axis. The reason for the complicated form of the solution is that we took the exponential coordinates of the *absolute* transformation between the B and A coordinate frames. Consider, instead, the exponential coordinates for the relative transformation

$$g(\alpha) = g_{ab}(\alpha)g_{ab}^{-1}(0),$$

where $g_{ab}(0)$ is the transformation corresponding to $\alpha = 0$ (a pure translation). It can be verified that the exponential coordinates for the relative transformation $g(\alpha)$

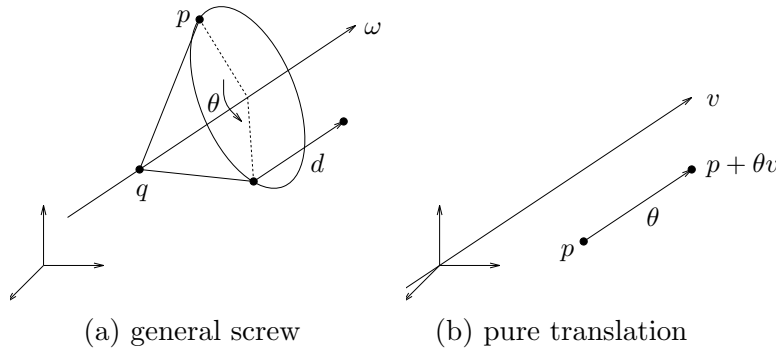


Figure 2.9: Screw motions.

exponential co-ordinates rigid motion for rigid motion—)
 twists! geometric attributes—(
 screws—(
 screws! geometric attributes of—(
 screw motions
 pitch of a screw
 axis of a screw

are

$$\xi = \begin{bmatrix} l_1 \\ 0 \\ 0 \\ 0 \\ 0 \\ 1 \end{bmatrix} \quad \theta = \alpha \neq 0.$$

3.3 Screws: a geometric description of twists

In this section, we explore some of the geometric attributes associated with a twist $\xi = (v, \omega)$. These attributes give additional insight into the use of twists to parameterize rigid body motions. We begin by defining a specific class of rigid body motions, called screw motions, and then show that a twist is naturally associated with a screw.

Consider a rigid body motion which consists of rotation about an axis in space through an angle of θ radians, followed by translation along the same axis by an amount d as shown in Figure 2.9a. We call such a motion a *screw motion*, since it is reminiscent of the motion of a screw, in so far as a screw rotates and translates about the same axis. To further encourage this analogy, we define the *pitch* of the screw to be the ratio of translation to rotation, $h := d/\theta$ (assuming $\theta \neq 0$). Thus, the net translational motion after rotating by θ radians is $h\theta$. We represent the axis as a directed line through a point; choosing $q \in \mathbb{R}^3$ to be a point on the axis and

screw motions
 screws!geometric
 attributes
 of—)
 screws!rigid
 body transfor-
 mations
 associated
 with

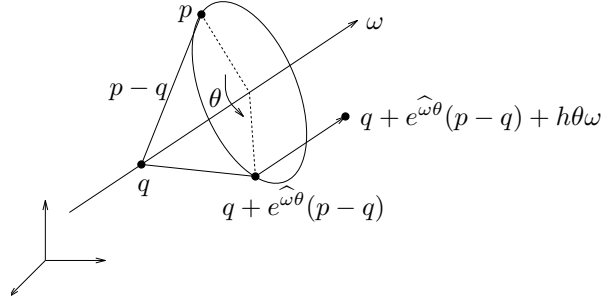


Figure 2.10: Generalized screw motion (with nonzero rotation).

$\omega \in \mathbb{R}^3$ to be a *unit* vector specifying the direction, the axis is the set of points

$$l = \{q + \lambda\omega : \lambda \in \mathbb{R}\}. \quad (2.46)$$

The above definitions hold when the screw motion consists of a nonzero rotation followed by translation.

In the case of zero rotation, the axis of the screw must be defined differently: we take the axis as the line through the origin in the direction v (i.e., v is a vector of magnitude 1), as shown in Figure 2.9b. By convention, the pitch of this screw is ∞ and the magnitude is the amount of translation along the direction v . Collecting these, we have the following definition of a screw:

Definition 2.2. Screw motion

A *screw* S consists of an *axis* l , a *pitch* h , and a *magnitude* M . A *screw motion* represents rotation by an amount $\theta = M$ about the axis l followed by translation by an amount $h\theta$ parallel to the axis l . If $h = \infty$ then the corresponding screw motion consists of a pure translation along the axis of the screw by a distance M .

To compute the rigid body transformation associated with a screw, we analyze the motion of a point $p \in \mathbb{R}^3$, as shown in Figure 2.10. The final location of the point is given by

$$gp = q + e^{\widehat{\omega}\theta}(p - q) + h\theta\omega$$

or, in homogeneous coordinates,

twists!screw
coordinates

$$g \begin{bmatrix} p \\ 1 \end{bmatrix} = \begin{bmatrix} e^{\hat{\omega}\theta} & (I - e^{\hat{\omega}\theta})q + h\theta\omega \\ 0 & 1 \end{bmatrix} \begin{bmatrix} p \\ 1 \end{bmatrix}.$$

Since this relationship must hold for all $p \in \mathbb{R}^3$, the rigid motion given by the screw is

$$g = \begin{bmatrix} e^{\hat{\omega}\theta} & (I - e^{\hat{\omega}\theta})q + h\theta\omega \\ 0 & 1 \end{bmatrix}. \quad (2.47)$$

As in the last section, this transformation maps points attached to the rigid body from their initial coordinates ($\theta = 0$) to their final coordinates, and all points are specified with respect to the fixed reference frame.

Note that the rigid body displacement given in equation (2.47) has the same form as the exponential of a twist, given in equation (2.43):

$$e^{\hat{\xi}\theta} = \begin{bmatrix} e^{\hat{\omega}\theta} & (I - e^{\hat{\omega}\theta})(\omega \times v) + \omega\omega^T v\theta \\ 0 & 1 \end{bmatrix}.$$

In fact, if we choose $v = -\omega \times q + h\omega$, then $\xi = (v, \omega)$ generates the screw motion in equation (2.47) (assuming $\|\omega\| = 1$, $\theta \neq 0$). In the case of a pure rotation, $h = 0$ and the twist associated with a screw motion is simply $\xi = (-\omega \times q, \omega)$. In the instance that the screw corresponds to pure translation, we let θ be the amount of translation, and the rigid body motion described by this “screw” is

$$g = \begin{bmatrix} I & \theta v \\ 0 & 1 \end{bmatrix}, \quad (2.48)$$

which is precisely the motion generated by $\exp(\hat{\xi}\theta)$ with $\xi = (v, 0)$. *Thus, we see that a screw motion corresponds to motion along a constant twist by an amount equal to the magnitude of the screw.*

In fact, we can go one step further and define a screw associated with every twist. Let $\hat{\xi} \in se(3)$ be a twist with twist coordinates $\xi = (v, \omega) \in \mathbb{R}^6$. We do not assume that $\|\omega\| = 1$, allowing both translation plus rotation as well as pure translation. The following are the screw coordinates of a twist:

pitch of a twist
axis of a twist
magnitude of a
twist
screws!twists
associated
with
twists!screw
motions
corresponding
to

1. *Pitch:*

$$h = \frac{\omega^T v}{\|\omega\|^2}. \quad (2.49)$$

The pitch of a twist is the ratio of translational motion to rotational motion.

If $\omega = 0$, we say that ξ has infinite pitch.

2. *Axis:*

$$l = \begin{cases} \left\{ \frac{\omega \times v}{\|\omega\|^2} + \lambda \omega : \lambda \in \mathbb{R} \right\}, & \text{if } \omega \neq 0 \\ \{0 + \lambda v : \lambda \in \mathbb{R}\}, & \text{if } \omega = 0. \end{cases} \quad (2.50)$$

The axis l is a directed line through a point. For $\omega \neq 0$, the axis is a line in the ω direction going through the point $\frac{\omega \times v}{\|\omega\|^2}$. For $\omega = 0$, the axis is a line in the v direction going through the origin.

3. *Magnitude:*

$$M = \begin{cases} \|\omega\|, & \text{if } \omega \neq 0 \\ \|v\|, & \text{if } \omega = 0. \end{cases} \quad (2.51)$$

The magnitude of a screw is the net rotation if the motion contains a rotational component, or the net translation otherwise. If we choose $\|\omega\| = 1$ (or $\|v\| = 1$ when $\omega = 0$), then a twist $\hat{\xi}\theta$ has magnitude $M = \theta$.

We next show that given a screw, we can define a twist which realizes the screw motion and has the proper geometric attributes. It suffices to prove that we can define a twist with a given set of attributes, since any twist with those attributes will generate the correct screw motion.

Proposition 2.10. Screw motions correspond to twists

Given a screw with axis l , pitch h , and magnitude M , there exists a unit magnitude twist ξ such that the rigid motion associated with the screw is generated by the twist $M\xi$.

Proof. The proof is by construction. We split the proof into the usual cases: pure translation and translation plus rotation. For consistency, we generate a screw of the form $\hat{\xi}\theta$, where $\theta = M$. We will assume that q is a point on the axis of the screw.

Case 1 ($h = \infty$). Let $l = \{q + \lambda v : \|v\| = 1, \lambda \in \mathbb{R}\}$, $\theta = M$, and define

$$\hat{\xi} = \begin{bmatrix} 0 & v \\ 0 & 0 \end{bmatrix}.$$

The rigid body motion $\exp(\hat{\xi}\theta)$ corresponds to pure translation along the screw axis by an amount θ .

Case 2 (h finite). Let $l = \{q + \lambda\omega : \|\omega\| = 1, \lambda \in \mathbb{R}\}$, $\theta = M$, and define

$$\hat{\xi} = \begin{bmatrix} \hat{\omega} & -\omega \times q + h\omega \\ 0 & 0 \end{bmatrix}. \quad (2.52)$$

The fact that the rigid body motion $\exp(\hat{\xi}\theta)$ is the appropriate screw motion is verified by direct calculation. \square

There are several important special cases of screw motion of which we shall make frequent use. A *zero pitch screw* is a screw motion for which $h = 0$, corresponding to a pure rotation about an axis. Zero pitch screws are used to model the action of a revolute joint of a manipulator. The axis of the screw corresponds to the axis of rotation of the joint. An *infinite pitch screw* is a motion for which $h = \infty$, as previously mentioned. This case corresponds to a pure translation and is the model for the action of a prismatic joint. The axis of the screw is defined to be a line through the origin which points in the direction of translation (a line through any other point could also be used). The magnitude of the screw gives the amount of the displacement. Finally, we define a *unit twist* to be a twist such that either $\|\omega\| = 1$, or $\omega = 0$ and $\|v\| = 1$; that is, a unit twist has magnitude $M = 1$. Unit twists are useful since they allow us to express rigid motions due to revolute and prismatic joints as $g = \exp(\hat{\xi}\theta)$, where θ corresponds to the amount of rotation or translation.

translational
motion
zero pitch screw
revolute
joint!twist
associated
with
infinite pitch
screw
screws!infinite
pitch
prismatic
joint!twist
associated
with
unit twist
axis of a
screw!choice of
point on

Some comments about the point q on the axis of the screw in the formulas above are in order. For instance, it is important to note that the formulas do not change for different choices of points on the axis of the screw. Thus, if $q' = q + \lambda\omega$ is some other point on the axis of the screw, the formula in equation (2.47) would be unchanged. It is also instructive to verify that for points on the axis of the screw, the screw motion is purely translational of magnitude $h\theta$, as may be verified by applying equation (2.47) to points on the axis.

The twist space $se(3)$ is also referred to as the *Lie algebra* of the Lie group $SE(3)$. The Lie bracket structure on $se(3)$ is defined by

$$[\hat{\xi}_1, \hat{\xi}_2] : se(3) \times se(3) \longrightarrow se(3) : (\hat{\xi}_1, \hat{\xi}_2) \mapsto [\hat{\xi}_1, \hat{\xi}_2] = \hat{\xi}_1 \hat{\xi}_2 - \hat{\xi}_2 \hat{\xi}_1 \quad (2.53)$$

In twist coordinates, we have

$$[\hat{\xi}_1, \hat{\xi}_2] = \begin{bmatrix} \widehat{\omega_1 \times \omega_2} & \omega_1 \times v_2 - \omega_2 \times v_1 \\ 0 & 0 \end{bmatrix}$$

The bilinear map specified in (2.53) has the following properties

- (i) $[\hat{\xi}_1, \hat{\xi}_2] = -[\hat{\xi}_2, \hat{\xi}_1]$ (skew-symmetry)
- (ii) $[\hat{\xi}_1, [\hat{\xi}_2, \hat{\xi}_3]] + [\hat{\xi}_3, [\hat{\xi}_1, \hat{\xi}_2]] + [\hat{\xi}_2, [\hat{\xi}_3, \hat{\xi}_1]] = 0$ (Jacobi's identity)

In both $SE(3)$ and $SO(3)$ cases, the exponential map relates the Lie group with its corresponding Lie algebra. This is in fact true for any Lie group, a result which we will explore further in a later section when we study modelling of constrained rigid motions.

One final remark is that the twist in (2.52) can be rewritten as the sum of two commuting twists, $\hat{\xi} = \hat{\xi}_1 + \hat{\xi}_2$, with

$$\hat{\xi}_1 = \begin{bmatrix} \hat{\omega} & -\omega \times q \\ 0 & 0 \end{bmatrix}, \quad \hat{\xi}_2 = \begin{bmatrix} 0 & h\omega \\ 0 & 0 \end{bmatrix}$$

and $[\hat{\xi}_1, \hat{\xi}_2] = 0$. Thus, we have

$$e^{\hat{\xi}\theta} = e^{\hat{\xi}_1\theta} e^{\hat{\xi}_2\theta}$$

This gives a formal proof of the following classic theorem on rigid body kinematics by Chasles.

Theorem 2.11 (Chasles [10]). *Every rigid body motion can be realized by a rotation about an axis combined with a translation parallel to that axis.*

As mentioned previously, it is important to keep in mind that the exponential of a twist represents the *relative* motion of a rigid body. As a mapping, $\exp(\hat{\xi}\theta)$ takes points from their initial coordinates, $p(0) \in \mathbb{R}^3$, to their coordinates after the rigid motion is applied:

$$p(\theta) = e^{\hat{\xi}\theta} p(0).$$

Both $p(0)$ and $p(\theta)$ are specified with respect to a single reference frame. If a coordinate frame B is attached to a rigid body undergoing a screw motion, the instantaneous configuration of the coordinate frame B , relative to a fixed frame A , is given by

$$g_{ab}(\theta) = e^{\hat{\xi}\theta} g_{ab}(0). \quad (2.54)$$

This transformation can be interpreted as follows: multiplication by $g_{ab}(0)$ maps the coordinates of a point relative to the B frame into A 's coordinates, and the exponential map transforms the point to its final location (still in A coordinates).

Example 2.3. Rotation about a line

Consider the motion of a rigid body rotating about a fixed axis in space, as shown in Figure 2.11. This motion corresponds to a zero-pitch screw about an axis in the $\omega = (0, 0, 1)$ direction passing through the point $q = (0, l_1, 0)$. The corresponding twist is

$$\xi = \begin{bmatrix} -\omega \times q \\ \omega \end{bmatrix} = \begin{bmatrix} l_1 \\ 0 \\ 0 \\ 0 \\ 0 \\ 1 \end{bmatrix}.$$

screws!
Chasles'
theorem
Chasles'
theorem
exponential
map!
as
relative
transformation
rotation about a
line!
as a screw
motion

screws—)
 twists!geometric
 attributes—)
 rigid body
 motion—)

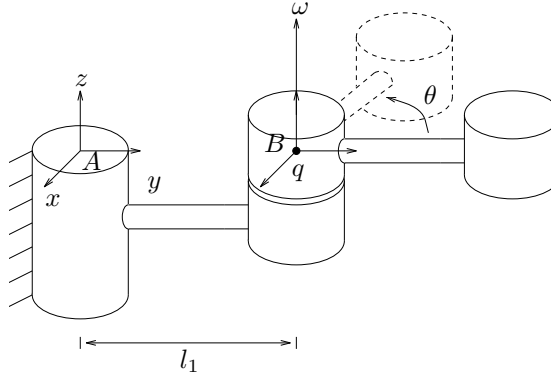


Figure 2.11: Rigid body motion generated by rotation about a fixed axis.

The exponential of this twist is given by

$$e^{\hat{\xi}\theta} = \begin{bmatrix} e^{\hat{\omega}\theta} & (I - e^{\hat{\omega}\theta})(\omega \times v) \\ 0 & 1 \end{bmatrix} = \begin{bmatrix} \cos \theta & -\sin \theta & 0 & l_1 \sin \theta \\ \sin \theta & \cos \theta & 0 & l_1(1 - \cos \theta) \\ 0 & 0 & 1 & 0 \\ 0 & 0 & 0 & 1 \end{bmatrix}.$$

When applied to the homogeneous representation of a point, this matrix maps the coordinates of a point on the rigid body, specified relative to the frame A with $\theta = 0$, to the coordinates of the same point after rotating by θ radians about the axis.

The rigid transformation which maps points in B coordinates to A coordinates—and hence describes the configuration of the rigid body—is given by $g_{ab}(\theta) = \exp(\hat{\xi}\theta)g_{ab}(0)$ where

$$g_{ab}(0) = \begin{bmatrix} I & \begin{bmatrix} 0 \\ l_1 \\ 0 \end{bmatrix} \\ 0 & 1 \end{bmatrix}.$$

Taking the exponential and performing the matrix multiplication yields

$$g_{ab} = \begin{bmatrix} \cos \theta & -\sin \theta & 0 & 0 \\ \sin \theta & \cos \theta & 0 & l_1 \\ 0 & 0 & 1 & 0 \\ 0 & 0 & 0 & 1 \end{bmatrix},$$

which can be verified by inspection.

4 Velocity of a Rigid Body

rotational
velocity—(
spatial frame
body frame

In this section, we derive a formula for the velocity of a rigid body whose motion is given by $g(t)$, a curve parameterized by time t in $SE(3)$. This is not such a naive question as in the case of a single particle following a curve $q(t) \in \mathbb{R}^3$, where the velocity of the particle is $v_q(t) = \frac{d}{dt}q(t)$, because this notion of velocity cannot be generalized since $SE(3)$ is not Euclidean. In particular, the quantity $\dot{g}(t) \notin SE(3)$ and $\dot{g}(t) \notin se(3)$ and the question of its connection with rotational and translational velocity needs to be handled with care. Further, the definition of velocity needs to relate to our informal understanding of rotational and translational velocity. We will show that the proper representation of rigid body velocity is through the use of twists.

4.1 Rotational velocity

Consider first the case of pure rotational motion in \mathbb{R}^3 . Let $R_{ab}(t) \in SO(3)$ be a curve representing a trajectory of an object frame B , with origin at the origin of frame A , but rotating relative to the fixed frame A . We call A the *spatial* coordinate frame and B the *body* coordinate frame.¹ Any point q attached to the rigid body follows a path in spatial coordinates given by

$$q_a(t) = R_{ab}(t)q_b.$$

Note that the coordinates q_b are fixed in the body frame. The velocity of the point in spatial coordinates is

$$v_{q_a}(t) = \frac{d}{dt}q_a(t) = \dot{R}_{ab}(t)q_b. \quad (2.55)$$

Thus \dot{R}_{ab} maps the body coordinates of a point to the spatial velocity of that point.

This representation of the rotational velocity is somewhat inefficient, since it requires

¹The word “spatial” is sometimes used to differentiate between planar motions in \mathbb{R}^2 and general (spatial) motions in \mathbb{R}^3 . In this chapter we reserve the word spatial to mean “relative to a fixed (inertial) coordinate frame.”

rotational
velocity!body
versus spatial
spatial angular
velocity
body angular
velocity

nine numbers to describe the velocity of a rotating body. One may use the special structure in the matrix \dot{R}_{ab} to derive a more compact representation. To this end, we rewrite equation (2.55) as

$$v_{q_a}(t) = \dot{R}_{ab}(t)R_{ab}^{-1}(t)R_{ab}(t)q_b. \quad (2.56)$$

The following lemma shows that $\dot{R}_{ab}(t)R_{ab}^{-1}(t) \in so(3)$; i.e., it is skew-symmetric.

Lemma 2.12. *Given $R(t) \in SO(3)$, the matrices $\dot{R}(t)R^{-1}(t) \in \mathbb{R}^{3 \times 3}$ and $R^{-1}(t)\dot{R}(t) \in \mathbb{R}^{3 \times 3}$ are skew-symmetric.*

Proof. Differentiating the identity

$$R(t)R(t)^T = I$$

we have, dropping the dependence of the matrices on t ,

$$\dot{R}R^T + R\dot{R}^T = 0,$$

so that

$$\dot{R}R^T = -(\dot{R}R^T)^T.$$

Hence, $\dot{R}R^{-1} = \dot{R}R^T$ is a skew-symmetric matrix. The proof that $R^{-1}\dot{R}$ is skew-symmetric follows by differentiating the identity $R^TR = I$. \square

Lemma 2.12 allows us to represent the velocity of a rotating body using a 3-vector. We define the *instantaneous spatial angular velocity*, denoted $\omega_{ab}^s \in \mathbb{R}^3$, as

$$\hat{\omega}_{ab}^s := \dot{R}_{ab}R_{ab}^{-1}. \quad (2.57)$$

The vector ω_{ab}^s corresponds to the instantaneous angular velocity of the object as seen from the spatial (A) coordinate frame. Similarly, we define the *instantaneous body angular velocity*, denoted $\omega_{ab}^b \in \mathbb{R}^3$, as

$$\hat{\omega}_{ab}^b := R_{ab}^{-1}\dot{R}_{ab}. \quad (2.58)$$

The body angular velocity describes the angular velocity as viewed from the instantaneous body (B) coordinate frame. From these two equations, it follows that the relationship between the two angular velocities is

velocity of a point!rotational@ rotational motion

$$\hat{\omega}_{ab}^b = R_{ab}^{-1} \hat{\omega}_{ab}^s R_{ab} \quad \text{or} \quad \omega_{ab}^b = R_{ab}^{-1} \omega_{ab}^s. \quad (2.59)$$

Thus the body angular velocity can be determined from the spatial angular velocity by rotating the angular velocity vector into the instantaneous body frame.

Returning now to equation (2.56), we can express the velocity of a point in terms of the instantaneous angular velocity of the rigid body. Substituting equation (2.57) into equation (2.56),

$$v_{q_a}(t) = \hat{\omega}_{ab}^s R_{ab}(t) q_b = \omega_{ab}^s(t) \times q_a(t). \quad (2.60)$$

Alternatively, using equation (2.59), the velocity of the point in body frame is given by

$$v_{q_b}(t) := R_{ab}^T(t) v_{q_a}(t) = \omega_{ab}^b(t) \times q_b. \quad (2.61)$$

Equations (2.60) and (2.61) constitute a compact description of the velocity of all particles of the body in terms of the body and spatial angular velocities, ω_{ab}^b and ω_{ab}^s .

Example 2.4. Rotational motion of a one degree of freedom manipulator

Consider the motion of the one degree of freedom manipulator shown in Figure 2.12. Let $\theta(t)$ be the angle of rotation about some reference configuration. The trajectory of the manipulator is given by

$$R(t) = \begin{bmatrix} \cos \theta(t) & -\sin \theta(t) & 0 \\ \sin \theta(t) & \cos \theta(t) & 0 \\ 0 & 0 & 1 \end{bmatrix}.$$

The spatial velocity is

$$\hat{\omega}^s = \dot{R} R^T = \begin{bmatrix} -\dot{\theta} \sin \theta & -\dot{\theta} \cos \theta & 0 \\ \dot{\theta} \cos \theta & -\dot{\theta} \sin \theta & 0 \\ 0 & 0 & 0 \end{bmatrix} \begin{bmatrix} \cos \theta & \sin \theta & 0 \\ -\sin \theta & \cos \theta & 0 \\ 0 & 0 & 1 \end{bmatrix} = \begin{bmatrix} 0 & -\dot{\theta} & 0 \\ \dot{\theta} & 0 & 0 \\ 0 & 0 & 0 \end{bmatrix},$$

rotational
velocity—)
rigid body
velocity—(

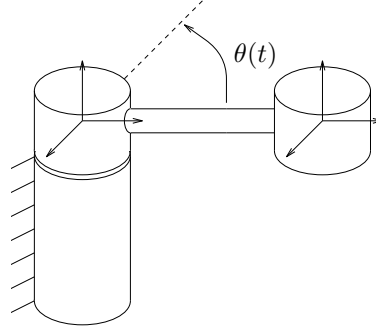


Figure 2.12: Rotational motion of a one degree of freedom manipulator.

hence,

$$\omega^s = \begin{bmatrix} 0 \\ 0 \\ \dot{\theta} \end{bmatrix}.$$

The body velocity is

$$\hat{\omega}^b = R^T \dot{R} = \begin{bmatrix} 0 & -\dot{\theta} & 0 \\ \dot{\theta} & 0 & 0 \\ 0 & 0 & 0 \end{bmatrix} \quad \text{or} \quad \omega^b = \begin{bmatrix} 0 \\ 0 \\ \dot{\theta} \end{bmatrix}.$$

4.2 Rigid body velocity

Let us now consider the general case where $g_{ab}(t) \in SE(3)$ is a one-parameter curve (parameterized by time) representing a trajectory of a rigid body: more specifically, the rigid body motion of the frame B attached to the body, relative to a fixed or inertial frame A . As in the case of rotation, $\dot{g}_{ab}(t)$ by itself is not particularly useful, but the two terms $\dot{g}_{ab}g_{ab}^{-1}$ and $g_{ab}^{-1}\dot{g}_{ab}$ have some special significance. With

$$g_{ab}(t) = \begin{bmatrix} R_{ab}(t) & p_{ab}(t) \\ 0 & 1 \end{bmatrix},$$

we have that

$$\dot{g}_{ab}g_{ab}^{-1} = \begin{bmatrix} \dot{R}_{ab} & \dot{p}_{ab} \\ 0 & 0 \end{bmatrix} \begin{bmatrix} R_{ab}^T & -R_{ab}^T p_{ab} \\ 0 & 1 \end{bmatrix} = \begin{bmatrix} \dot{R}_{ab}R_{ab}^T & -\dot{R}_{ab}R_{ab}^T p_{ab} + \dot{p}_{ab} \\ 0 & 0 \end{bmatrix},$$

which has the form of a twist. By analogy to the rotational velocity, we define the *spatial velocity* $\hat{V}_{ab}^s \in se(3)$ as

spatial velocity
spatial velocity!
geometric interpretation

$$\hat{V}_{ab}^s = \dot{g}_{ab} g_{ab}^{-1} \quad V_{ab}^s = \begin{bmatrix} v_{ab}^s \\ \omega_{ab}^s \end{bmatrix} = \begin{bmatrix} -\dot{R}_{ab} R_{ab}^T p_{ab} + \dot{p}_{ab} \\ (\dot{R}_{ab} R_{ab}^T)^\vee \end{bmatrix}. \quad (2.62)$$

The spatial velocity \hat{V}_{ab}^s can be used to find the velocity of a point in spatial coordinates. The coordinates of a point q attached to the rigid body in spatial coordinates are given by

$$q_a(t) = g_{ab}(t) q_b.$$

Differentiating yields

$$v_{q_a} = \dot{q}_a = \dot{g}_{ab} q_b = \dot{g}_{ab} g_{ab}^{-1} q_a$$

and thus,

$$v_{q_a} = \hat{V}_{ab}^s q_a = \omega_{ab}^s \times q_a + v_{ab}^s. \quad (2.63)$$

The interpretation of the components of the spatial velocity of a rigid motion is somewhat unintuitive. The angular component, ω_{ab}^s , is the instantaneous angular velocity of the body as viewed in the spatial frame. The linear component, v_{ab}^s , is *not the velocity of the origin of the body frame*, which is apparent from equation (2.62). Rather, $v_{ab}^s(t)$ is the velocity of a (possibly imaginary) point on the rigid body which is traveling through the origin of the spatial frame at time t . That is, if one stands at the origin of the spatial frame and measures the instantaneous velocity of a point attached to the rigid body and traveling through the origin at that instant, this is $v_{ab}^s(t)$.

A somewhat more natural interpretation of the spatial velocity is obtained by using the relationship between twists and screws described in the previous section. The screw associated with the twist \hat{V}_{ab}^s gives the instantaneous axis, pitch, and magnitude of the rigid motion relative to the spatial frame.

body velocity
body velocity!
geometric
interpretation

It is also possible to specify the velocity of a rigid body with respect to the (instantaneous) body frame. We define

$$\hat{V}_{ab}^b = g_{ab}^{-1} \dot{g}_{ab} = \begin{bmatrix} R_{ab}^T \dot{R}_{ab} & R_{ab}^T \dot{p}_{ab} \\ 0 & 0 \end{bmatrix} \quad V_{ab}^b = \begin{bmatrix} v_{ab}^b \\ \omega_{ab}^b \end{bmatrix} = \begin{bmatrix} R_{ab}^T \dot{p}_{ab} \\ (R_{ab}^T \dot{R}_{ab})^\vee \end{bmatrix} \quad (2.64)$$

to be the *body velocity* of a rigid motion $g_{ab}(t) \in SE(3)$. The velocity of the point in the body frame is given by

$$v_{q_b} = g_{ab}^{-1} v_{q_a} = g_{ab}^{-1} \dot{g}_{ab} q_b = \hat{V}_{ab}^b(t) q_b.$$

Thus, the action of \hat{V}_{ab}^b is to take the body coordinates of a point, q_b , and return the velocity of that point written in body coordinates, v_{q_b} :

$$v_{q_b} = \hat{V}_{ab}^b q_b = \omega_{ab}^b \times q_b + v_{ab}^b. \quad (2.65)$$

The interpretation of the body velocity is straightforward: v_{ab}^b is the velocity of the origin of the body coordinate frame relative to the spatial frame, as viewed in the current body frame. ω_{ab}^b is the angular velocity of the coordinate frame, also as viewed in the current body frame. Note that the body velocity is *not* the velocity of the body relative to the body frame; this latter quantity is always zero.

The spatial and body velocity of a rigid motion are related by a similarity transformation. To calculate this relationship, we note that

$$\hat{V}_{ab}^s = \dot{g}_{ab} g_{ab}^{-1} = g_{ab} (g_{ab}^{-1} \dot{g}_{ab}) g_{ab}^{-1} = g_{ab} \hat{V}_{ab}^b g_{ab}^{-1}.$$

Alternatively, we can write

$$\begin{aligned} \omega_{ab}^s &= R_{ab} \omega_{ab}^b \\ v_{ab}^s &= -\omega_{ab}^s \times p_{ab} + \dot{p}_{ab} = p_{ab} \times (R_{ab} \omega_{ab}^b) + R_{ab} v_{ab}^b. \end{aligned}$$

In either case, we may summarize the calculation as

$$V_{ab}^s = \begin{bmatrix} v_{ab}^s \\ \omega_{ab}^s \end{bmatrix} = \begin{bmatrix} R_{ab} & \hat{p}_{ab} R_{ab} \\ 0 & R_{ab} \end{bmatrix} \begin{bmatrix} v_{ab}^b \\ \omega_{ab}^b \end{bmatrix}. \quad (2.66)$$

The 6×6 matrix which transforms twists from one coordinate frame to another is referred to as the *adjoint transformation* associated with g , written Ad_g . Thus, given $g \in SE(3)$ which maps one coordinate system into another, $\text{Ad}_g : \mathbb{R}^6 \rightarrow \mathbb{R}^6$ is given as

$$\text{Ad}_g = \begin{bmatrix} R & \hat{p}R \\ 0 & R \end{bmatrix} \quad (2.67)$$

In the calculation that we have just performed, Ad_g maps body velocity twist coordinates to spatial velocity twist coordinates. Ad_g is invertible, and its inverse is given by

$$\text{Ad}_g^{-1} = \begin{bmatrix} R^T & -(R^T p)^\wedge R^T \\ 0 & R^T \end{bmatrix} = \begin{bmatrix} R^T & -R^T \hat{p} \\ 0 & R^T \end{bmatrix} = \text{Ad}_{g^{-1}}$$

(see Exercise 17).

We shall make frequent use of the adjoint transformations throughout the book. The calculations performed above give the following useful characterization of the adjoint associated with a rigid transformation $g \in SE(3)$:

Lemma 2.13. *If $\hat{\xi} \in se(3)$ is a twist with twist coordinates $\xi \in \mathbb{R}^6$, then for any $g \in SE(3)$, $g\hat{\xi}g^{-1}$ is a twist with twist coordinates $\text{Ad}_g \xi \in \mathbb{R}^6$.*

Physically, if ξ is a twist expressed in one coordinate frame, then $\text{Ad}_g \xi$ is the expression of the same twist relative to another coordinate frame displaced by g^{-1} .

It will often be convenient to define velocity without explicit reference to coordinate frames. For a rigid body with configuration $g \in SE(3)$, we define the spatial velocity as

$$\hat{V}^s = \dot{g}g^{-1} \quad V^s = \begin{bmatrix} v^s \\ \omega^s \end{bmatrix} = \begin{bmatrix} -\dot{R}R^T p + \dot{p} \\ (\dot{R}R^T)^\vee \end{bmatrix} \quad (2.68)$$

and the body velocity as

$$\hat{V}^b = g^{-1}\dot{g} \quad V^b = \begin{bmatrix} v^b \\ \omega^b \end{bmatrix} = \begin{bmatrix} R^T \dot{p} \\ (R^T \dot{R})^\vee \end{bmatrix}. \quad (2.69)$$

adjoint
transformation
between
body and
spatial
velocities
body velocity
relationship
with spatial
velocity
spatial velocity
relationship
with body
velocity

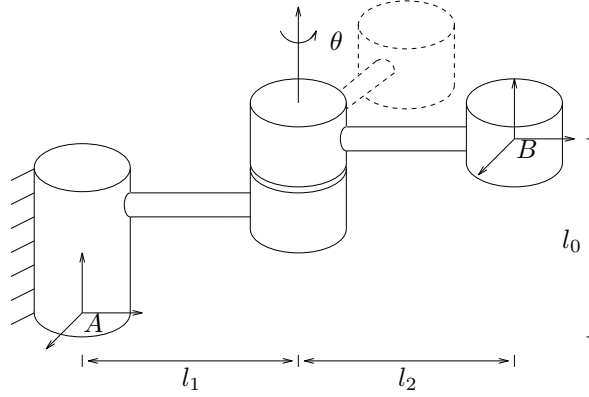


Figure 2.13: Rigid body motion generated by rotation about a fixed axis.

The body and spatial velocities are related by the adjoint transformation,

$$V^s = \text{Ad}_g V^b. \quad (2.70)$$

Example 2.5. One degree of freedom manipulator

Consider the one degree of freedom manipulator shown in Figure 2.13. The configuration of the coordinate frame B relative to the fixed frame A is given by

$$g(t) = \begin{bmatrix} \cos \theta(t) & -\sin \theta(t) & 0 & -l_2 \sin \theta(t) \\ \sin \theta(t) & \cos \theta(t) & 0 & l_1 + l_2 \cos \theta(t) \\ 0 & 0 & 1 & l_0 \\ 0 & 0 & 0 & 1 \end{bmatrix},$$

where we drop all subscripts for simplicity. The spatial velocity of the rotating rigid body is given by

$$V^s = \begin{bmatrix} v^s \\ \omega^s \end{bmatrix} \quad \begin{aligned} v^s &= -\dot{R}R^T p + \dot{p} \\ \omega^s &= (\dot{R}R^T)^\vee. \end{aligned}$$

Using the calculation of ω^s from the previous example, we have

$$v^s = \begin{bmatrix} l_1 \dot{\theta} \\ 0 \\ 0 \end{bmatrix} \quad \omega^s = \begin{bmatrix} 0 \\ 0 \\ \dot{\theta} \end{bmatrix}.$$

Note that v^s is precisely the velocity of a point attached to the rigid body as it travels through the origin of the A coordinate frame.

The body velocity is

$$V^b = \begin{bmatrix} v^b \\ \omega^b \end{bmatrix} \quad \begin{aligned} v^b &= R^T \dot{p} \\ \omega^b &= (R^T \dot{R})^\vee, \end{aligned}$$

which gives

$$v^b = \begin{bmatrix} -l_2 \dot{\theta} \\ 0 \\ 0 \end{bmatrix} \quad \omega^b = \begin{bmatrix} 0 \\ 0 \\ \dot{\theta} \end{bmatrix}.$$

The body velocity can be interpreted by imagining the velocity of the origin of the B coordinate frame, as seen in the B coordinates. Thus, the linear velocity is always in the $-x$ direction and the angular velocity is always in the z direction. The magnitude of the linear component of the velocity is dependent on the length of the link connecting the B frame to the joint.

4.3 Velocity of a screw motion

In the previous example, we calculated the spatial velocity of a rigid motion generated by a screw action, $\exp(\hat{\xi}\theta)$. Referring back to Example 2.3 in the previous section, we see that the spatial velocity V^s in the example above is identical to ξ when $\dot{\theta} = 1$. Consider the more general case where

$$g_{ab}(\theta) = e^{\hat{\xi}\theta} g_{ab}(0)$$

represents the configuration of coordinate frame B relative to frame A . Using the fact that for a constant twist $\hat{\xi}$,

$$\frac{d}{dt} \left(e^{\hat{\xi}\theta} \right) = \hat{\xi} \dot{\theta} e^{\hat{\xi}\theta}$$

velocity!screw@of
a screw
motion
screw mo-
tions!instantaneous
velocity of

coordinate
transforma-
tions!velocities@on
velocities
spatial veloc-
ity!transformation
of
spatial veloc-
ity!addition
of

(see Exercise 9), the spatial velocity for this rigid body motion is

$$\begin{aligned}\widehat{V}_{ab}^s &= \dot{g}_{ab}(\theta)g_{ab}^{-1}(\theta) \\ &= \left(\widehat{\xi}\dot{\theta}e^{\widehat{\xi}\theta}g_{ab}(0)\right)\left(g_{ab}^{-1}(0)e^{-\widehat{\xi}\theta}\right) \\ &= \widehat{\xi}\dot{\theta}.\end{aligned}$$

Thus, the spatial velocity corresponding to this motion is precisely the velocity generated by the screw.

The body velocity of a screw motion can be calculated in a similar manner:

$$\begin{aligned}\widehat{V}_{ab}^b &= g_{ab}^{-1}(\theta)\dot{g}_{ab}(\theta) \\ &= \left(g_{ab}^{-1}(0)e^{-\widehat{\xi}\theta}\right)\left(\widehat{\xi}\dot{\theta}e^{\widehat{\xi}\theta}g_{ab}(0)\right) \\ &= \left(g_{ab}^{-1}(0)\widehat{\xi}g_{ab}(0)\right)\dot{\theta} = \left(\text{Ad}_{g_{ab}^{-1}(0)}\widehat{\xi}\right)^\wedge \dot{\theta}.\end{aligned}$$

For $\dot{\theta} = 1$, \widehat{V}_{ab}^b is a constant vector in the moving body frame. The direction of the body velocity twist is given by the adjoint transformation generated by the initial configuration of the rigid body, $g_{ab}^{-1}(0)$. In particular, if $g_{ab}(0) = I$, i.e., the body frame and spatial frame coincide at $\theta = 0$, then $V_{ab}^s = V_{ab}^b = \widehat{\xi}\dot{\theta}$, where ξ is the constant twist which generates the screw motion.

4.4 Coordinate transformations

Just as we can compose rigid body transformations to find $g_{ac} \in SE(3)$ given $g_{ab}, g_{bc} \in SE(3)$, it is possible to determine the velocity of one coordinate frame relative to a third given the relative velocities between the first and second and second and third coordinate frames. We state the main results as a set of propositions.

Proposition 2.14. Transformation of spatial velocities

Consider the motion of three coordinate frames, A , B , and C . The following relation exists between their spatial velocities:

$$V_{ac}^s = V_{ab}^s + \text{Ad}_{g_{ab}} V_{bc}^s.$$

Proof. The configuration of frame C relative to A is given by

$$g_{ac} = g_{ab}g_{bc}.$$

By definition and the chain rule,

$$\begin{aligned}\hat{V}_{ac}^s &= \dot{g}_{ac}g_{ac}^{-1} \\ &= (\dot{g}_{ab}g_{bc} + g_{ab}\dot{g}_{bc})(g_{bc}^{-1}g_{ab}^{-1}) \\ &= \dot{g}_{ab}g_{ab}^{-1} + g_{ab}(\dot{g}_{bc}g_{bc}^{-1})g_{ab}^{-1} \\ &= \hat{V}_{ab}^s + g_{ab}\hat{V}_{bc}^sg_{ab}^{-1},\end{aligned}$$

and converting to twist coordinates,

$$V_{ac}^s = V_{ab}^s + \text{Ad}_{g_{ab}} V_{bc}^s.$$

□

Proposition 2.15. Transformation of body velocities

Consider motion of three coordinate frames, A , B , and C . The following relation exists between their relative body velocities:

$$V_{ac}^b = \text{Ad}_{g_{bc}^{-1}} V_{ab}^b + V_{bc}^b.$$

Proof. Application of the chain rule, as above. □

Propositions 2.14 and 2.15 are used to transform the velocity of a rigid body between different coordinate frames. Often, two of the coordinate frames are stationary with respect to each other and the velocity relationships can be simplified. As an example, if A and B are two inertial frames which are fixed relative to each other, then the spatial velocity of a frame C satisfies

$$V_{ac}^s = \text{Ad}_{g_{ab}} V_{bc}^s. \quad (2.71)$$

The corresponding relationship for body velocities is

$$V_{ac}^b = V_{bc}^b, \quad (2.72)$$

body veloc-
ity!transformation
and addition
of
adjoint
transforma-
tion!velocities@of
velocities

adjoint
transformation!
twists@of
twists!
transformation
of
coordinate
transformations!
twists@on
twists

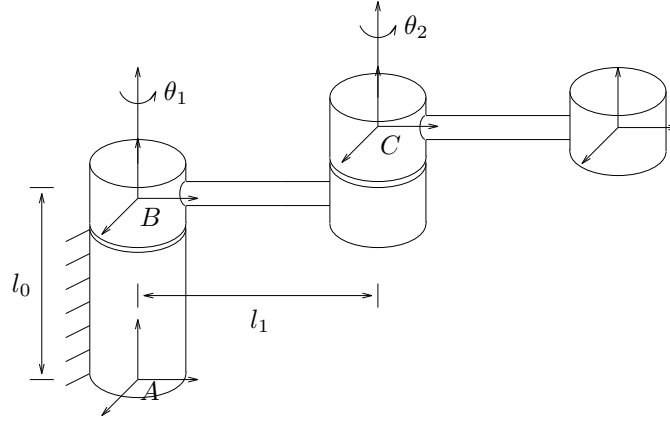


Figure 2.14: Two degree of freedom manipulator.

since the body velocity is independent of the inertial frame with respect to which it is measured.

The transformation rules given by Propositions 2.14 and 2.15 can also be applied to constant twists, such as those used to model revolute and prismatic joints. If ξ is a twist which represents the motion of a screw and we move the screw by applying a rigid body motion $g \in SE(3)$, the new twist can be obtained using equation (2.71). We interpret g as a fixed rigid motion and equate ξ with a spatial velocity vector. In this case, $\dot{g} = 0$ and hence

$$\xi' = \text{Ad}_g \xi \quad \text{or} \quad \hat{\xi}' = g \hat{\xi} g^{-1}. \quad (2.73)$$

This formula is of tremendous importance in the chapters to come, where we will need to keep track of the different twist axes corresponding to the joints of a robot when they are moved.

Example 2.6. Velocity of a two-link mechanism

Consider the two degree of freedom manipulator shown in Figure 2.14. We wish to find the velocity of frame C relative to A , given the joint velocities $\dot{\theta}_1, \dot{\theta}_2 \in \mathbb{R}$. Since

each motion is a screw motion, we write

$$\begin{aligned} V_{ab}^s &= \begin{bmatrix} v_{ab} \\ \omega_{ab} \end{bmatrix} \dot{\theta}_1 & v_{ab} &= \begin{bmatrix} 0 \\ 0 \\ 0 \end{bmatrix} & \omega_{ab} &= \begin{bmatrix} 0 \\ 0 \\ 1 \end{bmatrix}, \\ V_{bc}^s &= \begin{bmatrix} v_{bc} \\ \omega_{bc} \end{bmatrix} \dot{\theta}_2 & v_{bc} &= \begin{bmatrix} l_1 \\ 0 \\ 0 \end{bmatrix} & \omega_{bc} &= \begin{bmatrix} 0 \\ 0 \\ 1 \end{bmatrix}. \end{aligned}$$

body velocity
relationship
with spatial
velocity
spatial velocity
relationship
with body
velocity
rigid body
velocity—)

We also calculate $\text{Ad}_{g_{ab}}$:

$$\text{Ad}_{g_{ab}} = \begin{bmatrix} R_{ab} & \left(\begin{smallmatrix} 0 \\ 0 \\ l_0 \end{smallmatrix} \right)^\wedge R_{ab} \\ 0 & R_{ab} \end{bmatrix}.$$

Using Proposition 2.14,

$$V_{ac}^s = V_{ab}^s + \text{Ad}_{g_{ab}} V_{bc}^s = \begin{bmatrix} 0 \\ 0 \\ 0 \\ 0 \\ 0 \\ 1 \end{bmatrix} \dot{\theta}_1 + \begin{bmatrix} l_1 \cos \theta_1 \\ l_1 \sin \theta_1 \\ 0 \\ 0 \\ 0 \\ 1 \end{bmatrix} \dot{\theta}_2.$$

Note that the velocity consists of two components, one from each of the joints, and that they add together linearly.

A few other identities between body and spatial velocities will prove useful in subsequent chapters. We give them here in the form of a lemma. Their proof is left as an exercise.

Lemma 2.16. Rigid body velocity identities

Using the notation given above for the velocity of one coordinate frame relative to another, the following relationships hold:

$$\begin{aligned} V_{ab}^b &= -V_{ba}^s \\ V_{ab}^b &= -\text{Ad}_{g_{ba}} V_{ba}^b. \end{aligned}$$

5 Wrenches and Reciprocal Screws

In this section we consider forces and moments acting on rigid bodies and use this to introduce the notion of screw systems and reciprocal screws.

wrenches—(work, between twist and wrench equivalent wrenches transformation of

5.1 Wrenches

A generalized force acting on a rigid body consists of a linear component (pure force) and an angular component (pure moment) acting at a point. We can represent this generalized force as a vector in \mathbb{R}^6 :

$$F = \begin{bmatrix} f \\ \tau \end{bmatrix} \quad \begin{array}{ll} f \in \mathbb{R}^3 & \text{linear component} \\ \tau \in \mathbb{R}^3 & \text{rotational component} \end{array}$$

We will refer to a force/moment pair as a *wrench*.

The values of the wrench vector $F \in \mathbb{R}^6$ depend on the coordinate frame in which the force and moment are represented. If B is a coordinate frame attached to a rigid body, then we write $F_b = (f_b, \tau_b)$ for a wrench applied at the origin of B , with f_b and τ_b specified with respect to the B coordinate frame.

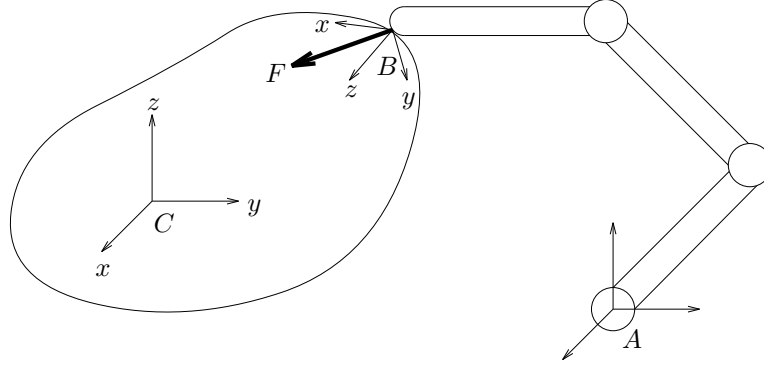
Wrenches combine naturally with twists to define instantaneous work. Consider the motion of a rigid body parameterized by $g_{ab}(t)$, where A is an inertial frame and B is a frame attached to the rigid body. Let $V_{ab}^b \in \mathbb{R}^6$ represent the instantaneous body velocity of the rigid body and let F_b represent an applied wrench. Both of these quantities are represented relative to the B coordinate frame and their dot product is the infinitesimal work:

$$\delta W = V_{ab}^b \cdot F_b = (v \cdot f + \omega \cdot \tau).$$

The net work generated by applying the wrench F_b through a twist V_{ab}^b over a time interval $[t_1, t_2]$ is given by

$$W = \int_{t_1}^{t_2} V_{ab}^b \cdot F_b dt.$$

Two wrenches are said to be *equivalent* if they generate the same work for every possible rigid body motion. Equivalent wrenches can be used to rewrite a given wrench in terms of a wrench applied at a different point (and with respect to a different coordinate frame). An example of this is shown in Figure 2.15: given the wrench F_b applied at the origin of contact coordinate frame B , we wish to determine



coordinate
transformations!
wrenches@of
wrenches
adjoint
transforma-
tion!
wrenches@of
wrenches

Figure 2.15: Transformation of wrenches between coordinate frames.

the equivalent wrench applied at the origin of the object coordinate frame C . In order to compute the equivalent wrench, we use the instantaneous work performed by the wrench as the body undergoes an arbitrary rigid motion. Let $g_{bc} = (p_{bc}, R_{bc})$ be the configuration of frame C relative to B . By equating the instantaneous work done by the wrench F_b and the wrench F_c over an arbitrary interval of time, we have that

$$V_{ac}^b \cdot F_c = V_{ab}^b \cdot F_b = \left(\text{Ad}_{g_{bc}} V_{ac}^b \right)^T F_b = V_{ac}^b \cdot \text{Ad}_{g_{bc}}^T F_b,$$

and since V_{ac}^b is free,

$$F_c = \text{Ad}_{g_{bc}}^T F_b. \quad (2.74)$$

Equation (2.74) transforms a wrench applied at the origin of the B frame into an equivalent wrench applied at the origin of the C frame. The components of F_c are specified relative to the C coordinate frame. Expanding equation (2.74),

$$\begin{bmatrix} f_c \\ \tau_c \end{bmatrix} = \begin{bmatrix} R_{bc}^T & 0 \\ -R_{bc}^T \hat{p}_{bc} & R_{bc}^T \end{bmatrix} \begin{bmatrix} f_b \\ \tau_b \end{bmatrix}, \quad (2.75)$$

we see that the adjoint transformation rotates the force and torque vectors from the B frame into the C frame and includes an additional torque of the form $-p_{bc} \times f_b$, which is the torque generated by applying a force f_b at a distance $-p_{bc}$.

wrenches!addition
of
wrenches!body
and spatial
representations
body wrench
spatial wrench

It is also possible to represent a wrench with respect to a coordinate frame which is not inside the rigid body. Consider for example the coordinate frame A shown in Figure 2.15. The wrench F written in A 's coordinate frame is given by

$$F_a = \text{Ad}_{g_{ba}}^T F_b.$$

This wrench represents the equivalent force/moment pair applied as if the coordinate frame A were rigidly attached to the object. This is *not* the same as simply rewriting the components of F_b in A 's coordinates, since the point of application for F_a is the origin of the A frame and not the origin of the B frame.

If several wrenches are all applied to a single rigid body, then the net wrench acting on the rigid body can be constructed by adding the wrench vectors. In order for this addition to make sense, all of the wrenches must be represented with respect to the same frame. Thus, given a set of wrenches F_i , each wrench is first written as an equivalent wrench relative to a single coordinate frame and then the equivalent wrenches are added to determine the net wrench acting on the rigid body. This helps explain why equivalent wrenches include a shift of origin: one can only add wrenches if they represent forces and torques applied at a single point (such as the center of mass or a fixed spatial frame).

A net wrench F acting on a rigid body with configuration $g_{ab} \in SE(3)$ has two natural representations. The *body* representation of the wrench is written as F_b and represents the equivalent force and moment applied at the origin of the B frame (and written in B 's coordinates). The *spatial* representation of the wrench is the equivalent wrench written in A 's coordinate frame. These representations are analogous to the spatial and body representations of the velocity of a rigid body.

As with velocities, it will be convenient to define the spatial and body representations of a wrench without explicit reference to a given set of coordinate frames. If $g \in SE(3)$ is the configuration of a rigid body, then we write F^b for the body wrench and F^s for the spatial wrench. These wrenches are related by the transpose of the

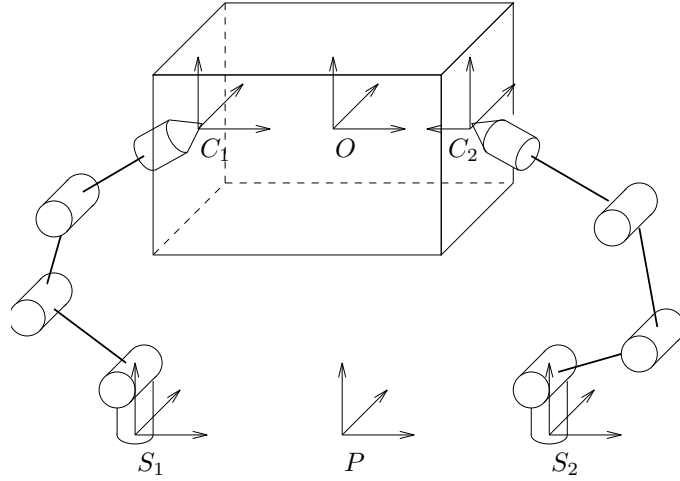


Figure 2.16: Coordinate frames for a simple grasping example.

adjoint matrix:

$$F^b = \text{Ad}_g^T F^s. \quad (2.76)$$

This notation mirrors that used for body and spatial velocities of a rigid body allowing the instantaneous work performed by a wrench F moving through a rigid motion with instantaneous velocity V to be written as

$$\delta W = V^b \cdot F^b = V^s \cdot F^s.$$

We leave the proof of this statement as an exercise.

Example 2.7. Preview of multifingered grasping

Consider the multifingered grasp shown in Figure 2.16. Let F_{C_i} be the wrench exerted by the i^{th} finger on the grasped object, represented in the frame C_i . The net wrench on the body, in the body coordinate frame O , is given by

$$F_o = \sum \text{Ad}_{g_{oc_i}}^T F_{C_i}.$$

This is the basic calculation which is used in grasping to determine the net effect of forces applied at the contact points between the fingers and the object.

adjoint
transformation
of wrenches

wrenches!screw
coordinates of
screws!associated
with wrenches
Poinsot's
theorem
Poinsot's
theorem

5.2 Screw coordinates for a wrench

As with twists, it is possible to generate a wrench by applying a force along an axis in space and simultaneously applying a torque about the same axis. The dual of Chasles' theorem, which showed that *every* twist could be generated by a screw, is called *Poinsot's theorem* [56]. It asserts that every wrench is equivalent to a force and torque applied along the same axis. We begin by defining the notion of a wrench acting along a screw.

With respect to some fixed spatial coordinate frame A , let S be a screw with axis $l = \{q + \lambda\omega : \lambda \in \mathbb{R}\}$, $\|\omega\| = 1$, pitch h , and magnitude M . We construct a wrench from this screw by applying a force of magnitude M along the directed line l and a torque of magnitude hM about the line. If $h = \infty$, we generate a wrench by applying a pure torque about l . The resulting wrench, in A 's coordinates, is given by

$$\begin{aligned} F &= M \begin{bmatrix} \omega \\ -\omega \times q + h\omega \end{bmatrix} & h \text{ finite} \\ F &= M \begin{bmatrix} 0 \\ \omega \end{bmatrix} & h = \infty, \end{aligned} \tag{2.77}$$

where the term $-\omega \times q$ accounts for the offset between the axis of the screw and the origin of A . We call F the *wrench along the screw* S . Note that F (and q and ω) are all specified with respect to the fixed coordinate frame A and hence F represents the spatial wrench applied to the rigid body. (We omit the use of subscripts in this section since all quantities are specified with respect to a single coordinate frame.)

To find the screw coordinates for a wrench, we solve equation (2.77) for ω , q , h , and M given $F = (f, \tau)$. This leads to the following theorem:

Theorem 2.17 (Poinsot [56]). *Every collection of wrenches applied to a rigid body is equivalent to a force applied along a fixed axis plus a torque about the same axis.*

Proof. The proof is constructive. Let $F = (f, \tau)$ be the net wrench applied to the object. We ignore the trivial case, $F = 0$. pitch of a wrench
axis of a wrench

Case 1: ($f = 0$, pure torque). Set $M = \|\tau\|$, $\omega = \tau/M$, and $h = \infty$. Equation (2.77) verifies that these are the appropriate screw coordinates.

Case 2: ($f \neq 0$). Set $M = \|f\|$, and $\omega = f/M$. It remains to solve

$$M(q \times \omega + h\omega) = \tau$$

for q and h . One solution is given by

$$h = \frac{f^T \tau}{\|f\|^2} \quad q = \frac{f \times \tau}{\|f\|^2}.$$

This solution is not unique since any $q' = q + \lambda\omega$ will also satisfy equation (2.77).

□

Using Poincot's theorem, we can define the screw coordinates of a wrench, $F = (f, \tau)$:

1. *Pitch:*

$$h = \frac{f^T \tau}{\|f\|^2} \tag{2.78}$$

The pitch of a wrench is the ratio of angular torque to linear force. If $f = 0$, we say that F has infinite pitch.

2. *Axis:*

$$l = \begin{cases} \left\{ \frac{f \times \tau}{\|f\|^2} + \lambda f : \lambda \in \mathbb{R} \right\}, & \text{if } f \neq 0 \\ \{0 + \lambda \tau : \lambda \in \mathbb{R}\}, & \text{if } f = 0 \end{cases} \tag{2.79}$$

The axis l is a directed line through a point. For $f \neq 0$, the axis is a line in the f direction going through the point $q = \frac{f \times \tau}{\|f\|^2}$. For $f = 0$, the axis is a line in the τ direction going through the origin.

magnitude of a
wrench
zero pitch screw
wrenches—)
reciprocal
screws—(
wrenches!reciprocal
to a twist
twists!reciprocal
to a wrench
reciprocal
screws!definition
reciprocal
product

3. *Magnitude:*

$$M = \begin{cases} \|f\|, & \text{if } f \neq 0 \\ \|\tau\|, & \text{if } f = 0 \end{cases} \quad (2.80)$$

The magnitude of a screw is the net linear force, if the motion contains a linear component, or the net torque, otherwise.

The dual nature of twists and wrenches is evident in the screw coordinates for twists and wrenches. For example, a zero pitch twist corresponds to pure rotation, while a zero pitch wrench corresponds to a pure force (no angular component).

5.3 Reciprocal screws

The dot product between twists and wrenches gives the instantaneous power associated with moving a rigid body through an applied force. As in the previous subsection, we carry out all calculations relative to a single coordinate frame and omit the use of subscripts. A wrench F is said to be *reciprocal* to a twist V if the instantaneous power is zero: $F \cdot V = 0$. Since both twists and wrenches can be represented by screws, we can use this to define the notion of reciprocal screws:

Definition 2.3. Reciprocal screws

Two screws S_1 and S_2 are *reciprocal* if the twist V about S_1 and the wrench F along S_2 are reciprocal.

Classically, reciprocal screws are defined by using the *reciprocal product* between screws. Let S_i be a screw with axis $l_i = \{q_i + \lambda\omega_i : \lambda \in \mathbb{R}\}$, pitch h_i , and magnitude M_i . Given two screws S_1 and S_2 , we define the distance d between the screws as the minimum distance between l_1 and l_2 ; this distance will be achieved along a line perpendicular to both l_1 and l_2 . We denote this line as dn where n is a unit vector and $d > 0$. The angle α between S_1 and S_2 is the angle between the vectors ω_1 and ω_2 ,

$$\alpha = \text{atan2}(\omega_1 \times \omega_2 \cdot n, \omega_1 \cdot \omega_2)$$

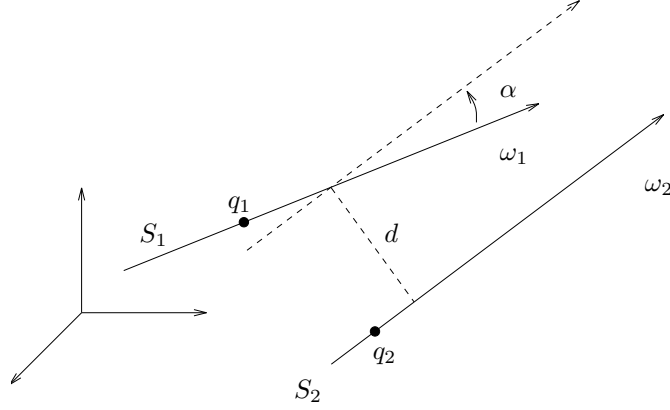


Figure 2.17: Notation for reciprocal screws.

(see Figure 2.17). The reciprocal product between two screws is defined as

$$S_1 \odot S_2 = M_1 M_2 ((h_1 + h_2) \cos \alpha - d \sin \alpha). \quad (2.81)$$

Proposition 2.18. Characterization of reciprocal screws

Two screws S_1 and S_2 are reciprocal if and only if

$$S_1 \odot S_2 = 0.$$

Proof. We consider only the case where h_1 and h_2 are finite. The other cases are left as exercises. Let V be the twist about the screw S_1 and F be the wrench along the screw S_2 :

$$V = M_1 \begin{bmatrix} q_1 \times \omega_1 + h_1 \omega_1 \\ \omega_1 \end{bmatrix} \quad F = M_2 \begin{bmatrix} \omega_2 \\ q_2 \times \omega_2 + h_2 \omega_2 \end{bmatrix}.$$

Without loss of generality we can assume that q_1 and q_2 are the points at which the axes are closest and hence q_2 can be rewritten as $q_2 = q_1 + dn$ where n is the unit normal vector connecting the two axes. The instantaneous work between V and F is

$$\begin{aligned} V \cdot F &= M_1 M_2 (\omega_2 \cdot (q_1 \times \omega_1 + h_1 \omega_1) + \omega_1 \cdot (q_2 \times \omega_2 + h_2 \omega_2)) \\ &= M_1 M_2 (\omega_2 \cdot q_1 \times \omega_1 + h_1 \omega_1 \cdot \omega_2 + \omega_1 \cdot (q_1 + dn) \times \omega_2 + h_2 \omega_1 \cdot \omega_2) \\ &= M_1 M_2 ((h_1 + h_2) \cos \alpha - d \sin \alpha), \end{aligned}$$

reciprocal
screws!use in
analyzing
mechanisms
screw system

which is precisely the reciprocal product. Hence, by definition, the screws are reciprocal if and only if the reciprocal product is zero. \square

If we represent screws using twist coordinates, then we can define the reciprocal product directly in terms of the components of the twists. Let $V_1, V_2 \in \mathbb{R}^6$ be two arbitrary twists. Then we define the reciprocal product between V_1 and V_2 as

$$V_1 \odot V_2 = v_1^T \omega_2 + v_2^T \omega_1.$$

A similar relationship holds if we associate screws with wrenches.

Reciprocal screws play an important role in analyzing the kinematic properties of mechanisms. For example, in a grasping context we can view the wrenches applied to an object as a set of constraining screws and ask if there are any instantaneous rigid motions (twists) that do not violate the constraints. Such twists, if they exist, correspond to motions of the grasped object which cannot be restricted by the fingers. This specific situation is considered in detail in Chapter 5, but we can give some preliminary indications of how the analysis might proceed using the concept of a system of screws.

As a motivating example, consider the grasping situation depicted in Figure 2.18. Suppose we constrain the motion of a rigid body by applying normal forces at several points around the rigid body. We would like to ascertain if there are any motions of the rigid body which cannot be resisted by these forces. Let $\{S_1, \dots, S_k\}$ represent the screws corresponding to the wrenches. Suppose that there exists another screw S_f such that $S_f \odot S_i = 0$. Then, interpreting S_f as a twist and each S_i as a wrench, we see that motion along S_f causes no work to be performed against any of the wrenches. Hence, the wrenches cannot resist this type of motion and the object is free to move (instantaneously) along S_f .

If we interpret a set of screws $\{S_1, \dots, S_k\}$ as twists, then the twists form a linear space over the reals and hence we can talk about scaling and adding screws by interpreting this in terms of regular addition and multiplication on twists. We

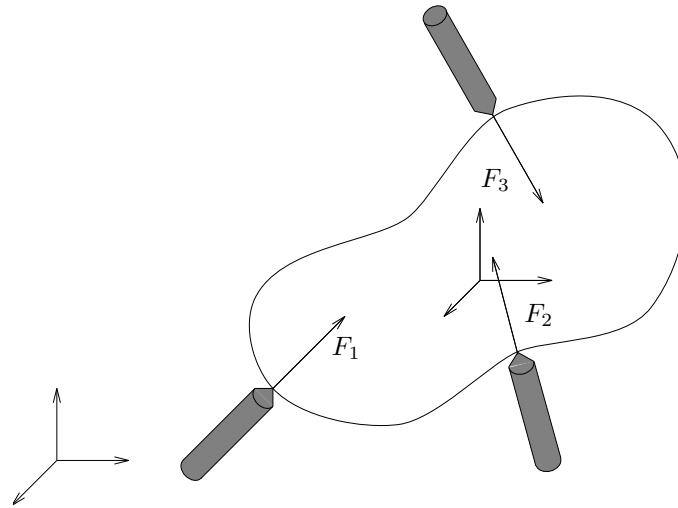


Figure 2.18: A set of pure forces acting on a rigid body.

reciprocal
screws!systems
of
reciprocal
screws!use in
analyzing
mechanisms

call the set of screws $\{S_1, \dots, S_k\}$ a *system of screws* and we define addition and scaling of screws by associating each screw with a unique twist.

It follows immediately from the definition of the reciprocal product that if S is reciprocal to S_1 and S_2 , then it is reciprocal to any linear combination of S_1 and S_2 (with the linear combination performed in twist coordinates). Using this linearity property, we can define the set of all screws which are reciprocal to a given system of screws as the *reciprocal screw system*. A reciprocal screw system defines a linear subspace of twists. If we interpret a screw system as a set of wrenches (or constrained directions), then the reciprocal screw system describes the instantaneous motions which are possible under the constraints. Conversely, if we interpret the screw system as a set of twists, then the reciprocal screw system is the set of wrenches which cause no net motion of the object. Both of these interpretations follow directly from the definition of the reciprocal product between a twist and a wrench.

In addition to applications in grasping, screw systems and reciprocal screw systems can be also used to analyze the mobility of mechanisms, as we shall see in

detail in the next chapter. The following proposition is one of the main tools in this type of analysis. Its proof follows directly from the fact that the space of twists is a 6-dimensional linear space and that screws can be naturally associated with this linear space.

Proposition 2.19. Dimensionality of reciprocal screw systems

Let r be the dimension of system of screws $\{S_1, \dots, S_k\}$ (determined by converting the screws into either twists or wrenches) and let n be the dimension of the corresponding reciprocal system. Then,

$$r + n = 6.$$

Applying this proposition to the example in Figure 2.18, we see that the subspace of twists which cannot be resisted is at least 3-dimensional. It may have greater dimension if the applied normal forces do not generate independent wrenches.

6 Constrained Rigid Motions

In the previous sections, we used $SE(3)$ to model the configuration space of a *free* rigid body. In robotics, however, most rigid motions we deal with are *constrained*, e.g., relative motions between two adjacent links of a manipulator, coupled through a revolute or a prismatic joint, and the end-effector motions of a manipulator when it performs an assembly task. In this section, we will develop models for certain types of constrained rigid motions using subgroups and submanifolds of $SE(3)$.

In classic mechanics literature, a constraint is said to be *scleronomic* if the constraint equation does not contain the time as an explicit variable and *rheonomic* otherwise. A scleronomic constraint is further classified as *holonomic* if it can be expressed as a function of the form

$$f : Q \rightarrow \mathbb{R}^m : q \mapsto f(q) = 0 \quad (2.82)$$

where Q is the configuration space of the free system, and *nonholonomic* otherwise. We will leave the treatment of nonholonomic constraint to a later chapter and study, in this section, rigid motions subject to holonomic constraints.

The set $H := f^{-1}(0) \subset SE(3)$ is referred to as the configuration space of the *constrained rigid body or system*. If the constraint is linearly independent (see Appendix A for more details), then H is well-behaved in the sense that it constitutes a smooth submanifold of $SE(3)$. In many cases, H could even have additional structures such as that of a Lie subgroup of $SE(3)$. Roughly speaking, if H is an algebraic subgroup of $SE(3)$, i.e., closed under the group multiplication, and a closed subset, then H is a Lie subgroup of $SE(3)$.

6.1 Subgroup Motions

We list some well known examples of Lie subgroups of $SE(3)$. Later, we classify all of its Lie subgroups, which will be used as model spaces or for mechanism synthesis.

Example 6.1. One-dimensional Lie subgroups

Fix $\hat{\xi} \in se(3)$, then

$$H = \{e^{\hat{\xi}\theta} \mid \theta \in \mathbb{R}\}$$

is a Lie subgroup of $SE(3)$, known as an one-parameter subgroup generated by $\hat{\xi}$. More specifically, for $\xi = (z, 0)$, $H = T(z)$ represents the set of translational motions along the z -axis direction, for $\xi = (0, z)$, $H = R(o, z)$ the set of rotational motions about the z -axis, and for $\xi = (-q \times z + \rho z, z)$, $H = H_\rho(q, z)$ the set of helical (or screw) motions of pitch ρ about the axis passing through q and in the direction z .

Example 6.2. Two-dimensional Lie subgroups

$$T_2(z) = T(x)T(y)$$

and

$$C(z) = T(z)R(o, z)$$

are referred to, respectively, as the planar translational subgroup about the xy -plane and the cylindrical subgroup about the z -axis. The order of the product in the above definitions is immaterial because $T(z)$ is invariant under rotations about the z -axis with $R^{-1}(0, z)T(z)R(o, z) = T(z)$.

Example 6.3. Three-dimensional Lie subgroups

$$T(3) = T_2(z)T(z)$$

$$PL(z) = T_2(z)R(o, z)$$

$$Y_\rho(z) = T_2(z)H_\rho(o, z)$$

are referred to, respectively, as the spatial translational subgroup, the group of planar rigid motions about the xy -plane and the group of planar translations about the xy -plane and helical motions (of pitch ρ) along the z -axis. Note again that the order of the product in the definition of $PL(z)$ is immaterial since $T_2(z)$ is invariant with respect to $R(0, z)$. A similar property holds for $Y_\rho(z)$ and $T(3)$ as well. Another 3-dimensional subgroup is obtained by embedding $SO(3)$ in $SE(3)$,

$$S(o) = \left\{ \begin{bmatrix} R & 0 \\ 0 & 1 \end{bmatrix} \mid R \in SO(3) \right\}$$

which is characterized as the set of rotations about the origin point o .

Example 6.4. Four-dimensional Lie subgroup

$$X(z) = T(3)R(o, z)$$

that consists of spatial translations and rotations about the z -axis is referred to as the Schonflies group. It can be expressed in more than one ways as the products of two Lie subgroups such as $T(3)H_\rho(o, z)$, $T(z)PL(z)$ and $T_2(z)C(z)$.

There is no five-dimensional Lie subgroup of $SE(3)$.

Given a Lie subgroup $H \subset SE(3)$, let $h(t) \in H, t \in (-\epsilon, \epsilon)$, be a curve such that $h(0) = e$. Then, $\hat{\xi} = \frac{d}{dt} |_{t=0} h(t)$ is a velocity vector tangent to H at e , and the set of all such tangent vectors forms a linear space, known as the Lie algebra \mathfrak{h} of H . It is not difficult to see that \mathfrak{h} is closed under the Lie bracket operation (2.53) (Exercise 23) and is thus referred to as a Lie subalgebra of $se(3)$.

Example 6.5. Lie algebras of Lie subgroups

Let $\{e_i\}_{i=1}^6 \in \mathbb{R}^6$ be the canonical basis of \mathbb{R}^6 , i.e., e_i has an 1 in the i^{th} entry and 0 otherwise. The Lie algebra of $T(3), S(o)$ and $X(z)$ are given by, respectively, $t(3) = \{\hat{e}_1, \hat{e}_2, \hat{e}_3\}$, $s(o) = \{\hat{e}_4, \hat{e}_5, \hat{e}_6\}$ and $x(z) = \{\hat{e}_1, \hat{e}_2, \hat{e}_3, \hat{e}_6\}$, where $\{\hat{e}_i, \hat{e}_j\}$ denotes the span of \hat{e}_i and \hat{e}_j .

The exponential map

$$\exp : se(3) \longrightarrow SE(3),$$

when restricted to \mathfrak{h} , takes a neighborhood of 0 in \mathfrak{h} diffeomorphically to a neighborhood of the identity in H . In particular, let $\{\hat{\xi}_i\}_{i=1}^k$ be a basis of \mathfrak{h} , and $g \in H$ near the identity. Then, there exist unique $\alpha, \beta \in \mathbb{R}^k$ such that

$$g = e^{\alpha_1 \hat{\xi}_1 + \dots + \alpha_k \hat{\xi}_k}$$

and

$$g = e^{\beta_1 \hat{\xi}_1} \dots e^{\beta_k \hat{\xi}_k}.$$

$\alpha \in \mathbb{R}^k$ is referred to as the *canonical coordinates of the first kind* and $\beta \in \mathbb{R}^k$ the *canonical coordinates of the second kind*.

Let $H \subset SE(3)$ be a Lie subgroup, and $g \in SE(3)$. The conjugate subgroup of H , denoted $I_g(H)$, is the Lie subgroup

$$I_g(H) = \{ghg^{-1} \mid h \in H\}.$$

Two subgroups H_1 and H_2 are said to belong to the same conjugacy class if they are conjugate to each other. In this case, their Lie algebras are related by the adjoint transformation $\mathfrak{h}_1 = \text{Ad}_g(\mathfrak{h}_2)$.

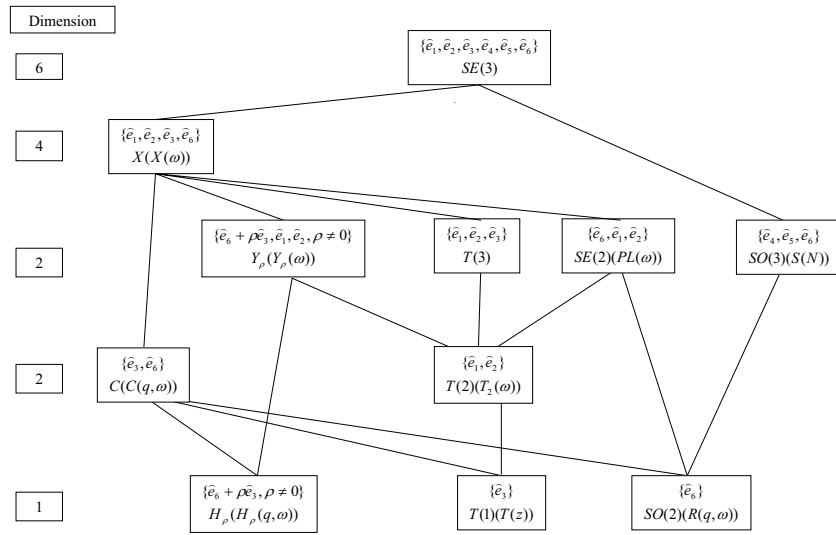
Example 6.6. Let $H = \{e^{\hat{\xi}\theta} \mid \theta \in \mathbb{R}\}$ be an one-parameter subgroup of screw motions about the axis of $\hat{\xi} \in \mathfrak{se}(3)$. Then,

$$I_g(H) = \{e^{(\text{Ad}_{g_0}\hat{\xi})^\wedge\theta} \mid \theta \in \mathbb{R}\}$$

corresponds to the one-parameter subgroup of screw motions about a displaced twist axis $(\text{Ad}_{g_0}\hat{\xi})^\wedge \in \mathfrak{se}(3)$. Since the pitch of a twist is Ad_g -invariant (see Exercise 16), screw motions with the same pitch belong to the same conjugacy class. For instance, the conjugate subgroups of $T(z)$, $R(o, z)$ and $H_\rho(o, z)$ are, respectively, of the form $T(v)$, $R(p, v)$ and $H_\rho(p, v)$ for arbitrary $p, v \in \mathbb{R}^3$. We will denote by T (or $T(1)$), R (or $SO(2)$) and H_ρ the conjugacy class of these subgroups and refer to $T(z)$, $R(o, z)$ and $H_\rho(o, z)$, respectively, their the *normal form subgroup*.

Example 6.7. The conjugate subgroups of $C(o, z)$, $PL(z)$ and $S(o)$ are, respectively, of the form $C(p, v)$, $PL(v)$ and $S(p)$ for arbitrary $p, v \in \mathbb{R}^3$. The conjugacy classes of these subgroups are denoted by C , $SE(2)$ and $SO(3)$, respectively.

It is interesting to classify, *up to a conjugation*, all Lie subgroups of $SE(3)$. This is achieved by first classifying all Lie subalgebras of $\mathfrak{se}(3)$ (see Exercise 23) and then applying the exponential map to the results. Figure 2.19 displays the classification results, with 10 types of proper Lie subgroups of $SE(3)$ identified. The Lie algebra that generates the normal form subgroup is shown in the upper part of each box. The conjugacy class together with a generic element enclosed in the parenthesis are shown in the lower part of the box. A line between two subgroups indicates an inclusion relation when both subgroups are in their normal form or obtained with the same conjugation action applied, i.e., $H_\rho(p, \omega) \subset Y_\rho(\omega) \subset X(\omega)$.

Figure 2.19: A classification of Lie subgroups of $SE(3)$

Subgroups:			Submanifolds:	
DoF	Notation	Description	Notation	Applications
1	T	Prismatic joint	P_a	Parallelogram joint
	R	Revolute joint		
	H_ρ	Helical joint		
2	T_2	Planar translation	$R(o, z)T(x)$	
	C	Cylindrical motion	$U(o, x, y)$	Pan-tilting motion
3	$T(3)$	Spatial translation	$T(z)U(o, x, y)$	Z3 spindle module
	$SE(2)$	Planar rigid motion	$U(o, x, y)T(z)$	Telescopic leg
	$SO(3)$	Rotational motions	$R(o, z)T_2(y)$	Wafer handling
4	X	SCARA motion	$T_2(z)U(o, x, y)$	Haptic device
			$T(z)S(o)$	Helicopter simulator
5			$T(3)U(o, x, y)$	5-axis machining
			$T_2(z)S(o)$	

Table 2.1: Model spaces by Lie subgroups and submanifolds of $SE(3)$

The three 1-dimensional subgroups, R, T and H_ρ are used to model, respectively, rigid motions generated by a revolute, a prismatic and a helical joint of pitch ρ . These joints are collectively referred to as lower pairs by Reuleaux. Other lower pairs include the cylindrical subgroup C , the planar subgroup $SE(2)$ and the rotation subgroup $SO(3)$. The subgroups $T(2), T(3)$, $SO(3)$, $SE(2)$ and X are used to model end-effector motions of manipulators having less than 6 degrees of freedom. For example, $T(3)$ is used to model purely translational manipulators, X the SCARA type of manipulators and $SO(3)$ orientational type of manipulators. These manipulators are sometimes referred to as *lower-mobility* manipulators. The subgroup Y_ρ is less often used as a model space but often finds its applications in parallel manipulator synthesis.

The left column of Table 2.1 summarizes joint and end-effector motions of commonly used robotic manipulators modeled by Lie subgroups of $SE(3)$.

6.2 Submanifold Motions

While Lie subgroups provide an important class of model spaces for robotic manipulators, there are important exceptions which defy such a modeling. For example, end-effector motions of a five degree of freedom manipulator or a five-axis machine tool could not be modeled by a Lie subgroup, as such a subgroup does not exist at all. Neither could the set of rigid motions generated by the plane-hinged parallelogram joint shown in Figure 2.20, or other composite joints. In these cases, there is a need to broaden the class of modeling spaces to include submanifolds of $SE(3)$.

There are three types of submanifolds: immersed, embedded and regular, with the last being the most natural and most important. We will use *regular submanifolds* as our extended model spaces to complement that of Lie subgroups.

Example 6.8. A plane-hinged parallelogram is a four-bar mechanism in which the opposing links have the same length, see Figure 2.20. It can be considered as a composite joint, and is widely used in design of parallel manipulators such as the Delta robots. Let ω be the unit vector normal to the parallelogram, and \mathbf{v} the vector of link 2 or 4 at the home or reference configuration, then the set of rigid motions generated by a parallelogram has the form

$$P_a(\omega, \mathbf{v}) = \left\{ \begin{bmatrix} I & (e^{\hat{\omega}\theta} - I)\mathbf{v} \\ 0 & 1 \end{bmatrix} \mid \theta \in (-\frac{\pi}{2}, \frac{\pi}{2}) \right\}.$$

Define the map $f : S^1 \rightarrow \mathbb{R}^3 : e^{i\theta} \mapsto (e^{\hat{\omega}\theta} - I)\mathbf{v}$. Clearly, f is an embedding and $f(S^1)$ is a regular submanifold of \mathbb{R}^3 and thus $SE(3)$ (see Exercise 24). Being an open subset of $f(S^1)$, $P_a(\omega, \mathbf{v})$ is an 1-dimensional submanifold of $SE(3)$. A parallelogram joint thus generates linear motions along an open subset of the unit circle S^1 if $\|\mathbf{v}\| = 1$.

Example 6.9. A U-joint consists of two consecutive R joints with orthogonally intersecting axes. The set of rigid motions generated by a U -joint that has its axes

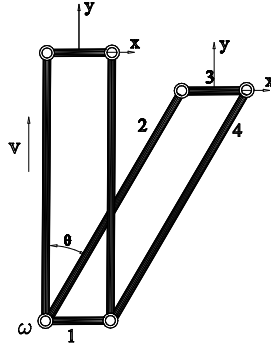


Figure 2.20: Composite joint: A plane-hinged Parallelogram

initially aligned with the x - and y - axes, respectively, has the form

$$\begin{aligned} U(0, x, y) &= R(0, x) \cdot R(0, y) \\ &= \left\{ \begin{bmatrix} e^{\hat{x}\alpha} e^{\hat{y}\beta} & 0 \\ 0 & 1 \end{bmatrix}, \alpha, \beta \in [0, 2\pi] \right\} \end{aligned}$$

which is a 2-dimensional submanifold of $SO(3)$ and thus $SE(3)$.

In general, it is difficult to enumerate all regular submanifolds of $SE(3)$. There are, however, two special families of regular submanifolds that play an important role in motion modeling and mechanism synthesis. They are referred to as *category I* and *category II* submanifolds, and are defined by the following propositions (see Exercise 25 and 26).

Proposition 6.1. Category I submanifolds

Let M_1 and M_2 be a regular submanifold of $T(3)$ and $SO(3)$, of dimension n_1 and n_2 , respectively. Then, $M_1 \cdot M_2$ (or $M_2 \cdot M_1$) is a regular submanifold of $SE(3)$, of dimension $n_1 + n_2$.

The \cdot product above is to be viewed as the product of two sets of homogeneous transformations. In general, $M_1 \cdot M_2 \neq M_2 \cdot M_1$.

Example 6.10. Model spaces for task motions

The set of rigid motions generated by a five-axis machine tool can be described by

$$T(3) \cdot U(0, x, y)$$

or in a general configuration by

$$I_q(T(3) \cdot U(o, x, y)) = T(3) \cdot U(q, \omega_1, \omega_2), \quad \omega_1 \perp \omega_2.$$

Similarly, the set of rigid motions generated by a wafer handling robot can be modeled by

$$T(z)R(o, z)T(x) = R(o, z)T_2(y).$$

The right column of Table 2.1 lists some rigid motions modeled using category I submanifolds.

Proposition 6.2. Category II submanifolds

Let H_1 and H_2 be a closed Lie subgroup of $SE(3)$, of dimension n_1 and n_2 , respectively. Let $H = H_1 \cap H_2$, and $n = \dim(H)$. Then, the product $H_1 \cdot H_2$ is a regular submanifold of $SE(3)$ of dimension $n_1 + n_2 - n$.

Note that if H_1 and H_2 commute, then $H_1 \cdot H_2$ is a Lie subgroup of $SE(3)$.

Example 6.11. From Figure 2.19, the following Lie subgroups can be factorized into

$$\begin{aligned} C(o, z) &= T(z)R(o, z), & T_2(z) &= T(x)T(y), \\ Y_\rho(z) &= H_\rho(o, z)T_2(z), & T(3) &= T_2(z)T(z), \\ PL(z) &= T_2(z)R(o, z), \\ X(z) &= T(3)R(o, z) = PL(z)T(z) = C(z)T_2(z). \end{aligned}$$

The order of the products above can be reversed.

If H_1 and H_2 do not commute, then $H_1 \cdot H_2$ and $H_2 \cdot H_1$ are distinct submanifolds. If $H_1 \cap H_2$ is nontrivial, one may use the factorizations of Example 6.11 to eliminate the common component and obtain a simpler (or irreducible) representation of the product.

Example 6.12. The product $C(o, z)X(x)$ can be simplified into

$$\begin{aligned}
 C(o, z)X(x) &= (R(o, z)T(z)) \cdot (T(3)R(o, x)) \\
 &= R(o, z)T(3)R(o, x) \\
 &= T(3)R(o, z)R(o, x) \\
 &= T(3)U(o, z, x),
 \end{aligned}$$

or in a general position, for $u \neq v$,

$$C(p, u)X(v) = T(3)U(p, u, v).$$

The product $S(o)S(p)$ is a five dimensional submanifold since $S(o) \cap S(p) = R(o, p/\|p\|)$. However, this product can not be further simplified as $S(o)$ is not trivial.

In general, *the product of three or more subgroups may not be a regular submanifold because of possible singularities.*

Two subgroups are said to be dependant if their intersection is nontrivial. The product of two dependant subgroups is referred to as a *dependant product*. There are all together 25 types of dependant products, which in their normal forms are displayed in Table 2.2 (see Exercise 27).

Intersection subgroup: $T(z)$				
No.	DoF	Product	Irreducible representation	Realizations
P1	3	$T_2(x)T_2(y)$	$T(3)$	1(8)
P2		$C(o, z)C(p, z)$	$C(o, z)R(p, z)$	24(32)
P3		$C(o, z)T_2(x)$	$R(o, z)T_2(x)$	7(18)
p4	4	$C(o, z)Y_\rho(x)$	$R(o, z)Y_\rho(x)$	29(57)
P5		$C(o, z)T(3)$	$X(z)$	7(34)
P6		$C(o, z)PL(x)$	$U(o, z, x)T_2(x)$	29(57)
P7		$T_2(x)PL(y)$	$X(y)$	7(42)
P8		$T_2(x)Y_\rho(y)$		7(42)
P9	5	$C(o, z)X(x)$	$T(3)U(0, z, x)$	288(708)
P10		$Y_\rho(x)PL(y)$		42(160)
P11		$PL(x)PL(y)$		
P12		$Y_\rho(x)Y_\rho(y)$		
Intersection subgroup: $H_\rho(o, z)$				
P13	4	$C(o, z)Y_\rho(z)$	$X(z)$	34(77)
Intersection subgroup: $R(o, z)$				
P14	4	$C(o, z)S(o)$	$T(z)S(o)$	7
P15		$C(o, z)PL(z)$	$X(z)$	34(77)
P16	5	$PL(z)S(o)$	$T_2(z)S(o)$	11(25)
P17		$S(o)S(p)$		2
P18	6	$S(o)X(z)$	$SE(3)$	79(219)
Intersection subgroup: $T_2(z)$				
P19	4	$Y_{\rho_1}(z)Y_{\rho_2}(z)$	$X(z)$	17(37)
P20		$Y_\rho(z)T(3)$		9(25)
P21		$Y_\rho(z)PL(z)$		17(37)
P22		$T(3)PL(z)$		9(25)
P23	5	$PL(z)X(x)$	$T(3)U(o, z, x)$	127(363)
P24		$Y_\rho(z)X(x)$		
Intersection subgroup: $T(3)$				
P25	5	$X(y)X(z)$	$T(3)U(0, y, z)$	564(1452)

Table 2.2: Category II submanifolds of $SE(3)$: 25 products of dependant subgroups

7 Summary

The following are the key concepts covered in this chapter:

1. The *configuration* of a rigid body is represented as an element $g \in SE(3)$. An element $g \in SE(3)$ may also be viewed as a mapping $g : \mathbb{R}^3 \rightarrow \mathbb{R}^3$ which preserves distances and angles between points. In homogeneous coordinates, we write

$$g = \begin{bmatrix} R & p \\ 0 & 1 \end{bmatrix} \quad \begin{array}{l} R \in SO(3) \\ p \in \mathbb{R}^3. \end{array}$$

The same representation can also be used for a rigid body transformation between two coordinate frames.

2. *Rigid body transformations* can be represented as the exponentials of twists:

$$g = \exp(\hat{\xi}\theta) \quad \hat{\xi} = \begin{bmatrix} \hat{\omega} & v \\ 0 & 0 \end{bmatrix}, \quad \begin{array}{l} \hat{\omega} \in so(3), \\ v \in \mathbb{R}^3, \theta \in \mathbb{R}. \end{array}$$

The twist coordinates of $\hat{\xi}$ are $\xi = (v, \omega) \in \mathbb{R}^6$.

3. A twist $\xi = (v, \omega)$ is associated with a *screw* having attributes

$$\begin{array}{ll} \text{pitch:} & h = \frac{\omega^T v}{\|\omega\|^2}; \\ \text{axis:} & l = \begin{cases} \{\frac{\omega \times v}{\|\omega\|^2} + \lambda \omega : \lambda \in \mathbb{R}\}, & \text{if } \omega \neq 0 \\ \{0 + \lambda v : \lambda \in \mathbb{R}\}, & \text{if } \omega = 0; \end{cases} \\ \text{magnitude:} & M = \begin{cases} \|\omega\|, & \text{if } \omega \neq 0 \\ \|v\|, & \text{if } \omega = 0. \end{cases} \end{array}$$

Conversely, given a screw we can write the associated twist. Two special cases are *pure rotation* about an axis $l = \{q + \lambda \omega\}$ by an amount θ and *pure translation* along an axis $l = \{0 + \lambda v\}$:

$$\xi = \begin{bmatrix} -\omega \times q \\ \omega \end{bmatrix} \theta \quad (\text{pure rotation}) \quad \xi = \begin{bmatrix} v \\ 0 \end{bmatrix} \theta \quad (\text{pure translation}).$$

4. The *velocity* of a rigid motion $g(t) \in SE(3)$ can be specified in two ways. The *spatial velocity*,

$$\hat{V}^s = \dot{g}g^{-1},$$

is a twist which gives the velocity of the rigid body as measured by an observer at the origin of the reference frame. The *body velocity*,

$$\hat{V}^b = g^{-1}\dot{g},$$

is the velocity of the object in the instantaneous body frame. These velocities are related by the *adjoint transformation*

$$V^s = \text{Ad}_g V^b \quad \text{Ad}_g = \begin{bmatrix} R & \hat{p}R \\ 0 & R \end{bmatrix},$$

which maps $\mathbb{R}^6 \rightarrow \mathbb{R}^6$. To transform velocities between coordinate frames, we use the relations

$$V_{ac}^s = V_{ab}^s + \text{Ad}_{g_{ab}} V_{bc}^s$$

$$V_{ac}^b = \text{Ad}_{g_{bc}^{-1}} V_{ab}^b + V_{bc}^b,$$

where V_{ab}^s is the spatial velocity of coordinate frame B relative to frame A and V_{ab}^b is the body velocity.

5. *Wrenches* are represented as a force, moment pair

$$F = (f, \tau) \in \mathbb{R}^6.$$

If B is a coordinate frame attached to a rigid body, then we write $F_b = (f_b, \tau_b)$ for a wrench applied at the origin of B , with f_b and τ_b specified with respect to the B coordinate frame. If C is a second coordinate frame, then we can write F_b as an *equivalent wrench* applied at C :

$$F_c = \text{Ad}_{g_{bc}}^T F_b.$$

For a rigid body with configuration g_{ab} , $F^s := F_a$ is called the *spatial wrench* and $F^b := F_b$ is called the *body wrench*.

6. A wrench $F = (f, \tau)$ is associated with a screw having attributes

$$\begin{aligned} \text{pitch:} \quad h &= \frac{f^T \tau}{\|f\|^2}; \\ \text{axis:} \quad l &= \begin{cases} \left\{ \frac{f \times \tau}{\|f\|^2} + \lambda f : \lambda \in \mathbb{R} \right\}, & \text{if } f \neq 0 \\ \{0 + \lambda \tau : \lambda \in \mathbb{R}\}, & \text{if } f = 0; \end{cases} \\ \text{magnitude:} \quad M &= \begin{cases} \|f\|, & \text{if } f \neq 0 \\ \|\tau\|, & \text{if } f = 0. \end{cases} \end{aligned}$$

Conversely, given a screw we can write the associated wrench. Two special cases are *pure force*

7. A wrench F and a twist V are *reciprocal* if $F \cdot V = 0$. Two screws S_1 and S_2 are reciprocal if the twist V_1 about S_1 and the wrench F_2 along S_2 are reciprocal. The *reciprocal product* between two screws is given by

$$S_1 \odot S_2 = V_1 \cdot F_2 = V_1 \odot V_2 = v_1 \cdot \omega_2 + v_2^T \omega_1$$

where $V_i = (v_i, \omega_i)$ represents the twist associated with the screw S_i . Two screws are reciprocal if the reciprocal product between the screws is zero.

8. A *system of screws* $\{S_1, \dots, S_k\}$ describes the vector space of all linear combinations of the screws $\{S_1, \dots, S_k\}$. A *reciprocal screw system* is the set of all screws which are reciprocal to S_i . The dimensions of a screw system and its reciprocal system sum to 6 (in $se(3)$).
9. A Lie subgroup of $SE(3)$ is used to model constrained rigid motions. The three one dimensional Lie subgroups R, T and H_ρ are used to model rigid motions generated by primitive joints, and the Lie subgroups $T(3), SO(3), SE(2), X$ and $SE(3)$ are often used to model a manipulator's end-effector motions.
10. Two special families of regular submanifolds of $SE(3)$, category I and category II submanifolds, are used to model constrained rigid motions that lack a group structure.

All of the concepts presented in this chapter can also be applied to planar rigid body motions (see Exercises 11 and 12).

8 Bibliography

The treatment of rigid motion described here, particularly the geometry of twists, was inspired by the work of Paden [51]. The use of exponential coordinates for representing robotic motion was introduced by Brockett [7]. Brockett's derivation also forms the basis of the next chapter. Related treatments can be found in the classical work by Ball [3] and the more recent texts by Hunt [28], Bottema and Roth [6], Duffy [17], Angeles [1], McCarthy [46] and Selig [66]. Goldstein [22] has a more detailed treatment of constraints. Classification of Lie subgroups of $SE(3)$ is first studied in [4], and introduced to the robotics community by Loncaric [42]. The use of submanifolds as modeling spaces for constrained rigid motions is introduced by Herve in [26, 27, 40, 37], and Meng, Liu and Li [47]. A more abstract version of the developments of this chapter can be made in the framework of matrix Lie groups and is presented in Appendix A.

cross prod-
uct!properties
of
rotation matri-
ces!properties
of
eigenvalues of a
rotation
matrix
cross prod-
uct!properties
of
skew-symmetric
matri-
ces!properties
of

9 Exercises

1. Let $a, b, c \in \mathbb{R}^3$ be 3-vectors and let \cdot and \times denote the dot product and cross product in \mathbb{R}^3 . Let $[\hat{a}, \hat{b}] = \hat{a}\hat{b} - \hat{b}\hat{a}$. Verify the following identities:

- (a) $a \cdot (b \times c) = (a \times b) \cdot c$
- (b) $a \times (b \times c) = (a \cdot c)b - (a \cdot b)c$
- (c) $[\hat{a}, \hat{b}] = (a \times b)^\wedge$

2. Using the homogeneous representation, show that $SE(3)$ satisfies the axioms of a group, with the group multiplication given by the usual matrix multiplication.

3. Properties of rotation matrices

Let $R \in SO(3)$ be a rotation matrix generated by rotating about a unit vector ω by θ radians. That is, R satisfies $R = \exp(\hat{\omega}\theta)$.

- (a) Show that the eigenvalues of $\hat{\omega}$ are 0, i , and $-i$, where $i = \sqrt{-1}$. What are the corresponding eigenvectors?
- (b) Show that the eigenvalues of R are 1, $e^{i\theta}$, and $e^{-i\theta}$. What is the eigenvector whose eigenvalue is 1?
- (c) Let R be a rotation matrix. Show that the characteristic polynomial of R is given by

$$-\lambda^3 + \lambda^2 \text{trace}(R) - \lambda \text{trace}(R) + 1 = 0$$

and the eigenvalues of R are $1, \cos \theta \pm i \sin \theta$, with $\cos \theta = \frac{\text{trace}(R)-1}{2}$.

- (d) Let $R = \begin{bmatrix} r_1 & r_2 & r_3 \end{bmatrix}$ be a rotation matrix. Show that $\det R = r_1^T(r_2 \times r_3)$.

4. Properties of skew-symmetric matrices

Show that the following properties of skew-symmetric matrices are true:

- (a) If $R \in SO(3)$ and $\omega \in \mathbb{R}^3$, then $R\hat{\omega}R^T = (R\omega)^\wedge$. Cayley parameters
- (b) If $R \in SO(3)$ and $v, w \in \mathbb{R}^3$, then $R(v \times w) = (Rv) \times (Rw)$. quaternions
- (c) Show that $so(3)$ is a vector space. Determine its dimension and give a unit quaternion basis for $so(3)$. pure quaternion

5. Cayley parameters

Another parameterization of $SO(3)$, which does not involve transcendental functions, is *Cayley's parameterization*. Let a be a vector in \mathbb{R}^3 and let \hat{a} be the associated 3×3 skew-symmetric matrix.

- (a) Show that $R_a = (I - \hat{a})^{-1}(I + \hat{a}) \in SO(3)$.
- (b) Verify that

$$R_a = \frac{1}{1 + \|a\|^2} \begin{bmatrix} 1 + a_1^2 - a_2^2 - a_3^2 & 2(a_1a_2 - a_3) & 2(a_1a_3 + a_2) \\ 2(a_1a_2 + a_3) & 1 - a_1^2 + a_2^2 - a_3^2 & 2(a_2a_3 - a_1) \\ 2(a_1a_3 - a_2) & 2(a_2a_3 + a_1) & 1 - a_1^2 - a_2^2 + a_3^2 \end{bmatrix}$$

- (c) Given a rotation matrix R , compute the Cayley parameters a . What is the geometric meaning of a ?

6. Unit quaternions

Let $Q = (q_0, \vec{q})$ and $P = (p_0, \vec{p})$ be quaternions, where $q_0, p_0 \in \mathbb{R}$ are the scalar parts of Q and P and \vec{q}, \vec{p} are the vector parts.

- (a) Show that the set of *unit* quaternions satisfies the axioms of a group.
- (b) Let x be a point and let X be a quaternion whose scalar part is zero and whose vector part is equal to x (such a quaternion is called a *pure* quaternion). Show that if Q is a unit quaternion, the product QXQ^* is a pure quaternion and the vector part of QXQ^* satisfies

$$(q_0^2 - \vec{q} \cdot \vec{q})\vec{x} + 2(q_0(\vec{q} \times \vec{x}) + (x \cdot \vec{q})\vec{q}).$$

Verify that the vector part describes the point to which x is rotated under the rotation associated with Q .

(c) Show that the set of unit quaternions is a two-to-one covering of $SO(3)$. That is, for each $R \in SO(3)$, there exist two distinct unit quaternions which can be used to represent this rotation.

(d) Compare the number of additions and multiplications needed to perform the following operations:

- i. Compose two rotation matrices.
- ii. Compose two quaternions.
- iii. Apply a rotation matrix to a vector.
- iv. Apply a quaternion to a vector [as in part (b)].

Count a subtraction as an addition, and a division as a multiplication.

(e) Show that a rigid body rotating at unit velocity about a unit vector in $\omega \in \mathbb{R}^3$ can be represented by the quaternion differential equations

$$\dot{Q} \cdot Q^* = (0, \omega/2),$$

where \cdot represents quaternion multiplication.

7. Denote by $SU(2)$ the set of 2×2 complex unitary matrices with unit determinant,

$$SU(2) = \left\{ M \in \mathbb{C}^{2 \times 2} \mid M^* M = M M^* = I, \det M = 1 \right\}$$

and write $M \in SU(2)$ as

$$M = \begin{bmatrix} \alpha & \beta \\ -\bar{\beta} & \bar{\alpha} \end{bmatrix} \quad \begin{array}{l} \alpha = q_0 + iq_1 \quad \beta = q_2 + iq_3 \\ q_0^2 + q_1^2 + q_2^2 + q_3^2 = 1. \end{array}$$

Thus, $SU(2)$ can be identified with both the set of unit quaternions and the unit sphere in \mathbb{R}^4 .

(a) Show, using ordinary matrix multiplication, that $SU(2)$ satisfies the axioms of a group.

- (b) Let $su(2)$ be the set of complex 2×2 skew-Hermitian matrices with trace zero, matrix exponential properties of

$$su(2) = \left\{ iA \mid A = \begin{bmatrix} x_1 & x_2 + ix_3 \\ x_2 - ix_3 & -x_1 \end{bmatrix}, x_i \in \mathbb{R} \right\}$$

Show that

$$\exp : su(2) \rightarrow SU(2) : iA \mapsto \exp iA = I \cos \|A\| + i \frac{A}{\|A\|} \sin \|A\|$$

$$\log : SU(2) \rightarrow su(2) : M \mapsto \log M = \frac{\phi/2}{2 \sin \phi/2} (M - M^*)$$

where $\cos \phi/2 = \text{trace}(M)/2$.

- (c) Show that there exists a 2-to-1 group homomorphism between $SU(2)$ and $SO(3)$, and thus $SU(2)$ is a double covering of $SO(3)$. Interpret your results.

8. A rigid body moving in \mathbb{R}^2 has three degrees of freedom (two components of translation and one of rotation), a rigid body moving in \mathbb{R}^3 has six degrees of freedom (three each of translation and rotation). Show that a rigid body moving in \mathbb{R}^n will have $\frac{1}{2}(n + n^2)$ degrees of freedom. How many are translational and how many are rotational?

9. Properties of the matrix exponential

Let Λ be a matrix in $\mathbb{R}^{n \times n}$. The exponential of Λ is defined as

$$e^\Lambda = I + \Lambda + \frac{\Lambda^2}{2!} + \frac{\Lambda^3}{3!} + \cdots$$

- (a) Choose a matrix norm and show that the above series converges.
 (b) Let $g \in \mathbb{R}^{n \times n}$ be an invertible matrix. Show the following equality:

$$ge^\Lambda g^{-1} = e^{g\Lambda g^{-1}}.$$

- (c) Verify that

$$\frac{d}{dt} e^{\Lambda \theta} = (\Lambda \dot{\theta}) e^{\Lambda \theta} = e^{\Lambda \theta} (\Lambda \dot{\theta}).$$

projection maps
planar
rotational
motion
rotational
motion!planar

10. *Projection maps and proof of Proposition 2.9*

This problem completes the proof of Proposition 2.9 using the properties of projection maps on linear spaces. Assume $\hat{\omega} \in so(3)$ and $\|\omega\| = 1$.

- (a) Given a vector $\omega \in \mathbb{R}^3$, let N_ω denote the subspace spanned by ω and N_ω^\perp denote the orthogonal complement. Show that

$$\text{image } \hat{\omega} = N_\omega^\perp \quad \text{and} \quad \text{kernel } \hat{\omega} = N_\omega.$$

- (b) Let $V \subset \mathbb{R}^n$ be a linear subspace. A *projection map* is a linear mapping $P_V : \mathbb{R}^n \rightarrow V$ which satisfies $\text{image } (P_V) = V$ and $P_V(x) = x$ for all $x \in V$. Show that

$$P_{N_\omega} = \omega\omega^T \quad \text{and} \quad P_{N_\omega^\perp} = (I - \omega\omega^T)$$

are both projection maps.

- (c) Calculate the null space of $I - e^{\hat{\omega}\theta}$ for $\hat{\omega} \in so(3)$ and $\theta \in (0, \pi)$ and show that $(I - e^{\hat{\omega}\theta}) : N_\omega^\perp \rightarrow N_\omega^\perp$ is bijective.
- (d) Let $A = (I - e^{\hat{\omega}\theta})\hat{\omega} + \omega\omega^T\theta$, where $\theta \in (0, \pi)$. Show that $A : \mathbb{R}^3 \rightarrow \mathbb{R}^3$ is invertible.

11. *Planar rotational motion*

Let $SO(2)$ be the set of all 2×2 orthogonal matrices with determinant equal to +1.

- (a) Show that $SO(2)$ can be identified with the \mathbb{S}^1 , the unit circle in \mathbb{R}^2 .
- (b) Let $\omega \in \mathbb{R}$ be a real number and define $\hat{\omega} \in so(2)$ as the skew-symmetric matrix

$$\hat{\omega} = \begin{bmatrix} 0 & -\omega \\ \omega & 0 \end{bmatrix}.$$

Show that

$$e^{\hat{\omega}\theta} = \begin{bmatrix} \cos \omega\theta & -\sin \omega\theta \\ \sin \omega\theta & \cos \omega\theta \end{bmatrix}.$$

Is the exponential map $\exp : so(2) \rightarrow SO(2)$ surjective? injective?

planar rigid
body
transformations
rigid body
transformations!

(c) Show that for $R \in SO(2)$ and $\hat{\omega} \in so(2)$, $R\hat{\omega}R^T = \hat{\omega}$.

12. Planar rigid body transformations

A transformation $g = (p, R) \in SE(2)$ consists of a translation $p \in \mathbb{R}^2$ and a 2×2 rotation matrix R . We represent this in homogeneous coordinates as a 3×3 matrix:

$$g = \begin{bmatrix} R & p \\ 0 & 1 \end{bmatrix}.$$

A twist $\hat{\xi} \in se(2)$ can be represented by a 3×3 matrix of the form:

$$\hat{\xi} = \begin{bmatrix} \hat{\omega} & v \\ 0 & 0 \end{bmatrix} \quad \hat{\omega} = \begin{bmatrix} 0 & -\omega \\ \omega & 0 \end{bmatrix} \quad \omega \in \mathbb{R}, v \in \mathbb{R}^2.$$

The twist coordinates for $\hat{\xi} \in se(2)$ have the form $\xi = (v, \omega) \in \mathbb{R}^3$. Note that v is a vector in the plane and ω is a scalar.

- (a) Show that the exponential of a twist in $se(2)$ gives a rigid body transformation in $SE(2)$. Consider both the pure translation case, $\xi = (v, 0)$, and the general case, $\xi = (v, \omega), \omega \neq 0$.
- (b) Show that the planar twists which correspond to pure rotation about a point q and pure translation in a direction v are given by

$$\xi = \begin{bmatrix} q_y \\ -q_x \\ 1 \end{bmatrix} \quad (\text{pure rotation}) \quad \xi = \begin{bmatrix} v_x \\ v_y \\ 0 \end{bmatrix} \quad (\text{pure translation}).$$

- (c) Show that every planar rigid body motion can be described as either pure rotation about a point (called the *pole* of the motion) or pure translation.
- (d) Show that the matrices $\hat{V}^s = \dot{g}g^{-1}$ and $\hat{V}^b = g^{-1}\dot{g}$ are both twists. Define and interpret the spatial velocity $V^s \in \mathbb{R}^3$ and the body velocity $V^b \in \mathbb{R}^3$.

adjoint
transforma-
tion!planar@for
planar motions
Rodrigues'
formula
twists!transformation
of
coordinate
transforma-
tions!twists@on
twists

- (e) The adjoint transformation is used to map body velocities $V^b \in \mathbb{R}^3$ into spatial velocities $V^s \in \mathbb{R}^3$. Show that the adjoint transformation for planar rigid motions is given by

$$\text{Ad}_g = \begin{bmatrix} R & \begin{bmatrix} p_y \\ -p_x \end{bmatrix} \\ 0 & 1 \end{bmatrix}.$$

13. Verify that for $\omega \in \mathbb{R}^3$, $\|\omega\| \neq 1$

$$e^{\hat{\omega}\theta} = I + \frac{\hat{\omega}}{\|\omega\|} \sin(\|\omega\|\theta) + \frac{\hat{\omega}^2}{\|\omega\|^2} (1 - \cos(\|\omega\|\theta)).$$

14. Let $\xi_a = (-\omega_a \times q_a + h\omega_a, \omega_a)$ be the twist associated with a screw having pitch h and axis $l = \{q_a + \lambda\omega_a : \lambda \in \mathbb{R}\}$, where all quantities are specified relative to a coordinate frame A .

- (a) Let B be a second coordinate frame with configuration $g_{ab} \in SE(3)$. Show that the representation of the twist relative to B is given by

$$\xi_b = \text{Ad}_{g_{ab}}^{-1} \xi_a = \text{Ad}_{g_{ba}} \xi_a.$$

- (b) Suppose instead that we move the screw via a rigid body transformation $g \in SE(3)$. Show that the transformed screw can be represented by the twist

$$\xi'_a = \text{Ad}_g \xi_a,$$

still relative to the A coordinate frame.

15. Attach two coordinate frames A and B to a rigid body to describe its motion relative to a reference configuration (of the body). Let $g_1(t) \in SE(3)$ and $g_2(t) \in SE(3)$ be the representation of the same motion with respect to A and B , respectively, and $g_0 \in SE(3)$ the (fixed) transformation from A to B . Show that the following relations holds

$$g_2(t) = g_0 g_1(t) g_0^{-1}$$

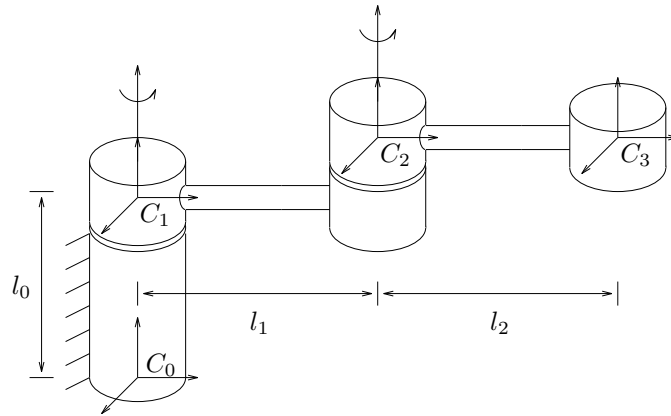


Figure 2.21: A two degree of freedom manipulator.

and

$$V_2^b = \text{Ad}_{g_0} V_1^b$$

16. Show that the pitch of a twist is invariant under the Adjoint transformation.

17. Use homogeneous representations to show that the following identities hold:

(a) $(\text{Ad}_g)^{-1} = \text{Ad}_{g^{-1}}$ for all $g \in SE(3)$.

(b) $\text{Ad}_{g_1 g_2} = \text{Ad}_{g_1} \text{Ad}_{g_2}$ for all $g_1, g_2 \in SE(3)$.

18. Prove Proposition 2.15: $V_{ac}^b = \text{Ad}_{g_{bc}^{-1}} V_{ab}^b + V_{bc}^b$.

19. Figure 2.21 shows a two degree of freedom manipulator. Let l_0, l_1, l_2 be the link length parameters and θ_1, θ_2 the joint angle variables of link 1 and link 2, respectively.

(a) Express the position and orientation of frame C_3 relative to frame C_0 in terms of the joint angle variables and the link parameters.

(b) Compute the spatial velocity of C_3 relative to C_0 as functions of the joint angles and the joint rates.

adjoint
transformation!
properties
of

reciprocal
screws!systems
of
frame invariance
coordinate
transforma-
tions!invariance
under

- (c) Compute the body velocity of C_3 relative to C_0 as functions of the joint angles and the joint rates.
- (d) *Optional:* Find the spatial velocity of the origin of C_3 and use this to check your answer for parts (b) and (c).

You may want to use a symbolic math package, such as the one described in Appendix B, to carry out the computations in this exercise.

20. *Frame invariance and reciprocal screw systems*

An operator is said to be *frame invariant* if it does not depend on the choice of coordinate frame used to carry out the calculations. Operations which are frame invariant can be computed relative to *any* coordinate frame, which can simplify calculations.

- (a) Show that the reciprocal product between two screws is frame invariant.
- (b) Show that the inner product between two twists is *not* frame invariant.
- (c) Calculate a basis for the system of screws reciprocal to a zero-pitch screw through a point q . Give a geometric interpretation for the screws which form your basis. (Hint: perform your calculations relative to a specially chosen frame.)
- (d) Calculate a basis for the system of screws reciprocal to an infinite pitch screw. Give a geometric interpretation for the screws which form your basis.
- (e) Using reciprocal screws, show that three parallel, coplanar, zero-pitch screws are dependent. That is, exhibit a system of four independent screws which are reciprocal to each of the coplanar screws.

21. *Hybrid representation of velocity*

A seemingly natural way of representing the velocity of a rigid body is to use

\dot{p} to represent the linear velocity and ω^s to represent the angular velocity. We call $V_{ab}^h = (\dot{p}, \omega^s)$ the *hybrid velocity* of a rigid body.

- (a) Show that the hybrid velocity is related to the body velocity by the relationship

$$V^h = \begin{bmatrix} R & 0 \\ 0 & R \end{bmatrix} V^b$$

and hence represents the velocity of the rigid body relative to a frame attached to the origin of the rigid body, but whose orientation remains fixed relative to the inertial frame.

- (b) Consider the motion of three coordinate frames, A , B , and C . Show that the following relationship holds between their hybrid velocities:

$$V_{ac}^h = \text{Ad}_{(-R_{ab}p_{bc})} V_{ab}^h + \text{Ad}_{R_{ab}} V_{bc}^h.$$

where Ad_p denotes the adjoint map corresponding to a pure translation by p and Ad_R denotes the adjoint map corresponding to pure rotation.

- (c) Show that the hybrid velocity of a rigid body is independent of the position of the spatial frame, but not its orientation.
- (d) Show that the hybrid velocity of a rigid body is independent of the orientation of the body frame, but not its position.
- (e) Interpret a wrench in hybrid coordinates and calculate the change of basis formulas for a change in spatial and/or body frames.
22. Define the Lie algebra \mathfrak{h} of a Lie subgroup H of $\text{SE}(3)$ to be the set of velocity vectors tangent to H at e . Let $h_i(t) \in H, i = 1, 2$ be two curves in H that passes through e at $t = 0$, and $\hat{\xi}_1 = \dot{h}_1(0)$ and $\hat{\xi}_2 = \dot{h}_2(0)$. Show that $h(s, t) = h_1(s)h_2(t)h_1^{-1}(s)$ is a curve in H that passes through e at $t = 0$ with the following properties

$$\frac{d}{dt} \Big|_{t=0} h(s, t) = h_1(s)\hat{\xi}_2 h_1^{-1}(s) \in \mathfrak{h}$$

and

$$\frac{d}{ds} \Big|_{s=0} \frac{d}{dt} \Big|_{t=0} h(s, t) = \widehat{\xi}_1 \widehat{\xi}_2 - \widehat{\xi}_2 \widehat{\xi}_1 \in \mathfrak{h}.$$

Thus, \mathfrak{h} is a Lie subalgebra of $\mathfrak{se}(3)$.

23. *Classification of Lie subalgebras of $\mathfrak{se}(3)$*

Let $\{e_i\}_{i=1}^6$ be the canonical basis of \mathbb{R}^6 , and $t(3) = \{\widehat{e}_1, \widehat{e}_2, \widehat{e}_3\}$.

(a) Show that $t(3)$ is an ideal of $\mathfrak{se}(3)$ in the sense that

$$[\widehat{\xi}, t(3)] \subset t(3), \quad \forall \widehat{\xi} \in \mathfrak{se}(3)$$

(b) Let $\widehat{\xi}_1 = \widehat{\xi} + \widehat{t}_1, \widehat{\eta}_1 = \widehat{\eta} + \widehat{s}_1$, where $\widehat{t}_1, \widehat{s}_1 \in t(3)$, be two elements of $\mathfrak{se}(3)/t(3)$. Show that

$$[\widehat{\xi}_1, \widehat{\eta}_1] = [\widehat{\xi} + \widehat{t}_1, \widehat{\eta} + \widehat{s}_1] = [\widehat{\xi}, \widehat{\eta}] + t(3)$$

defines a Lie bracket structure on $\mathfrak{se}(3)/t(3)$.

(c) Show that the projection map

$$\pi : \mathfrak{se}(3) \longrightarrow \mathfrak{se}(3)/t(3)$$

is a Lie algebra homomorphism. Find all the pre-images under π for the three Lie subalgebras of $\mathfrak{so}(3)$: $0 = \{0\}$, $\mathfrak{so}(2) = \{\widehat{e}_6\}$, and $\mathfrak{so}(3)$ itself.

24. Show that the map $f : S^1 \longrightarrow \mathbb{R}^3 : e^{i\theta} \longmapsto (e^{\widehat{\omega}\theta} - I)\mathbf{v}$ is an one-to-one immersion, and $f(S^1)$ is a regular submanifold of $SE(3)$ (See also Theorem 5.7, Boothby [5]).

25. Prove Proposition 6.1.

26. Prove Proposition 6.2.

27. Use the inclusion relations of Figure 2.19 to identify all subgroups containing a desired intersection subgroup and derive the 25 dependent products shown in Table 2.2.

Chapter 3

Manipulator Kinematics

The kinematics of a robot manipulator describes the relationship between the motion of the joints of the manipulator and the resulting motion of the rigid bodies which form the robot. This chapter gives a description of the kinematics for a general n degrees of freedom, open-chain robot manipulator using the tools presented in Chapter 2. We also present a brief treatment of redundant manipulators using this same framework.

1 Introduction

Most modern manipulators consist of a set of rigid links connected together by a set of joints. Motors are attached to the joints so that the overall motion of the mechanism can be controlled to perform a given task. A tool, typically a gripper of some sort, is attached to the end of the robot to interact with the environment.

Although any type of joint mechanism can be used to connect the links of a robot, traditionally the joints are chosen from a set of six mechanisms called *lower pairs*. These special types of joint mechanisms correspond to subgroups of the special Euclidean group $SE(3)$. They represent revolute, prismatic, helical, cylindrical, spherical, and planar joints.

The *revolute*, *prismatic*, and *helical* joints each correspond to screw motions,

cylindrical joint
spherical joint
planar joint
open-chain
manipulators
product of
exponentials
formula

with the helical joint corresponding to a general screw with finite, nonzero pitch. A *cylindrical joint* has two independent degrees of freedom and is typically constructed by combining a revolute and a prismatic joint such that their axes are coincident. Revolute and prismatic joints are by far the most common type of joint encountered in robotics.

A *spherical joint* is a mechanism which is capable of arbitrary rotations. Passive spherical joints often consist of a ball inserted into a socket, and are therefore referred to as *ball and socket joints*. Unfortunately, this type of mechanism does not work well if the joint is to exert forces and torques, and hence actuated spherical joints are most often constructed by combining three revolute joints (with motors) such that their axes all intersect at a point. Spherical mechanisms are often used as wrists in robot manipulators to allow arbitrary orientation of the gripper or tool at the end of the robot.

Planar joints allow for arbitrary translation and rotation in the plane. Along with helical joints, they are the least commonly used of the lower-pair mechanisms. A planar joint can be built from a revolute joint attached to two independent prismatic joints. The motion of a planar joint is restricted to $SE(2)$, regarded as a 3-dimensional subgroup of $SE(3)$.

Modern robot manipulators, and kinematic mechanisms in general, are typically constructed by connecting different lower-pair joints together using rigid links. Since each of the joints restricts the motion of adjacent links to a subgroup of $SE(3)$, the tools developed in the last chapter provide a natural starting point for the analysis of such mechanisms. In this and the chapters that follow, we concentrate on the kinematics, dynamics, trajectory generation and control of open-chain robot manipulators, in which a number of links are attached serially by a set of actuated joints. By controlling the forces and torques on each of the links, we seek to move the robot in a specified way.

The heart of the formulation which we present here is the *product of exponentials*

formula, which represents the kinematics of an open-chain mechanism as the product of exponentials of twists. This setting works whenever the joints of the robot consist of either revolute, prismatic, or helical joints, which is the case for practically all commercially available robot manipulators. It provides a global, geometric representation of the kinematics of a manipulator which greatly simplifies the analysis of the mechanism and provides a very structured parameterization for open-chain robots.

This chapter is organized as follows: Section 2 contains a derivation of the product of exponentials (POE) formula for the forward kinematics of an arbitrary open-chain manipulator. We concentrate on the most general case, where the end-effector configuration lies in $SE(3)$. Cases in which the end-effector space is a subgroup of $SE(3)$ are highlighted. Section 3 discusses the inverse problem of finding a set of joint angles which causes the end-effector to have a desired configuration. We make extensive use of a set of subproblems originally proposed by Paden and Kahan which are very closely related to the exponential representation of rigid body motion. Section 4 derives the velocity and force relationships between the end-effector and the joints, and introduces the manipulator Jacobian for a robot. Finally, in Section 5 we extend some of the main results of this chapter to redundant manipulators and parallel mechanisms.

2 Forward Kinematics

2.1 Problem statement

The *forward kinematics* of a robot determines the configuration of the end-effector (the gripper or tool mounted on the end of the robot) given the relative configurations of each pair of adjacent links of the robot. In this section, we restrict ourselves to open-chain manipulators in which the links form a single serial chain and each pair of links is connected either by a revolute joint or a prismatic (sliding) joint. To

SCARA
manipulator
joint
space!open-
chain@for
open-chain
manipulators
configuration
space
revolute joint
joint angle

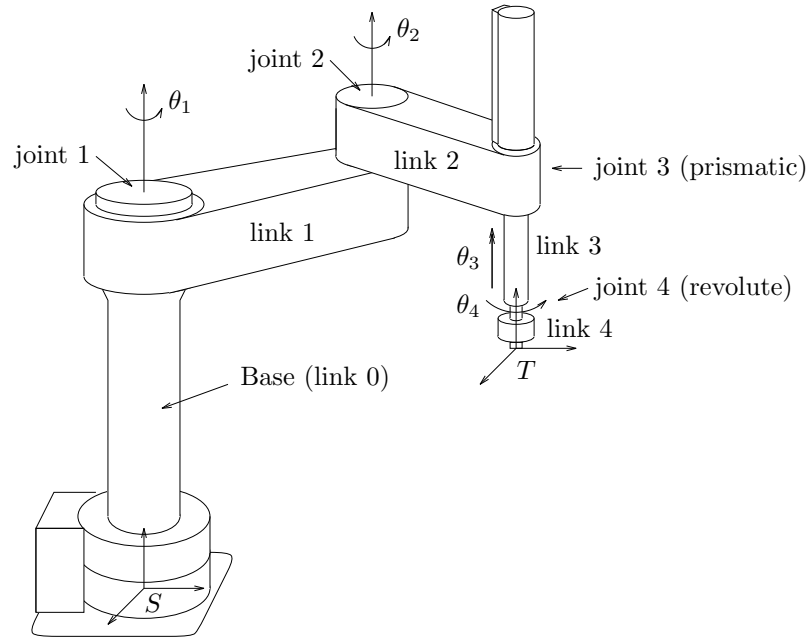


Figure 3.1: Numbering conventions for an AdeptOne robot.

fix notation, we number the joints from 1 to n , starting at the base, and number the links such that joint i connects links $i - 1$ and i . Link 0 is taken to be the base of the manipulator and link n is attached rigidly to the end-effector. Figure 3.1 illustrates our choice of notational conventions for an AdeptOne robot (a type of SCARA manipulator, with its task space being the Schonflies subgroup X).

The *joint space* Q of a manipulator consists of all possible values of the joint variables of the robot. This is also the configuration space of the robot, since specifying the joint angles specifies location of all of the links of the robot. For revolute joints, the joint variable is given by an angle $\theta_i \in [0, 2\pi)$ with the angle 2π equated to the angle 0. This set of joint angles is naturally associated with a unit circle in the plane, denoted \mathbb{S}^1 , and hence we write $\theta_i \in \mathbb{S}^1$ for revolute joints. We measure all joint angles using a right-handed coordinate system, so that an angle about a directed axis is positive if it represents a clockwise rotation as viewed along the

direction of the axis. Prismatic joints are described by a linear displacement $\theta_i \in \mathbb{R}$ along a directed axis, where positive displacement is taken along the direction of the axis.

prismatic joint
degrees of
freedom
base frame
tool frame

The joint space Q is the Cartesian product between each of these individual joint spaces. The number of degrees of freedom of an open-chain manipulator is equal to the the number of joints in the manipulator. For the four degree of freedom SCARA robot of Figure 3.1, for instance, we have $\theta = (\theta_1, \theta_2, \theta_3, \theta_4) \in \mathbb{S}^1 \times \mathbb{S}^1 \times \mathbb{R} \times \mathbb{S}^1 = Q$. For manipulators with multiple revolute joints, we use \mathbb{T}^p to represent the p -torus, defined to be the Cartesian product of p copies of \mathbb{S}^1 : $\mathbb{T}^p = \mathbb{S}^1 \times \cdots \times \mathbb{S}^1$. The joint space of a manipulator with p revolute joints and r prismatic joints is $Q = \mathbb{T}^p \times \mathbb{R}^r$ and has $p + r$ degrees of freedom. In practice, Q may be defined to be a subset of this unrestricted joint space in order to account for joint constraints such as finite displacements and rotations.

We attach two coordinate frames to the manipulator, as illustrated in Figure 3.1. The *base frame*, S , is attached to a point on the manipulator which is stationary with respect to link 0. Usually, S is attached directly to link 0, although this need not be the case, as we shall see later. (The reason for the use of the letter S instead of B is to avoid confusing the base frame with the body frame, which is ordinarily attached to a moving object.) The *tool frame*, T , is attached to the end-effector of the robot, so that the tool frame moves when the joints of the robot move.

The forward kinematics problem can now be formalized. For simplicity, we refer to all joint variables as angles, although both angles and displacements are allowed, depending on the joint type. Given a set of joint angles $\theta \in Q$, we wish to determine the configuration of the tool frame T relative to the base frame S . The forward kinematics is represented by a mapping $g_{st} : Q \rightarrow SE(3)$ which describes this relationship. The goal of this section is to show how to explicitly construct g_{st} for a given open-chain robot manipulator and explore the structure of this mapping.

Classically, the forward kinematics map for an open-chain manipulator is con-

product of
exponentials
formula—(
forward
kinemat-
ics!product of
exponentials
formula—(

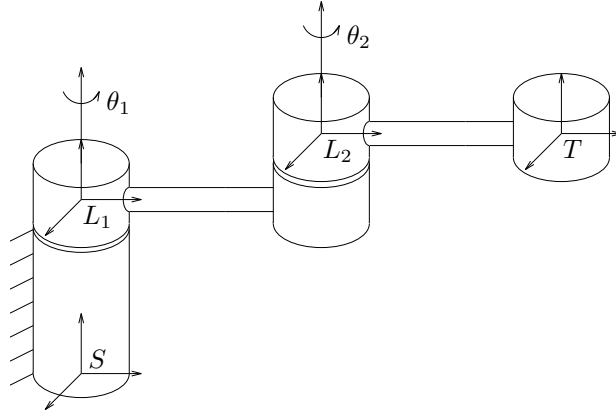


Figure 3.2: A two degree of freedom manipulator.

structured by composing the rigid motions due to the individual joints. Consider, for example, the two degree of freedom manipulator shown in Figure 3.2. To compute the configuration of the tool frame T relative to the base frame S , we concatenate the rigid motions between adjacent frames:

$$g_{st}(\theta_1, \theta_2) = g_{sl_1}(\theta_1)g_{l_1l_2}(\theta_2)g_{l_2t}.$$

The mapping $g_{st} : \mathbb{T}^2 \rightarrow SE(3)$ represents the forward kinematics of the manipulator: it gives the end-effector configuration as a function of the joint angles.

This procedure is easily extended to any open-chain mechanism. If we define $g_{l_{i-1}l_i}(\theta_i)$ as the transformation between the adjacent link frames, then the overall kinematics are given by

$$g_{st}(\theta) = g_{sl_1}(\theta_1)g_{l_1l_2}(\theta_2) \cdots g_{l_{n-1}l_n}(\theta_n)g_{l_nt}. \quad (3.1)$$

Equation (3.1) is a general formula for the forward kinematics map of an open-chain manipulator in terms of the relative transformations between adjacent link frames.

2.2 The product of exponentials (POE) formula

A more geometric description of the kinematics can be obtained by using the fact that motion of the individual joints is generated by a twist associated with the joint axis. Recall that if ξ is a twist, then the rigid motion associated with rotating and translating along the axis of the twist is given by

product of
exponentials
for-
mula!independen
on order of
joint motions

$$g_{ab}(\theta) = e^{\widehat{\xi}\theta} g_{ab}(0).$$

If ξ corresponds to a prismatic (infinite pitch) joint, then $\theta \in \mathbb{R}$ is the amount of translation; otherwise, $\theta \in \mathbb{S}^1$ measures the angle of rotation about the axis.

Consider again the two degrees of freedom manipulator shown in Figure 3.2. Suppose that we fix the first joint and consider the configuration of the tool frame as a function of θ_2 only. This is a simple revolute (zero-pitch) screw motion about the axis of the second joint and hence we can write

$$g_{st}(\theta_2) = e^{\widehat{\xi}_2\theta_2} g_{st}(0),$$

where ξ_2 is the twist corresponding to rotation about the second joint. Next, fix θ_2 and move only θ_1 . By composition, the end-effector configuration becomes

$$g_{st}(\theta_1, \theta_2) = e^{\widehat{\xi}_1\theta_1} g_{st}(\theta_2) = e^{\widehat{\xi}_1\theta_1} e^{\widehat{\xi}_2\theta_2} g_{st}(0), \quad (3.2)$$

where ξ_1 is the twist associated with the first joint. Equation (3.2) is an alternative formula for the manipulator forward kinematics. Note that ξ_1 and ξ_2 are constant twists obtained by evaluating the screw motion for each joint at the $\theta_1 = \theta_2 = 0$ configuration of the manipulator.

The simple form of equation (3.2) appears to rely on moving θ_2 first, followed by θ_1 . This allowed us to represent the joint motions as twists about constant axes. To show that this representation does not depend on the order in which we move the joints, we can derive the forward kinematics by moving θ_1 first, and then θ_2 . In this case,

$$g_{st}(\theta_1) = e^{\widehat{\xi}_1\theta_1} g_{st}(0)$$

reference configuration is the motion due to moving θ_1 with θ_2 fixed. This motion moves the axis of θ_2 , and rotation of the second link occurs around a *new* axis,

revolute and prismatic joints

$$\xi'_2 = \text{Ad}_{e^{\hat{\xi}_1 \theta_1}} \xi_2.$$

joint twists

rotation about a line

revolute joint

twist associated with

Using the properties of the matrix exponential (see Exercise 9 in Chapter 2), the rigid body transformation

$$e^{\hat{\xi}'_2 \theta_2} = e^{\hat{\xi}_1 \theta_1} \left(e^{\hat{\xi}_2 \theta_2} \right) e^{-\hat{\xi}_1 \theta_1}$$

describes motion about the new axis. Thus,

$$\begin{aligned} g_{st}(\theta_1, \theta_2) &= e^{\hat{\xi}'_2 \theta_2} e^{\hat{\xi}_1 \theta_1} g_{st}(0) \\ &= e^{\hat{\xi}_1 \theta_1} \left(e^{\hat{\xi}_2 \theta_2} \right) e^{-\hat{\xi}_1 \theta_1} e^{\hat{\xi}_1 \theta_1} g_{st}(0) \\ &= e^{\hat{\xi}_1 \theta_1} e^{\hat{\xi}_2 \theta_2} g_{st}(0), \end{aligned}$$

as before.

We can generalize this procedure to find the forward kinematics map for an arbitrary open-chain manipulator with n degrees of freedom. Let S be a frame attached to the base of the manipulator and T be a frame attached to the last link of the manipulator. Define the *reference configuration* of the manipulator to be the configuration of the manipulator corresponding to $\theta = 0$ and let $g_{st}(0)$ represent the rigid body transformation between T and S when the manipulator is in its reference configuration. For each joint, construct a twist ξ_i which corresponds to the screw motion for the i^{th} joint with all other joint angles held fixed at $\theta_j = 0$. For a revolute joint, the twist ξ_i has the form

$$\xi_i = \begin{bmatrix} -\omega_i \times q_i \\ \omega_i \end{bmatrix},$$

where $\omega_i \in \mathbb{R}^3$ is a unit vector in the direction of the twist axis and $q_i \in \mathbb{R}^3$ is any

point on the axis.¹ For a prismatic joint,

$$\xi_i = \begin{bmatrix} v_i \\ 0 \end{bmatrix},$$

where $v_i \in \mathbb{R}^3$ is a unit vector pointing in the direction of translation. All vectors and points are specified relative to the base coordinate frame S .

Combining the individual joint motions, the forward kinematics map, $g_{st} : Q \rightarrow SE(3)$, is given by

$$g_{st}(\theta) = e^{\hat{\xi}_1 \theta_1} e^{\hat{\xi}_2 \theta_2} \dots e^{\hat{\xi}_n \theta_n} g_{st}(0) \quad (3.3)$$

The ξ_i 's must be numbered sequentially starting from the base, but $g_{st}(\theta)$ gives the configuration of the tool frame independently of the order in which the rotations and translations are actually performed. Equation (3.3) is called the *product of exponentials formula* (POE) for the manipulator forward kinematics.

Example 3.1. SCARA forward kinematics

Consider the SCARA manipulator shown in Figure 3.3. It consists of four joints—three revolute and one prismatic (note that we have chosen to order the joints differently than for the AdeptOne robot in Figure 3.1). We let $\theta = 0$ correspond to the fully extended configuration and attach base and tool frames as shown in the figure.

The transformation between tool and base frames at $\theta = 0$ is given by

$$g_{st}(0) = \begin{bmatrix} I & \begin{pmatrix} 0 \\ l_1 + l_2 \\ l_0 \end{pmatrix} \\ 0 & 1 \end{bmatrix}.$$

To construct the twists for the revolute joints, note that

$$\omega_1 = \omega_2 = \omega_3 = \begin{bmatrix} 0 \\ 0 \\ 1 \end{bmatrix}$$

¹We choose the convention $-\omega \times q$ instead of $q \times \omega$ since the former can be correctly interpreted in both the spatial and planar cases (see Exercise 12 in Chapter 2).

prismatic
joint!twist
associated
with
product of
exponentials
formula!basic
formula
SCARA manip-
ulator!forward
kinematics
forward
kinemat-
ics!SCARA@for
SCARA
manipulator

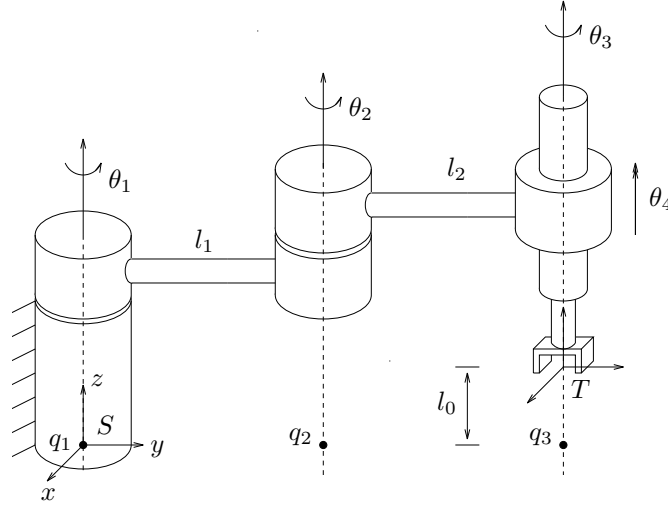


Figure 3.3: SCARA manipulator in its reference configuration.

and we can choose axis points

$$q_1 = \begin{bmatrix} 0 \\ 0 \\ 0 \end{bmatrix} \quad q_2 = \begin{bmatrix} 0 \\ l_1 \\ 0 \end{bmatrix} \quad q_3 = \begin{bmatrix} 0 \\ l_1 + l_2 \\ 0 \end{bmatrix}.$$

This yields twists

$$\xi_1 = \begin{bmatrix} 0 \\ 0 \\ 0 \\ 0 \\ 1 \end{bmatrix} \quad \xi_2 = \begin{bmatrix} l_1 \\ 0 \\ 0 \\ 0 \\ 1 \end{bmatrix} \quad \xi_3 = \begin{bmatrix} l_1 + l_2 \\ 0 \\ 0 \\ 0 \\ 1 \end{bmatrix}.$$

The prismatic joint points in the z direction and has an associated twist

$$\xi_4 = \begin{bmatrix} v_4 \\ 0 \end{bmatrix} = \begin{bmatrix} 0 \\ 0 \\ 1 \\ 0 \\ 0 \end{bmatrix}.$$

The forward kinematics map of the manipulator has the form

$$g_{st}(\theta) = e^{\hat{\xi}_1 \theta_1} e^{\hat{\xi}_2 \theta_2} e^{\hat{\xi}_3 \theta_3} e^{\hat{\xi}_4 \theta_4} g_{st}(0) = \begin{bmatrix} R(\theta) & p(\theta) \\ 0 & 1 \end{bmatrix}.$$

The individual exponentials are given by

$$\begin{aligned}
 e^{\hat{\xi}_1 \theta_1} &= \begin{bmatrix} \cos \theta_1 & -\sin \theta_1 & 0 & 0 \\ \sin \theta_1 & \cos \theta_1 & 0 & 0 \\ 0 & 0 & 1 & 0 \\ 0 & 0 & 0 & 1 \end{bmatrix} \\
 e^{\hat{\xi}_2 \theta_2} &= \begin{bmatrix} \cos \theta_2 & -\sin \theta_2 & 0 & l_1 \sin \theta_2 \\ \sin \theta_2 & \cos \theta_2 & 0 & l_1 (1 - \cos \theta_2) \\ 0 & 0 & 1 & 0 \\ 0 & 0 & 0 & 1 \end{bmatrix} \\
 e^{\hat{\xi}_3 \theta_3} &= \begin{bmatrix} \cos \theta_3 & -\sin \theta_3 & 0 & (l_1 + l_2) \sin \theta_3 \\ \sin \theta_3 & \cos \theta_3 & 0 & (l_1 + l_2)(1 - \cos \theta_3) \\ 0 & 0 & 1 & 0 \\ 0 & 0 & 0 & 1 \end{bmatrix} \\
 e^{\hat{\xi}_4 \theta_4} &= \begin{bmatrix} 1 & 0 & 0 & 0 \\ 0 & 1 & 0 & 0 \\ 0 & 0 & 1 & \theta_4 \\ 0 & 0 & 0 & 1 \end{bmatrix}.
 \end{aligned}$$

Expanding the terms in the product of exponentials formula yields

$$\begin{aligned}
 g_{st}(\theta) &= \begin{bmatrix} R(\theta) & p(\theta) \\ 0 & 1 \end{bmatrix} \\
 R(\theta) &= \begin{bmatrix} \cos(\theta_1 + \theta_2 + \theta_3) & -\sin(\theta_1 + \theta_2 + \theta_3) & 0 \\ \sin(\theta_1 + \theta_2 + \theta_3) & \cos(\theta_1 + \theta_2 + \theta_3) & 0 \\ 0 & 0 & 1 \end{bmatrix} \\
 p(\theta) &= \begin{bmatrix} -l_1 \sin \theta_1 - l_2 \sin(\theta_1 + \theta_2) \\ l_1 \cos \theta_1 + l_2 \cos(\theta_1 + \theta_2) \\ l_0 + \theta_4 \end{bmatrix}.
 \end{aligned} \tag{3.4}$$

Note that the image of $g_{st}(\theta)$ lies actually in the subgroup $X(z)$.

Example 3.2. Elbow manipulator forward kinematics

Consider the elbow manipulator shown in Figure 3.4. The mechanism consists of two intersecting axes at the shoulder, an elbow, and a spherical wrist (modeled as three intersecting axes). The reference configuration ($\theta = 0$) is fully extended, as shown.

elbow manipula-
tor!forward
kinematics
forward
kinemat-
ics!elbow@for
elbow
manipulator

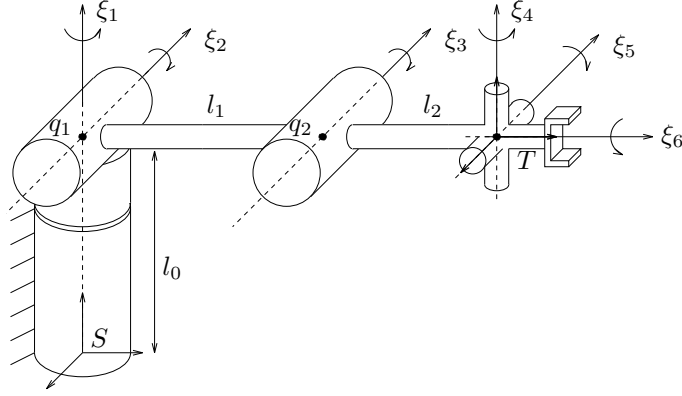


Figure 3.4: Elbow manipulator.

The forward kinematics is computed by calculating the individual twist motions for each joint. The transformation between the tool and base frames at $\theta = 0$ is given by

$$g_{st}(0) = \begin{bmatrix} I & \begin{pmatrix} 0 \\ l_1+l_2 \\ l_0 \\ 1 \end{pmatrix} \\ 0 & 1 \end{bmatrix}.$$

The first two joints have twists

$$\xi_1 = \begin{bmatrix} -\begin{pmatrix} 0 \\ 0 \\ 1 \end{pmatrix} \times \begin{pmatrix} 0 \\ 0 \\ l_0 \end{pmatrix} \\ \begin{pmatrix} 0 \\ 0 \\ 1 \end{pmatrix} \end{bmatrix} = \begin{bmatrix} 0 \\ 0 \\ 0 \\ 0 \\ 1 \end{bmatrix} \quad \xi_2 = \begin{bmatrix} -\begin{pmatrix} -1 \\ 0 \\ 0 \end{pmatrix} \times \begin{pmatrix} 0 \\ 0 \\ l_0 \end{pmatrix} \\ \begin{pmatrix} -1 \\ 0 \\ 0 \end{pmatrix} \end{bmatrix} = \begin{bmatrix} 0 \\ -l_0 \\ 0 \\ -1 \\ 0 \end{bmatrix}.$$

Note that we have used $q_1 = (0, 0, l_0)$ for the first twist; we could just as well have used the origin or any other point on the axis of the twist. The other twists are calculated in a similar manner:

$$\xi_3 = \begin{bmatrix} 0 \\ -l_0 \\ l_1 \\ -1 \\ 0 \\ 0 \end{bmatrix} \quad \xi_4 = \begin{bmatrix} l_1+l_2 \\ 0 \\ 0 \\ 0 \\ 0 \\ 1 \end{bmatrix} \quad \xi_5 = \begin{bmatrix} 0 \\ -l_0 \\ l_1+l_2 \\ -1 \\ 0 \\ 0 \end{bmatrix} \quad \xi_6 = \begin{bmatrix} -l_0 \\ 0 \\ 0 \\ 0 \\ 1 \\ 0 \end{bmatrix}.$$

The full forward kinematics are

$$g_{st}(\theta) = e^{\hat{\xi}_1 \theta_1} \dots e^{\hat{\xi}_6 \theta_6} g_{st}(0) = \begin{bmatrix} R(\theta) & p(\theta) \\ 0 & 1 \end{bmatrix}$$

where

$$R(\theta) = \begin{bmatrix} r_{11} & r_{12} & r_{13} \\ r_{21} & r_{22} & r_{23} \\ r_{31} & r_{32} & r_{33} \end{bmatrix}$$

$$p(\theta) = \begin{bmatrix} -\sin \theta_1 (l_1 \cos \theta_2 + l_2 \cos(\theta_2 + \theta_3)) \\ \cos \theta_1 (l_1 \cos \theta_2 + l_2 \cos(\theta_2 + \theta_3)) \\ l_0 - l_1 \sin \theta_2 - l_2 \sin(\theta_2 + \theta_3) \end{bmatrix},$$

and, using the notation $c_i = \cos \theta_i$, $s_i = \sin \theta_i$, $c_{ij} = \cos(\theta_i + \theta_j)$, $s_{ij} = \sin(\theta_i + \theta_j)$,

$$r_{11} = c_6(c_1c_4 - s_1c_{23}s_4) + s_6(s_1s_{23}c_5 + s_1c_{23}c_4s_5 + c_1s_4s_5)$$

$$r_{12} = -c_5(s_1c_{23}c_4 + c_1s_4) + s_1s_{23}s_5$$

$$r_{13} = c_6(-c_5s_1s_{23} - (c_{23}c_4s_1 + c_1s_4)s_5) + (c_1c_4 - c_{23}s_1s_4)s_6$$

$$r_{21} = c_6(c_4s_1 + c_1c_{23}s_4) - (c_1c_5s_{23} + (c_1c_{23}c_4 - s_1s_4)s_5)s_6$$

$$r_{22} = c_5(c_1c_{23}c_4 - s_1s_4) - c_1s_{23}s_5$$

$$r_{23} = c_6(c_1c_5s_{23} + (c_1c_{23}c_4 - s_1s_4)s_5) + (c_4s_1 + c_1c_{23}s_4)s_6$$

$$r_{31} = -(c_6s_{23}s_4) - (c_{23}c_5 - c_4s_{23}s_5)s_6$$

$$r_{32} = -(c_4c_5s_{23}) - c_{23}s_5$$

$$r_{33} = c_6(c_{23}c_5 - c_4s_{23}s_5) - s_{23}s_4s_6.$$

product of
exponentials
formula—)
forward
kinemat-
ics!product of
exponentials
formula—)
twists!parameterizi-
manipulators
via—(
base frame
product of
exponentials
formula!choice
of base frame

2.3 Parameterization of manipulators via twists

Using the product of exponentials formula, the kinematics of a manipulator is completely characterized by the twist coordinates for each of the joints. We now consider some issues related to parameterizing robot motion using twists.

Choice of base frame and reference configuration

In the examples above, we chose the base frame for the manipulator to be at the base of the robot. Other choices of the base frame are possible, and can sometimes lead

reference configuration!choice of
product of
exponentials
formula!choice of base frame
SCARA manipulator!forward kinematics
forward kinematics!SCARA@for SCARA manipulator

to simplified calculations. One natural choice is to place the base frame coincident with the tool frame in the reference configuration. That is, we choose a base frame which is fixed relative to the base of the robot and which lines up with the tool frame when $\theta = 0$. This simplifies calculations since $g_{st}(0) = I$ with this choice of base frame and hence

$$g_{st}(\theta) = e^{\hat{\xi}_1 \theta_1} \dots e^{\hat{\xi}_n \theta_n}.$$

A further degree of freedom in specifying the manipulator kinematics is the choice of the reference configuration for the manipulator. Recall that the reference configuration was the configuration corresponding to setting all of the joint variables to 0. By adding or subtracting a fixed offset from each joint variable, we can define *any* configuration of the manipulator as the reference configuration. The twist coordinates for the individual joints of a manipulator depend on the choice of reference configuration (as well as base frame) and so the reference configuration is usually chosen such that the kinematic analysis is as simple as possible. For example, a common choice is to define the reference configuration such that points on the twist axes for the joints have a simple form, as in all of the examples above.

Example 3.3. SCARA forward kinematics with alternate base frame

Consider the SCARA manipulator with base frame coincident with the tool frame at $\theta = 0$, as shown in Figure 3.5. The twists are now calculated with respect to the new base frame:

$$\begin{aligned}\xi_1 &= \begin{bmatrix} -\begin{pmatrix} 0 \\ 0 \\ 1 \end{pmatrix} \times \begin{pmatrix} 0 \\ -l_1 - l_2 \\ 0 \end{pmatrix} \\ \begin{pmatrix} 0 \\ 0 \\ 1 \end{pmatrix} \end{bmatrix} = \begin{bmatrix} -l_1 - l_2 \\ 0 \\ 0 \\ 0 \\ 1 \end{bmatrix} \\ \xi_2 &= \begin{bmatrix} -\begin{pmatrix} 0 \\ 0 \\ 1 \end{pmatrix} \times \begin{pmatrix} 0 \\ -l_2 \\ 0 \end{pmatrix} \\ \begin{pmatrix} 0 \\ 0 \\ 1 \end{pmatrix} \end{bmatrix} = \begin{bmatrix} -l_2 \\ 0 \\ 0 \\ 0 \\ 1 \end{bmatrix}\end{aligned}$$

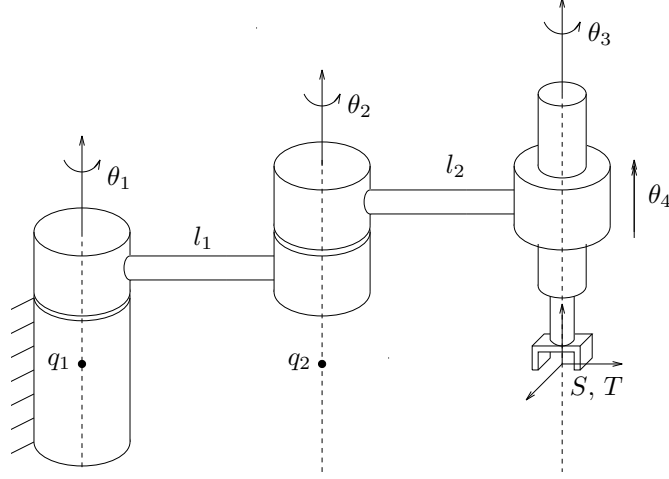


Figure 3.5: SCARA manipulator in its reference configuration, with base frame coincident with tool frame.

and similar calculations yield:

$$\xi_3 = \begin{bmatrix} 0 \\ 0 \\ 0 \\ 0 \\ 1 \end{bmatrix} \quad \xi_4 = \begin{bmatrix} 0 \\ 0 \\ 1 \\ 0 \\ 0 \end{bmatrix}.$$

Expanding the product of exponentials formula gives

$$\begin{aligned} g_{st}(\theta) &= \begin{bmatrix} R(\theta) & p(\theta) \\ 0 & 1 \end{bmatrix} \\ R(\theta) &= \begin{bmatrix} \cos(\theta_1 + \theta_2 + \theta_3) & -\sin(\theta_1 + \theta_2 + \theta_3) & 0 \\ \sin(\theta_1 + \theta_2 + \theta_3) & \cos(\theta_1 + \theta_2 + \theta_3) & 0 \\ 0 & 0 & 1 \end{bmatrix} \\ p(\theta) &= \begin{bmatrix} -l_1 \sin \theta_1 - l_2 \sin(\theta_1 + \theta_2) \\ -l_1 - l_2 + l_1 \cos \theta_1 + l_2 \cos(\theta_1 + \theta_2) \\ \theta_4 \end{bmatrix}. \end{aligned} \tag{3.5}$$

Note that $g_{st}(0) = I$, which is consistent with the fact that the base and tool frames are coincident at $\theta = 0$. Compare this formula with the kinematics map derived in Example 3.1.

product of
exponentials
formula!
Denavit-
Hartenberg
parameters
Denavit-
Hartenberg
parameters
link frames

Relationship with Denavit-Hartenberg parameters

Given a base frame S and a tool frame T , the coordinates of the twists corresponding to each joint of a robot manipulator provide a complete parameterization of the kinematics of the manipulator. An alternative parameterization, which is the de facto standard in robotics, is the use of *Denavit-Hartenberg parameters* [16]. In this section, we discuss the relationships between these two parameterizations and their relative merits.

Denavit-Hartenberg parameters are obtained by applying a set of rules which specify the position and orientation of frames L_i attached to each link of the robot and then constructing the homogeneous transformations between frames, denoted $g_{l_{i-1}l_i}$. By convention, we identify the base frame S with L_0 . The kinematics of the mechanism can be written as

$$g_{st}(\theta) = g_{l_0l_1}(\theta_1)g_{l_1l_2}(\theta_2) \cdots g_{l_{n-1}l_n}(\theta_n)g_{l_nt}, \quad (3.6)$$

just as in equation (3.1). Each of the transformations $g_{l_{i-1}l_i}$ has the form

$$g_{l_{i-1}l_i} = \begin{bmatrix} \cos \phi_i & -\sin \phi_i \cos \alpha_i & \sin \phi_i \sin \alpha_i & a_i \cos \phi_i \\ \sin \phi_i & \cos \phi_i \cos \alpha_i & -\cos \phi_i \sin \alpha_i & a_i \sin \phi_i \\ 0 & \sin \alpha_i & \cos \alpha_i & d_i \\ 0 & 0 & 0 & 1 \end{bmatrix},$$

where the four scalars α_i , a_i , d_i , and ϕ_i are the parameters for the i^{th} link. For revolute joints, ϕ_i corresponds to the joint variable θ_i , while for prismatic joints, d_i corresponds to the joint variable θ_i . Denavit-Hartenberg parameters are available for standard industrial robots and are used by most commercial robot simulation and programming systems.

It may seem somewhat surprising that only four parameters are needed to specify the relative link displacements, since the twists for each joint have six independent parameters. This is achieved by cleverly choosing the link frames so that certain cancellations occur. In fact, it is possible to give physical interpretations to the

various parameters based on the relationships between adjacent link frames. An excellent discussion can be found in Spong and Vidyasagar [69].

adjoint
transformation
of
twists

There is not a simple one-to-one mapping between the twist coordinates for the joints of a robot manipulator and the Denavit-Hartenberg parameters. This is because the twist coordinates for each joint are specified with respect to a single base frame and hence do not directly represent the relative motions of each link with respect to the previous link. To see this, let $\xi_{i-1,i}$ be the twist for the i^{th} link *relative to the previous link frame*. Then, $g_{l_{i-1}l_i}$ is given by

$$g_{l_{i-1}l_i} = e^{\widehat{\xi}_{i-1,i}\theta_i} g_{l_{i-1}l_i}(0) \quad (3.7)$$

and the forward kinematics map becomes

$$g_{st}(\theta) = e^{\widehat{\xi}_{01}\theta_1} g_{l_0l_1}(0) e^{\widehat{\xi}_{12}\theta_2} g_{l_1l_2}(0) \cdots e^{\widehat{\xi}_{n-1,n}\theta_n} g_{l_{n-1}l_n}(0). \quad (3.8)$$

This is evidently not the same as the product of exponentials formula, though it bears some resemblance to it.

The relationship between the twists ξ_i and the pairs $g_{l_{i-1}l_i}(0)$ and $\xi_{i-1,i}$ can be determined using the adjoint mapping. We first rewrite equation (3.8) as

$$g_{st}(\theta) = e^{\widehat{\xi}_{01}\theta_1} \left(g_{l_0l_1}(0) e^{\widehat{\xi}_{12}\theta_2} g_{l_0l_1}^{-1}(0) \right) \cdot \left(g_{l_0l_2}(0) e^{\widehat{\xi}_{23}\theta_3} g_{l_0l_2}^{-1}(0) \right) \cdots \left(g_{l_0l_{n-1}}(0) e^{\widehat{\xi}_{n-1,n}\theta_n} g_{l_0l_{n-1}}^{-1}(0) \right) g_{l_0t}(0). \quad (3.9)$$

We can simplify this equation by making use of the relationship

$$g e^{\widehat{\xi}\theta} g^{-1} = e^{(\text{Ad}_g \xi)^\wedge \theta}$$

to obtain

$$g_{st}(\theta) = e^{\widehat{\xi}_{01}\theta_1} e^{(\text{Ad}_{g_{l_0l_1}}(0) \xi_{12})^\wedge \theta_2} \cdots e^{(\text{Ad}_{g_{l_0l_{n-1}}}(0) \xi_{n-1,n})^\wedge \theta_n} g_{l_0t}(0).$$

It follows immediately that

$$\xi_i = \text{Ad}_{g_{l_0l_{i-1}}(0)} \xi_{i-1,i}. \quad (3.10)$$

joint
twists!given
Denavit-
Hartenberg
parameters

This formula verifies that the twist ξ_i is the joint twist for the i^{th} joint in its reference configuration and written relative to the base coordinate frame.

twists!parameterizing
manipulators
via—)

workspace of a
manipulator—(
complete
workspace
reachable
workspace

Given the Denavit-Hartenberg parameters for a manipulator, the corresponding twists ξ_i can be determined by first parameterizing $g_{i-1,i}$ using exponential coordinates, as in equation (3.7), and then applying equation (3.10). However, in almost all instances it is substantially easier to construct the joint twists ξ_i directly, by writing down the direction of the joint axes and, in the case of revolute joints, choosing a convenient point on each axis. Indeed, one of the most attractive features of the product of exponentials formula is its usage of only two coordinate frames, the base frame S , and the tool frame T . This property, combined with the geometric significance of the twists ξ_i , make the product of exponentials representation a superior alternative to the use of Denavit-Hartenberg parameters.

2.4 Manipulator workspace

The *workspace* of a manipulator is defined as the set of all end-effector configurations which can be reached by some choice of joint angles. If Q is the configuration space of a manipulator and $g_{st} : Q \rightarrow SE(3)$ is the forward kinematics map, then the workspace W is defined as the set

$$W = \{g_{st}(\theta) : \theta \in Q\} \subset SE(3). \quad (3.11)$$

The workspace is used when planning a task for the manipulator to execute; all desired motions of the manipulator must remain within the workspace. We refer to this notion of workspace as the *complete workspace* of a manipulator.

Characterizing the workspace as a subset of $SE(3)$ is often somewhat difficult to interpret. Instead, one can consider the set of positions (in \mathbb{R}^3) which can be reached by some choice of joint angles. This set is called the *reachable workspace* and is defined as

$$W_R = \{p(\theta) : \theta \in Q\} \subset \mathbb{R}^3, \quad (3.12)$$

where $p(\theta) : Q \rightarrow \mathbb{R}^3$ is the position component of the forward kinematics map g_{st} . The reachable workspace is the volume of \mathbb{R}^3 which can be reached at *some* orientation.

Since the reachable workspace does not consider ability to arbitrarily orient the end-effector, for some tasks it is not a useful measure of the range of a manipulator. The *dextrous workspace* of a manipulator is the volume of space which can be reached by the manipulator with arbitrary orientation:

$$W_D = \{p \in \mathbb{R}^3 : \forall R \in SO(3), \exists \theta \text{ with } g_{st}(\theta) = (p, R)\} \subset \mathbb{R}^3. \quad (3.13)$$

The dextrous workspace is useful in the context of task planning since it allows the orientation of the end-effector to be ignored when positioning objects in the dextrous workspace.

For a general robot manipulator, the dextrous workspace can be very difficult to calculate. A common feature of industrial manipulators is to place a spherical wrist at the end of the manipulator, as in the elbow manipulator given in Example 3.2. Recall that a spherical wrist consists of three orthogonal revolute axes which intersect at a point. If the end-effector frame is placed at the origin of the wrist axes, then the spherical wrist can be used to achieve any orientation at a given end-effector position. Hence, for a manipulator with a spherical wrist, the dextrous workspace is equal to the reachable workspace, $W_D = W_R$. Furthermore, the complete workspace for the end-effector satisfies $W = W_R \times SO(3)$. This analysis only holds when the end-effector frame is placed at the center of the spherical wrist; if an offset is present, the analysis becomes more complex.

Example 3.4. Workspace for a planar three-link robot

Consider the planar manipulator shown in Figure 3.6a. Let $g = (x, y, \phi)$ represent the position and orientation of the end-effector. The forward kinematics of the mechanism can be derived using the product of exponentials formula, but are more

workspace of a
manipulator!dextr
dextrous
workspace
spherical
wrist!effect on
workspace

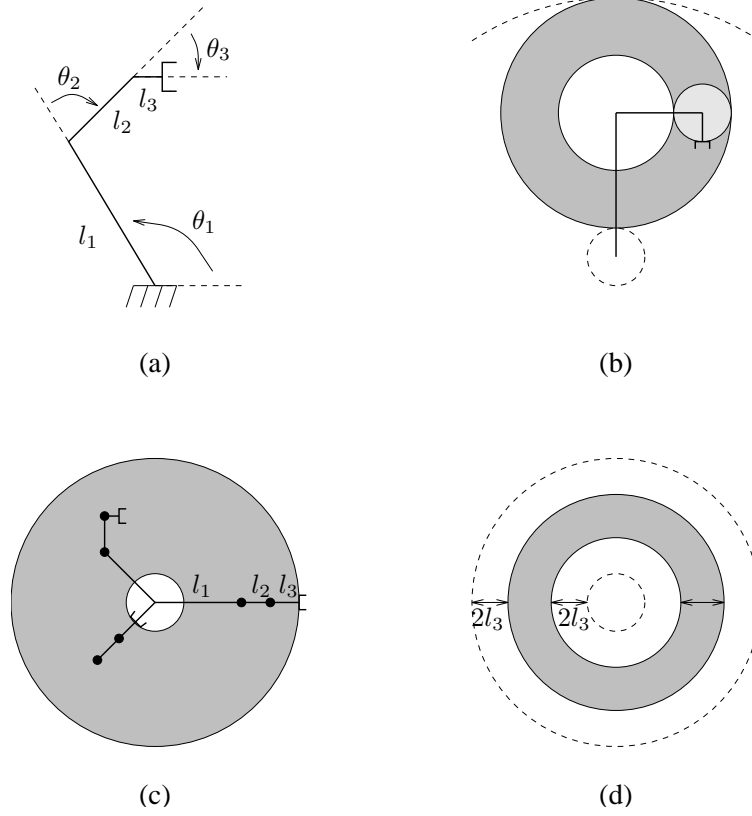


Figure 3.6: Workspace calculations for a planar three-link robot (a). The construction of the workspace is illustrated in (b). The reachable workspace is shown in (c) and the dextrous workspace is shown in (d).

easily derived using plane geometry:

$$\begin{aligned} x &= l_1 \cos \theta_1 + l_2 \cos(\theta_1 + \theta_2) + l_3 \cos(\theta_1 + \theta_2 + \theta_3) \\ y &= l_1 \sin \theta_1 + l_2 \sin(\theta_1 + \theta_2) + l_3 \sin(\theta_1 + \theta_2 + \theta_3) \\ \phi &= \theta_1 + \theta_2 + \theta_3. \end{aligned} \tag{3.14}$$

workspace of a
manipulator—)
forward
kinematics—)

We take $l_1 > l_2 > l_3$, and assume $l_1 > l_2 + l_3$.

The reachable workspace is calculated by ignoring the orientation of the end-effector. To generate it, we first take θ_1 and θ_2 as fixed. The set of reachable points becomes a circle of radius l_3 formed by sweeping θ_3 through all angles (see Figure 3.6b). We now let θ_2 vary through all angles to get an annulus with inner radius $l_2 - l_3$ and outer radius $l_2 + l_3$ centered at the end of the first link. Finally, we generate the reachable workspace by sweeping the annulus through all values of θ_1 , to give the reachable workspace. The final construction is shown in Figure 3.6c. W_R is an annulus with inner radius $l_1 - l_2 - l_3$ and outer radius $l_1 + l_2 + l_3$.

The dextrous workspace for this manipulator is somewhat subtle. Although the manipulator has the planar equivalent of a spherical wrist, the end-effector frame is not aligned with the center of the wrist. This reduces the size of the dextrous workspace by $2l_3$ on the inner and outer edges, as shown in Figure 3.6d.

Example 3.5. Reachable workspace of the elbow manipulator

We calculate the reachable workspace by the spherical wrist center point of the elbow manipulator shown in Figure 3.4, and determine the workspace shape, volume and its intersection with the yz -plane.

The forward kinematic map of the elbow manipulator is derived in Example 3.2, with the wrist center point having coordinates $p = (0, l_1 + l_2, l_0)^T$. Assuming no joint limit constraints, the reachable workspace has the form

$$W_R = \{e^{\hat{\xi}_1 \theta_1} e^{\hat{\xi}_2 \theta_2} e^{\hat{\xi}_3 \theta_3} p, \theta_i \in [0, 2\pi], i = 1, \dots, 3\}. \tag{3.15}$$

inverse
kinematics—(

For better visualization of how W_R is generated we define, for $i = 2, 3$,

$$g_{i0} = \begin{bmatrix} I & -\omega_i \times v_i \\ 0 & 1 \end{bmatrix} = \begin{bmatrix} I & \hat{\omega}_i^2 q_i \\ 0 & 1 \end{bmatrix}$$

where ω_i is the direction of, and q_i a point on the i^{th} axis, and let

$$\xi'_i = Ad_{g_{i0}} \xi_i = \begin{bmatrix} 0 \\ \omega_i \end{bmatrix}.$$

We can rewrite 3.15 as

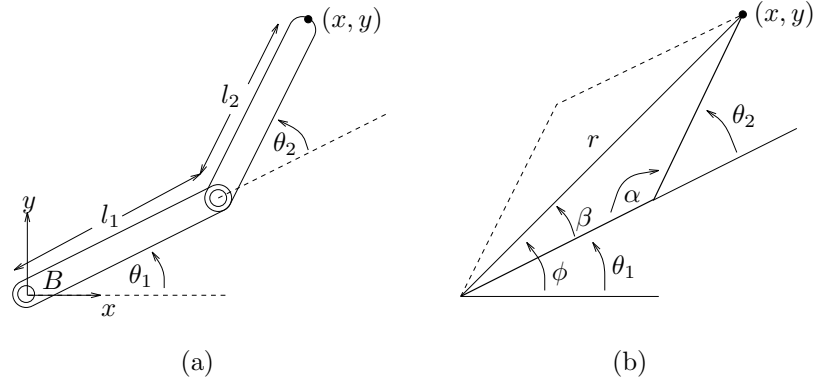
$$W_R = \{e^{\hat{\xi}_1 \theta_1} g_{20}^{-1} e^{\hat{\xi}_2 \theta_2} g_{20} g_{30}^{-1} e^{\hat{\xi}_3 \theta_3} g_{30} p, \theta_i \in [0, 2\pi], i = 1, \dots, 3\} \quad (3.16)$$

Since the g'_{i0} s and their associated inverses consist of simple translations, W_R can be viewed as simple rotations about axes passing through the origin of a certain translated points or sets. We can derive W_R successively as follows: First, with $g_{30}p = (0, l_2, 0)^T$, $W_3 := \{e^{\hat{\xi}_3 \theta_3} g_{30}p, \theta_3 \in [0, 2\pi]\}$ is a circle in the yz -plane, centered at the origin and with radius l_2 ; $W'_3 := g_{20}g_{30}^{-1}W_3$ is W_3 shifted to the right of the y -axis by l_1 . The minimum and maximum distance of W'_3 to the axis of ξ'_2 (x -axis) are $l_2 - l_1$ and $l_2 + l_1$, respectively. Then, $W_2 := \{e^{\hat{\xi}_2 \theta_2} W'_3, \theta_2 \in [0, 2\pi]\}$ is an annulus in the yz -plane, centered at the origin, of outer radius $l_2 + l_1$ and inner radius $l_2 - l_1$; $W'_2 = g_{20}^{-1}W_2$ is W_2 shifted up along the z -axis by l_0 ; Finally, $W_R = W_1 := \{e^{\hat{\xi}_1 \theta_1} W'_2, \theta_1 \in [0, 2\pi]\}$ is a solid shell, centered at $(0, 0, l_0)$, of inner radius $l_2 - l_1$ and outer radius $l_2 + l_1$. The volume of W_R is $\frac{4}{3}\pi((l_2 + l_1)^3 - (l_2 - l_1)^3)$. Note that if $l_2 \neq l_1$, then W_R contains an void.

Exercise 3 shows calculation of reachable workspace for PUMA 600 manipulator under joint limit constraints.

3 Inverse Kinematics

We now consider the inverse kinematics problem: given a desired configuration for the tool frame, find joint angles which achieve that configuration. That is, given a



inverse kinematics!
simple example
two-link planar manipulator!
inverse kinematics

Figure 3.7: Inverse kinematics of a planar two-link manipulator.

forward kinematics map $g_{st} : Q \rightarrow SE(3)$ and a desired configuration $g_d \in SE(3)$, we would like to solve the equation

$$g_{st}(\theta) = g_d \quad (3.17)$$

for some $\theta \in Q$. This problem may have multiple solutions, a unique solution, or no solution.

3.1 A planar example

To illustrate some of the issues in inverse kinematics, we first consider the inverse kinematics of the planar two-link manipulator shown in Figure 3.7a. The forward kinematics can be determined using plane geometry:

$$\begin{aligned} x &= l_1 \cos \theta_1 + l_2 \cos(\theta_1 + \theta_2) \\ y &= l_1 \sin \theta_1 + l_2 \sin(\theta_1 + \theta_2). \end{aligned}$$

The inverse problem is to solve for θ_1 and θ_2 , given x and y . A standard trick is to solve the problem using polar coordinates, (r, ϕ) , as shown in Figure 3.7b. From this viewpoint, θ_2 is determined by $r = \sqrt{x^2 + y^2}$, and the law of cosines gives

$$\theta_2 = \pi \pm \alpha \quad \alpha = \cos^{-1} \left(\frac{l_1^2 + l_2^2 - r^2}{2l_1 l_2} \right). \quad (3.18)$$

inverse kinemat-
ics!solving
using
subproblems
inverse kinemat-
ics!number of
solutions

If $\alpha \neq 0$, there are two distinct values of θ_2 which give the appropriate radius; the second is referred to as the “flip solution” and is shown as a dashed line in Figure 3.7b. The complete solution is given by solving for ϕ and using this to determine θ_1 . This problem must be solved for each possible value of θ_2 , yielding

$$\theta_1 = \text{atan2}(y, x) \pm \beta \quad \beta = \cos^{-1} \left(\frac{r^2 + l_1^2 - l_2^2}{2l_1 r} \right),$$

where the sign used for β agrees with that used for α .

This planar example illustrates several important features of inverse kinematics problems. In solving an inverse kinematics problem, one first divides the problem into specific subproblems, such as solving for θ_2 given r and then using θ_1 to rotate the end-effector to the proper position. Each subproblem may have zero, one, or many solutions depending on the desired end-effector location. If the configuration is outside of the workspace of the manipulator, then no solution can exist and one of the subproblems must fail to have a solution (consider what happens if $r > l_1 + l_2$ in the example above). Multiple solutions occur when the desired configuration is within the workspace but there are multiple joint configurations which all map to the same end-effector location. If a subproblem generates multiple solutions, then we must complete the solution procedure for all joint angles generated by the subproblem.

Traditionally, inverse kinematics solutions are separated into classes: closed-form solutions and numerical solutions. Closed-form solutions, such as the one given above, allow for fast and efficient calculation of the joint angles which give a desired end-effector configuration. Numerical solutions rely on an interactive procedure to solve equation (3.17). Most industrial manipulators have closed-form solutions. These solutions are obtained in a manner similar to that described above: using geometric and algebraic identities, solve the set of nonlinear, coupled, algebraic equations which define the inverse kinematics problem. An introduction to classical techniques for solving inverse kinematics problems is given in Craig [13].

3.2 Paden-Kahan subproblems

Paden-Kahan subproblems—(rotation about a line

Using the product of exponentials formula for the forward kinematics map, it is possible to develop a geometric algorithm to solve the inverse kinematics problem. This method was originally presented by Paden [51] and built on the unpublished work of Kahan [31].

To solve the inverse kinematics problem, we first solve a number of subproblems which occur frequently in inverse solutions for common manipulator designs. One then seeks to reduce the full inverse kinematics problem into appropriate subproblems whose solutions are known. One feature of the subproblems presented here is that they are both geometrically meaningful and numerically stable. Note that this set of subproblems is by no means exhaustive and there may exist manipulators which cannot be solved using these canonical problems. Additional subproblems are explored in the exercises.

For each of the subproblems presented below, we give a statement of the geometric problem to be solved and a detailed solution. On a first reading of this section, it may be difficult to understand the relevance of the specific subproblems presented here. We recommend that the first-time reader skip the solutions until she sees how the subproblems are used in the examples presented later in this section.

Subproblem 1. Rotation about a single axis

Let ξ be a zero-pitch twist with unit magnitude and $p, q \in \mathbb{R}^3$ two points. Find θ such that

$$e^{\hat{\xi}\theta}p = q. \quad (3.19)$$

Solution. This problem corresponds to rotating a point p about a given axis ξ until it coincides with a second point q , as shown in Figure 3.8a. Let r be a point on the axis of ξ . Define $u = (p - r)$ to be the vector between r and p , and $v = (q - r)$ the vector between r and q . It follows from equation (3.19) and the fact that $\exp(\hat{\xi}\theta)r = r$

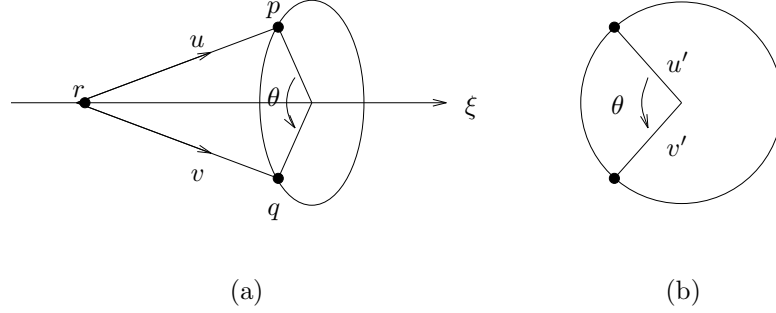


Figure 3.8: Subproblem 1: (a) Rotate p about the axis of ξ until it is coincident with q . (b) The projection of u and v onto the plane normal to the twist axis.

(since r is on the axis of ξ) that

$$e^{\widehat{\omega}\theta}u = v, \quad (3.20)$$

where we have used the fact that u and v are vectors, and hence we have $\exp(\widehat{\xi}\theta)u = \exp(\widehat{\omega}\theta)u$.

To determine when the problem has a solution, define u' and v' to be the projections of u and v onto the plane perpendicular to the axis of ξ . If $\omega \in \mathbb{R}^3$ is a unit vector in the direction of the axis of ξ , then

$$u' = u - \omega\omega^T u \quad \text{and} \quad v' = v - \omega\omega^T v.$$

The problem has a solution only if the projections of u and v onto the ω -axis and onto the plane perpendicular to ω have equal lengths. More formally, if we project equation (3.20) onto the span of ω and the null space of ω^T , we obtain the necessary conditions

$$\omega^T u = \omega^T v \quad \text{and} \quad \|u'\| = \|v'\|. \quad (3.21)$$

If equation (3.21) is satisfied, then we can find θ by looking only at the projected vectors u' and v' as shown in Figure 3.8b. If $u' \neq 0$, then we can determine θ using

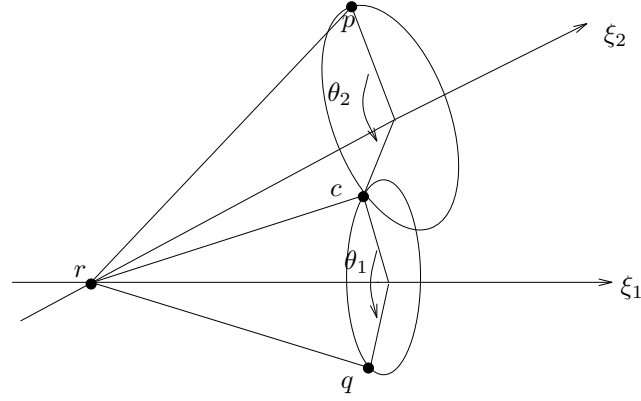
rotation about
two axes

Figure 3.9: Subproblem 2: Rotate p about the axis of ξ_2 followed by a rotation around the axis of ξ_1 such that the final location of p is coincident with q .

the relationships

$$\begin{aligned} u' \times v' &= \omega \sin \theta \|u'\| \|v'\| \\ u' \cdot v' &= \cos \theta \|u'\| \|v'\| \end{aligned} \quad \Rightarrow \quad \theta = \text{atan2}(\omega^T(u' \times v'), u'^T v').$$

If $u' = 0$, then there are an infinite number of solutions since, in this case, $p = q$ and both points lie on the axis of rotation. \square

Subproblem 2. Rotation about two subsequent axes

Let ξ_1 and ξ_2 be two zero-pitch, unit magnitude twists with intersecting axes and $p, q \in \mathbb{R}^3$ two points. Find θ_1 and θ_2 such that

$$e^{\hat{\xi}_1 \theta_1} e^{\hat{\xi}_2 \theta_2} p = q. \quad (3.22)$$

Solution. This problem corresponds to rotating a point p first about the axis of ξ_2 by θ_2 and then about the axis of ξ_1 by θ_1 , so that the final location of p is coincident with the point q . This motion is depicted in Figure 3.9. If the axes of ξ_1 and ξ_2 coincide, this problem reduces to Subproblem 1 and any θ_1, θ_2 such that $\theta_1 + \theta_2 = \theta$ is a solution, where θ is the solution to Subproblem 1.

If the two axes are not parallel, i.e., $\omega_1 \times \omega_2 \neq 0$, then let c be a point such that

$$e^{\widehat{\xi}_2 \theta_2} p = c = e^{-\widehat{\xi}_1 \theta_1} q. \quad (3.23)$$

In other words, c represents the point to which p is rotated about the axis of ξ_2 by θ_2 . Let r be the point of intersection of the two axes, so that

$$e^{\widehat{\xi}_2 \theta_2} (p - r) = c - r = e^{-\widehat{\xi}_1 \theta_1} (q - r). \quad (3.24)$$

As before, define vectors $u = (p - r)$, $v = (q - r)$, and $z = (c - r)$. Substituting these expressions into equation (3.24) gives

$$e^{\widehat{\omega}_2 \theta_2} u = z = e^{-\widehat{\omega}_1 \theta_1} v,$$

which implies that

$$\omega_2^T u = \omega_2^T z \quad \text{and} \quad \omega_1^T v = \omega_1^T z \quad (3.25)$$

and $\|u\|^2 = \|z\|^2 = \|v\|^2$. Furthermore, since ω_1 , ω_2 , and $\omega_1 \times \omega_2$ are linearly independent, we can write

$$z = \alpha \omega_1 + \beta \omega_2 + \gamma (\omega_1 \times \omega_2) \quad (3.26)$$

and

$$\|z\|^2 = \alpha^2 + \beta^2 + 2\alpha\beta\omega_1^T\omega_2 + \gamma^2\|\omega_1 \times \omega_2\|^2. \quad (3.27)$$

Substituting equation (3.26) into equation (3.25) gives a system of two equations in two unknowns:

$$\begin{aligned} \omega_2^T u &= \alpha \omega_2^T \omega_1 + \beta \\ \omega_1^T v &= \alpha + \beta \omega_1^T \omega_2 \end{aligned} \quad \Longrightarrow \quad \begin{aligned} \alpha &= \frac{(\omega_1^T \omega_2) \omega_2^T u - \omega_1^T v}{(\omega_1^T \omega_2)^2 - 1} \\ \beta &= \frac{(\omega_1^T \omega_2) \omega_1^T v - \omega_2^T u}{(\omega_1^T \omega_2)^2 - 1}. \end{aligned}$$

Solving equation (3.27) for γ^2 and using $\|z\|^2 = \|u\|^2$ yields

rotation to a
given distance

$$\gamma^2 = \frac{\|u\|^2 - \alpha^2 - \beta^2 - 2\alpha\beta\omega_1^T\omega_2}{\|\omega_1 \times \omega_2\|^2}.$$

This equation may have zero, one, or two real solutions. In the case that a solution exists, we can find z —and hence c —given α , β , and γ .

To find θ_1 and θ_2 , we solve

$$e^{\widehat{\xi}_2\theta_2}p = c \quad \text{and} \quad e^{-\widehat{\xi}_1\theta_1}q = c$$

using Subproblem 1. If there are multiple solutions for c , each of these solutions gives a value for θ_1 and θ_2 . Two solutions exist in the case where the circles in Figure 3.9 intersect at two points, one solution when the circles are tangential, and none when the circles fail to intersect. \square

Subproblem 3. Rotation to a given distance

Let ξ be a zero-pitch, unit magnitude twist; $p, q \in \mathbb{R}^3$ two points; and δ a real number > 0 . Find θ such that

$$\|q - e^{\widehat{\xi}\theta}p\| = \delta. \quad (3.28)$$

Solution. This problem corresponds to rotating a point p about axis ξ until the point is a distance δ from q , as shown in Figure 3.10a. A solution exists if the circle defined by rotating p around ξ intersects the sphere of radius δ centered at q .

To find the explicit solution, we again consider the projection of all points onto the plane perpendicular to ω , the direction of the axis of ξ . Let r be a point on the axis of ξ , and define $u = (p - r)$ and $v = (q - r)$ so that

$$\|v - e^{\widehat{\omega}\theta}u\|^2 = \delta^2. \quad (3.29)$$

The projections of u and v are

$$u' = u - \omega\omega^T u \quad \text{and} \quad v' = v - \omega\omega^T v.$$

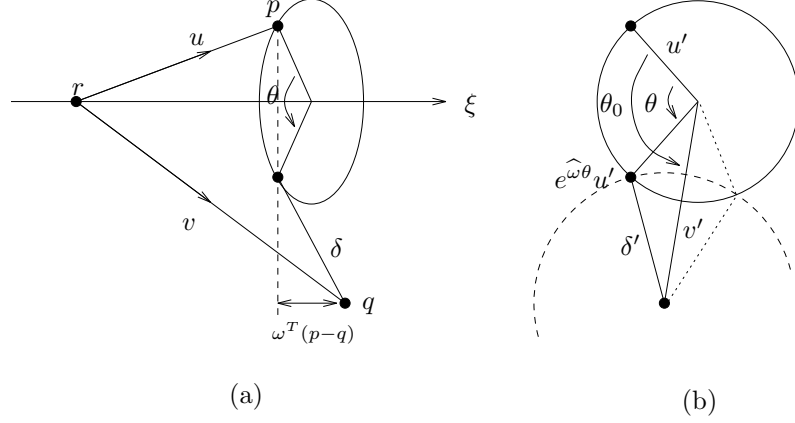


Figure 3.10: Subproblem 3: (a) Rotate p about the axis of ξ until it is a distance δ from q . (b) The projection onto the plane perpendicular to the axis. The dashed line is the “flip” solution.

We can also “project” δ by subtracting the component of $p - q$ in the ω direction,

$$\delta'^2 = \delta^2 - |\omega^T(p - q)|^2,$$

so that equation (3.29) becomes

$$\|v' - e^{\widehat{\omega}\theta} u'\|^2 = \delta'^2$$

(see Figure 3.10b). If we let θ_0 be the angle between the vectors u' and v' , we have

$$\theta_0 = \text{atan2}(\omega^T(u' \times v'), u'^T v'). \quad (3.30)$$

We can now use the law of cosines to solve for the angle $\phi = \theta_0 - \theta$. The triangle formed by the center of the axis, $\exp(\widehat{\omega}\theta)u'$, and v' satisfies

$$\|u'\|^2 + \|v'\|^2 - 2\|u'\|\|v'\|\cos\phi = \delta'^2$$

and therefore

$$\theta = \theta_0 \pm \cos^{-1} \left(\frac{\|u'\|^2 + \|v'\|^2 - \delta'^2}{2\|u'\|\|v'\|} \right). \quad (3.31)$$

Equation (3.31) has either zero, one, or two solutions, depending on the number of points in which the circle of radius $\|u'\|$ intersects the circle of radius δ' .

Paden-Kahan
subproblems—)
□ inverse kinemat-
ics!solving
using
subproblems
Paden-Kahan
subprob-
lems!solving
inverse
kinematics
using

3.3 Solving inverse kinematics using subproblems

Given the solutions to the subproblems presented above, we must now find techniques for converting the complete inverse kinematics problem into the appropriate subproblems.

The basic technique for simplification is to apply the kinematic equations to special points, such as the intersection of two or more axes. This is a potentially powerful operation since $\exp(\widehat{\xi}\theta)p = p$ if p is on the axis of a revolute twist ξ . Using this, we can eliminate the dependence of certain joint angles by appropriate selection of points. For example, if we wish to solve

$$e^{\widehat{\xi}_1\theta_1}e^{\widehat{\xi}_2\theta_2}e^{\widehat{\xi}_3\theta_3} = g,$$

with ξ_1 , ξ_2 , and ξ_3 all zero-pitch twists, then applying both sides to a point p on the axis of ξ_3 yields

$$e^{\widehat{\xi}_1\theta_1}e^{\widehat{\xi}_2\theta_2}p = gp,$$

which can be solved using Subproblem 2 (in the case that ξ_1 and ξ_2 intersect).

Another common trick for reducing a problem to a subproblem is to subtract a point from both sides of an equation and take the norm of the result. Since rigid motions preserve norm, some dependencies can be eliminated. For example, if we wish to solve

$$e^{\widehat{\xi}_1\theta_1}e^{\widehat{\xi}_2\theta_2}e^{\widehat{\xi}_3\theta_3} = g$$

for ξ_3 , and ξ_1, ξ_2 intersect at a point q , then we can apply both sides of the equation to a point p that is not on the axis of ξ_3 and subtract the point q . Taking the norm

elbow manipulator!
inverse kinematics!
inverse kinematics!
elbow@for
manipulator

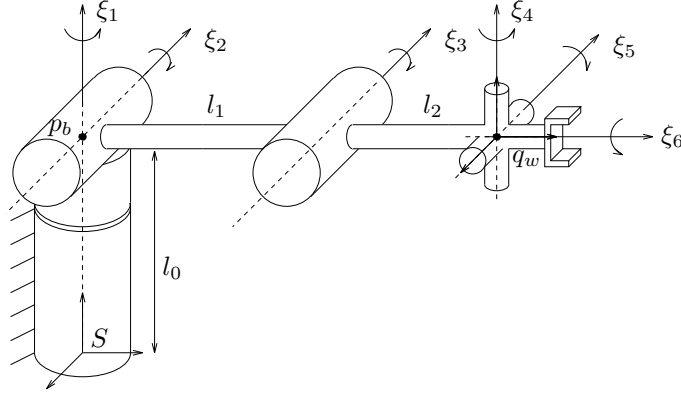


Figure 3.11: Elbow manipulator.

of the result yields

$$\begin{aligned}\delta &:= \|gp - q\| = \|e^{\hat{\xi}_1\theta_1}e^{\hat{\xi}_2\theta_2}e^{\hat{\xi}_3\theta_3}p - q\| \\ &= \|e^{\hat{\xi}_1\theta_1}e^{\hat{\xi}_2\theta_2}(e^{\hat{\xi}_3\theta_3}p - q)\| \\ &= \|e^{\hat{\xi}_3\theta_3}p - q\|\end{aligned}$$

which is Subproblem 3.

We now show how the subproblems of Section 3.2 can be used to solve the inverse kinematics of some common manipulators. Additional examples appear in the exercises.

Example 3.6. Elbow manipulator inverse kinematics

The elbow manipulator in Figure 3.11 consists of a three degree of freedom manipulator with a spherical wrist. This special structure simplifies the inverse kinematics and fits nicely with the subproblems presented earlier.

The equation we wish to solve is

$$g_{st}(\theta) = e^{\hat{\xi}_1\theta_1} \dots e^{\hat{\xi}_6\theta_6} g_{st}(0) = g_d,$$

where $g_d \in SE(3)$ is the desired configuration of the tool frame. Post-multiplying

this equation by $g_{st}^{-1}(0)$ isolates the exponential maps:

$$e^{\hat{\xi}_1\theta_1} \dots e^{\hat{\xi}_6\theta_6} = g_d g_{st}^{-1}(0) =: g_1. \quad (3.32)$$

We determine the requisite joint angles in four steps.

Step 1 (solve for the elbow angle, θ_3). Apply both sides of equation (3.32) to a point $p_w \in \mathbb{R}^3$ which is the common point of intersection for the wrist axes. Since $\exp(\hat{\xi}\theta)p_w = p_w$ if p_w is on the axis of ξ , this yields

$$e^{\hat{\xi}_1\theta_1} e^{\hat{\xi}_2\theta_2} e^{\hat{\xi}_3\theta_3} p_w = g_1 p_w. \quad (3.33)$$

Subtract from both sides of equation (3.33) a point p_b which is at the intersection of the first two axes, as shown in Figure 3.11:

$$e^{\hat{\xi}_1\theta_1} e^{\hat{\xi}_2\theta_2} e^{\hat{\xi}_3\theta_3} p_w - p_b = e^{\hat{\xi}_1\theta_1} e^{\hat{\xi}_2\theta_2} \left(e^{\hat{\xi}_3\theta_3} p_w - p_b \right) = g_1 p_w - p_b. \quad (3.34)$$

Using the property that the distance between points is preserved by rigid motions, take the magnitude of both sides of equation (3.34):

$$\|e^{\hat{\xi}_3\theta_3} p_w - p_b\| = \|g_1 p_w - p_b\|. \quad (3.35)$$

This equation is in the form required for Subproblem 3, with $p = p_w$, $q = p_b$, and $\delta = \|g_1 p_w - p_b\|$. Applying Subproblem 3, we solve for θ_3 .

Step 2 (solve for the base joint angles). Since θ_3 is known, equation (3.33) becomes

$$e^{\hat{\xi}_1\theta_1} e^{\hat{\xi}_2\theta_2} (e^{\hat{\xi}_3\theta_3} p_w) = g_1 p_w. \quad (3.36)$$

Applying Subproblem 2 with $p = \exp(\hat{\xi}_3\theta_3)p_w$ and $q = g_1 p_w$ gives the values for θ_1 and θ_2 .

Step 3 (solve for two of three wrist angles). The remaining kinematics can be written as

$$e^{\hat{\xi}_4\theta_4} e^{\hat{\xi}_5\theta_5} e^{\hat{\xi}_6\theta_6} = e^{-\hat{\xi}_3\theta_3} e^{-\hat{\xi}_2\theta_2} e^{-\hat{\xi}_1\theta_1} g_d g_{st}^{-1}(0) =: g_2. \quad (3.37)$$

SCARA manipulator!
inverse kinematics
inverse kinematics!
SCARA@for SCARA
manipulator

Apply both sides of equation (3.37) to a point p which is on the axis of ξ_6 but *not* on the ξ_4, ξ_5 axes. This gives

$$e^{\hat{\xi}_4\theta_4}e^{\hat{\xi}_5\theta_5}p = g_2p. \quad (3.38)$$

Apply Subproblem 2 to find θ_4 and θ_5 .

Step 4 (solve for the remaining wrist angle). The only remaining unknown is θ_6 . Rearranging the kinematics equation and applying both sides to any point p which is not on the axis of ξ_6 ,

$$e^{\hat{\xi}_6\theta_6}p = e^{-\hat{\xi}_5\theta_5}e^{-\hat{\xi}_4\theta_4} \dots e^{-\hat{\xi}_1\theta_1}g_d g_{st}^{-1}(0)p =: q. \quad (3.39)$$

Apply Subproblem 1 to find θ_6 .

At the end of this procedure, θ_1 through θ_6 are determined. There are a maximum of eight possible solutions, due to multiple solutions for equations (3.35), (3.36), and (3.38). Note that the overall procedure is to first solve for the three angles which determine the position of the center of the wrist and then solve for the wrist angles.

Example 3.7. Inverse kinematics of a SCARA manipulator

Consider the four degree of freedom SCARA manipulator shown in Figure 3.12. From the forward kinematics derived in Example 3.1 on page 105, the tool configuration has the form

$$g_{st}(\theta) = e^{\hat{\xi}_1\theta_1} \dots e^{\hat{\xi}_4\theta_4} g_{st}(0) = \begin{bmatrix} \cos \phi & -\sin \phi & 0 & x \\ \sin \phi & \cos \phi & 0 & y \\ 0 & 0 & 1 & z \\ 0 & 0 & 0 & 1 \end{bmatrix} =: g_d \quad (3.40)$$

and hence we can solve the inverse kinematics given x, y, z , and ϕ as in equation (3.40). We begin by solving for θ_4 . Applying both sides of equation (3.40) to

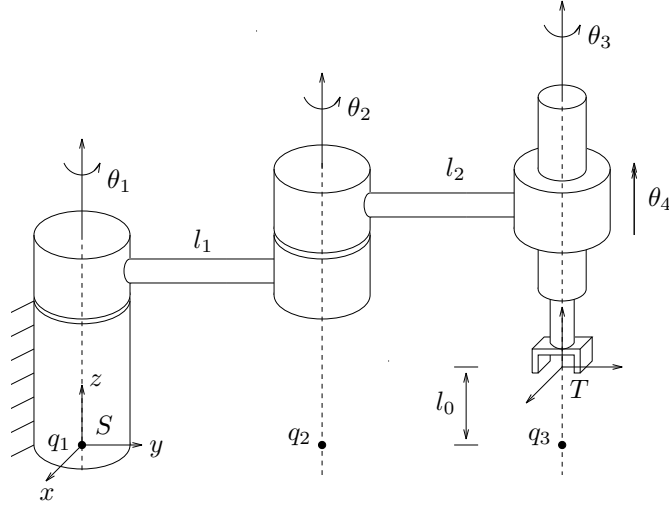


Figure 3.12: SCARA manipulator in its reference configuration.

the origin of the tool frame gives

$$p(\theta) = \begin{bmatrix} -l_1 \sin \theta_1 - l_2 \sin(\theta_1 + \theta_2) \\ l_1 \cos \theta_1 + l_2 \cos(\theta_1 + \theta_2) \\ l_0 + \theta_4 \end{bmatrix} = \begin{bmatrix} x \\ y \\ z \end{bmatrix},$$

where $p(\theta)$ is the position component of the forward kinematics, given by equation (3.4). From the form of $p(\theta)$, we see that $\theta_4 = z - l_0$. Notice that finding θ_4 did not make use of any of the previously defined subproblems.

Once θ_4 is known, we can rearrange equation (3.40) to read

$$e^{\hat{\xi}_1 \theta_1} e^{\hat{\xi}_2 \theta_2} e^{\hat{\xi}_3 \theta_3} = g_d g_{st}^{-1}(0) e^{-\hat{\xi}_4 \theta_4} =: g_1. \quad (3.41)$$

Let p be a point on the axis of ξ_3 and q be a point on the axis of ξ_1 . Applying equation (3.41) to p , subtracting q from both sides, and applying norms,

$$\begin{aligned} \|e^{\hat{\xi}_1 \theta_1} e^{\hat{\xi}_2 \theta_2} p - q\| &= \|e^{\hat{\xi}_1 \theta_1} (e^{\hat{\xi}_2 \theta_2} p - q)\| \\ &= \|e^{\hat{\xi}_2 \theta_2} p - q\| = \|g_1 p - q\| =: \delta. \end{aligned} \quad (3.42)$$

Application of Subproblem 3 gives the value of θ_2 . θ_1 can now be found by applying equation (3.41) to a point p' on the axis of ξ_3 and solving Subproblem 1:

$$e^{\widehat{\xi}_1\theta_1}e^{\widehat{\xi}_2\theta_2}e^{\widehat{\xi}_3\theta_3}p' = e^{\widehat{\xi}_1\theta_1}\left(e^{\widehat{\xi}_2\theta_2}p'\right) = g_1p'.$$

Finally, we rearrange equation (3.41), shifting the (known) θ_1 and θ_2 terms to the right-hand side:

$$e^{\widehat{\xi}_3\theta_3} = e^{-\widehat{\xi}_2\theta_2}e^{-\widehat{\xi}_1\theta_1}g_dg_{st}^{-1}(\theta)e^{-\widehat{\xi}_4\theta_4}. \quad (3.43)$$

Applying equation (3.43) to any point p which is not on the axis of ξ_3 and solving Subproblem 1 a final time gives θ_3 and completes the solution.

There are a maximum of two possible solutions for the SCARA manipulator, corresponding to the solutions of equation (3.42).

Many industrial robots are designed so that motion of a certain joint is decoupled from that of the rest. This property can be used, in conjunction with special feature points, for inverse kinematics problems. For example, the fourth joint of the SCARA manipulator is decoupled from the rest, leading to direct isolation of θ_4 from the inverse kinematics problem, as in Example 3.7. We explore the use of this technique for the ABB IRB4400 robot shown in Figure 3.13.

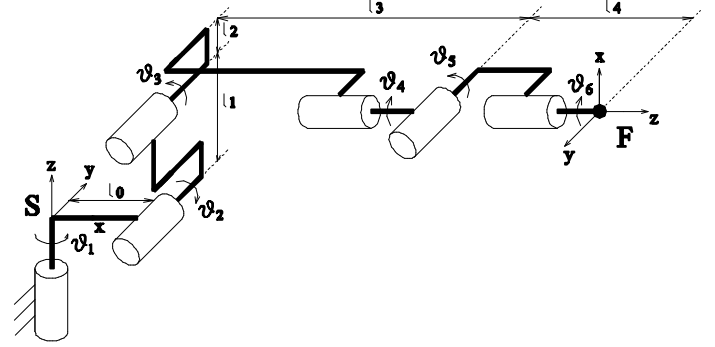
Example 3.8. Inverse kinematics of elbow manipulator with axes offset

This manipulator employs a five-bar (or parallelogram) mechanism to drive the second and third joint. As the joint angle θ_3 is the difference between the third and second actuated angles, an equivalent open-chain representation of the manipulator can be obtained, and is shown in Figure 3.13(b). The twist parameters for the joint axes are given by

$$\omega_1 = \begin{bmatrix} 0 \\ 0 \\ 1 \end{bmatrix}, \quad \omega_2 = -\omega_3 = -\omega_5 \begin{bmatrix} 0 \\ 1 \\ 0 \end{bmatrix}, \quad \omega_4 = \omega_6 = \begin{bmatrix} -1 \\ 0 \\ 0 \end{bmatrix}$$



(a)



(b)

Figure 3.13: ABB IRB4400 robot and its equivalent open-chain model (Courtesy of ABB Inc.)

and

$$q_1 = \begin{bmatrix} 0 \\ 0 \\ 0 \end{bmatrix}, \quad q_2 = \begin{bmatrix} l_0 \\ 0 \\ 0 \end{bmatrix}, \quad q_3 = \begin{bmatrix} l_0 \\ 0 \\ l_1 \end{bmatrix}, \quad p_w := q_4 = q_5 = q_6 = \begin{bmatrix} l_0 + l_3 \\ 0 \\ l_1 + l_2 \end{bmatrix}.$$

With $\xi_i = (-\omega_i \times q_i, \omega_i)$, the inverse kinematics equation we need to solve has the form

$$g_{st}(\theta) = e^{\hat{\xi}_1 \theta_1} e^{\hat{\xi}_2 \theta_2} e^{\hat{\xi}_3 \theta_3} e^{\hat{\xi}_4 \theta_4} e^{\hat{\xi}_5 \theta_5} e^{\hat{\xi}_6 \theta_6} := g_d \quad (3.44)$$

where $g_d \in SE(3)$ is a desired transformation. Since the last three axes intersect at a point we can, as in Example 3.6, separate the inverse kinematics problem into an orientation part and a position part. Applying both sides of equation (3.44) to the intersection point p_w yields,

$$e^{\hat{\xi}_1 \theta_1} e^{\hat{\xi}_2 \theta_2} e^{\hat{\xi}_3 \theta_3} p_w = g_d p_w =: q. \quad (3.45)$$

Because of the offset between the first and second axes, we premultiply both sides of equation (3.45) by $e^{-\hat{\xi}_1\theta_1}$ to get

$$e^{\hat{\xi}_2\theta_2}e^{\hat{\xi}_3\theta_3}p_w = e^{-\hat{\xi}_1\theta_1}q. \quad (3.46)$$

From the structure of the manipulator, joint two and three generate motions only in the xz -plane. Thus, with $q = (q_x, q_y, q_z)$, we have from the above equation that

$$0 = (0, 1, 0) \cdot (e^{-\hat{\xi}_1\theta_1}q) = \cos\theta_1 q_y - \sin\theta_1 q_x.$$

A solution for θ_1 is found to be

$$\theta_1 = \tan^{-1}(q_y/q_x).$$

Hence, there are two solutions of θ_1 . Specifically, if $\theta_1 = \theta_1^*$ is a solution, $\theta_1 = \theta_1^* + \pi$ is also a solution, where $-\pi/2 < \theta_1^* < \pi/2$. We call θ_1^* the front-reach solution, and $\theta_1 = \theta_1^* + \pi$ the back-reach solution. Because of the mechanism constraints, the back-reach solution is physically impossible.

With θ_1 determined, we subtract q_2 from both sides of equation (3.46), and take the norm,

$$\|e^{\hat{\xi}_3\theta_3}p_w - q_2\| = \|e^{-\hat{\xi}_1\theta_1}q - q_2\| =: \delta.$$

Subproblem 3 can be used to solve for θ_3 from the above equation. The result is then applied to equation (3.46) to solve for θ_2 , using Subproblem 1.

With θ_1, θ_2 and θ_3 determined, we can solve for the remaining angles θ_4, θ_5 and θ_6 from equation (3.44), employing the same technique as in Example 3.6. Note that for each solution set of the first three joint angles, there are two possible wrist configurations. Since there are four possible upper arm configurations, a total of eight manipulator postures are possible. However, due to mechanical limits, fewer than eight manipulator postures are physically realizable.

4 The Manipulator Jacobian

In addition to the relationship between the joint angles and the end-effector configuration, one often makes use of the relationship between the joint and end-effector velocities. In this section, we derive a formula for this relationship and study its structure and properties. We also study the dual relationship between end-effector wrenches and joint torques.

Traditionally, one describes the Jacobian for a manipulator by differentiating the forward kinematics map. This works when the forward kinematics is represented as a mapping $g : \mathbb{R}^n \rightarrow \mathbb{R}^p$, in which case the Jacobian is the linear map $\frac{\partial g}{\partial \theta}(\theta) : \mathbb{R}^n \rightarrow \mathbb{R}^p$. However, if we represent the forward kinematics more completely as $g : \mathbb{R}^n \rightarrow SE(3)$, the Jacobian is not so easily obtained. The problem is that $\frac{\partial g}{\partial \theta}(\theta)$ is not a natural quantity since g is a matrix-valued function. Of course, one could always choose coordinates for $SE(3)$, but this description only holds locally. More importantly, choosing a local parameterization for $SE(3)$ destroys the natural geometric structure of rigid body motion.

To correct this problem, we use the tools of Chapter 2 to write the Jacobian of the forward kinematics map in terms of twists. We shall see that the product of exponentials formula leads to a very natural and explicit description of the manipulator Jacobian, which highlights the geometry of the mechanism and has none of the drawbacks of a local representation.

4.1 End-effector velocity

Let $g_{st} : Q \rightarrow SE(3)$ be the forward kinematics map for a manipulator. If the joints move along a path $\theta(t) \in Q$, then the end-effector traverses a path $g_{st}(\theta(t)) \in SE(3)$. The instantaneous spatial velocity of the end-effector is given by the twist

$$\hat{V}_{st}^s = \dot{g}_{st}(\theta)g_{st}^{-1}(\theta).$$

manipulator
Jacobian—(
manipulator
Jaco-
bian!Jacobian@ve
Jacobian of a
mapping
velocity!end-
effector
end-effector
veloc-
ity!manipulator@
manipulator
Jacobian

manipulator
Jacobian!spatial
product of
exponentials
for-
mula!manipulator
Jacobian using
manipulator
Jacobian!spatial

Applying the chain rule,

$$\hat{V}_{st}^s = \sum_{i=1}^n \left(\frac{\partial g_{st}}{\partial \theta_i} \dot{\theta}_i \right) g_{st}^{-1}(\theta) = \sum_{i=1}^n \left(\frac{\partial g_{st}}{\partial \theta_i} g_{st}^{-1}(\theta) \right) \dot{\theta}_i, \quad (3.47)$$

and we see that the end-effector velocity is linearly related to the velocity of the individual joints. In twist coordinates, equation (3.47) can be written as

$$V_{st}^s = J_{st}^s(\theta) \dot{\theta},$$

where

$$J_{st}^s(\theta) = \begin{bmatrix} \left(\frac{\partial g_{st}}{\partial \theta_1} g_{st}^{-1} \right)^\vee & \cdots & \left(\frac{\partial g_{st}}{\partial \theta_n} g_{st}^{-1} \right)^\vee \end{bmatrix}. \quad (3.48)$$

We call the matrix $J_{st}^s(\theta) \in \mathbb{R}^{6 \times n}$ the *spatial manipulator Jacobian*. At each configuration θ , it maps the joint velocity vector into the corresponding velocity of the end-effector.

If we represent the forward kinematics using the product of exponentials formula, we can obtain a more explicit and elegant formula for J_{st}^s . Let

$$g_{st}(\theta) = e^{\hat{\xi}_1 \theta_1} \cdots e^{\hat{\xi}_n \theta_n} g_{st}(0)$$

represent the mapping $g_{st} : Q \rightarrow SE(3)$, where $\hat{\xi}_i \in se(3)$ are unit twists. Then,

$$\begin{aligned} \left(\frac{\partial g_{st}}{\partial \theta_i} \right) g_{st}^{-1} &= e^{\hat{\xi}_1 \theta_1} \cdots e^{\hat{\xi}_{i-1} \theta_{i-1}} \frac{\partial}{\partial \theta_i} \left(e^{\hat{\xi}_i \theta_i} \right) e^{\hat{\xi}_{i+1} \theta_{i+1}} \cdots e^{\hat{\xi}_n \theta_n} g_{st}(0) g_{st}^{-1} \\ &= e^{\hat{\xi}_1 \theta_1} \cdots e^{\hat{\xi}_{i-1} \theta_{i-1}} (\hat{\xi}_i) e^{\hat{\xi}_i \theta_i} \cdots e^{\hat{\xi}_n \theta_n} g_{st}(0) g_{st}^{-1} \\ &= e^{\hat{\xi}_1 \theta_1} \cdots e^{\hat{\xi}_{i-1} \theta_{i-1}} (\hat{\xi}_i) e^{-\hat{\xi}_{i-1} \theta_{i-1}} \cdots e^{-\hat{\xi}_1 \theta_1} \end{aligned}$$

and, converting to twist coordinates,

$$\left(\frac{\partial g_{st}}{\partial \theta_i} g_{st}^{-1} \right)^\vee = \text{Ad}_{(e^{\hat{\xi}_1 \theta_1} \cdots e^{\hat{\xi}_{i-1} \theta_{i-1}})} \xi_i. \quad (3.49)$$

The spatial manipulator Jacobian becomes

$$\boxed{\begin{aligned} J_{st}^s(\theta) &= \begin{bmatrix} \xi_1 & \xi_2' & \cdots & \xi_n' \end{bmatrix} \\ \xi_i' &= \text{Ad}_{(e^{\hat{\xi}_1 \theta_1} \cdots e^{\hat{\xi}_{i-1} \theta_{i-1}})} \xi_i \end{aligned}} \quad (3.50)$$

$J_{st}^s(\theta) : \mathbb{R}^n \rightarrow \mathbb{R}^6$ is a configuration-dependent matrix which maps joint velocities to end-effector velocities.

manipulator
Jaco-
bian!
geometric
interpretation
manipulator
Jacobian!
body

Equation (3.50) shows that the manipulator Jacobian has a very special structure. By virtue of the definition of ξ' , the i^{th} column of the Jacobian depends only on $\theta_1, \dots, \theta_{i-1}$. In other words, the contribution of the i^{th} joint velocity to the end-effector velocity is independent of the configuration of later joints in the chain. Furthermore, the i^{th} column of the Jacobian,

$$\xi'_i = \text{Ad}_{(e^{\hat{\xi}_1 \theta_1} \dots e^{\hat{\xi}_{i-1} \theta_{i-1}})} \xi_i,$$

corresponds to the i^{th} joint twist, ξ_i , transformed by the rigid transformation $\exp(\hat{\xi}_1 \theta_1) \dots \exp(\hat{\xi}_{i-1} \theta_{i-1})$. This is precisely the rigid body transformation which takes the i^{th} joint frame from its reference configuration to the current configuration of the manipulator. Thus, *the i^{th} column of the spatial Jacobian is the i^{th} joint twist, transformed to the current manipulator configuration.* This powerful structural property means that we can calculate $J_{st}^s(\theta)$ “by inspection,” as we shall see shortly in an example.

It is also possible to define a *body manipulator Jacobian*, J_{st}^b , which is defined by the relationship

$$V_{st}^b = J_{st}^b(\theta) \dot{\theta}.$$

A calculation similar to that performed previously yields

$$\boxed{\begin{aligned} J_{st}^b(\theta) &= \begin{bmatrix} \xi_1^\dagger & \dots & \xi_{n-1}^\dagger & \xi_n^\dagger \end{bmatrix} \\ \xi_i^\dagger &= \text{Ad}_{(e^{\hat{\xi}_i \theta_i} \dots e^{\hat{\xi}_n \theta_n} g_{st}(0))}^{-1} \xi_i \end{aligned}} \quad (3.51)$$

The columns of J_{st}^b correspond to the joint twists written with respect to the tool frame at the current configuration. Note that $g_{st}(0)$ appears explicitly; choosing S such that $g_{st}(0) = I$ simplifies the calculation of J_{st}^b . The spatial and body Jacobians

adjoint
transformation
between
body and
spatial
manipulator
Jacobian
manipulator
Jacobian
relationship
between body
and spatial
velocity of a
point attached
to end-effector
trajectory
generation,
using
manipulator
Jacobian

are related by an adjoint transformation:

$$J_{st}^s(\theta) = \text{Ad}_{g_{st}(\theta)} J_{st}^b(\theta). \quad (3.52)$$

The spatial and body manipulator Jacobians can be used to compute the instantaneous velocity of a point attached to the end-effector. Let q^b represent a point attached to the end-effector, written in body (tool) coordinates. The velocity of q^b , also in body coordinates, is given by

$$v_q^b = \hat{V}_{st}^b q^b = \left(J_{st}^b(\theta) \dot{\theta} \right)^\wedge q^b.$$

Similarly, if we represent our point relative to the spatial (base) frame, then

$$v_q^s = \hat{V}_{st}^s q^s = \left(J_{st}^s(\theta) \dot{\theta} \right)^\wedge q^s.$$

If we desire the velocity of the origin of the tool frame, then $q^b = 0$ but $q^s = g_{st}(\theta)q^b = p(\theta)$, the position component of the forward kinematics map. Thus, using homogeneous coordinates explicitly,

$$v_q^s = \begin{bmatrix} \dot{p}(\theta) \\ 0 \end{bmatrix} = R_{st} \hat{V}_{st}^b \begin{bmatrix} 0 \\ 1 \end{bmatrix} = \hat{V}_{st}^s \begin{bmatrix} p(\theta) \\ 1 \end{bmatrix}$$

are all equivalent expressions for the velocity of the origin of the tool frame.

The relationship between joint velocity and end-effector velocity can be used to move a robot manipulator from one end-effector configuration to another without calculating the inverse kinematics for the manipulator. If J_{st} is invertible, then we can write

$$\dot{\theta}(t) = (J_{st}^s(\theta))^{-1} V_{st}^s(t). \quad (3.53)$$

If $V_{st}^s(t)$ is known, equation (3.53) is an ordinary differential equation for θ . To move the end-effector between two configurations g_1 and g_2 , we pick *any* workspace path $g(t)$ with $g(0) = g_1$ and $g(T) = g_2$, calculate the spatial velocity $\hat{V}^s = \dot{g}g^{-1}$, and integrate equation (3.53) over the interval $[0, T]$.

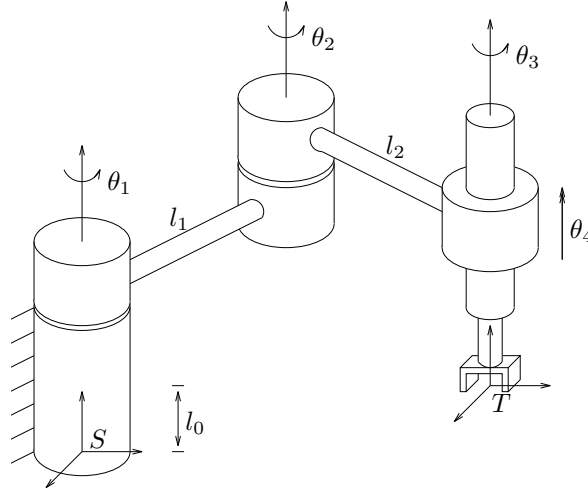


Figure 3.14: SCARA manipulator in non-reference configuration.

Example 3.9. Jacobian for a SCARA robot

Consider the SCARA robot at an arbitrary configuration $\theta \in Q$, as shown in Figure 3.14. The spatial Jacobian can be evaluated by writing the twists associated with each joint in its current configuration. For the SCARA, the directions of the twists are fixed and only the points through which the axes of the twists pass are functions of θ . By inspection,

$$q'_1 = \begin{bmatrix} 0 \\ 0 \\ 0 \end{bmatrix} \quad q'_2 = \begin{bmatrix} -l_1 \sin \theta_1 \\ l_1 \cos \theta_1 \\ 0 \end{bmatrix} \quad q'_3 = \begin{bmatrix} -l_1 \sin \theta_1 - l_2 \sin(\theta_1 + \theta_2) \\ l_1 \cos \theta_1 + l_2 \cos(\theta_1 + \theta_2) \\ 0 \end{bmatrix}$$

are points on the axes. Calculating the associated twists yields

$$J_{st}^s = \begin{bmatrix} 0 & l_1 \cos \theta_1 & l_1 \cos \theta_1 + l_2 \cos(\theta_1 + \theta_2) & 0 \\ 0 & l_1 \sin \theta_1 & l_1 \sin \theta_1 + l_2 \sin(\theta_1 + \theta_2) & 0 \\ 0 & 0 & 0 & 1 \\ 0 & 0 & 0 & 0 \\ 0 & 0 & 0 & 0 \\ 1 & 1 & 1 & 0 \end{bmatrix}.$$

As a check, one can calculate the linear velocity of the end-effector using the formula $(J_{st}^s \dot{\theta})^\wedge p(\theta)$ and verify that it agrees with $\dot{p}(\theta)$.

SCARA
manipula-
tor!manipulator
Jacobian
manipulator
Jaco-
bian!SCARA@for
SCARA
manipulator

Stanford
manipula-
tor!manipulator
Jacobian
manipulator
Jaco-
bian!Stanford@for
Stanford
manipulator

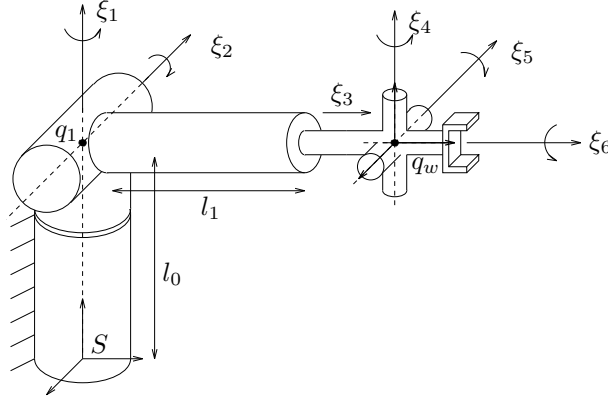


Figure 3.15: An idealized version of the Stanford arm.

Example 3.10. Jacobian for the Stanford arm

The Stanford arm, shown in Figure 3.15, is a six degree of freedom robot with two revolute joints at the base, a prismatic joint, and a spherical wrist. It is very similar to an elbow manipulator, with the “elbow” replaced by a prismatic joint.

The spatial manipulator Jacobian for the Stanford arm is computed by determining the location and directions of the joint twists as a function of the joint angles. For example, the first two joints pass through the point $q_1 = q_2 = (0, 0, l_0)$ and point in the directions $\omega_1 = (0, 0, 1)$ and $\omega'_2 = (-\cos \theta_1, -\sin \theta_1, 0)$. This gives joint twists

$$\xi_1 = \begin{bmatrix} -\omega_1 \times q_1 \\ \omega_1 \end{bmatrix} = \begin{bmatrix} 0 \\ 0 \\ 0 \\ 0 \\ 0 \\ 1 \end{bmatrix} \quad \xi'_2 = \begin{bmatrix} -\omega'_2 \times q_1 \\ \omega'_2 \end{bmatrix} = \begin{bmatrix} l_0 \sin \theta_1 \\ -l_0 \cos \theta_1 \\ 0 \\ -\cos \theta_1 \\ -\sin \theta_1 \\ 0 \end{bmatrix}.$$

The third joint is prismatic and hence we care only about its direction. Taking into account the change in orientation due to the first two joints, we have

$$\xi'_3 = \begin{bmatrix} e^{\widehat{z}\theta_1} e^{-\widehat{x}\theta_2} \begin{bmatrix} 0 \\ 1 \\ 0 \end{bmatrix} \\ 0 \end{bmatrix} = \begin{bmatrix} -\sin \theta_1 \cos \theta_2 \\ \cos \theta_1 \cos \theta_2 \\ -\sin \theta_2 \\ 0 \\ 0 \\ 0 \end{bmatrix} = \begin{bmatrix} v'_3 \\ 0 \end{bmatrix}.$$

Finally, we compute the twists corresponding to the wrist. The wrist is located at

the point

$$q'_w = \begin{bmatrix} 0 \\ 0 \\ l_0 \end{bmatrix} + e^{\widehat{\mathbf{z}}\theta_1} e^{-\widehat{\mathbf{x}}\theta_2} \begin{bmatrix} 0 \\ l_1 + \theta_3 \\ 0 \end{bmatrix} = \begin{bmatrix} -(l_1 + \theta_3) \sin \theta_1 \cos \theta_2 \\ (l_1 + \theta_3) \cos \theta_1 \cos \theta_2 \\ l_0 - (l_1 + \theta_3) \sin \theta_2 \end{bmatrix}.$$

The directions of the wrist axes depend on θ_1 and θ_2 as well as the preceding wrist axes. These are given by

$$\begin{aligned} \omega'_4 &= e^{\widehat{\mathbf{z}}\theta_1} e^{-\widehat{\mathbf{x}}\theta_2} \begin{bmatrix} 0 \\ 0 \\ 1 \end{bmatrix} = \begin{bmatrix} -s_1 s_2 \\ c_1 s_2 \\ c_2 \end{bmatrix} \\ \omega'_5 &= e^{\widehat{\mathbf{z}}\theta_1} e^{-\widehat{\mathbf{x}}\theta_2} e^{\widehat{\mathbf{z}}\theta_4} \begin{bmatrix} -1 \\ 0 \\ 0 \end{bmatrix} = \begin{bmatrix} -c_1 c_4 + s_1 c_2 s_4 \\ -s_1 c_4 - c_1 c_2 s_4 \\ s_2 s_4 \end{bmatrix} \\ \omega'_6 &= e^{\widehat{\mathbf{z}}\theta_1} e^{-\widehat{\mathbf{x}}\theta_2} e^{\widehat{\mathbf{z}}\theta_4} e^{-\widehat{\mathbf{x}}\theta_5} \begin{bmatrix} 0 \\ 1 \\ 0 \end{bmatrix} = \begin{bmatrix} -c_5(s_1 c_2 c_4 + c_1 s_4) + s_1 s_2 s_5 \\ c_5(c_1 c_2 c_4 - s_1 s_4) - c_1 s_2 s_5 \\ -s_2 c_4 c_5 - c_2 s_5 \end{bmatrix}. \end{aligned}$$

Combining these directions with our calculations for q'_w , we can now write the complete manipulator Jacobian:

$$J_{st}^s = \begin{bmatrix} 0 & -\omega'_2 \times q_1 & v'_3 & -\omega'_4 \times q'_w & -\omega'_5 \times q'_w & -\omega'_6 \times q'_w \\ \omega_1 & \omega'_2 & 0 & \omega'_4 & \omega'_5 & \omega'_6 \end{bmatrix}, \quad (3.54)$$

where the various quantities are defined above.

Note that we were able to calculate the entire manipulator Jacobian without explicitly differentiating the forward kinematics map.

As a final comment, we re-emphasize that the manipulator Jacobian differs from the Jacobian of a mapping $f: \mathbb{R}^n \rightarrow \mathbb{R}^p$. For instance, in Example 3.9 (the SCARA manipulator), it is possible to define the configuration of the end-effector as $x = (p(\theta), \phi(\theta))$, where $p(\theta)$ is the xyz position of the tool frame and $\phi(\theta) = \theta_1 + \theta_2 + \theta_3$ is the angle of rotation of the tool frame about the z -axis. The kinematics is then represented by the mapping $x = f(\theta)$ and by the chain rule

$$\dot{x} = \frac{\partial f}{\partial \theta} \dot{\theta}.$$

manipulator
Jaco-
bian! Jacobian@ve
Jacobian of a
mapping
SCARA
manipula-
tor! manipulator
Jacobian

The matrix $\frac{\partial f}{\partial \theta}$ is the Jacobian of the mapping $f : Q \rightarrow \mathbb{R}^4$, but it is *not* the manipulator Jacobian (body or spatial). In particular, the columns of $\frac{\partial f}{\partial \theta}$ cannot be interpreted as the instantaneous twist axes corresponding to each joint.

Similarly, for a general manipulator, one can choose a local parameterization for $SE(3)$ and write the kinematics as $f : Q \rightarrow \mathbb{R}^6$. Once again, the Jacobian of the mapping $f : Q \rightarrow \mathbb{R}^6$ has no direct geometric interpretation, even though it has the same dimensions as the manipulator Jacobian. Furthermore, for manipulators which generate full rotation of the end-effector, the parameterization of $SE(3)$ by a vector of six numbers introduces singularities which are solely an artifact of the parameterization. These singularities may lead to false conclusions about the ability of the manipulator to reach certain configurations or achieve certain velocities. The use of the manipulator Jacobian, as we have defined it here, avoids these difficulties.

4.2 End-effector forces

The manipulator Jacobian can also be used to describe the relationship between wrenches applied at the end-effector and joint torques. This relationship is fundamental in understanding how to program robots to interact with their environment by application of forces. We shall see that the duality of wrenches and twists discussed in Chapter 2 extends to manipulator kinematics.

To derive the relationship between wrenches and torques, we calculate the work associated with applying a wrench through a displacement of the end-effector. If we let $g_{st}(\theta(t))$ represent the motion of the end-effector, the net work performed by applying a (body) wrench F_t over an interval of time $[t_1, t_2]$ is

$$W = \int_{t_1}^{t_2} V_{st}^b \cdot F_t dt,$$

where V_{st}^b is the body velocity of the end-effector. The work will be the same as that performed by the joints (assuming no friction), and hence

$$\int_{t_1}^{t_2} \dot{\theta} \cdot \tau dt = W = \int_{t_1}^{t_2} V_{st}^b \cdot F_t dt.$$

Since this relationship must hold for any choice of time interval, the integrands must be equal. Using the manipulator Jacobian to relate V_{st}^b to $\dot{\theta}$, we have

$$\dot{\theta}^T \tau = \dot{\theta}^T (J_{st}^b)^T F_t.$$

It follows that since $\dot{\theta}$ is free,

$$\tau = (J_{st}^b)^T F_t. \quad (3.55)$$

This equation relates the end-effector wrench to the joint torques by giving the torques that are equivalent to a (body) wrench applied at the end-effector.

A similar analysis can be used to derive the relationship between a spatial wrench F_s applied at the end-effector and the corresponding joint torques:

$$\tau = (J_{st}^s)^T F_s. \quad (3.56)$$

The full derivation of this equation is left as an exercise.

The interpretation of the Jacobian transpose as a mapping from end-effector forces to joint torques must be made carefully. If the Jacobian is square and full rank, there are no difficulties. However, in all other cases, the relationship can be misleading. We defer the discussion of singularities to the next section, and consider only the case when J_{st} is not square.

The formulas given by equations (3.55) and (3.56) describe the force relationship that must hold between the end-effector forces and joint torques. We can use these equations to ask two separate questions:

1. If we apply an end-effector force, what joint torques are required to resist that force?
2. If we apply a set of joint torques, what is the resulting end-effector wrench (assuming that the wrench is resisted by some external agent)?

joint
torques
end-
effector
and
end-effector
forces
Jacobian
transpose

redundant
manipulators
structurally
dependent
forces

SCARA
manipula-
tor!manipulator
Jacobian

manipulator
Jaco-
bian!SCARA@for
SCARA
manipulator

Equation (3.55) answers the first question in all cases. However, in manipulation tasks, we are often more interested in answering the second question, which can be recast as: what joint torques must be applied to generate a given end-effector wrench?

If the number of joints is larger than the dimension of the workspace, then we say the manipulator is *kinematically redundant*. In this case, we can generically find a vector of joint torques which generates the appropriate end-effector force, as given by equation (3.55). However, since there are more joints than the minimum number required, internal motions may exist which allow the manipulator to move while keeping the position of the end-effector fixed. Redundant manipulators are discussed in more detail in Section 5.

If, on the other hand, the number of joints is smaller than the dimension of the workspace, then there may be no torque which satisfies equation (3.55) for arbitrary end-effector wrenches, and therefore some end-effector wrenches cannot be applied. They can, however, be *resisted* by the manipulator. This is a consequence of our assumption that the allowable motion of the manipulator is completely parameterized by the joint angles θ . If a wrench causes no joint torques, it must be resisted by structural forces generated by the mechanism. Such a situation occurs when F lies in the null space of J_{st}^T . In this case, the force balance equation is satisfied with $\tau = 0$; the resisting forces are supplied completely by the robot's mechanical structure.

Example 3.11. End-effector forces for a SCARA robot

Consider again the SCARA robot from the Example 3.9. The transpose of the spatial manipulator Jacobian is

$$(J_{st}^s)^T = \begin{bmatrix} 0 & 0 & 0 & 0 & 0 & 1 \\ l_1 c_1 & l_1 s_1 & 0 & 0 & 0 & 1 \\ l_1 c_1 + l_2 c_{12} & l_1 s_1 + l_2 s_{12} & 0 & 0 & 0 & 1 \\ 0 & 0 & 1 & 0 & 0 & 0 \end{bmatrix}.$$

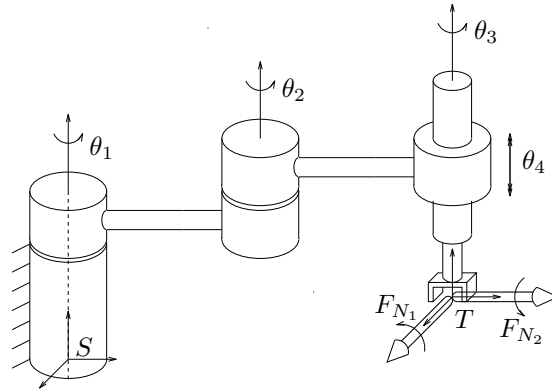


Figure 3.16: End-effector wrenches which generate no joint torques.

The null space of this matrix is spanned by

$$F_{N_1} = \begin{bmatrix} 0 \\ 0 \\ 0 \\ 1 \\ 0 \\ 0 \end{bmatrix} \quad F_{N_2} = \begin{bmatrix} 0 \\ 0 \\ 0 \\ 0 \\ 1 \\ 0 \end{bmatrix};$$

hence, workspace torques about the x - and y -axes of the manipulator cannot be applied by the manipulator. For example, twisting the manipulator as shown in Figure 3.16 generates no joint torques and no motion of the manipulator.

4.3 Singularities

At a given configuration, the manipulator Jacobian describes the relationship between the instantaneous velocity of the end-effector and the joint velocities:

$$V_{bt}^s = J_{bt}^s(\theta)\dot{\theta}.$$

A *singular configuration* of a robot manipulator is a configuration at which the manipulator Jacobian drops rank. For a six degree of freedom manipulator in $SE(3)$, the Jacobian fails to be invertible at singular points and hence the manipulator is not able to achieve instantaneous motion in certain directions. Near singular

end-effector
wrench!manipulat
manipulator
Jacobian—)
manipulator
Jaco-
bian!mapping@for
mapping
forces—)
kinematic
singularities—(
singular
configurations

degrees of freedom!loss of configurations, the size of the joint velocities required to maintain a desired end-effector wrench!singular@at singular configuration effector velocity in certain directions can be extremely large.

Jacobian transpose If a manipulator has fewer than six degrees of freedom, a singular configuration corresponds to a configuration in which the number of degrees of freedom of the end-effector drops. This is again characterized by the manipulator Jacobian dropping rank, i.e., two or more of the columns of $J_{st}^s(\theta) \in \mathbb{R}^{6 \times n}$ become linearly dependent.

kinematic singularities!open-chain@for open-chain manipulators—(Since most manipulators are designed for tasks in which all of the degrees of freedom are needed, singular configurations should usually be avoided, if possible.

collinear revolute joints

Singularities also affect the size of the end-effector forces that the manipulator can apply. At a singular configuration, some end-effector wrenches will lie in the null space of the Jacobian transpose. These wrenches can be balanced without applying *any* joint torques, as the mechanism will generate the opposing wrenches. On the other hand, *applying* an end-effector wrench in a singular direction is not possible. Such a wrench could be balanced by any wrench in the singular direction, and hence it can be balanced by the zero wrench. If no other external forces are present, no forces will be generated.

In order to avoid these difficulties, it is necessary to identify singular configurations of a manipulator. We concentrate on classifying several common singularities for six degree of freedom manipulators and show how these can be determined by analyzing the geometry of the system. The cases presented here can be extended to consider more general open-chain manipulators. For each of the geometric conditions given below, we give a sketch of the proof of singularity. To illustrate some of the different ways in which singularities can be analyzed, we use a different proof technique for each example.

Example 3.12. Two collinear revolute joints

The Jacobian for a six degree of freedom manipulator is singular if there exist two

revolute joints with twists

spherical wrist

$$\xi_1 = \begin{bmatrix} -\omega_1 \times q_1 \\ \omega_1 \end{bmatrix} \quad \xi_2 = \begin{bmatrix} -\omega_2 \times q_2 \\ \omega_2 \end{bmatrix}$$

which satisfy the following conditions:

1. The axes are parallel: $\omega_1 = \pm\omega_2$.
2. The axes are collinear: $\omega_i \times (q_1 - q_2) = 0$, $i = 1, 2$.

Proof. In analyzing the singularity of a matrix, we are permitted to pre- or post-multiply the matrix by a nonsingular matrix of the proper dimensions. Pre-multiplication by a nonsingular matrix can be used to add one row to another or switch two rows, while post-multiplication can be used to perform the same operations on columns.

Assume, without loss of generality, that the columns of the Jacobian which are linearly dependent are the *first* two columns of J . The Jacobian has the form

$$J(\theta) = \begin{bmatrix} -\omega_1 \times q_1 & -\omega_2 \times q_2 & \cdots \\ \omega_1 & \omega_2 & \cdots \end{bmatrix} \in \mathbb{R}^{6 \times 6}$$

and we can assume $\omega_1 = \omega_2$ by negating the second column if necessary. Subtracting column 1 from column 2 yields

$$J(\theta) \sim \begin{bmatrix} -\omega_1 \times q_1 & -\omega_2 \times (q_2 - q_1) & \cdots \\ \omega_1 & 0 & \cdots \end{bmatrix},$$

where the symbol \sim denotes equivalence of two matrices (up to elementary column operations). Using condition 2, the second column is zero, so that $J(\theta)$ is singular.

□

This type of singularity is common in spherical wrist assemblies that are composed of three mutually orthogonal revolute joints whose axes intersect at a point. By rotating the second joint in the wrist, it is possible to align the first and third axes and the manipulator Jacobian becomes singular. In this configuration, rotation about the axis normal to the plane defined by the first and second joints is not possible.

coplanar
revolute axes
coordinate
transforma-
tions!use in
analyzing
singularities
adjoint
transforma-
tion!between
body and
spatial
manipulator
Jacobian

Example 3.13. Three parallel coplanar revolute joint axes

The Jacobian for a six degree of freedom manipulator is singular if there exist three revolute joints which satisfy the following conditions:

1. The axes are parallel: $\omega_i = \pm\omega_j$ for $i, j = 1, 2, 3$.
2. The axes are coplanar: there exists a plane with unit normal n such that $n^T\omega_i = 0$ and

$$n^T(q_i - q_j) = 0, \quad i, j = 1, 2, 3.$$

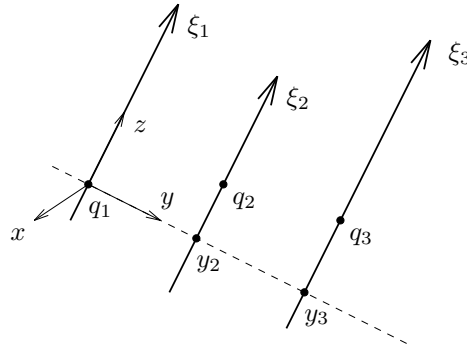
Proof. Another type of transformation which can be used in analyzing singularities is to change the frame of reference used to express the twists that form the columns of the Jacobian. A change of coordinates affects twists (and hence the Jacobian) by pre-multiplying by the adjoint matrix corresponding to the change of basis. Since the adjoint is an invertible transformation ($\text{Ad}_g^{-1} = \text{Ad}_{g^{-1}}$), this does not affect the singularity of the matrix.

After an initial column permutation, assume $J(\theta)$ has the form

$$J(\theta) = \begin{bmatrix} -\omega_1 \times q_1 & -\omega_2 \times q_2 & -\omega_3 \times q_3 & \cdots \\ \omega_1 & \omega_2 & \omega_3 & \cdots \end{bmatrix}.$$

Attach a coordinate frame to the point q_1 with the z -axis of the frame pointing in the direction of ω_1 (see Figure 3.17). Further, choose the frame such that the plane formed by the axes is the yz plane in the new coordinates. Thus, each axis has a point of intersection which lies on the y -axis. Call these points $y_1(=0)$, y_2 , and y_3 . Now, with respect to this frame, the Jacobian has the form

$$\text{Ad}_g J(\theta) = \begin{bmatrix} 0 & \pm y_2 & \pm y_3 & \\ 0 & 0 & 0 & \cdots \\ 0 & 0 & 0 & \\ 0 & 0 & 0 & \\ 0 & 0 & 0 & \cdots \\ 1 & \pm 1 & \pm 1 & \end{bmatrix}.$$



intersecting
joint axes
reciprocal
screws!use in
analyzing
mechanisms

Figure 3.17: Three coplanar, parallel, revolute twists.

The first three columns are clearly linearly dependent. \square

The elbow manipulator exhibits this singularity in its reference configuration (see Figure 3.11).

Example 3.14. Four intersecting revolute joint axes

The Jacobian for a six degree of freedom manipulator is singular if there exist four revolute joint axes that intersect at a point q :

$$\omega_i \times (q_i - q) = 0, \quad i = 1, \dots, 4.$$

Proof. This example is trivial if we choose a frame whose origin is at the common point of intersection of the four revolute twists. However, we can also show singularity by making use of reciprocal screw systems. Recall from Section 5.3 of Chapter 2 that a wrench is reciprocal to a twist when the inner product between the wrench and the twist is zero (indicating that no work is done by applying the wrench and moving along the twist). Since we are in a 6-dimensional space, if we can show that the dimension of the reciprocal system is sufficiently large (three for this example), then we can show singularity of the system of twists. This technique works well when there are a large number of twists and hence the size of the reciprocal system is small.

degrees of freedom!loss of kinematic singularities!open-chain@for open-chain manipulators—) origin: kinematic singularities—)

For this example, we make use of the following fact: every revolute twist is reciprocal to a pure force, in any direction, applied to a point on the axis of the revolute twist. To see this, it suffices to consider a twist and wrench through the

$$V = \begin{bmatrix} 0 \\ \omega \end{bmatrix} \quad F = \begin{bmatrix} f \\ 0 \end{bmatrix} \quad \implies \quad V^T F = 0.$$

It is left to the reader to verify that this case generalizes appropriately.

We can now use this fact to construct the reciprocal system for the four twists which intersect at a point. Since any pure force through this point corresponds to a reciprocal wrench, it follows that the dimension of the reciprocal system is three and hence the four twists must be singular. \square

This type of singularity occurs in the inverse elbow manipulator (see Exercise ??) when the final joint axis intersects the shoulder adding a fourth axis as shown.

The singularities given here and in the exercises are by no means exhaustive. However, they do occur frequently and are often easy to determine just by examining the geometry of the manipulator. It is also possible for a manipulator to exhibit different types of singularities at a single configuration. In this case, depending on the number and type of the singularities, the manipulator may lose the ability to move in several different directions at once. For example, if the arm of the elbow manipulator shown in Figure 3.4 is held vertically over the base, it exhibits all three of the singularities we have just illustrated. However, it still has four degrees of freedom (instead of three) since two of the singularities restrict motion in the same direction.

In addition to singularities of the manipulator Jacobian, a robot can also lose degrees of freedom when the joint variables are constrained to lie in a closed interval. In this case, a loss of freedom of motion can occur when one or more of the joints is at the limit of its travel. At such a configuration, motion past the joint limit is not allowed and the motion of the end-effector is restricted.

4.4 Manipulability

As we saw in the previous section, when a manipulator is at a singular configuration there are directions of movement which require high joint rates and forces. Near a singularity, movement may also be difficult in certain directions. The *manipulability* of a robot describes its ability to move freely in all directions in the workspace.

manipulability
measures—
(manipulator
Jaco-
bian!manipulabili-
manipulability
measures
singular values
of a matrix

Manipulability measures can be divided into two rough classes:

1. The ability to *reach* a certain position or set of positions
2. The ability to *change* the position or orientation at a given configuration

The first of these measures is directly related to the workspace of a manipulator. Depending on the task, we may want to use the complete, reachable, or dextrous workspaces to characterize the manipulability of a manipulator. The second class of measures concerns the manipulability of a manipulator around a given configuration; that is, it is a local property.

To study local manipulability, we examine the Jacobian of the manipulator, which relates infinitesimal joint motions to infinitesimal workspace motions. Throughout this section we write J for the manipulator Jacobian J_{st} . Either the spatial or body Jacobian can be used, but the body Jacobian is preferred since the body velocity of the end-effector is independent of the choice of base frame.

There are many different local manipulability measures that have been proposed in the literature and which are useful in different situations. We present a small sample of some of the more common measures here. Many of these measures rely on the singular values of J . Recall that for a matrix $A \in \mathbb{R}^{p \times n}$, the singular values of A are the square roots of the eigenvalues of $A^T A$. We write $\sigma(A)$ for the set of singular values of A and $\lambda(A)$ to denote the set of eigenvalues of A . The maximum singular value of a matrix is equal to the induced two-norm of the matrix:

$$\sigma_{\max}(A) = \max_{\|x\|_2=1} \|Ax\|_2 = \|A\|_2.$$

condition
number of a
matrix

If a matrix is singular, then at least one of its singular values is zero.

Example 3.15. Minimum singular value of J

$$\mu_1(\theta) = \sigma_{\min}(J(\theta))$$

The minimum singular value of the Jacobian corresponds to the minimum workspace velocity that can be produced by a unit joint velocity vector. The corresponding eigenvector gives the direction (twist) in which the motion of the end-effector is most limited. At a singular configuration, the minimum singular value of J is zero.

Example 3.16. Inverse of the condition number of J

$$\mu_2(\theta) = \frac{\sigma_{\min}(J(\theta))}{\sigma_{\max}(J(\theta))}$$

The condition number of a matrix A is defined as the ratio of the maximum singular value of A to the minimum singular value of A . For the Jacobian, the inverse condition number gives a measure of the sensitivity of the magnitude of the end-effector velocity V to the direction of the joint velocity vector $\dot{\theta}$. It provides a normalized measure of the minimum singular value of J . At a singular configuration, the inverse condition number is zero.

Example 3.17. Determinant of J

$$\mu_3(\theta) = \det J(\theta)$$

The determinant of the Jacobian measures the volume of the velocity ellipsoid (in the workspace) generated by unit joint velocity vectors. It is important to note that $\mu_3(\theta)$ does not contain information about the condition number of J . In particular, since $\det J(\theta)$ is the product of the singular values of $J(\theta)$, it can be large even if $\sigma_{\min}(J(\theta))$ is small, by having a large $\sigma_{\max}(J(\theta))$.

These manipulability measures can be used to provide an alternate definition for the dextrous workspace of a manipulator. For any of the measures given above, define the set W'_D as

$$W'_D = \{g_{st}(\theta) : \theta \in Q, \mu_i(\theta) \neq 0\} \subset SE(3). \quad (3.57)$$

W'_D is the set of end-effector configurations for which the manipulator can move infinitesimally in any direction. Note that W'_D is a subset of $SE(3)$, unlike our previous definition (in equation (3.13)) which consisted of the subset of \mathbb{R}^3 at which the manipulator could achieve *any* orientation.

Additional manipulability measures are given in the exercises.

5 Redundant and Parallel Manipulators

In this section, we briefly consider some other kinematic mechanisms that occur frequently in robotic manipulation. We focus on two particular types of structures—redundant manipulators and parallel manipulators—and indicate how to extend some of the results of this chapter to cover these cases.

5.1 Redundant manipulators

In order to perform a given task, a robot must have enough degrees of freedom to accomplish that task. In the analysis presented so far, we have concentrated on the case in which the robot has precisely the required degrees of freedom. A *kinematically redundant* manipulator has more than the minimal number of degrees of freedom required to complete a set of tasks.

A redundant manipulator can have an infinite number of joint configurations which give the same end-effector configuration. The extra degrees of freedom present in redundant manipulators can be used to avoid obstacles and kinematic singularities or to optimize the motion of the manipulator relative to a cost function. Addition-

ally, if joint limits are present, redundant manipulators can be used to increase the workspace of the manipulator.

The derivation of the forward kinematics of a redundant manipulator is no different from the derivation presented in Section 2. Using the product of exponentials formula,

$$g_{st}(\theta) = e^{\hat{\xi}_1 \theta_1} \dots e^{\hat{\xi}_n \theta_n} g_{st}(0),$$

where n is greater than p , the dimension of the workspace ($p = 3$ for planar manipulators and $p = 6$ for spatial manipulators). The Jacobian of a redundant manipulator has the form

$$J_{st}^s(\theta) = \begin{bmatrix} \xi_1 & \xi_2' & \dots & \xi_n' \end{bmatrix},$$

where ξ_i' is the twist corresponding to the i^{th} joint axis in the current configuration. $J_{st}^s \in \mathbb{R}^{p \times n}$ has more columns than rows.

The inverse kinematics problem for a redundant manipulator is ill-posed: there may exist infinitely many configurations of the robot which give the desired end-effector configuration. In fact, if we keep the end-effector configuration fixed, the robot is still free to move along any trajectory which satisfies

$$g_{st}(\theta(t)) = g_d, \quad (3.58)$$

where $g_d \in SE(3)$ is the desired configuration of the end-effector. The set of all θ which satisfy this equation is called the *self-motion manifold* for the configuration g_d . Differentiating equation (3.58), we obtain

$$J_{st}^s(\theta(t))\dot{\theta} = (\dot{g}_{st}g_{st}^{-1})^\vee = 0.$$

Thus, the motions which are allowed must have joint velocities which lie in the null space of the manipulator Jacobian. A motion along the self-motion manifold is called an *internal motion*.

More generally, given an end-effector path $g(t)$, we would like to find a corresponding joint trajectory $\theta(t)$. Since there may be an infinite number of joint trajectories which give the requisite end-effector path, additional criteria are used to choose among them. One common solution is to choose the minimum joint velocity which gives the desired workspace velocity. This is achieved by choosing

$$\dot{\theta} = J_{st}^\dagger(\theta)V_{st},$$

where $J^\dagger = J^T(JJ^T)^{-1}$ is the Moore-Penrose generalized inverse of J . The properties of this and other kinematic redundancy resolution algorithms are discussed briefly in Chapter 7.

The manipulator Jacobian can also be used to relate joint torques to end-effector wrenches for redundant manipulators. Since the links of the manipulator are free to move even when the end-effector is fixed, a thorough understanding of the relationship between joint forces and end-effector wrenches requires a study of the dynamics of the manipulator. In particular, the possible existence of internal motions, combined with the inertial coupling between the links, can cause forces to be applied to the end-effector even if no joint torques are applied. We defer a complete discussion of this situation until Chapter 6, in which we study the dynamics of constrained systems in full detail. Using the results of that chapter, it will be possible to show that when a manipulator is in *static equilibrium*, the previous relationship,

$$\tau = J_{st}^T F, \quad (3.59)$$

still holds. This relationship gives the joint torques necessary to produce a given end-effector wrench when the system is stationary. Either the body or spatial Jacobian can be used, as long as the wrench F is represented appropriately.

Example 3.18. Self-motion manifold for a planar manipulator

Consider the planar manipulator shown in Figure 3.18a. Holding the position of the

pseudo-inverse
for resolving
redundancy
manipulator
Jaco-
bian!mapping@for
mapping
forces
end-effector
wrench!manipulat
manipulator
Jacobian
end-effector
wrench!redundant
redundant
manipulators

redundant
manipulators!kinematics—)

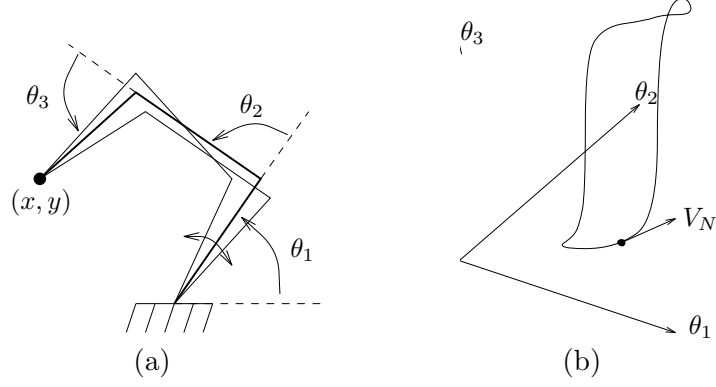


Figure 3.18: Self-motion manifold for a redundant planar manipulator.

end-effector fixed, the system obeys the following kinematic constraints:

$$\begin{aligned} l_1 \cos \theta_1 + l_2 \cos(\theta_1 + \theta_2) + l_3 \cos(\theta_1 + \theta_2 + \theta_3) &= x \\ l_1 \sin \theta_1 + l_2 \sin(\theta_1 + \theta_2) + l_3 \sin(\theta_1 + \theta_2 + \theta_3) &= y. \end{aligned}$$

This is a set of two equations in three variables and hence there exist multiple solutions. A self-motion manifold for this manipulator is shown in Figure 3.18b.

The Jacobian for the mapping $p : \theta \mapsto (x, y)$ is

$$\frac{\partial p}{\partial \theta} = \begin{bmatrix} -l_1 s_1 - l_2 s_{12} - l_3 s_{123} & -l_2 s_{12} - l_3 s_{123} & -l_3 s_{123} \\ l_1 c_1 + l_2 c_{12} + l_3 c_{123} & l_2 c_{12} + l_3 c_{123} & l_3 c_{123} \end{bmatrix}, \quad (3.60)$$

where $s_{ijk} = \sin(\theta_i + \theta_j + \theta_k)$ and similarly for c_{ijk} . The Jacobian has a null space spanned by the vector

$$V_N = \begin{bmatrix} l_2 l_3 \sin \theta_3 \\ -l_2 l_3 \sin \theta_3 - l_1 l_3 \sin(\theta_2 + \theta_3) \\ l_1 l_2 \sin \theta_2 + l_1 l_3 \sin(\theta_2 + \theta_3) \end{bmatrix}.$$

Any velocity $\dot{\theta} = \alpha V_N$ is tangent to the self-motion manifold and maintains the position of the end-effector. One such velocity is shown as an arrow on Figure 3.18b.

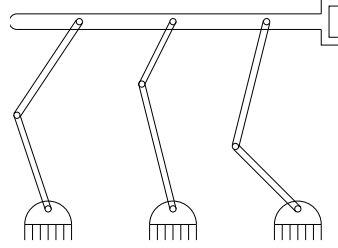


Figure 3.19: A parallel manipulator consisting of three series chains connected to a single end-effector.

5.2 Parallel manipulators

A *parallel* manipulator is one in which two or more series chains connect the end-effector to the base of the robot. An example is shown in Figure 3.19. Parallel manipulators can offer advantages over open-chain manipulators in terms of rigidity of the mechanism and placement of the actuators. For example, the manipulator in Figure 3.19 can be completely actuated by controlling only the first link in each chain, eliminating the need to place motors at the distal links of the manipulator. Parallel manipulators are also called *closed-chain* manipulators, since they contain one or more closed kinematic chains.

Structure equation for a parallel mechanism

The forward kinematics for a parallel manipulator are described by equating the end-effector location specified by each chain. Suppose we have a manipulator with n_1 joints in the first chain (including the end-effector) and n_2 joints in the second chain (including the end-effector). Then, the forward kinematics is described in exponential coordinates as

$$g_{st} = e^{\hat{\xi}_{11}\theta_{11}} \dots e^{\hat{\xi}_{1n_1}\theta_{1n_1}} g_{st}(0) = e^{\hat{\xi}_{21}\theta_{21}} \dots e^{\hat{\xi}_{2n_2}\theta_{2n_2}} g_{st}(0), \quad (3.61)$$

where all quantities are specified relative to a single base and tool frame. Equation (3.61) is called the *structure equation* (or loop equation) for the manipulator

parallel
manipulators—
structure
equations—
forward
kinemat-
ics!parallel@for
parallel
manipulators

joint space!parallel@for parallel manipulators and introduces constraints between the possible joint angles of the manipulator. It is because of these constraints that we can control the end-effector location by specifying only a subset of the joint variables: the other joint variables must take on values such that equation (3.61) is satisfied.

Gruebler's formula Since the joint variables are constrained by equation (3.61), the joint space for a parallel manipulator is not simply the Cartesian product of the individual joint spaces, as in the open-chain case. Rather, it is the subset $Q' \subset Q$ which also satisfies equation (3.61). Determining the dimension of Q' , and hence the number of degrees of freedom for the parallel manipulator, requires careful inspection of the number of joints and links in the mechanism.

inverse kinematics!parallel@for parallel manipulators Let N be the number of links in the mechanism, g the number of joints, and f_i the number of degrees of freedom for the i^{th} joint. The number of degrees of freedom can be obtained by taking the total degrees of freedom for all of the links and subtracting the number of constraints imposed by the joints attached to the links. If all of the joints define independent constraints, the number of degrees of freedom for the mechanism is

$$F = 6N - \sum_{i=1}^g (6 - f_i) = 6(N - g) + \sum_{i=1}^g f_i. \quad (3.62)$$

Equation (3.62) is called *Gruebler's formula*. Gruebler's formula only holds when the constraints imposed by the joints are independent. For planar motions, Gruebler's formula holds with 6 replaced by 3.

Although the forward kinematics of a parallel manipulator is complicated by the closed loop nature of the mechanism, the inverse problem is no more difficult than in the open-chain case. Namely, the inverse kinematics problem for a parallel manipulator is solved by considering the inverse problem for each open-chain mechanism which connects the ground to the end-effector. This can be done using the methods presented in Section 3.

Velocity and force relationships

The velocity of the end-effector of a parallel manipulator is related to the velocity of the joints of the manipulator by differentiating the structure equation (3.61). This gives a Jacobian matrix for each chain:

$$V_{st}^s = J_1^s \begin{bmatrix} \dot{\theta}_{11} \\ \vdots \\ \dot{\theta}_{1n_1} \end{bmatrix} = J_2^s \begin{bmatrix} \dot{\theta}_{21} \\ \vdots \\ \dot{\theta}_{2n_2} \end{bmatrix}, \quad (3.63)$$

where

$$J_1^s = \begin{bmatrix} \xi_{11} & \xi'_{12} & \cdots & \xi'_{1n_1} \end{bmatrix} \quad J_2^s = \begin{bmatrix} \xi_{21} & \xi'_{22} & \cdots & \xi'_{2n_2} \end{bmatrix}.$$

Since the mechanism contains closed kinematic chains, not all joint velocities can be specified independently.

The manipulator Jacobian can be written in more conventional form by stacking the Jacobians for each chain:

$$\begin{bmatrix} J_1^s & 0 \\ 0 & J_2^s \end{bmatrix} \dot{\theta} = \begin{bmatrix} I \\ I \end{bmatrix} V_{st}^s. \quad (3.64)$$

This equation has a form very similar to one which we shall use in Chapter 5 to describe the kinematics of a multifingered grasp. Indeed, if we view each of the chains as grasping the end-effector link via a prismatic or revolute joint, then a parallel manipulator is very similar to a multifingered hand grasping an object.

The relationship between joint torques and end-effector forces for a parallel manipulator is more complicated than for an open-chain manipulator. The basic problem is that two or more chains can fight against each other and apply forces which cause no net end-effector wrench. A set of joint torques which causes no net end-effector wrench is called an *internal force*. We defer a discussion of internal forces until Chapter 5, where they arise naturally in the context of grasping.

Singularities

end-effector
veloc-
ity!parallel@for
parallel
manipulators
manipulator
Jaco-
bian!parallel@for
parallel
manipulators
grasping!similarity
to parallel
mechanisms
end-effector
wrench!parallel@f
parallel
manipulators
internal forces
structure
equations—)
kinematic
singulari-
ties!parallel@for
parallel
manipulators
parallel
manipula-
tors!kinematic
singularities

admissible
velocities, for
parallel
manipulators
rank of
structure
equations

Determining the singularities of parallel mechanisms is more involved than it is for serial mechanisms. Consider a general parallel mechanism with k chains and let Θ_i denote the joint variables in the i^{th} chain. The Jacobian of the structure equations has the form

singular
configura-
tions!parallel@for
parallel
manipulators
kinematic

$$V_{st}^s = J_1(\Theta_1)\dot{\Theta}_1 = \cdots = J_k(\Theta_k)\dot{\Theta}_k. \quad (3.65)$$

singularity
ties!actuator@versus
actuator
singularities

We say that an end-effector velocity is *admissible* at a configuration $\Theta = (\Theta_1, \dots, \Theta_k)$ if there exist $\dot{\Theta}_i$ which satisfy equation (3.65). The set of admissible velocities forms a linear space, since it is the intersection of the range spaces of $J_i(\theta)$, $i = 1, \dots, k$.

actuator
singularities
four-bar
linkage—(

Hence, we can define the *rank of the structure equations*, ρ , at a configuration Θ as the dimension of the space of admissible velocities,

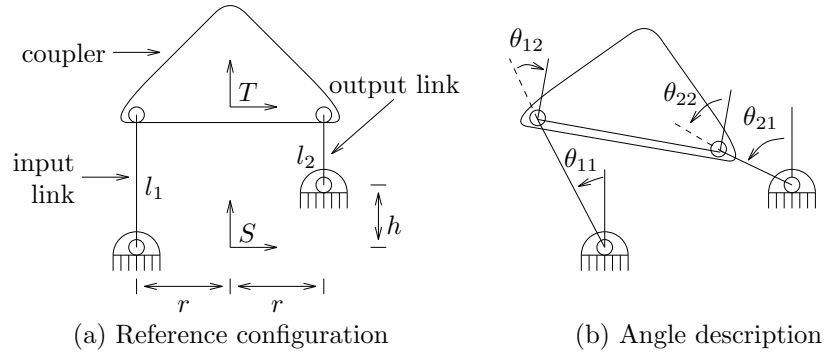
$$\rho = \dim \bigcap_{i=1}^k \mathcal{R}(\mathcal{J}_i(\theta)), \quad (3.66)$$

where $\mathcal{R}(\mathcal{A})$ denotes the range space of the matrix A .

A parallel mechanism is *kinematically singular* at a point if the rank of the structure equations drops at that point. In this case, the tool loses the ability to move instantaneously in some direction. This is analogous to our description of singularities in serial mechanisms. However, at this point we have not yet identified which joints in the mechanism are actuated and which are passive. If a parallel mechanism is fully actuated, then these are the only types of singularities that can occur. However, in most instances, only some of the joints of a parallel manipulator are actuated and this can lead to additional singularities. We call this second type of singularity an *actuator singularity* and give an example of it when we study the Stewart platform in Section 5.4.

5.3 Four-bar linkage

To illustrate some of the concepts introduced above, we consider the four-bar linkage shown in Figure 3.20. The mechanism consists of three rigid bodies connected



degrees of freedom of four-bar mechanism

Figure 3.20: Four-bar linkage.

together by revolute joints. The links attached to the ground frame are called the *input* and *output* links, the rigid body which connects the input and output links is called the *coupler*. It is called a four-bar mechanism even though there are only three links, since historically the ground frame is considered to be the fourth link.

Four-bar linkages are usually studied in the context of mechanism synthesis. For example, we might try to find a mechanism such that the input and output links satisfy a given functional relationship, creating a type of mechanical computer. Alternatively, one might wish to design the mechanism so that a point on the coupler traces a specified path or passes through a set of points. Many other variations exist, but for all of these problems one tries to choose the kinematic parameters which describe the mechanism—the lengths of the links, shape of the coupler, location of the joints—so that a given task is performed. In this section, we bypass the synthesis problem and concentrate on kinematic analysis of a given mechanism.

The number of degrees of freedom of a four-bar mechanism is given by Gruebler's formula:

$$N = 3 \text{ links}$$

$$g = 4 \text{ joints} \quad \implies \quad F = 3(3 - 4) + 4 = 1.$$

$$f_i = 1 \text{ DOF/link}$$

The fact that there is only one degree of freedom helps explain the terminology of

structure equations
for
four-bar
mechanism

the input and output links. Note that we used the planar version of Gruebler's formula to calculate the mobility of the mechanism. A quick calculation shows that the spatial version of the formula gives $F = 6(3 - 4) + 4 = -2$ (!). We leave the resolution of this apparent paradox as an exercise.

To write the structure equations, we must first assign base and tool frames and choose a reference configuration. The tool and base frames are assigned as shown in the figure. We choose the reference configuration ($\theta = 0$) to be the configuration shown in Figure 3.20a. Note that this is not the usual reference configuration if we had considered each of the kinematic chains as independent two-link robots. However, it will be convenient to have the reference configuration satisfy the kinematic constraints and hence we define the angles as shown in Figure 3.20b. With respect to this configuration, the structure equations have the form

$$g_{st} = e^{\hat{\xi}_{11}\theta_{11}} e^{\hat{\xi}_{12}\theta_{12}} g_{st}(0) = e^{\hat{\xi}_{21}\theta_{21}} e^{\hat{\xi}_{22}\theta_{22}} g_{st}(0).$$

Note that in the plane this gives three constraints in terms of four variables, leaving one degree of freedom as expected.

The twists can be calculated using the formulas for twists in the plane derived in the exercises at the end of Chapter 2. In particular, a revolute joint in the plane through a point $q = (q_x, q_y)$ is described by a planar twist

$$\xi = \begin{bmatrix} q_y \\ -q_x \\ 1 \end{bmatrix} \in \mathbb{R}^3.$$

This yields

$$\begin{aligned} \xi_{11} &= \begin{bmatrix} 0 \\ r \\ 1 \end{bmatrix} & \xi_{12} &= \begin{bmatrix} l_1 \\ r \\ 1 \end{bmatrix} & \xi_{21} &= \begin{bmatrix} h \\ -r \\ 1 \end{bmatrix} & \xi_{22} &= \begin{bmatrix} h + l_2 \\ -r \\ 1 \end{bmatrix} \\ g_{st}(0) &= \begin{bmatrix} I & \begin{bmatrix} 0 \\ h+l_2 \end{bmatrix} \\ 0 & 1 \end{bmatrix}. \end{aligned}$$

Expanding the product of exponentials formula gives

$$\begin{aligned} -r - l_1 \sin \theta_{11} + r \cos(\theta_{11} + \theta_{12}) &= x = r - l_2 \sin \theta_{21} - r \cos(\theta_{21} + \theta_{22}) \\ l_1 \cos \theta_{11} + r \sin(\theta_{11} + \theta_{12}) &= y = h + l_2 \cos \theta_{21} - r \sin(\theta_{21} + \theta_{22}) \\ \theta_{11} + \theta_{12} &= \phi = \theta_{21} + \theta_{22} \end{aligned}$$

kinematic
singularities!four-
bar@for
four-bar
mechanism

where ϕ is the angle the tool frame makes with the horizontal. From the form of this equation, it is clear that solving for the forward kinematics is a complicated task, though it turns out that in many cases it can be done in closed form.

The Jacobian of the structure equation has the form

$$V_{st}^s = \begin{bmatrix} \xi_{11} & \xi'_{12} \end{bmatrix} \begin{bmatrix} \dot{\theta}_{11} \\ \dot{\theta}_{12} \end{bmatrix} = \begin{bmatrix} \xi_{21} & \xi'_{22} \end{bmatrix} \begin{bmatrix} \dot{\theta}_{21} \\ \dot{\theta}_{22} \end{bmatrix}.$$

To calculate the individual columns of the Jacobian, we write the twists at the current configuration of the manipulator. Thus,

$$V_{st}^s = \begin{bmatrix} 0 & l_1 \cos \theta_{11} \\ r & r + l_1 \sin \theta_{11} \\ 1 & 1 \end{bmatrix} \begin{bmatrix} \dot{\theta}_{11} \\ \dot{\theta}_{12} \end{bmatrix} = \begin{bmatrix} h & h + l_2 \cos \theta_{21} \\ -r & -r + l_2 \sin \theta_{21} \\ 1 & 1 \end{bmatrix} \begin{bmatrix} \dot{\theta}_{21} \\ \dot{\theta}_{22} \end{bmatrix}.$$

This gives the velocity constraints on the system. Since the individual Jacobians for each chain only have two columns, it is clear that the dimension of the space of admissible velocities is at most two. To examine the mobility more closely, we rearrange the Jacobian to isolate the actuated and passive joints.

Suppose we take $\theta = \theta_{11}$ as the actuated joint and let $\alpha = (\theta_{12}, \theta_{21}, \theta_{22})$ represent the passive joints. The Jacobian of the structure equation can be rearranged as

$$\xi_{11} \dot{\theta} = \begin{bmatrix} -\xi'_{12} & \xi_{21} & \xi'_{22} \end{bmatrix} \dot{\alpha} \quad (3.67)$$

(this type of rearrangement works only in the special case where we have two serial chains or a single kinematic loop). The form of this equation suggests that if we specify the velocity of the actuated joint θ , then we can solve for the velocity of the passive joints if the right-hand side of equation (3.67) is nonsingular.

uncertainty
configuration

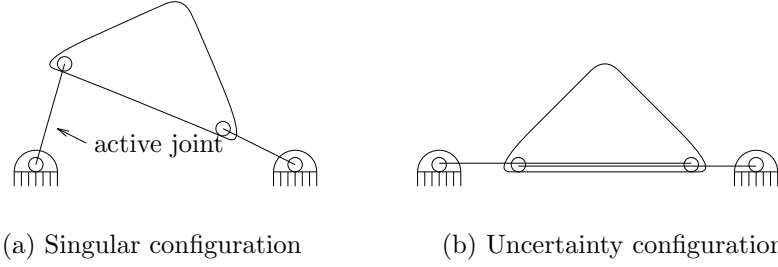


Figure 3.21: Potential singular configurations for four-bar mechanisms.

The right-hand side of equation (3.67) corresponds to the twists generated by three parallel, revolute joints. We know from our study of singularities of twists that if the three axes are coplanar in addition to being parallel, then the twists are linearly dependent. In the planar case, this means that if the passive joints are collinear, then the right-hand side of equation (3.67) loses rank and the mechanism may not be able to move. However, this condition is not sufficient since it may happen that ξ_{11} is in the range of $\{\xi'_{12}, \xi_{21}, \xi'_{22}\}$ even though they are singular. These two different situations are shown in Figure 3.21. Note that switching the role of the input and output links changes the singular configurations of the mechanism. For example, the singularity shown in Figure 3.21a is only a singularity if the left-hand link is chosen as the input link (since this choice gives three collinear passive joints).

The configuration shown in Figure 3.21b is known as an *uncertainty configuration* in the kinematics literature. In this case, it is actually possible for the mechanism to move instantaneously in two independent directions. Examining the structure equations, we see that

$$\begin{bmatrix} 0 & 0 \\ r & r - l_1 \\ 1 & 1 \end{bmatrix} \begin{bmatrix} \dot{\theta}_{11} \\ \dot{\theta}_{12} \end{bmatrix} = \begin{bmatrix} 0 & 0 \\ -r & -r + l_1 \\ 1 & 1 \end{bmatrix} \begin{bmatrix} \dot{\theta}_{21} \\ \dot{\theta}_{22} \end{bmatrix}$$

and hence

$$\dot{\theta}_{N_1} = \begin{bmatrix} 1 \\ -1 \\ -1 \\ 1 \end{bmatrix} \quad \text{and} \quad \dot{\theta}_{N_2} = \begin{bmatrix} r - l_1 \\ -r \\ r - l_1 \\ -r \end{bmatrix}$$

represent two independent, instantaneously admissible velocities. These two independent velocities exist only if the mechanism is perfectly aligned and hence uncertainty configurations rarely occur in practice.

5.4 Stewart platform

Another common example of a parallel mechanism is the Stewart platform, an example of which is shown in Figure 3.22. The mechanism consists of two rigid bodies, connected by a set of prismatic joints. Each prismatic joint is connected to the rigid body by a spherical joint, allowing complete rotational motion. Only the prismatic joints are actuated.

Stewart platforms are commonly used in aircraft flight simulators to move an aircraft cockpit along the motion indicated by the (simulated) dynamics of the system. Although the concept of a Stewart platform is quite old (it was studied by Stewart in the 1950s [72]), it is only recently that the kinematics for a general Stewart platform have been solved in complete generality.

In order to write the structure equation for a Stewart platform, we must first take a slight detour and discuss the modeling of a spherical joint. For the manipulators we have considered previously, we have always modeled a spherical joint as three revolute joints intersecting at a point. This made physical sense since this is how most actuated spherical wrists are built. However, spherical wrists always have singularities when any two of the axes become parallel (it can be shown that this will always happen for some choice of joint angles). In a Stewart platform, the spherical joints are completely passive and hence will never become singular. This requires that we define spherical joints slightly differently than spherical wrists.

four-bar
linkage—)
Stewart
platform—(
spherical joint
spherical
wrist!spherical@v
spherical joint

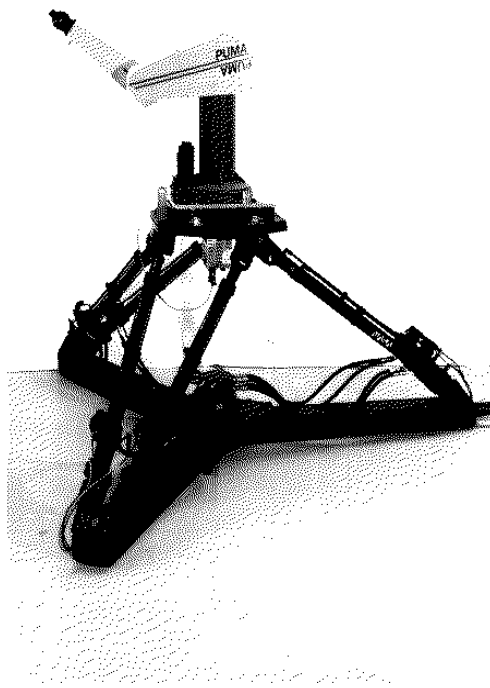


Figure 3.22: A Stewart platform with a PUMA robot attached. (Photo courtesy of Steve Dubowsky, MIT)

The rigid motion generated by a spherical joint has the form

$$g(R) = \begin{bmatrix} R & (I - R)q \\ 0 & 1 \end{bmatrix} \quad R \in SO(3),$$

structure equations!
stewart@for
Stewart
platform

where R is a free parameter and q is the location of the center of the wrist. Similarly, the velocity of a spherical joint has the form

$$V^s = \begin{bmatrix} -\omega \times q \\ \omega \end{bmatrix} \quad \omega \in \mathbb{R}^3,$$

where ω is a free parameter (the velocity). To cast this equation into a more useful framework, we rewrite V^s as

$$V^s = \begin{bmatrix} -e_1 \times q & -e_2 \times q & -e_3 \times q \\ e_1 & e_2 & e_3 \end{bmatrix} \begin{bmatrix} \omega_1 \\ \omega_2 \\ \omega_3 \end{bmatrix},$$

where e_i is the i^{th} unit vector in \mathbb{R}^3 . Notice that the columns of the matrix which defines V^s are *never* linearly dependent.

We can now write the structure equations for the Stewart platform. Let $g_{s_i}(R_{s_i})$ represent the orientation of the i^{th} spherical joint attached to the base and $g_{t_i}(R_{t_i})$ represent the i^{th} spherical joint attached to the tool. Then, the structure equation for the Stewart platform is given by

$$g_{st} = g_{s_1}(R_{s_1})e^{\hat{\xi}_1\theta_1}g_{t_1}(R_{t_1})g_{st}(0) = \cdots = g_{s_6}(R_{s_6})e^{\hat{\xi}_6\theta_6}g_{t_6}(R_{t_6})g_{st}(0), \quad (3.68)$$

where ξ_i and θ_i model the motion of the i^{th} prismatic joint.

Solving the forward kinematics for a Stewart platform is a very difficult problem due to the large number and complicated form of the constraints. Abstractly, given the length of the links, we can solve the structure equations to find the orientations of the ball and socket joints and then determine the configuration of the tool frame. As the problem has been specified here, there is an extra degree of freedom in each

parallel manipulators!inverse kinematics
inverse kinematics!parallel@for parallel manipulators
inverse kinematics!stewart@for Stewart platform

link corresponding to rotation of the prismatic joint about its own axis. This further complicates the forward kinematics problem.

The inverse kinematics problem for the Stewart platform is remarkably simple. Given the desired configuration of the platform, we find the locations of the pivot points and solve for the distance between each base and the appropriate pivot. Let q_{s_i} be the location of the i^{th} pivot point on the base and q_{t_i} be the location of the tool pivot point (written relative to the base and tool frames, respectively). Then, the extension of the prismatic joints is given by

$$\theta_i = \|q_{s_i} - g_{st}q_{t_i}\|.$$

It is possible to derive this result in a manner similar to that used in solving the subproblems of Section 3; but in this case, the solution is obvious from the geometry of the manipulator.

We may now study the mobility of the Stewart platform by calculating the Jacobian of the structure equation. Taking the Jacobian of equation (3.68) yields

$$\begin{aligned} V_{st}^s &= \begin{bmatrix} \xi_{s_1,1} & \xi_{s_1,2} & \xi_{s_1,3} & \xi'_1 & \xi'_{t_1,1} & \xi'_{t_1,2} & \xi'_{t_1,3} \end{bmatrix} \begin{bmatrix} \omega_{s_1} \\ \dot{\theta}_1 \\ \omega_{t_1} \end{bmatrix} \\ &= \dots \\ &= \begin{bmatrix} \xi_{s_6,1} & \xi_{s_6,2} & \xi_{s_6,3} & \xi'_6 & \xi'_{t_6,1} & \xi'_{t_6,2} & \xi'_{t_6,3} \end{bmatrix} \begin{bmatrix} \omega_{s_6} \\ \dot{\theta}_6 \\ \omega_{t_6} \end{bmatrix}. \end{aligned} \quad (3.69)$$

It can be shown that the Jacobian matrices are never singular as long as θ_i is nonzero (see Exercise 29). Hence, all tool velocities are admissible.

However, an interesting problem occurs when the tool frame and base frame are coplanar. In this case, the actuated joints can only generate forces in the plane, and hence the mechanism cannot resist (or apply) nonplanar forces or torques. Note that the mechanism is still not kinematically singular: the joints can accommodate any motion of the tool frame. However, the *actuated* joints cannot generate the wrenches

necessary to actually achieve any motion. This is an example of the second class of singularity that was mentioned previously. We call this type of singularity an *actuator singularity* since it corresponds to a failure of the actuated joints to be able to generate arbitrary wrenches in the tool frame. This type of singularity is very closely related to the failure of the force-closure conditions which occur in grasping.

actuator
singularities
kinematic
singularities!actuator@ver
actuator
singularities
planar Stewart
platform

A geometric interpretation of this singularity in the Stewart platform can be obtained by noting that the system of wrenches which can be applied to the tool frame is given by the set of all zero-pitch (pure force) wrenches generated by the actuated joints through the points q_{t_i} . Since the prismatic joints generate zero-pitch wrenches, we can use the previously derived examples of singularities of zero-pitch screws to locate some of the singularities of the Stewart platform. In this context, when the base and tool frames are coplanar, we get a singularity because we have four (actually six) coplanar, zero-pitch screws. A separate singularity occurs whenever two of the prismatic joints are collinear.

Example 3.19. Singularities for a planar Stewart platform

Consider the planar parallel mechanism shown in Figure 3.23. Three actuated prismatic joints are used to control the position and orientation of the platform. The revolute joints at the end of each link are passive. Kinematically, this mechanism shares some of the properties of the Stewart platform.

We concentrate on the singularities of the mechanism. As with the Stewart platform, it can be shown that there are no kinematic singularities where the dimension of the space of achievable velocities drops rank (it is always three). Since the actuated joints are all prismatic, the wrenches generated by the joints correspond to zero-pitch screws. In the plane, it can be shown that three zero-pitch screws intersecting at a point are singular. This is exactly the configuration in which the mechanism is drawn in Figure 3.23 (see the wrench diagram to the right).

Hence, in this configuration, it is not possible for the mechanism to generate pure

Stewart
platform—)
parallel
manipulators—)

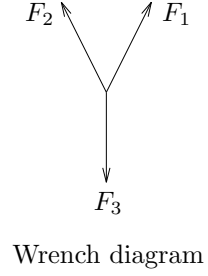
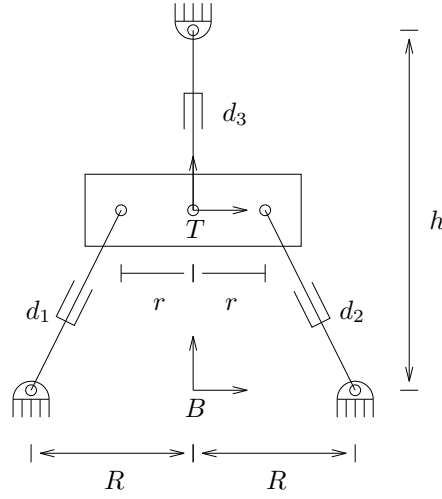


Figure 3.23: A planar version of the Stewart platform.

torques around the point of common intersection. This is clear if we write down the wrenches relative to a coordinate frame attached at the intersection point. In this set of coordinates, we have

$$F = \begin{bmatrix} v_1 & v_2 & v_3 \\ 0 & 0 & 0 \end{bmatrix} \begin{bmatrix} f_1 \\ f_2 \\ f_3 \end{bmatrix},$$

where v_i is the direction of the i^{th} prismatic axis and f_i is the force exerted by the i^{th} actuator. It is clear that we cannot generate a pure torque around the intersection point since

$$\begin{bmatrix} 0 \\ 1 \end{bmatrix} \notin \text{range} \begin{bmatrix} v_1 & v_2 & v_3 \\ 0 & 0 & 0 \end{bmatrix}.$$

6 Summary

The following are the key concepts covered in this chapter:

1. The *forward kinematics* of a manipulator is described by a mapping $g_{st} : Q \rightarrow SE(3)$ which describes the end-effector configuration as a function of the robot joint variables. For open-chain manipulators consisting of revolute and prismatic joints, the kinematics can be written using the *product of exponentials formula*:

$$g_{st}(\theta) = e^{\hat{\xi}_1 \theta_1} e^{\hat{\xi}_2 \theta_2} \dots e^{\hat{\xi}_n \theta_n} g_{st}(0),$$

where ξ_i is the twist corresponding to the i^{th} joint axis in the reference ($\theta = 0$) configuration.

2. The (*complete*) *workspace* of a manipulator is the set of end-effector configurations which can be reached by some choice of joint angles. The *reachable workspace* defines end-effector positions which can be reached at some orientation. The *dextrous workspace* defines end-effector positions which can be reached at any orientation.
3. The *inverse kinematics* of a manipulator describes the relationship between the end-effector configuration and the joint angles which achieve that configuration. For many manipulators, we can find the inverse kinematics by making use of the following subproblems:

Subproblem 1:	$e^{\hat{\xi} \theta} p = q$	rotate one point onto another
Subproblem 2:	$e^{\hat{\xi}_1 \theta_1} e^{\hat{\xi}_2 \theta_2} p = q$	rotate about two intersecting twists
Subproblem 3:	$\ q - e^{\hat{\xi} \theta} p\ = \delta$	move one point to a specified distance from another

To find a complete solution, we apply the manipulator kinematics to a set of points which reduce the complete problem into an appropriate set of subproblems.

4. The *manipulator Jacobian* relates the joint velocities $\dot{\theta}$ to the end-effector velocity V_{st} and the joint torques τ to the end-effector wrench F :

$$\begin{aligned} V_{st}^s &= J_{st}^s(\theta)\dot{\theta} & \tau &= (J_{st}^s)^T F_s & (\text{spatial}) \\ V_{st}^b &= J_{st}^b(\theta)\dot{\theta} & \tau &= (J_{st}^b)^T F_t & (\text{body}). \end{aligned}$$

If the manipulator kinematics is written using the product of exponentials formula, then the manipulator Jacobians have the form:

$$\begin{aligned} J_{st}^s(\theta) &= \begin{bmatrix} \xi_1 & \xi'_2 & \cdots & \xi'_n \end{bmatrix} & \xi'_i &= \text{Ad}_{(e^{\hat{\xi}_1\theta_1} \cdots e^{\hat{\xi}_{i-1}\theta_{i-1}})} \xi_i \\ J_{st}^b(\theta) &= \begin{bmatrix} \xi_1^\dagger & \cdots & \xi_{n-1}^\dagger & \xi_n^\dagger \end{bmatrix} & \xi_i^\dagger &= \text{Ad}_{(e^{\hat{\xi}_i\theta_i} \cdots e^{\hat{\xi}_n\theta_n} g_{st}(0))}^{-1} \xi_i. \end{aligned}$$

5. A configuration is *singular* if the manipulator Jacobian loses rank at that configuration. Examples for a general six degree of freedom arm include:
- (a) Two collinear revolute joints
 - (b) Three parallel, coplanar revolute joint axes
 - (c) Four intersecting revolute joint axes

The *manipulability* of a robot provides a measure of the nearness to singularity.

6. A manipulator is *kinematically redundant* if it has more than the minimally required degrees of freedom. The *self-motion manifold* describes the set of joint values which can be used to achieve a desired configuration of the end-effector. *Internal motions* correspond to motions along the self-motion manifold and satisfy

$$J_{st}(\theta)\dot{\theta} = 0.$$

7. A *parallel manipulator* has multiple kinematic chains connecting the base to the end-effector. For the case of two chains, the kinematics satisfies the structure equation

$$g_{st} = e^{\widehat{\xi}_{11}\theta_{11}} \dots e^{\widehat{\xi}_{1n_1}\theta_{1n_1}} g_{st}(0) = e^{\widehat{\xi}_{21}\theta_{21}} \dots e^{\widehat{\xi}_{2n_2}\theta_{2n_2}} g_{st}(0),$$

where ξ_{ij} is twist for the the j^{th} joint on the i^{th} chain. The Jacobian of the structure equation has the form

$$V_{st}^s = J_1^s(\Theta_1)\dot{\Theta}_1 = J_2^s(\Theta_2)\dot{\Theta}_2,$$

where $\Theta_i = (\theta_{i1}, \dots, \theta_{in_i})$. A kinematic singularity occurs when the dimension of the space of admissible forces drops rank. Other singularities can occur when the set of end-effector forces which can be generated by the actuated joints drops rank.

7 Bibliography

There is a vast literature on robot kinematics, including a number of textbooks devoted to analysis, design, and control of manipulators. For an introductory treatment of the topics presented here, consult the textbook by Craig [13]. See also [21, 23, 49, 55, 76, 70]. The product of exponentials formula was initially described by Brockett [7]; the presentation given here was inspired by the dissertation of Paden [51]. A selection of advanced topics in the flavor of the tools presented in this section can be found in a collection of papers edited by Brockett [8].

Roth [63] presented a pioneer study on the relationship between the kinematic geometry and manipulator performance including workspace. Further studies on this topic are given in [36, 24]. The recursive algorithm for workspace calculation of Example 3.5 was developed by Yang and Lee [?, 39], but using the Denavit-Hartenberg notation.

In terms of bounds on the number of inverse kinematic solutions to a six degree of freedom manipulator, Rastegar, Roth and Scheinman [64] established a bound of 32 using a non-constructive proof. This bound was made constructive by Duffy and Crane [18] and reduced to 16 by Primrose [57]. However, it was Lee and Liang [38] who gave a constructive procedure for finding the inverse kinematic solutions for a general manipulator. The procedure has been refined by Roth and Raghavan [59] and Manocha and Canny [43], whose account we follow in this chapter. Manseur and Doty [44] gave an example of a robot with 16 inverse kinematic solutions.

The treatment of parallel mechanisms given here is not the standard one. For a classical treatment of four-bar and other parallel mechanisms, see, for example, Hunt [28]. A detailed description of the four-bar synthesis problem, along with analytical and graphical solution techniques, can be found in the book by Erdman and Sandor [19], in addition to other textbooks on kinematics and design of mechanisms.

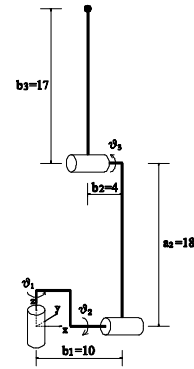
8 Exercises

1. Go to the web and create a database of popular industrial robots. Select three distinct models and draw the twist axes associated with each of the robots.
2. Show that the forward kinematics map for a manipulator is independent of the order in which rotations and translations are performed.
3. A reference configuration of the PUMA 500 (Figure 3.24(a)) is shown in Figure 3.24(b). At such a configuration, the joint limit constraints are symmetric, and are given by $\theta_i \in [-\theta_{i,max}, \theta_{i,max}]$, where $\theta_{1,max} = 160^\circ$, $\theta_{2,max} = 125^\circ$, and $\theta_{3,max} = 135^\circ$. Determine the reachable workspace volume of the wrist center point p , with coordinates given by $p = (b_1 - b_2, 0, a_2 + b_3)$, and plot its intersection with the xz -plane.

product of
exponentials
for-
mula!independen
of order of
joint motions



(a)



(b)

Figure 3.24: (a) PUMA 500 manipulator; (b) A reference configuration with symmetric joint limit constraints

4. Subproblem 4: Translation to a given distance

Let ξ be an infinite-pitch unit-magnitude twist; $p, q \in \mathbb{R}^3$ two points; and δ a real number > 0 . Find θ such that

$$\|q - e^{\widehat{\xi}\theta} p\| = \delta.$$

Use this subproblem to solve for the extension of the prismatic joint in the SCARA robot in Example 3.7.

5. Consider the wrist mechanism shown in Figure 3.25(a). Write down the forward kinematic map, and solve the inverse kinematics problem for a desired orientation using both the Paden-Kahan subproblems and the algebraic method of Chapter 2.

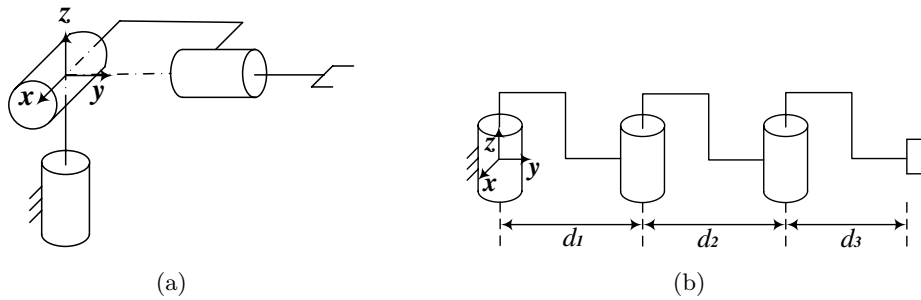


Figure 3.25: (a) A wrist mechanism; (b) A planar manipulator

6. For the three degrees of freedom planar manipulator shown in Figure 3.25(b):
 - (a) Find the forward kinematic map.
 - (b) Compute the spatial Jacobian.
 - (c) Given a desired end effector location $g_d \in SE(2)$, solve the inverse kinematics problem.
7. For each of the three degree of freedom manipulators shown in Figure 3.26:
 - (a) Find the forward kinematics map.
 - (b) Given a desired tip location, solve the inverse kinematics problem using the subproblems, including Subproblem 4 in Exercise 4.
 - (c) Derive the spatial Jacobian.

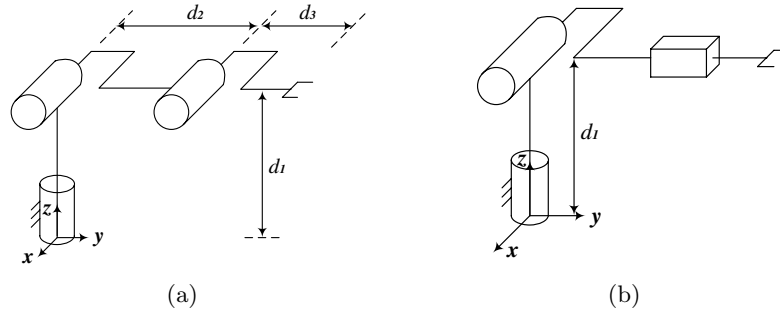


Figure 3.26: Two simple 3-DoF manipulators.

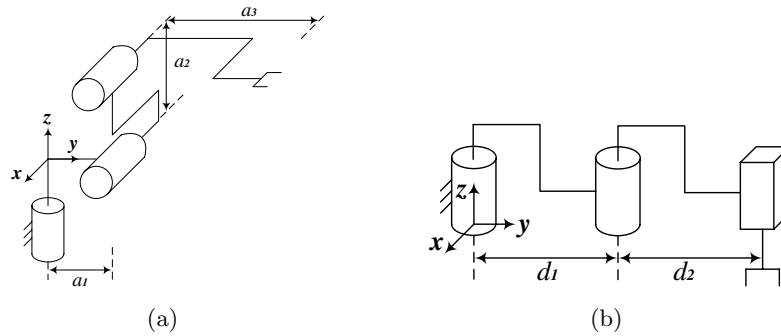


Figure 3.27: Two 3-degree-of-freedom manipulators.

8. For each of the manipulators shown in Figure 3.27:
 - (a) Find the forward kinematic map.
 - (b) Given a desired tip location, solve the inverse kinematics problem.
9. For the five degrees of freedom manipulator shown in Figure 3.28:
 - (a) Find the forward kinematic map.
 - (b) Given a desired tip location and approach vector (the z -axis of the tool frame), solve the inverse kinematics problem.
 - (c) Derive the spatial Jacobian.
 - (d) Give a geometric description of the singular configurations.

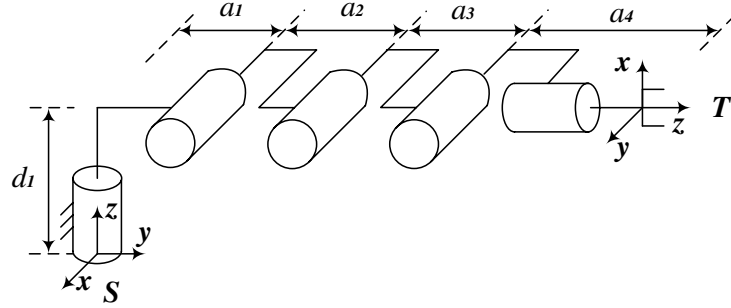


Figure 3.28: A 5-DoF manipulator

- (e) Sketch the reachable workspace.
10. Figure 3.29 shows the Motoman HP3 robot and its associated CAD model.
- Identify the twist associated with each joint axes.
 - Find the forward kinematic map.
 - Solve the inverse kinematics problem.
 - Compute the spatial Jacobian.
 - Sketch the reachable workspace of the tip point.
11. Repeat Exercise 10 for the Stanford manipulator shown in Figure 3.30.
12. *Inverse kinematics via Jacobian inverse*

Consider the manipulator shown in Figure 3.13, where the link parameters and joint travel limits are given in the table below:

Parameter	Value (mm)	Motion Range (degree)
l_0	150	$-170^\circ \leq \theta_1 \leq 170^\circ$
l_1	270	$-90^\circ \leq \theta_2 \leq 90^\circ$
l_3	440	$\theta_2 - 150^\circ \leq \theta_3 \leq \theta_2 + 150^\circ$
l_4	113.6	$-135^\circ \leq \theta_5 \leq 135^\circ$
$l_{12} = l_1 + l_2$	355	$-200^\circ \leq \theta_6 \leq 200^\circ$

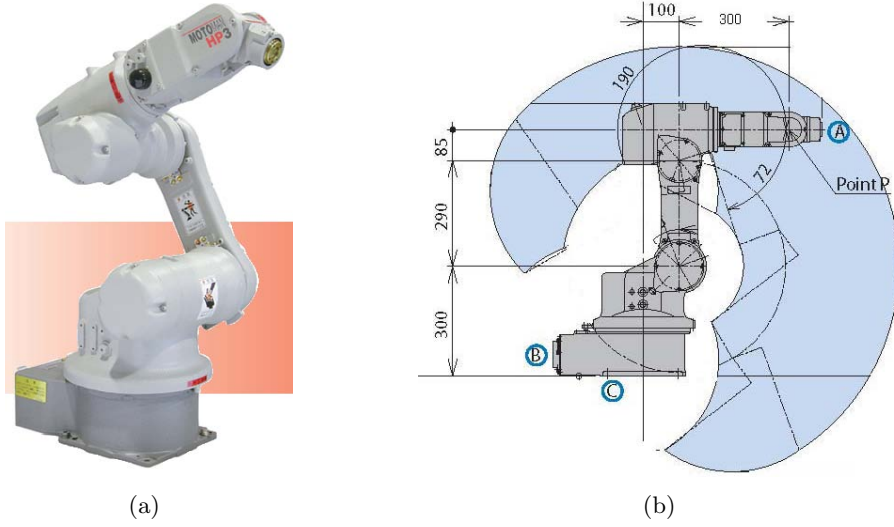


Figure 3.29: Motoman HP3 robot and its associated CAD model.

Let F and C_6 be two different end-effector frames, which are fixed relative to each other and related by

$$R_{6f} = I, p_{6f} = \begin{bmatrix} 0 \\ 0 \\ l_4 \end{bmatrix}.$$

In other words, C_6 is located at the wrist center point. Let $\theta = (\theta_1, \theta_2, \theta_{23}, \theta_4, \theta_5, \theta_6)$, where $\theta_{23} = \theta_3 - \theta_2$, be the joint position vector.

- (a) Determine the forward kinematic map $g_{s6}(\theta) \in SE(3)$.
- (b) Let $R_{s6}(\theta) = (R_1 \cdot R_2 \cdot R_3 \cdot R_4) \cdot (R_5 \cdot R_6 \cdot R_{s6}(0)) := R_{14} \cdot R_{56}$, and ω_{56} the body angular velocity of C_6 . Show that

$$\begin{bmatrix} \dot{p}_{s6} \\ R_{56}\omega_{s6} \end{bmatrix} = \begin{bmatrix} J_p & 0 \\ J_\omega^1 & J_\omega^2 \end{bmatrix} \dot{\theta} := J(\theta)\dot{\theta}$$

and

$$J(\theta)^{-1} = \begin{bmatrix} J_p^{-1} & 0 \\ -(J_\omega^2)^{-1}J_\omega^1J_p^{-1} & (J_\omega^2)^{-1} \end{bmatrix}.$$

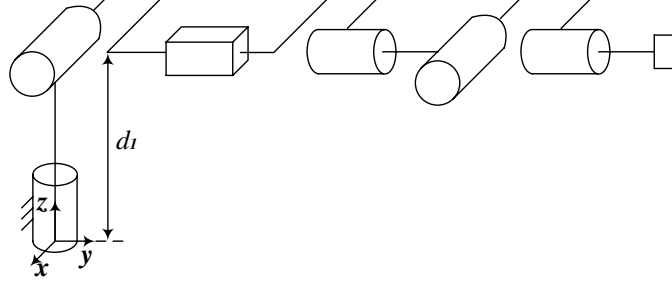


Figure 3.30: Representation of the Stanford manipulator

Give the analytic expression of J_p^{-1} and $(J_\omega^2)^{-1}$. Note that $(\dot{p}_{s6}, R_{56} \cdot \omega_{s6})$ can be readily computed from (v_{sf}, ω_{sf}) by

$$\begin{bmatrix} \dot{p}_{s6} \\ R_{56} \cdot \omega_{s6} \end{bmatrix} = \begin{bmatrix} R_{s6} & R_{s6} \hat{p}_{6f} \\ 0 & R_{56} \end{bmatrix} \begin{bmatrix} v_{sf} \\ \omega_{sf} \end{bmatrix}.$$

- (c) Let $g_d(t) \in SE(3), t \in [0, T]$, be a desired trajectory of the end-effector frame F , and T_0 the sampling period. Discretize the continuous trajectory by $g_d^i = g_d(iT_0), i = 1, \dots, n = \lceil T/T_0 \rceil$, where $\lceil T/T_0 \rceil$ denotes the nearest integer to T/T_0 . Let θ^0 be the initial joint angle, and $g(0) = g_{sf}(\theta^0)$ the initial configuration of the end-effector. A sequence of joint angles $(\theta^0, \dots, \theta^k, \theta^{k+1}, \dots, \theta^n)$ that realizes the desired trajectory $g_d(t)$ is constructed as follows: First, given θ^k , let $g^k = g_{sf}(\theta^k)$ and compute $\hat{\xi}_k \in se(3)$ from

$$e^{\hat{\xi}_k} = (g^k)^{-1} (g_d^{k+1})$$

or

$$\hat{\xi}_k = \log((g^k)^{-1} \cdot g_d^{k+1}).$$

Then, compute $\delta\theta^k$ from

$$J(\theta^k) \delta\theta^k = \begin{bmatrix} R_{s6} & R_{s6} \hat{p}_{6f} \\ 0 & R_{56} \end{bmatrix} \xi_k.$$

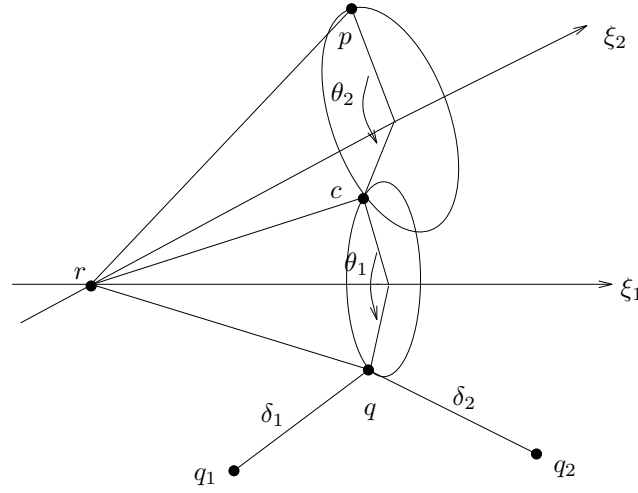


Figure 3.31: Subproblem 5: Rotate p about the axis of ξ_1 followed by a rotation about the axis of ξ_2 such that the final location of p is δ_1 from q_1 and δ_2 from q_2 .

Finally, set

$$\theta^{k+1} = \theta^k + \delta\theta^k.$$

Write a compute program to implement the above computations. Verify your program with several desired trajectories $g_d(t)$.

13. *Subproblem 5: Rotation about two axes to given distances*

Let ξ_1, ξ_2 be two zero-pitch unit magnitude twists with intersecting axes, and p, q_1 , and q_2 be points in \mathbb{R}^3 (see Figure 3.31). Find θ_1 and θ_2 such that

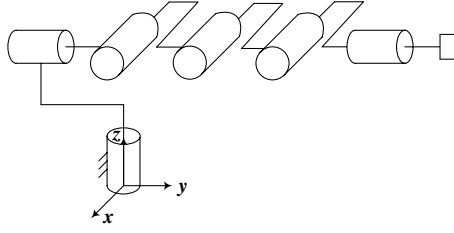
$$\|e^{\hat{\xi}_1\theta_1} e^{\hat{\xi}_2\theta_2} p - q_1\| = \delta_1$$

and

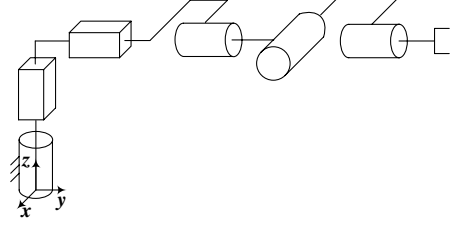
$$\|e^{\hat{\xi}_1\theta_1} e^{\hat{\xi}_2\theta_2} p - q_2\| = \delta_2.$$

(Hint: Find a point q such that $q = e^{\hat{\xi}_1\theta_1} e^{\hat{\xi}_2\theta_2} p$, and q is on the intersection of the three spheres centered at, respectively, q_1, q_2 , and r , of radii δ_1, δ_2 , and $\|p - r\|$.) Apply this and the Paden-Kahan subproblems to solve the inverse kinematics problem for the inverse elbow manipulator shown in Figure 3.32(a).

Paden-Kahan
subproblems—
singular values
of a matrix



(a)



(b)

Figure 3.32: (a) Inverse elbow manipulator, (b) A 6-DoF cylindrical manipulator

14. Solve the inverse kinematics problem for the cylindrical robot with a spherical wrist shown in Figure 3.32(b).
15. Show that the spatial velocity of a manipulator does not depend on the location of the tool frame (as long as it moves with the end-effector).
16. *Singular values of a matrix*

Let $A : \mathbb{R}^n \rightarrow \mathbb{R}^p$ represent a linear map and assume that r is the rank of A . Thus, $r \leq \min(n, p)$. Show that there exist matrices $U \in \mathbb{R}^{p \times p}$, $V \in \mathbb{R}^{n \times n}$ and $\Sigma \in \mathbb{R}^{p \times n}$ such that

$$A = U\Sigma V^T, \quad (3.70)$$

where

- (a) The columns of V are orthonormal, i.e., $V^T V = I$. Further, it may be partitioned as

$$V = \begin{bmatrix} v_1 & \cdots & v_r & v_{r+1} & \cdots & v_n \end{bmatrix} = \begin{bmatrix} V_1 & V_2 \end{bmatrix}$$

so that the range space of $A^T : \mathbb{R}^p \rightarrow \mathbb{R}^n$, denoted $\mathcal{R}(A^T)$, is spanned by the columns of V_1 , and the null space of A , denoted $\eta(A)$, is spanned by the columns of V_2 .

- (b) The columns of U are orthonormal, i.e., $U^T U = I$, and it may be partitioned as manipulability
measures

$$U = \begin{bmatrix} u_1 & \cdots & u_r & u_{r+1} & \cdots & u_p \end{bmatrix} = \begin{bmatrix} U_1 & U_2 \end{bmatrix}$$

so that $\mathcal{R}(A)$ is spanned by the columns of U_1 , and $\eta(A^T)$ is spanned by the columns of U_2 .

- (c) Σ is a matrix of dimension $p \times n$ of the form

$$\Sigma = \begin{bmatrix} \Sigma_1 & 0 \\ 0 & 0 \end{bmatrix}$$

with

$$\Sigma_1 = \begin{bmatrix} \sigma_1 & & 0 \\ & \ddots & \\ 0 & & \sigma_r \end{bmatrix} \in \mathbb{R}^{r \times r}, \quad \sigma_1 \geq \cdots \geq \sigma_r > 0$$

The σ_i are called the *singular values* of A , and $\Sigma \in \mathbb{R}^{p \times n}$ is the representation of A in terms of the V basis for \mathbb{R}^n and the U basis for \mathbb{R}^p .

17. Let $J(\theta) : \mathbb{R}^n \rightarrow \mathbb{R}^6$ be the Jacobian of a manipulator. Show that the manipulability measure $\mu_3(\theta)$ is given by the product of the singular values of $J(\theta)$; that is,

$$\mu_3(\theta) = \prod_{i=1}^6 \sigma_i(\theta).$$

Thus, $\mu_3(\theta)$ is zero if and only if the Jacobian is singular.

18. Let $A : \mathbb{R}^n \rightarrow \mathbb{R}^p$ be of rank r and have singular value decomposition (3.70). Let B_1 denote the ball of unit radius in \mathbb{R}^n ; that is,

$$B_1 = \{x \in \mathbb{R}^n, \|x\| \leq 1\}.$$

Use the description of the matrices U, V of Exercise 16 to find the map under A of B_1 . Distinguish between the cases that $p \geq n$ and $p \leq n$ and also when $r < \min(n, p)$.

isotropic points
Euler angles

19. Let $J(\theta) : \mathbb{R}^n \rightarrow \mathbb{R}^p$ be the Jacobian of a manipulator ($p = 3$ or 6). Assume that a task is modeled by an ellipsoid in the task space with its principal axes of length $\alpha_1, \dots, \alpha_p$. Let $E_\beta \subset \mathbb{R}^p$ be an ellipsoid of size scaled by β , namely

$$E_\beta := \{y : \left(\frac{y_1}{\alpha_1}\right)^2 + \dots + \left(\frac{y_p}{\alpha_p}\right)^2 \leq \beta\}$$

Define a manipulability measure on $J(\theta)$ which takes into account the task requirement as

$$\mu_t(\theta) := \max\{\beta : J(\theta)(B_1) \subset E_\beta\}.$$

Characterize $\mu_t(\theta)$ in terms of the singular values of $J(\theta)$ and lengths of the principal axes, $\alpha_1, \dots, \alpha_p$.

20. *Isotropic points*

A point in a manipulator's workspace is said to be *isotropic* if the condition number of the Jacobian is 1.

- (a) Calculate conditions under which a two-link planar manipulator has isotropic points and sketch their location in the plane.
- (b) Compute the isotropic points for an elbow manipulator without a wrist.
- (c) Discuss why isotropic points are useful for tasks which involve applying forces against the environment.

21. Euler angles can be used to represent rotations via the product of exponentials formula. If we think of (α, β, γ) as joints angles of a robot manipulator, then we can find the singularities of an Euler angle parameterization by calculating the Jacobian of the “forward kinematics,” where we are concerned only with the rotation portion of the forward kinematics map. Use this point of view to find singularities for the following classes of Euler angles:

- (a) ZYZ Euler angles

(b) ZYX Euler angles

(c) XYZ Euler angles

kinematic
singularities—(
coplanar
revolute axes
intersecting
joint axes

22. *Kinematic singularity: four coplanar revolute joints*

Four revolute joint axes with twists $\xi_i = (q_i \times \omega_i, \omega_i)$, $i = 1, \dots, 4$, are said to be coplanar if there exists a plane with unit normal n such that:

(a) Each axis direction is orthogonal to n : $n^T \omega_i = 0$, $i = 1, \dots, 4$.

(b) The vector from q_i to q_j is orthogonal to n : $n^T(q_i - q_j) = 0$, $i = 1, \dots, 4$.

Show that when four of its revolute joint axes are coplanar, a six degree of freedom manipulator is at a singular configuration. Give an example of a manipulator exhibiting such a singularity.

23. *Kinematic singularity: six revolute joints intersecting along a line*

Six revolute joint axes with twists $\xi_i = (q_i \times \omega_i, \omega_i)$, $i = 1, \dots, 6$, intersect along a line $(p \times n, n)$ if there exist constants $\gamma_i, \beta_i \in \mathbb{R}$, $i = 1, \dots, 6$, such that

$$q_i + \gamma_i \omega_i = p + \beta_i n.$$

Show that when the six revolute joint axes of a six degree of freedom manipulator intersect along a line, the manipulator is at a singular configuration.

24. *Kinematic singularity: prismatic joint perpendicular to two parallel coplanar revolute joints*

A prismatic joint with twist $\xi_3 = (v_3, 0)$ is normal to a plane containing two parallel revolute axes $\xi_i = (q_i \times \omega_i, \omega_i)$, $i = 1, 2$, if

(a) $v_3^T \omega_i = 0$, $i = 1, 2$

(b) $v_3^T(q_1 - q_2) = 0$

(c) $\omega_1 = \pm \omega_2$

kinematic
singularities—)
manipulability
measures

singular
configurations

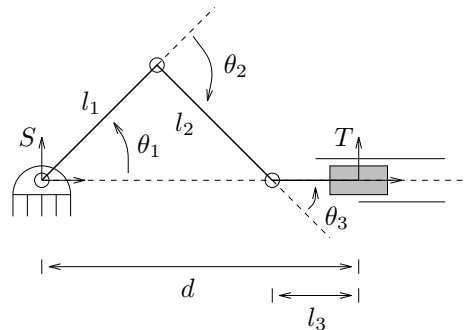
end-effector
wrench!singular@at
singular
configuration

slider-crank
mechanism

Show that when this occurs, a six degree of freedom manipulator is at a singular configuration. Give an example of a manipulator exhibiting such a singularity.

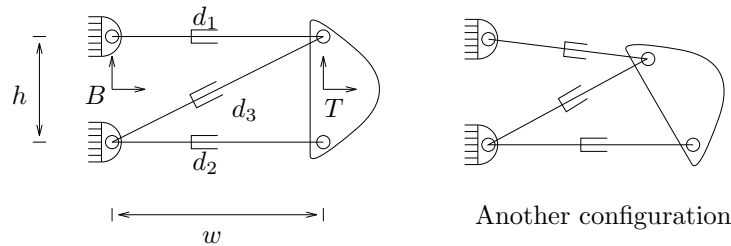
25. In general, the manipulator Jacobian depends on the choice of base and tool frames. Determine which of the manipulability measures described in Section 4.4 is independent of the choice of base and/or tool frames.
26. Show that if a manipulator is at a singular configuration, then there exists an end-effector wrench F which can be balanced without applying any joint torques. How is the wrench related to the twists which form the columns of the Jacobian?

27. Consider the slider-crank mechanism shown below:



- (a) Calculate the number of degrees of freedom of the mechanism. Explain why the spatial version of Gruebler's formula cannot be used.
- (b) Calculate the structure equations for the mechanism.
- (c) Calculate the Jacobian of the structure equations; give explicit expressions for the instantaneous twists for each of the joints.
- (d) Find the singular configurations of the mechanism if d is the active variable.
- (e) Find the singular configurations if θ_1 is treated as the active variable. Under what conditions (on l_1, l_2, l_3) do singular configurations exist?

28. The figure below shows a planar parallel manipulator called a “variable geometry truss.” Three actuated prismatic joints are used to control the position and orientation of the platform. The revolute joints at the end of each link are passive. Assume that there are no actuator limits.



- Use Gruebler's formula to calculate the number of degrees of freedom of the mechanism.
 - Write the structure equations for the mechanism. Be sure to clearly define your zero configuration.
 - Given $g_{st} = ([x, y], R_\phi)$, find explicit expressions for d_1 , d_2 , and d_3 .
 - Find the spatial Jacobian of the structure equations. Give an explicit answer. Use the fact that some links intersect at a point to minimize extra calculations.
 - Find the singular configurations of the mechanism. In addition to kinematic singularities, also identify any actuator singularities.
29. *Stewart platform*
- Consider the Stewart platform shown in Figure 3.22. Let θ_i represent the displacement of the i^{th} prismatic actuator.

- Use Gruebler's formula to compute the number of degrees of freedom of the mechanism.
- Show that if $\theta_i > 0$ for all i , then the mechanism is not at a singular configuration.

U-joint

- (c) Suppose that we replace the spherical joints in the Stewart platform with U-joints (a U-joint consists of two orthogonal revolute joints which intersect at a point). Use Gruebler's formula to compute the number of degrees of freedom of the mechanism.
- (d) Derive the structure equations for the mechanism in part (c). Are there any singular configurations?

Chapter 4

Robot Dynamics and Control

This chapter presents an introduction to the dynamics and control of robot manipulators. We derive the equations of motion for a general open-chain manipulator and, using the structure present in the dynamics, construct control laws for asymptotic tracking of a desired trajectory. In deriving the dynamics, we will make explicit use of twists for representing the kinematics of the manipulator and explore the role that the kinematics play in the equations of motion. We assume some familiarity with dynamics and control of physical systems.

1 Introduction

The kinematic models of robots that we saw in the last chapter describe how the motion of the joints of a robot is related to the motion of the rigid bodies that make up the robot. We implicitly assumed that we could command arbitrary joint level trajectories and that these trajectories would be faithfully executed by the real-world robot. In this chapter, we look more closely at how to execute a given joint trajectory on a robot manipulator.

Most robot manipulators are driven by electric, hydraulic, or pneumatic actuators, which apply torques (or forces, in the case of linear actuators) at the joints of the robot. The *dynamics* of a robot manipulator describes how the robot moves in

response to these actuator forces. For simplicity, we will assume that the actuators do not have dynamics of their own and, hence, we can command arbitrary torques at the joints of the robot. This allows us to study the inherent mechanics of robot manipulators without worrying about the details of how the joints are actuated on a particular robot.

We will describe the dynamics of a robot manipulator using a set of nonlinear, second-order, ordinary differential equations which depend on the kinematic and inertial properties of the robot. Although in principle these equations can be derived by summing all of the forces acting on the coupled rigid bodies which form the robot, we shall rely instead on a Lagrangian derivation of the dynamics. This technique has the advantage of requiring only the kinetic and potential energies of the system to be computed, and hence tends to be less prone to error than summing together the inertial, Coriolis, centrifugal, actuator, and other forces acting on the robot's links. It also allows the structural properties of the dynamics to be determined and exploited.

Once the equations of motion for a manipulator are known, the inverse problem can be treated: the *control* of a robot manipulator entails finding actuator forces which cause the manipulator to move along a given trajectory. If we have a perfect model of the dynamics of the manipulator, we can find the proper joint torques directly from this model. In practice, we must design a feedback control law which updates the applied forces in response to deviations from the desired trajectory. Care is required in designing a feedback control law to insure that the overall system converges to the desired trajectory in the presence of initial condition errors, sensor noise, and modeling errors.

In this chapter, we primarily concentrate on one of the simplest robot control problems, that of regulating the position of the robot. There are two basic ways that this problem can be solved. The first, referred to as *joint space control*, involves converting a given task into a desired path for the joints of the robot. A control law is

then used to determine joint torques which cause the manipulator to follow the given trajectory. A different approach is to transform the dynamics and control problem into the task space, so that the control law is written in terms of the end-effector position and orientation. We refer to this approach as *workspace control*.

Lagrange's
equa-
tions!mechanical@
mechanical
systems—(
Newton's law

A much harder control problem is one in which the robot is in contact with its environment. In this case, we must regulate not only the position of the end-effector but also the forces it applies against the environment. We discuss this problem briefly in the last section of this chapter and defer a more complete treatment until Chapter 6, after we have introduced the tools necessary to study constrained systems.

2 Lagrange's Equations

There are many methods for generating the dynamic equations of a mechanical system. All methods generate equivalent sets of equations, but different forms of the equations may be better suited for computation or analysis. We will use a Lagrangian analysis for our derivation, which relies on the energy properties of mechanical systems to compute the equations of motion. The resulting equations can be computed in closed form, allowing detailed analysis of the properties of the system.

2.1 Basic formulation

Consider a system of n particles which obeys Newton's second law—the time rate of change of a particle's momentum is equal to the force applied to a particle. If we let F_i be the applied force on the i^{th} particle, m_i be the particle's mass, and r_i be its position, then Newton's law becomes

$$F_i = m_i \ddot{r}_i \quad r_i \in \mathbb{R}^3, i = 1, \dots, n. \quad (4.1)$$

Our interest is not in a set of independent particles, but rather in particles which are attached to one another and have limited degrees of freedom. To describe

constraints!holonomic. In this interconnection, we introduce *constraints* between the positions of our particles.

Each constraint is represented by a function $g_j: \mathbb{R}^{3n} \rightarrow \mathbb{R}$ such that

$$g_j(r_1, \dots, r_n) = 0 \quad j = 1, \dots, k. \quad (4.2)$$

A constraint which can be written in this form, as an algebraic relationship between the positions of the particles, is called a *holonomic* constraint. More general constraints between rigid bodies—involving \dot{r}_i —can also occur, as we shall discover when we study multifingered hands.

A constraint acts on a system of particles through application of *constraint forces*. The constraint forces are determined in such a way that the constraint in equation (4.2) is always satisfied. If we view the constraint as a smooth surface in \mathbb{R}^n , the constraint forces are normal to this surface and restrict the velocity of the system to be tangent to the surface at all times. Thus, we can rewrite our system dynamics as a vector equation

$$F = \begin{bmatrix} m_1 I & & 0 \\ & \ddots & \\ 0 & & m_n I \end{bmatrix} \begin{bmatrix} \ddot{r}_1 \\ \vdots \\ \ddot{r}_n \end{bmatrix} + \sum_{j=1}^k \Gamma_j \lambda_j, \quad (4.3)$$

where the vectors $\Gamma_1, \dots, \Gamma_k \in \mathbb{R}^{3n}$ are a basis for the forces of constraint and λ_j is the scale factor for the j^{th} basis element. We do not require that $\Gamma_1, \dots, \Gamma_k$ be orthonormal. For constraints of the form in equation (4.2), Γ_j can be taken as the gradient of g_j , which is perpendicular to the level set $g_j(r) = 0$.

The scalars $\lambda_1, \dots, \lambda_k$ are called *Lagrange multipliers*. Formally, we determine the Lagrange multipliers by solving the $3n + k$ equations in equations (4.2) and (4.3) for the $3n + k$ variables $r \in \mathbb{R}^{3n}$ and $\lambda \in \mathbb{R}^k$. The λ_i values only give the relative magnitudes of the constraint forces since the vectors Γ_j are not necessarily orthonormal.

This approach to dealing with constraints is intuitively simple but computationally complex, since we must keep track of the state of all particles in the system even

though they are not capable of independent motion. A more appealing approach is to describe the motion of the system in terms of a smaller set of variables that completely describes the configuration of the system. For a system of n particles with k constraints, we seek a set of $m = 3n - k$ variables q_1, \dots, q_m and smooth functions f_1, \dots, f_n such that

Lagrange's
equations!
mechanical
mechanical
systems
Lagrange's
equations

$$\begin{aligned} r_i = f_i(q_1, \dots, q_m) \\ i = 1, \dots, n \end{aligned} \iff \begin{aligned} g_j(r_1, \dots, r_n) = 0 \\ j = 1, \dots, k. \end{aligned} \quad (4.4)$$

We call the q_i 's a set of *generalized coordinates* for the system. For a robot manipulator consisting of rigid links, these generalized coordinates are almost always chosen to be the angles of the joints. The specification of these angles uniquely determines the position of all of the particles which make up the robot.

Since the values of the generalized coordinates are sufficient to specify the position of the particles, we can rewrite the equations of motion for the system in terms of the generalized coordinates. To do so, we also express the external forces applied to the system in terms of components along the generalized coordinates. We call these forces *generalized forces* to distinguish them from physical forces, which are always represented as vectors in \mathbb{R}^3 . For a robot manipulator with joint angles acting as generalized coordinates, the generalized forces are the torques applied about the joint axes.

To write the equations of motion, we define the *Lagrangian*, L , as the difference between the kinetic and potential energy of the system. Thus,

$$L(q, \dot{q}) = T(q, \dot{q}) - V(q),$$

where T is the kinetic energy and V is the potential energy of the system, both written in generalized coordinates.

Theorem 4.1. Lagrange's equations

The equations of motion for a mechanical system with generalized coordinates $q \in \mathbb{R}^m$

and Lagrangian L are given by

$$\frac{d}{dt} \frac{\partial L}{\partial \dot{q}_i} - \frac{\partial L}{\partial q_i} = \Upsilon_i \quad i = 1, \dots, m, \quad (4.5)$$

where Υ_i is the external force acting on the i^{th} generalized coordinate.

The equations in (4.5) are called *Lagrange's equations*. We will often write them in vector form as

$$\frac{d}{dt} \frac{\partial L}{\partial \dot{q}} - \frac{\partial L}{\partial q} = \Upsilon,$$

where $\frac{\partial L}{\partial \dot{q}}$, $\frac{\partial L}{\partial q}$, and Υ are to be formally regarded as row vectors, though we often write them as column vectors for notational convenience. A proof of Theorem 4.1 can be found in most books on dynamics of mechanical systems (e.g., [62]).

Lagrange's equations are an elegant formulation of the dynamics of a mechanical system. They reduce the number of equations needed to describe the motion of the system from n , the number of particles in the system, to m , the number of generalized coordinates. Note that if there are *no* constraints, then we can choose q to be the components of r , giving $T = \frac{1}{2} \sum m_i \|\dot{r}_i\|^2$, and equation (4.5) then reduces to equation (4.1). In fact, rearranging equation (4.5) as

$$\frac{d}{dt} \frac{\partial L}{\partial \dot{q}} = \frac{\partial L}{\partial q} + \Upsilon$$

is just a restatement of Newton's law in generalized coordinates:

$$\frac{d}{dt} (\text{momentum}) = \text{applied force}.$$

The motion of the individual particles can be recovered through application of equation (4.4).

Example 4.1. Dynamics of a spherical pendulum

Consider an idealized spherical pendulum as shown in Figure 4.1. The system consists of a point with mass m attached to a spherical joint by a massless rod of length l . We parameterize the configuration of the point mass by two scalars, θ and ϕ ,

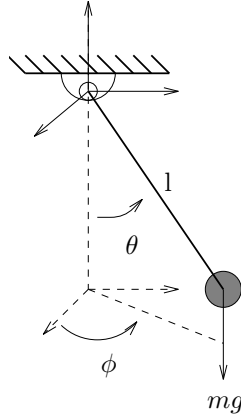


Figure 4.1: Idealized spherical pendulum. The configuration of the system is described by the angles θ and ϕ .

which measure the angular displacement from the z - and x -axes, respectively. We wish to solve for the motion of the mass under the influence of gravity.

We begin by deriving the Lagrangian for the system. The position of the mass, relative to the origin at the base of the pendulum, is given by

$$r(\theta, \phi) = \begin{bmatrix} l \sin \theta \cos \phi \\ l \sin \theta \sin \phi \\ -l \cos \theta \end{bmatrix}. \quad (4.6)$$

The kinetic energy is

$$T = \frac{1}{2} m l^2 \|\dot{r}\|^2 = \frac{1}{2} m l^2 (\dot{\theta}^2 + (1 - \cos^2 \theta) \dot{\phi}^2)$$

and the potential energy is

$$V = -mgl \cos \theta,$$

where $g \approx 9.8 \text{ m/sec}^2$ is the gravitational constant. Thus, the Lagrangian is given by

$$L(q, \dot{q}) = \frac{1}{2} m l^2 (\dot{\theta}^2 + (1 - \cos^2 \theta) \dot{\phi}^2) + mgl \cos \theta,$$

where $q = (\theta, \phi)$.

rigid
bodies—inertial
properties—(

Substituting L into Lagrange's equations gives

$$\begin{aligned}\frac{d}{dt} \frac{\partial L}{\partial \dot{\theta}} &= \frac{d}{dt} (ml^2 \dot{\theta}) = ml^2 \ddot{\theta} \\ \frac{\partial L}{\partial \theta} &= ml^2 \sin \theta \cos \theta \dot{\phi}^2 - mgl \sin \theta \\ \frac{d}{dt} \frac{\partial L}{\partial \dot{\phi}} &= \frac{d}{dt} (ml^2 \sin^2 \theta \dot{\phi}) = ml^2 \sin^2 \theta \ddot{\phi} + 2ml^2 \sin \theta \cos \theta \dot{\theta} \dot{\phi} \\ \frac{\partial L}{\partial \phi} &= 0\end{aligned}$$

and the overall dynamics satisfy

$$\begin{bmatrix} ml^2 & 0 \\ 0 & ml^2 \sin^2 \theta \end{bmatrix} \begin{bmatrix} \ddot{\theta} \\ \ddot{\phi} \end{bmatrix} + \begin{bmatrix} -ml^2 \sin \theta \cos \theta \dot{\phi}^2 \\ 2ml^2 \sin \theta \cos \theta \dot{\theta} \dot{\phi} \end{bmatrix} + \begin{bmatrix} mgl \sin \theta \\ 0 \end{bmatrix} = 0. \quad (4.7)$$

Given the initial position and velocity of the point mass, equation (4.7) uniquely determines the subsequent motion of the system. The motion of the mass in \mathbb{R}^3 can be retrieved from equation (4.6).

2.2 Inertial properties of rigid bodies

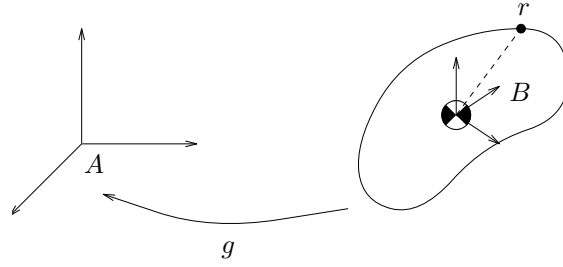
To apply Lagrange's equations to a robot, we must calculate the kinetic and potential energy of the robot links as a function of the joint angles and velocities. This, in turn, requires that we have a model for the mass distribution of the links. Since each link is a rigid body, its kinetic and potential energy can be defined in terms of its total mass and its moments of inertia about the center of mass.

Let $V \subset \mathbb{R}^3$ be the volume occupied by a rigid body, and $\rho(r)$, $r \in V$ be the mass distribution of the body. If the object is made from a homogeneous material, then $\rho(r) = \rho$, a constant. The mass of the body is the volume integral of the mass density:

$$m = \int_V \rho(r) dV.$$

The center of mass of the body is the weighted average of the density:

$$\bar{r} = \frac{1}{m} \int_V \rho(r) r dV.$$



rigid
bodies!kinetic
energy

Figure 4.2: Coordinate frames for calculating the kinetic energy of a moving rigid body.

Consider the rigid object shown in Figure 4.2. We compute the kinetic energy as follows: fix the body frame at the mass center of the object and let (p, R) be a trajectory of the object relative to an inertial frame, where we have dropped all subscripts to simplify notation. Let $r \in \mathbb{R}^3$ be the coordinates of a body point relative to the body frame. The velocity of the point in the inertial frame is given by

$$\dot{p} + \dot{R} r$$

and the kinetic energy of the object is given by the following volume integral:

$$T = \frac{1}{2} \int_V \rho(r) \|\dot{p} + \dot{R} r\|^2 dV. \quad (4.8)$$

Expanding the product in the kinetic energy integral yields

$$T = \frac{1}{2} \int_V \rho(r) \left(\|\dot{p}\|^2 + 2\dot{p}^T \dot{R} r + \|\dot{R} r\|^2 \right) dV.$$

The first term of the above expression gives the translational kinetic energy. The second term vanishes because the body frame is placed at the mass center of the object and

$$\int_V \rho(r) (\dot{p}^T \dot{R}) r dV = (\dot{p}^T \dot{R}) \int_V \rho(r) r dV = 0.$$

The last term can be simplified using properties of rotation and skew-symmetric

matrices:

$$\begin{aligned} \frac{1}{2} \int_V \rho(r) (\dot{R}r)^T (\dot{R}r) dV &= \frac{1}{2} \int_V \rho(r) (R\hat{\omega}r)^T (R\hat{\omega}r) dV \\ &= \frac{1}{2} \int_V \rho(r) (\hat{r}\omega)^T (\hat{r}\omega) dV \\ &= \frac{1}{2} \omega^T \left(\int_V \rho(r) \hat{r}^T \hat{r} dV \right) \omega =: \frac{1}{2} \omega^T \mathcal{I} \omega, \end{aligned}$$

where $\omega \in \mathbb{R}^3$ is the *body* angular velocity. The symmetric matrix $\mathcal{I} \in \mathbb{R}^{3 \times 3}$ defined by

$$\mathcal{I} = \begin{bmatrix} I_{xx} & I_{xy} & I_{xz} \\ I_{yx} & I_{yy} & I_{yz} \\ I_{zx} & I_{zy} & I_{zz} \end{bmatrix} = - \int_V \rho(r) \hat{r}^2 dV$$

is called the *inertia tensor* of the object expressed in the body frame. It has entries

$$\begin{aligned} I_{xx} &= \int_V \rho(r) (y^2 + z^2) dx dy dz \\ I_{xy} &= - \int_V \rho(r) (xy) dx dy dz, \end{aligned}$$

and the other entries are defined similarly.

The total kinetic energy of the object can now be written as the sum of a translational component and a rotational component,

$$\begin{aligned} T &= \frac{1}{2} m \|\dot{p}\|^2 + \frac{1}{2} \omega^T \mathcal{I} \omega \\ &= \frac{1}{2} (V^b)^T \begin{bmatrix} mI & 0 \\ 0 & \mathcal{I} \end{bmatrix} V^b =: \frac{1}{2} (V^b)^T \mathcal{M} V^b, \end{aligned} \tag{4.9}$$

where $\hat{V}^b = g^{-1} \dot{g} \in se(3)$ is the body velocity, and \mathcal{M} is called the *generalized inertia matrix* of the object, expressed in the body frame. The matrix \mathcal{M} is symmetric and positive definite.

Example 4.2. Generalized inertia matrix for a homogeneous bar

Consider a homogeneous rectangular bar with mass m , length l , width w , and height h , as shown in Figure 4.3. The mass density of the bar is $\rho = \frac{m}{lwh}$. We attach a

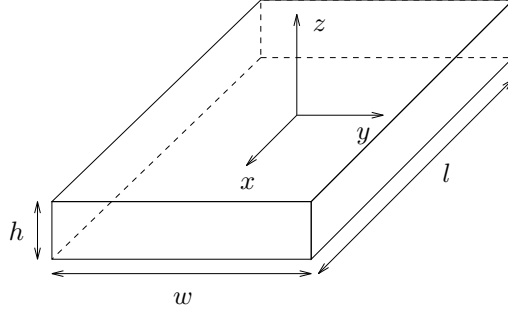


Figure 4.3: A homogeneous rectangular bar.

coordinate frame at the center of mass of the bar, with the coordinate axes aligned with the principal axes of the bar.

The inertia tensor is evaluated using the previous formula:

$$\begin{aligned}
 I_{xx} &= \int_V \frac{m}{lwh} (y^2 + z^2) dV = \frac{m}{lwh} \int_{-h/2}^{h/2} \int_{-w/2}^{w/2} \int_{-l/2}^{l/2} (y^2 + z^2) dx dy dz \\
 &= \frac{m}{lwh} \left(\frac{1}{12} (lw^3h + lwh^3) \right) = \frac{m}{12} (w^2 + h^2), \\
 I_{xy} &= - \int_V \frac{m}{lwh} (xy) dV = - \frac{m}{lwh} \int_{-h/2}^{h/2} \int_{-w/2}^{w/2} \int_{-l/2}^{l/2} (xy) dx dy dz \\
 &= - \frac{m}{lwh} \int_{-h/2}^{h/2} \int_{-w/2}^{w/2} \left(\frac{1}{2} x^2 y \Big|_{-l/2}^{l/2} \right) dy dz = 0.
 \end{aligned}$$

The other entries are calculated in the same manner and we have:

$$\mathcal{I} = \begin{bmatrix} \frac{m}{12}(w^2 + h^2) & 0 & 0 \\ 0 & \frac{m}{12}(l^2 + h^2) & 0 \\ 0 & 0 & \frac{m}{12}(l^2 + w^2) \end{bmatrix}.$$

The inertia tensor is diagonal by virtue of the fact that we aligned the coordinate axes with the principal axes of the box.

The generalized inertia matrix is given by

$$\mathcal{M} = \begin{bmatrix} mI & 0 \\ 0 & \mathcal{I} \end{bmatrix} = \begin{bmatrix} m & 0 & 0 & 0 & 0 & 0 \\ 0 & m & 0 & 0 & 0 & 0 \\ 0 & 0 & m & 0 & 0 & 0 \\ 0 & 0 & 0 & \frac{m}{12}(w^2 + h^2) & 0 & 0 \\ 0 & 0 & 0 & 0 & \frac{m}{12}(l^2 + h^2) & 0 \\ 0 & 0 & 0 & 0 & 0 & \frac{m}{12}(l^2 + w^2) \end{bmatrix}.$$

rigid
bodies!inertial
properties—)
two-link planar
manipulator!dynamics

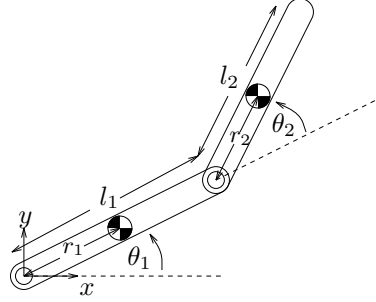


Figure 4.4: Two-link planar manipulator.

The block diagonal structure of this matrix relies on attaching the body coordinate frame at center of mass (see Exercise 3).

2.3 Example: Dynamics of a two-link planar robot

To illustrate how Lagrange's equations apply to a simple robotic system, consider the two-link planar manipulator shown in Figure 4.4. Model each link as a homogeneous rectangular bar with mass m_i and moment of inertia tensor

$$\mathcal{I}_i = \begin{bmatrix} I_{xi} & 0 & 0 \\ 0 & I_{yi} & 0 \\ 0 & 0 & I_{zi} \end{bmatrix}$$

relative to a frame attached at the center of mass of the link and aligned with the principle axes of the bar. Letting $v_i \in \mathbb{R}^3$ be the translational velocity of the center of mass for the i^{th} link and $\omega_i \in \mathbb{R}^3$ be the angular velocity, the kinetic energy of the manipulator is

$$T(\theta, \dot{\theta}) = \frac{1}{2} m_1 \|v_1\|^2 + \frac{1}{2} \omega_1^T \mathcal{I}_1 \omega_1 + \frac{1}{2} m_2 \|v_2\|^2 + \frac{1}{2} \omega_2^T \mathcal{I}_2 \omega_2.$$

Since the motion of the manipulator is restricted to the xy plane, $\|v_i\|$ is the magnitude of the xy velocity of the center of mass and ω_i is a vector in the direction of the z -axis, with $\|\omega_1\| = \dot{\theta}_1$ and $\|\omega_2\| = \dot{\theta}_1 + \dot{\theta}_2$.

We solve for the kinetic energy in terms of the generalized coordinates by using the kinematics of the mechanism. Let $p_i = (x_i, y_i, 0)$ denote the position of the i^{th}

center of mass. Letting r_1 and r_2 be the distance from the joints to the center of mass for each link, as shown in the figure, we have

$$\begin{aligned}\bar{x}_1 &= r_1 c_1 & \dot{\bar{x}}_1 &= -r_1 s_1 \dot{\theta}_1 \\ \bar{y}_1 &= r_1 s_1 & \dot{\bar{y}}_1 &= r_1 c_1 \dot{\theta}_1 \\ \bar{x}_2 &= l_1 c_1 + r_2 c_{12} & \dot{\bar{x}}_2 &= -(l_1 s_1 + r_2 s_{12}) \dot{\theta}_1 - r_2 s_{12} \dot{\theta}_2 \\ \bar{y}_2 &= l_1 s_1 + r_2 s_{12} & \dot{\bar{y}}_2 &= (l_1 c_1 + r_2 c_{12}) \dot{\theta}_1 + r_2 c_{12} \dot{\theta}_2,\end{aligned}$$

where $s_i = \sin \theta_i$, $s_{ij} = \sin(\theta_i + \theta_j)$, and similarly for c_i and c_{ij} . The kinetic energy becomes

$$\begin{aligned}T(\theta, \dot{\theta}) &= \frac{1}{2} m_1 (\dot{\bar{x}}_1^2 + \dot{\bar{y}}_1^2) + \frac{1}{2} \mathcal{I}_{z1} \dot{\theta}_1^2 + \frac{1}{2} m_2 (\dot{\bar{x}}_2^2 + \dot{\bar{y}}_2^2) + \frac{1}{2} \mathcal{I}_{z2} (\dot{\theta}_1 + \dot{\theta}_2)^2 \\ &= \frac{1}{2} \begin{bmatrix} \dot{\theta}_1 \\ \dot{\theta}_2 \end{bmatrix}^T \begin{bmatrix} \alpha + 2\beta c_2 & \delta + \beta c_2 \\ \delta + \beta c_2 & \delta \end{bmatrix} \begin{bmatrix} \dot{\theta}_1 \\ \dot{\theta}_2 \end{bmatrix},\end{aligned}\tag{4.10}$$

where

$$\begin{aligned}\alpha &= \mathcal{I}_{z1} + \mathcal{I}_{z2} + m_1 r_1^2 + m_2 (l_1^2 + r_2^2) \\ \beta &= m_2 l_1 r_2 \\ \delta &= \mathcal{I}_{z2} + m_2 r_2^2.\end{aligned}$$

Finally, we can substitute the Lagrangian $L = T$ into Lagrange's equations to obtain (after some calculation)

$$\begin{bmatrix} \alpha + 2\beta c_2 & \delta + \beta c_2 \\ \delta + \beta c_2 & \delta \end{bmatrix} \begin{bmatrix} \ddot{\theta}_1 \\ \ddot{\theta}_2 \end{bmatrix} + \begin{bmatrix} -\beta s_2 \dot{\theta}_2 & -\beta s_2 (\dot{\theta}_1 + \dot{\theta}_2) \\ \beta s_2 \dot{\theta}_1 & 0 \end{bmatrix} \begin{bmatrix} \dot{\theta}_1 \\ \dot{\theta}_2 \end{bmatrix} = \begin{bmatrix} \tau_1 \\ \tau_2 \end{bmatrix}.\tag{4.11}$$

The first term in this equation represents the inertial forces due to acceleration of the joints, the second represents the Coriolis and centrifugal forces, and the right-hand side is the applied torques.

2.4 Newton-Euler equations for a rigid body

Lagrange's equations provide a very general method for deriving the equations of motion for a mechanical system. However, implicit in the derivation of Lagrange's

configuration
space

equations is the assumption that the configuration space of the system can be parameterized by a subset of \mathbb{R}^n , where n is the number of degrees of freedom of the system. For a rigid body with configuration $g \in SE(3)$, Lagrange's equations cannot be directly used to determine the equations of motion unless we choose a local parameterization for the configuration space (for example, using Euler angles to parameterize the orientation of the rigid body). Since all parameterizations of $SE(3)$ are singular at some configuration, such a derivation can only hold locally.

In this section, we give a global characterization of the dynamics of a rigid body subject to external forces and torques. We begin by reviewing the standard derivation of the equations of rigid body motion and then examine the dynamics in terms of twists and wrenches.

Let $g = (p, R) \in SE(3)$ be the configuration of a coordinate frame attached to the center of mass of a rigid body, relative to an inertial frame. Let f represent a force applied at the center of mass, with the coordinates of f specified relative to the inertial frame. The translational equations of motion are given by Newton's law, which can be written in terms of the linear momentum $m\dot{p}$ as

$$f = \frac{d}{dt}(m\dot{p}).$$

Since the mass of the rigid body is constant, the translational motion of the center of mass becomes

$$f = m\ddot{p}. \quad (4.12)$$

These equations are independent of the angular motion of the rigid body because we have used the center of mass to represent the position of the body.

Similarly, the equations describing angular motion can be derived independently of the linear motion of the system. Consider the rotational motion of a rigid body about a point, subject to an externally applied torque τ . To derive the equations of motion, we equate the change in angular momentum to the applied torque. The

angular momentum relative to an inertial frame is given by $\mathcal{I}'\omega^f$, where

inertia tensor

$$\mathcal{I}' = \mathcal{R}\mathcal{I}\mathcal{R}^T$$

is the instantaneous inertia tensor relative to the inertial frame and ω^s is the spatial angular velocity. The angular equations of motion become

$$\tau = \frac{d}{dt}(\mathcal{I}'\omega^f) = \frac{\lceil}{\lfloor}(\mathcal{R}\mathcal{I}\mathcal{R}^T\omega^f),$$

where $\tau \in \mathbb{R}^3$ is specified relative to the inertial frame. Expanding the right-hand side of this equation, we have

$$\begin{aligned}\tau &= \mathcal{R}\mathcal{I}\mathcal{R}^T\dot{\omega}^s + \dot{\mathcal{R}}\mathcal{I}\mathcal{R}^T\omega^f + \mathcal{R}\mathcal{I}\dot{\mathcal{R}}^T\omega^f \\ &= \mathcal{I}'\dot{\omega}^f + \dot{\mathcal{R}}\mathcal{R}^T\mathcal{I}'\omega^f + \mathcal{I}'\mathcal{R}\dot{\mathcal{R}}^T\omega^f \\ &= \mathcal{I}'\dot{\omega}^f + \omega^f \times \mathcal{I}'\omega^f - \mathcal{I}'\omega^f \times \omega^f,\end{aligned}$$

where the last equation follows by differentiating the identity $\mathcal{R}\mathcal{R}^T = I$ and using the definition of ω^s . The last term of this equation is zero, and hence the dynamics are given by

$$\mathcal{I}'\dot{\omega}^f + \omega^f \times \mathcal{I}'\omega^f = \tau. \quad (4.13)$$

Equation (4.13) is called *Euler's equation*.

Equations (4.12) and (4.13) describe the dynamics of a rigid body in terms of a force and torque applied at the center of mass of the object. However, the coordinates of the force and torque vectors are not written relative to a body-fixed frame attached at the center of mass, but rather with respect to an inertial frame. Thus the pair $(f, \tau) \in \mathbb{R}^6$ is not the wrench applied to the rigid body, as defined in Chapter 2, since the point of application is not the origin of the inertial coordinate frame. Similarly, the velocity pair (\dot{p}, ω^s) does not correspond to the spatial or body velocity, since \dot{p} is not the correct expression for the linear velocity term in either body or spatial coordinates.

In order to express the dynamics in terms of twists and wrenches, we rewrite Newton's equation using the body velocity $v^b = R^T \dot{p}$ and body force $f^b = R^T f$. Expanding the right-hand side of equation (4.12),

$$\frac{d}{dt}(m\dot{p}) = \frac{d}{dt}(mRv^b) = Rm\dot{v}^b + \dot{R}mv^b,$$

and pre-multiplying by R^T , the translational dynamics become

$$m\dot{v}^b + \omega^b \times mv^b = f^b. \quad (4.14)$$

Equation (4.14) is Newton's law written in body coordinates.

Similarly, we can write Euler's equation in terms of the body angular velocity $\omega^b = R^T \omega^s$ and the body torque $\tau^b = R^T \tau$. A straightforward computation shows that

$$\mathcal{I}\dot{\omega}^b + \omega^b \times \mathcal{I}\omega^b = \tau^b. \quad (4.15)$$

Equation (4.15) is Euler's equation, written in body coordinates. Note that in body coordinates the inertia tensor is constant and hence we use \mathcal{I} instead of $\mathcal{I}' = \mathcal{R}\mathcal{I}\mathcal{R}^T$.

Combining equations (4.14) and (4.15) gives the equations of motion for a rigid body subject to an external wrench F applied at the center of mass and specified with respect to the body coordinate frame:

$$\boxed{\begin{bmatrix} mI & 0 \\ 0 & \mathcal{I} \end{bmatrix} \begin{bmatrix} \dot{v}^b \\ \dot{\omega}^b \end{bmatrix} + \begin{bmatrix} \omega^b \times mv^b \\ \omega^b \times \mathcal{I}\omega^b \end{bmatrix} = F^b} \quad (4.16)$$

This equation is called the *Newton-Euler equation* in body coordinates. It gives a global description of the equations of motion for a rigid body subject to an external wrench. Note that the linear and angular motions are coupled since the linear velocity in body coordinates depends on the current orientation.

It is also possible to write the Newton-Euler equations relative to a spatial coordinate frame. This version is explored in Exercises 4 and 5. Once again the

equations for linear and angular motion are coupled, so that the translational motion still depends on the rotational motion. In this book we shall always write the Newton-Euler equations in body coordinates, as in equation (4.16).

3 Dynamics of Open-Chain Manipulators

We now derive the equations of motion for an open-chain robot manipulator. We shall use the kinematics formulation presented in the previous chapter to write the Lagrangian for the robot in terms of the joint angles and joint velocities. Using this form of the dynamics, we explore several fundamental properties of robot manipulators which are of importance when proving the stability of robot control laws.

3.1 The Lagrangian for an open-chain robot

To calculate the kinetic energy of an open-chain robot manipulator with n joints, we sum the kinetic energy of each link. For this we define a coordinate frame, L_i , attached to the center of mass of the i^{th} link. Let

$$g_{sl_i}(\theta) = e^{\widehat{\xi}_1 \theta_1} \dots e^{\widehat{\xi}_i \theta_i} g_{sl_i}(0)$$

represent the configuration of the frame L_i relative to the base frame of the robot, S . The body velocity of the center of mass of the i^{th} link is given by

$$V_{sl_i}^b = J_{sl_i}^b(\theta) \dot{\theta},$$

where $J_{sl_i}^b$ is the body Jacobian corresponding to g_{sl_i} . $J_{sl_i}^b$ has the form

$$J_{sl_i}^b(\theta) = \begin{bmatrix} \xi_1^\dagger & \dots & \xi_i^\dagger & 0 & \dots & 0 \end{bmatrix},$$

where

$$\xi_j^\dagger = \text{Ad}_{(e^{\widehat{\xi}_j \theta_j} \dots e^{\widehat{\xi}_i \theta_i} g_{sl_i}(0))}^{-1} \xi_j \quad j \leq i$$

rigid
bodies!dynamics—
Newton-Euler
equations—)
Lagrange's
equa-
tions!mechanical@
mechanical
systems—)
dynamics!open-
chain
manipulators—(
Lagrangian!open-
chain@for
open-chain
manipulators

potential energy
for an
open-chain
manipulator

is the j^{th} instantaneous joint twist relative to the i^{th} link frame. To streamline notation, we write $J_{sl_i}^b$ as J_i for the remainder of this section.

The kinetic energy of the i^{th} link is

$$T_i(\theta, \dot{\theta}) = \frac{1}{2} (V_{sl_i}^b)^T \mathcal{M}_i V_{sl_i}^b = \frac{1}{2} \dot{\theta}^T J_i^T(\theta) \mathcal{M}_i J_i(\theta) \dot{\theta}, \quad (4.17)$$

where \mathcal{M}_i is the generalized inertia matrix for the i^{th} link. Now the total kinetic energy can be written as

$$T(\theta, \dot{\theta}) = \sum_{i=1}^n T_i(\theta, \dot{\theta}) =: \frac{1}{2} \dot{\theta}^T M(\theta) \dot{\theta}. \quad (4.18)$$

The matrix $M(\theta) \in \mathbb{R}^{n \times n}$ is the *manipulator inertia matrix*. In terms of the link Jacobians, J_i , the manipulator inertia matrix is defined as

$$M(\theta) = \sum_{i=1}^n J_i^T(\theta) \mathcal{M}_i J_i(\theta). \quad (4.19)$$

To complete our derivation of the Lagrangian, we must calculate the potential energy of the manipulator. Let $h_i(\theta)$ be the height of the center of mass of the i^{th} link (height is the component of the position of the center of mass opposite the direction of gravity). The potential energy for the i^{th} link is

$$V_i(\theta) = m_i g h_i(\theta),$$

where m_i is the mass of the i^{th} link and g is the gravitational constant. The total potential energy is given by the sum of the contributions from each link:

$$V(\theta) = \sum_{i=1}^n V_i(\theta) = \sum_{i=1}^n m_i g h_i(\theta).$$

Combining this with the kinetic energy, we have

$$L(\theta, \dot{\theta}) = \sum_{i=1}^n \left(T_i(\theta, \dot{\theta}) - V_i(\theta) \right) = \frac{1}{2} \dot{\theta}^T M(\theta) \dot{\theta} - V(\theta).$$

3.2 Equations of motion for an open-chain manipulator

Lagrange's
equations!open-
chain@for
open-chain
manipulators

Let $\theta \in \mathbb{R}^n$ be the joint angles for an open-chain manipulator. The Lagrangian is of the form

$$L(\theta, \dot{\theta}) = \frac{1}{2} \dot{\theta}^T M(\theta) \dot{\theta} - V(\theta),$$

where $M(\theta)$ is the manipulator inertia matrix and $V(\theta)$ is the potential energy due to gravity. It will be convenient to express the kinetic energy as a sum,

$$L(\theta, \dot{\theta}) = \frac{1}{2} \sum_{i,j=1}^n M_{ij}(\theta) \dot{\theta}_i \dot{\theta}_j - V(\theta). \quad (4.20)$$

The equations of motion are given by substituting into Lagrange's equations,

$$\frac{d}{dt} \frac{\partial L}{\partial \dot{\theta}_i} - \frac{\partial L}{\partial \theta_i} = \Upsilon_i,$$

where we let Υ_i represent the actuator torque and other nonconservative, generalized forces acting on the i^{th} joint. Using equation (4.20), we have

$$\begin{aligned} \frac{d}{dt} \frac{\partial L}{\partial \dot{\theta}_i} &= \frac{d}{dt} \left(\sum_{j=1}^n M_{ij} \dot{\theta}_j \right) = \sum_{j=1}^n \left(M_{ij} \ddot{\theta}_j + \dot{M}_{ij} \dot{\theta}_j \right) \\ \frac{\partial L}{\partial \theta_i} &= \frac{1}{2} \sum_{j,k=1}^n \frac{\partial M_{kj}}{\partial \theta_i} \dot{\theta}_k \dot{\theta}_j - \frac{\partial V}{\partial \theta_i}. \end{aligned}$$

The \dot{M}_{ij} term can now be expanded in terms of partial derivatives to yield

$$\begin{aligned} \sum_{j=1}^n M_{ij}(\theta) \ddot{\theta}_j + \sum_{j,k=1}^n \left(\frac{\partial M_{ij}}{\partial \theta_k} \dot{\theta}_j \dot{\theta}_k - \frac{1}{2} \frac{\partial M_{kj}}{\partial \theta_i} \dot{\theta}_k \dot{\theta}_j \right) + \frac{\partial V}{\partial \theta_i}(\theta) &= \Upsilon_i \\ i &= 1, \dots, n. \end{aligned}$$

Rearranging terms, we can write

$$\sum_{j=1}^n M_{ij}(\theta) \ddot{\theta}_j + \sum_{j,k=1}^n \Gamma_{ijk} \dot{\theta}_j \dot{\theta}_k + \frac{\partial V}{\partial \theta_i}(\theta) = \Upsilon_i \quad i = 1, \dots, n, \quad (4.21)$$

Coriolis and
centrifugal
forces

where Γ_{ijk} is given by

$$\Gamma_{ijk} = \frac{1}{2} \left(\frac{\partial M_{ij}(\theta)}{\partial \theta_k} + \frac{\partial M_{ik}(\theta)}{\partial \theta_j} - \frac{\partial M_{kj}(\theta)}{\partial \theta_i} \right). \quad (4.22)$$

Equation (4.21) is a second-order differential equation in terms of the manipulator joint variables. It consists of four pieces: inertial forces, which depend on the acceleration of the joints; centrifugal and Coriolis forces, which are quadratic in the joint velocities; potential forces, of the form $\frac{\partial V}{\partial \theta_i}$; and external forces, Υ_i .

The centrifugal and Coriolis terms arise because of the non-inertial frames which are implicit in the use of generalized coordinates. In the classical mechanics literature, one identifies terms of the form $\dot{\theta}_i \dot{\theta}_j$, $i \neq j$ as Coriolis forces and terms of the form $\dot{\theta}_i^2$ as centrifugal forces. The functions Γ_{ijk} are called the *Christoffel symbols* corresponding to the inertia matrix $M(\theta)$.

The external forces can be divided into two components. Let τ_i represent the applied torque at the joint and define $-N_i(\theta, \dot{\theta})$ to be any other forces which act on the i^{th} generalized coordinate, including conservative forces arising from a potential as well as frictional forces. (The reason for the negative sign in the definition of N_i will become apparent in a moment.) As an example, if the manipulator has viscous friction at the joints, then N_i would be defined as

$$-N_i(\theta, \dot{\theta}) = -\frac{\partial V}{\partial \theta_i} - \beta \dot{\theta}_i,$$

where β is the damping coefficient. Other forces acting on the manipulator, such as forces applied at the end-effector, can also be included by reflecting them to the joints (via the transpose of the appropriate Jacobian).

In order to put the equations of motion back into vector form, we define the matrix $C(\theta, \dot{\theta}) \in \mathbb{R}^{n \times n}$ as

$$C_{ij}(\theta, \dot{\theta}) = \sum_{k=1}^n \Gamma_{ijk} \dot{\theta}_k = \frac{1}{2} \sum_{k=1}^n \left(\frac{\partial M_{ij}}{\partial \theta_k} + \frac{\partial M_{ik}}{\partial \theta_j} - \frac{\partial M_{kj}}{\partial \theta_i} \right) \dot{\theta}_k. \quad (4.23)$$

We call the matrix C the *Coriolis matrix* for the manipulator; the vector $C(\theta, \dot{\theta})\dot{\theta}$ gives the Coriolis and centrifugal force terms in the equations of motion. Note that there are other ways to define the matrix $C(\theta, \dot{\theta})$ such that $C_{ij}(\theta, \dot{\theta})\dot{\theta}_j = \Gamma_{ijk}\dot{\theta}_j\dot{\theta}_k$. However, this particular choice has important properties which we shall later exploit.

Equation (4.21) can now be rewritten as

$$\boxed{M(\theta)\ddot{\theta} + C(\theta, \dot{\theta})\dot{\theta} + N(\theta, \dot{\theta}) = \tau} \quad (4.24)$$

where τ is the vector of actuator torques and $N(\theta, \dot{\theta})$ includes gravity terms and other forces which act at the joints. This is a second-order vector differential equation for the motion of the manipulator as a function of the applied joint torques. The matrices M and C , which summarize the inertial properties of the manipulator, have some important properties which we shall use in the sequel:

Lemma 4.2. Structural properties of the robot equations of motion

Equation (4.24) satisfies the following properties:

1. $M(\theta)$ is symmetric and positive definite.
2. $\dot{M} - 2C \in \mathbb{R}^{n \times n}$ is a skew-symmetric matrix.

Proof. Positive definiteness of the inertia matrix follows directly from its definition and the fact that the kinetic energy of the manipulator is zero only if the system is at rest. To show property 2, we calculate the components of the matrix $\dot{M} - 2C$:

$$\begin{aligned} (\dot{M} - 2C)_{ij} &= \dot{M}_{ij}(\theta) - 2C_{ij}(\theta) \\ &= \sum_{k=1}^n \frac{\partial M_{ij}}{\partial \theta_k} \dot{\theta}_k - \frac{\partial M_{ij}}{\partial \theta_k} \dot{\theta}_k - \frac{\partial M_{ik}}{\partial \theta_j} \dot{\theta}_k + \frac{\partial M_{kj}}{\partial \theta_i} \dot{\theta}_k \\ &= \sum_{k=1}^n \frac{\partial M_{kj}}{\partial \theta_i} \dot{\theta}_k - \frac{\partial M_{ik}}{\partial \theta_j} \dot{\theta}_k. \end{aligned}$$

Switching i and j shows $(\dot{M} - 2C)^T = -(\dot{M} - 2C)$. Note that the skew-symmetry property depends upon the particular definition of C given in equation (4.23). \square

dynamics!passivity
property

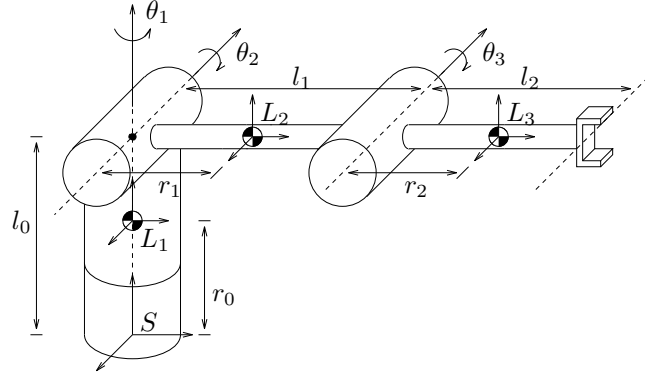


Figure 4.5: Three-link, open-chain manipulator.

Property 2 is often referred to as the *passivity* property since it implies, among other things, that in the absence of friction the net energy of the robot system is conserved (see Exercise 8). The passivity property is important in the proof of many control laws for robot manipulators.

Example 4.3. Dynamics of a three-link manipulator

To illustrate the formulation presented above, we calculate the dynamics of the three-link manipulator shown in Figure 4.5. The joint twists were computed in Chapter 3 (for the elbow manipulator) and are given by

$$\xi_1 = \begin{bmatrix} 0 \\ 0 \\ 0 \\ 0 \\ 1 \end{bmatrix} \quad \xi_2 = \begin{bmatrix} 0 \\ -l_0 \\ 0 \\ -1 \\ 0 \end{bmatrix} \quad \xi_3 = \begin{bmatrix} 0 \\ -l_0 \\ l_1 \\ -1 \\ 0 \end{bmatrix}.$$

To each link we attach a frame L_i at the center of mass and aligned with principle inertia axes of the link, as shown in the figure:

$$g_{sl_1(0)} = \begin{bmatrix} I & \begin{pmatrix} 0 \\ 0 \\ r_0 \end{pmatrix} \\ 0 & 1 \end{bmatrix} \quad g_{sl_2(0)} = \begin{bmatrix} I & \begin{pmatrix} 0 \\ r_1 \\ l_0 \end{pmatrix} \\ 0 & 1 \end{bmatrix} \quad g_{sl_3(0)} = \begin{bmatrix} I & \begin{pmatrix} 0 \\ l_1 + r_2 \\ l_0 \end{pmatrix} \\ 0 & 1 \end{bmatrix}.$$

With this choice of link frames, the link inertia matrices have the general form

$$\mathcal{M}_i = \left[\begin{array}{ccc|ccc} m_i & 0 & 0 & & & \\ 0 & m_i & 0 & & & \\ & 0 & m_i & & & \\ \hline & & 0 & I_{xi} & 0 & \\ & & & 0 & I_{yi} & \\ & & & & 0 & I_{zi} \end{array} \right],$$

where m_i is the mass of the object and I_{xi} , I_{yi} , and I_{zi} are the moments of inertia about the x -, y -, and z -axes of the i^{th} link frame.

To compute the manipulator inertia matrix, we first compute the body Jacobians corresponding to each link frame. A detailed, but straightforward, calculation yields

$$\begin{aligned} J_1 = J_{sl_1(0)}^b &= \begin{bmatrix} 0 & 0 & 0 \\ 0 & 0 & 0 \\ 0 & 0 & 0 \\ 0 & 0 & 0 \\ 0 & 0 & 0 \\ 1 & 0 & 0 \end{bmatrix} & J_2 = J_{sl_2(0)}^b &= \begin{bmatrix} -r_1 c_2 & 0 & 0 \\ 0 & 0 & 0 \\ 0 & -r_1 & 0 \\ 0 & -1 & 0 \\ -s_2 & 0 & 0 \\ c_2 & 0 & 0 \end{bmatrix} \\ J_3 = J_{sl_3(0)}^b &= \begin{bmatrix} -l_2 c_2 - r_2 c_{23} & 0 & 0 \\ 0 & l_1 s_3 & 0 \\ 0 & -r_2 - l_1 c_3 & -r_2 \\ 0 & -1 & -1 \\ -s_{23} & 0 & 0 \\ c_{23} & 0 & 0 \end{bmatrix}. \end{aligned}$$

The inertia matrix for the system is given by

$$M(\theta) = \begin{bmatrix} M_{11} & M_{12} & M_{13} \\ M_{21} & M_{22} & M_{23} \\ M_{31} & M_{32} & M_{33} \end{bmatrix} = J_1^T \mathcal{M}_\infty \mathcal{J}_\infty + \mathcal{J}_\epsilon^T \mathcal{M}_\epsilon \mathcal{J}_\epsilon + \mathcal{J}_\exists^T \mathcal{M}_\exists \mathcal{J}_\exists.$$

The components of M are given by

$$\begin{aligned} M_{11} &= I_{y2} s_2^2 + I_{y3} s_{23}^2 + I_{z1} + I_{z2} c_2^2 + I_{z3} c_{23}^2 \\ &\quad + m_2 r_1^2 c_2^2 + m_3 (l_1 c_2 + r_2 c_{23})^2 \end{aligned}$$

$$M_{12} = 0$$

$$M_{13} = 0$$

$$M_{21} = 0$$

$$M_{22} = I_{x2} + I_{x3} + m_3 l_1^2 + m_2 r_1^2 + m_3 r_2^2 + 2m_3 l_1 r_2 c_3$$

$$M_{23} = I_{x3} + m_3 r_2^2 + m_3 l_1 r_2 c_3$$

$$M_{31} = 0$$

$$M_{32} = I_{x3} + m_3 r_2^2 + m_3 l_1 r_2 c_3$$

$$M_{33} = I_{x3} + m_3 r_2^2.$$

Note that several of the moments of inertia of the different links do not appear in this expression. This is because the limited degrees of freedom of the manipulator do not allow arbitrary rotations of each joint around each axis.

The Coriolis and centrifugal forces are computed directly from the inertia matrix via the formula

$$C_{ij}(\theta, \dot{\theta}) = \sum_{k=1}^n \Gamma_{ijk} \dot{\theta}_k = \frac{1}{2} \sum_{k=1}^n \left(\frac{\partial M_{ij}}{\partial \theta_k} + \frac{\partial M_{ik}}{\partial \theta_j} - \frac{\partial M_{kj}}{\partial \theta_i} \right) \dot{\theta}_k.$$

A very messy calculation shows that the nonzero values of Γ_{ijk} are given by:

$$\begin{aligned} \Gamma_{112} &= (I_{y2} - I_{z2} - m_2 r_1^2) c_2 s_2 + (I_{y3} - I_{z3}) c_{23} s_{23} \\ &\quad - m_3 (l_1 c_2 + r_2 c_{23}) (l_1 s_2 + r_2 s_{23}) \end{aligned}$$

$$\Gamma_{113} = (I_{y3} - I_{z3}) c_{23} s_{23} - m_3 r_2 s_{23} (l_1 c_2 + r_2 c_{23})$$

$$\begin{aligned} \Gamma_{121} &= (I_{y2} - I_{z2} - m_2 r_1^2) c_2 s_2 + (I_{y3} - I_{z3}) c_{23} s_{23} \\ &\quad - m_3 (l_1 c_2 + r_2 c_{23}) (l_1 s_2 + r_2 s_{23}) \end{aligned}$$

$$\Gamma_{131} = (I_{y3} - I_{z3}) c_{23} s_{23} - m_3 r_2 s_{23} (l_1 c_2 + r_2 c_{23})$$

$$\begin{aligned} \Gamma_{211} &= (I_{z2} - I_{y2} + m_2 r_1^2) c_2 s_2 + (I_{z3} - I_{y3}) c_{23} s_{23} \\ &\quad + m_3 (l_1 c_2 + r_2 c_{23}) (l_1 s_2 + r_2 s_{23}) \end{aligned}$$

$$\Gamma_{223} = -l_1 m_3 r_2 s_3$$

$$\Gamma_{232} = -l_1 m_3 r_2 s_3$$

$$\Gamma_{233} = -l_1 m_3 r_2 s_3$$

$$\Gamma_{311} = (I_{z3} - I_{y3}) c_{23} s_{23} + m_3 r_2 s_{23} (l_1 c_2 + r_2 c_{23})$$

$$\Gamma_{322} = l_1 m_3 r_2 s_3$$

Finally, we compute the effect of gravitational forces on the manipulator. These

forces are written as

$$N(\theta, \dot{\theta}) = \frac{\partial V}{\partial \theta},$$

where $V : \mathbb{R}^n \rightarrow \mathbb{R}$ is the potential energy of the manipulator. For the three-link manipulator under consideration here, the potential energy is given by

$$V(\theta) = m_1 g h_1(\theta) + m_2 g h_2(\theta) + m_3 g h_3(\theta),$$

where h_i is the the height of the center of mass for the i^{th} link. These can be found using the forward kinematics map

$$g_{sl_i}(\theta) = e^{\hat{\xi}_1 \theta_1} \dots e^{\hat{\xi}_i \theta_i} g_{sl_i}(0),$$

which gives

$$h_1(\theta) = r_0$$

$$h_2(\theta) = l_0 - r_1 \sin \theta_2$$

$$h_3(\theta) = l_0 - l_1 \sin \theta_2 - r_2 \sin(\theta_2 + \theta_3).$$

Substituting these expressions into the potential energy and taking the derivative gives

$$N(\theta, \dot{\theta}) = \frac{\partial V}{\partial \theta} = \begin{bmatrix} 0 \\ -(m_2 g r_1 + m_3 g l_1) \cos \theta_2 - m_3 r_2 \cos(\theta_2 + \theta_3) \\ -m_3 g r_2 \cos(\theta_2 + \theta_3) \end{bmatrix}. \quad (4.25)$$

This completes the derivation of the dynamics.

3.3 Robot dynamics and the product of exponentials formula

The formulas and properties given in the last section hold for any mechanical system with Lagrangian $L = \frac{1}{2} \dot{\theta}^T M(\theta) \dot{\theta} - V(\theta)$. If the forward kinematics are specified using the product of exponentials formula, then it is possible to get more explicit formulas for the inertia and Coriolis matrices. In this section we derive these formulas, based on the treatments given by Brockett et al. [9] and Park et al. [52].

product of
exponentials
for-
mula!dynamics
using
dynamics!using
the product of
exponentials
formula
cross prod-
uct!Lie@and
Lie bracket

twists! Lie
bracket
between

In addition to the tools introduced in Chapters 2 and 3, we will make use of one additional operation on twists. Recall, first, that in $so(3)$ the cross product between two vectors $\omega_1, \omega_2 \in \mathbb{R}^3$ yields a third vector, $\omega_1 \times \omega_2 \in \mathbb{R}^3$. It can be shown by direct calculation that the cross product satisfies

$$(\omega_1 \times \omega_2)^\wedge = \hat{\omega}_1 \hat{\omega}_2 - \hat{\omega}_2 \hat{\omega}_1.$$

By direct analogy, we define the *Lie bracket* on $se(3)$ as

$$[\hat{\xi}_1, \hat{\xi}_2] = \hat{\xi}_1 \hat{\xi}_2 - \hat{\xi}_2 \hat{\xi}_1.$$

A simple calculation verifies that the right-hand side of this equation has the form of a twist, and hence $[\hat{\xi}_1, \hat{\xi}_2] \in se(3)$.

If $\xi_1, \xi_2 \in \mathbb{R}^6$ represent the coordinates for two twists, we define the bracket operation $[\cdot, \cdot] : \mathbb{R}^6 \times \mathbb{R}^6 \rightarrow \mathbb{R}^6$ as

$$[\xi_1, \xi_2] = \left(\hat{\xi}_1 \hat{\xi}_2 - \hat{\xi}_2 \hat{\xi}_1 \right)^\vee. \quad (4.26)$$

This is a generalization of the cross product on \mathbb{R}^3 to vectors in \mathbb{R}^6 . The following properties of the Lie bracket are also generalizations of properties of the cross product:

$$= -[\xi_2, \xi_1]$$

$$[\xi_1, [\xi_2, \xi_3]] + [\xi_2, [\xi_3, \xi_1]] + [\xi_3, [\xi_1, \xi_2]] = 0.$$

A more detailed (and abstract) description of the Lie bracket operation on $se(3)$ is given in Appendix A. For this chapter we shall only need the formula given in equation (4.26)

We now define some additional notation which we use in the sequel. Let $A_{ij} \in \mathbb{R}^{6 \times 6}$ represent the adjoint transformation given by

$$A_{ij} = \begin{cases} \text{Ad}_{(e^{\xi_{j+1}\theta_{j+1}} \dots e^{\xi_i\theta_i})}^{-1} & i > j \\ I & i = j \\ 0 & i < j. \end{cases} \quad (4.27)$$

Using this notation, the j^{th} column of the body Jacobian for the i^{th} link is given by

$\text{Ad}_{g_{sl_i}^{-1}} A_{ij} \xi_j$:

$$J_i(\theta) = \text{Ad}_{g_{sl_i(0)}^{-1}} \begin{bmatrix} A_{i1} \xi_1 & \cdots & A_{ii} \xi_i & 0 & \cdots & 0 \end{bmatrix}.$$

inertia
matrix!open-
chain@for
open-chain
manipulators
Coriolis matrix

We combine $\text{Ad}_{g_{sl_i(0)}^{-1}}$ with the link inertia matrix by defining the transformed inertia matrix for the i^{th} link:

$$\mathcal{M}'_i = \text{Ad}_{\mathcal{J}_{\uparrow}^{-\infty}(i)}^T \mathcal{M}_i \text{Ad}_{\mathcal{J}_{\uparrow}^{-\infty}(i)}. \quad (4.28)$$

The matrix \mathcal{M}'_i represents the inertia of the i^{th} link reflected into the base frame of the manipulator.

Using these definitions, we can obtain formulas for the inertial quantities which appear in the equation of motion. We state the results as a proposition.

Proposition 4.3. Formulas for inertia and Coriolis matrices

Using the notation defined above, the inertia and Coriolis matrices for an open-chain manipulator are given by

$$\begin{aligned} M_{ij}(\theta) &= \sum_{l=\max(i,j)}^n \xi_i^T A_{li}^T \mathcal{M}'_l \mathcal{A}_{\uparrow l} \xi_j \\ C_{ij}(\theta) &= \frac{1}{2} \sum_{k=1}^n \left(\frac{\partial M_{ij}}{\partial \theta_k} + \frac{\partial M_{ik}}{\partial \theta_j} - \frac{\partial M_{kj}}{\partial \theta_i} \right) \dot{\theta}_k, \end{aligned} \quad (4.29)$$

where

$$\begin{aligned} \frac{\partial M_{ij}}{\partial \theta_k} &= \sum_{l=\max(i,j)}^n \left([A_{ki} \xi_i, \xi_k]^T A_{lk}^T \mathcal{M}'_l \mathcal{A}_{\uparrow l} \xi_j \right. \\ &\quad \left. + \xi_i^T A_{li}^T \mathcal{M}'_l \mathcal{A}_{\uparrow l} [\mathcal{A}_{\parallel l} \xi_i, \xi_{\parallel}] \right). \end{aligned} \quad (4.30)$$

This proposition shows that all of the dynamic attributes of the manipulator can be determined directly from the joint twists ξ_i , the link frames $g_{sl_i(0)}$, and the link inertia matrices \mathcal{M}_i . The matrices A_{ij} are the only expressions in equations (4.29) and (4.30) which depend on the current configuration of the manipulator.

SCARA manipulator dynamics *Proof.* The only term which needs to be calculated in order to prove the proposition is $\frac{\partial}{\partial \theta_k}(A_{lj}\xi_j)$. For $i \geq j$, let $g_{ij} \in SE(3)$ be the rigid transformation given by

$$g_{ij} = \begin{cases} e^{-\hat{\xi}_i \theta_i} \dots e^{-\hat{\xi}_{j+1} \theta_{j+1}} & i > j \\ I & i = j, \end{cases}$$

so that $A_{ij} = \text{Ad}_{g_{ij}}$. Using this notation, if k is an integer such that $i \geq k \geq j$, then $g_{ij} = g_{ik}g_{kj}$. We now proceed to calculate $\frac{\partial}{\partial \theta_k}(A_{lj}\xi_j)$ for $i \geq k \geq j$:

$$\begin{aligned} \frac{\partial}{\partial \theta_k}(A_{lj}\xi_j) &= \left(\frac{\partial}{\partial \theta_k} (g_{lj} \hat{\xi}_j g_{lj}^{-1}) \right)^\vee = \left(\frac{\partial g_{lj}}{\partial \theta_k} \hat{\xi}_j g_{lj}^{-1} + g_{lj} \hat{\xi}_j \frac{\partial g_{lj}^{-1}}{\partial \theta_k} \right)^\vee \\ &= \left(-g_{l,k} \hat{\xi}_k g_{kj} \hat{\xi}_j g_{lj}^{-1} + g_{lj} \hat{\xi}_j g_{kj}^{-1} \hat{\xi}_k g_{lk}^{-1} \right)^\vee \\ &= \text{Ad}_{g_{lk}} \left(-\hat{\xi}_k g_{kj} \hat{\xi}_j g_{kj}^{-1} + g_{kj} \hat{\xi}_j g_{kj}^{-1} \hat{\xi}_k \right)^\vee \\ &= A_{lk}[A_{kj}\xi_j, \xi_k]. \end{aligned}$$

For all other values of k , $\frac{\partial}{\partial \theta_k}(A_{lj}\xi_j)$ is zero. The proposition now follows by direct calculation. \square

Example 4.4. Dynamics of an idealized SCARA manipulator

Consider the SCARA manipulator shown in Figure 4.6. The joint twists are given by

$$\xi_1 = \begin{bmatrix} 0 \\ 0 \\ 0 \\ 1 \end{bmatrix} \quad \xi_2 = \begin{bmatrix} l_1 \\ 0 \\ 0 \\ 1 \end{bmatrix} \quad \xi_3 = \begin{bmatrix} l_1+l_2 \\ 0 \\ 0 \\ 1 \end{bmatrix} \quad \xi_4 = \begin{bmatrix} 0 \\ 0 \\ 1 \\ 0 \end{bmatrix}.$$

Assuming that the link frames are initially aligned with the base frame and are located at the centers of mass of the links, the transformed link inertia matrices have the form

$$\mathcal{M}'_i = \begin{bmatrix} I & 0 \\ -\hat{p}_i & I \end{bmatrix} \begin{bmatrix} m_i I & 0 \\ 0 & \mathcal{I} \end{bmatrix} \begin{bmatrix} I & \hat{p}_i \\ 0 & I \end{bmatrix} = \begin{bmatrix} m_i I & m_i \hat{p}_i \\ -m_i \hat{p}_i & \mathcal{I} \end{bmatrix},$$

where p_i is the location of the origin of the i^{th} link frame relative to the base frame S .

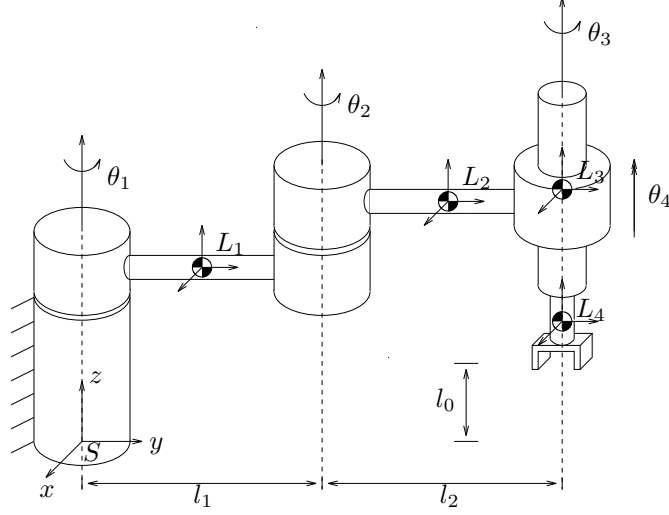


Figure 4.6: SCARA manipulator in its reference configuration.

Given the joint twists ξ_i and transformed link inertias \mathcal{M}'_i , the dynamics of the manipulator can be computed using the formulas in Proposition 4.3. This task is considerably simplified using the software described in Appendix B, so we omit a detailed computation and present only the final result. The inertia matrix $M(\theta) \in \mathbb{R}^{4 \times 4}$ is given by

$$M(\theta) = \begin{bmatrix} \alpha + \beta + 2\gamma \cos \theta_2 & \beta + \gamma \cos \theta_2 & \delta & 0 \\ \beta + \gamma \cos \theta_2 & \beta & \delta & 0 \\ \delta & \delta & \delta & 0 \\ 0 & 0 & 0 & m_4 \end{bmatrix},$$

where

$$\alpha = I_{z1} + r_1^2 m_1 + l_1^2 m_2 + l_1^2 m_3 + l_1^2 m_4$$

$$\beta = I_{z2} + I_{z3} + I_{z4} + l_2^2 m_3 + l_2^2 m_4 + m_2 r_2^2$$

$$\gamma = l_1 l_2 m_3 + l_1 l_2 m_4 + l_1 m_2 r_2$$

$$\delta = I_{z3} + I_{z4}.$$

dynamics!open-
chain
manipulators—)
Lyapunov
stability—(
stability
definitions—(
local stability

The Coriolis matrix is given by

$$C(\theta, \dot{\theta}) = \begin{bmatrix} -\gamma \sin \theta_2 \dot{\theta}_2 & -\gamma \sin \theta_2 (\dot{\theta}_1 + \dot{\theta}_2) & 0 & 0 \\ \gamma \sin \theta_2 \dot{\theta}_1 & 0 & 0 & 0 \\ 0 & 0 & 0 & 0 \\ 0 & 0 & 0 & 0 \end{bmatrix}.$$

The only remaining term in the dynamics is the gravity term, which can be determined by inspection since only θ_4 affects the potential energy of the manipulator. Hence,

$$N(\theta, \dot{\theta}) = \begin{bmatrix} 0 \\ 0 \\ 0 \\ m_4 g \end{bmatrix}.$$

Friction and other nonconservative forces can also be included in N .

4 Lyapunov Stability Theory

In this section we review the tools of Lyapunov stability theory. These tools will be used in the next section to analyze the stability properties of a robot controller. We present a survey of the results that we shall need in the sequel, with no proofs. The interested reader should consult a standard text, such as Vidyasagar [74] or Khalil [32], for details.

4.1 Basic definitions

Consider a dynamical system which satisfies

$$\dot{x} = f(x, t) \quad x(t_0) = x_0 \quad x \in \mathbb{R}^n. \quad (4.31)$$

We will assume that $f(x, t)$ satisfies the standard conditions for the existence and uniqueness of solutions. Such conditions are, for instance, that $f(x, t)$ is Lipschitz continuous with respect to x , uniformly in t , and piecewise continuous in t . A point $x^* \in \mathbb{R}^n$ is an *equilibrium point* of (4.31) if $f(x^*, t) \equiv 0$. Intuitively and somewhat

crudely speaking, we say an equilibrium point is *locally stable* if all solutions which start near x^* (meaning that the initial conditions are in a neighborhood of x^*) remain near x^* for all time. The equilibrium point x^* is said to be *locally asymptotically stable* if x^* is locally stable and, furthermore, all solutions starting near x^* tend towards x^* as $t \rightarrow \infty$. We say somewhat crude because the time-varying nature of equation (4.31) introduces all kinds of additional subtleties. Nonetheless, it is intuitive that a pendulum has a locally stable equilibrium point when the pendulum is hanging straight down and an unstable equilibrium point when it is pointing straight up. If the pendulum is damped, the stable equilibrium point is locally asymptotically stable.

By shifting the origin of the system, we may assume that the equilibrium point of interest occurs at $x^* = 0$. If multiple equilibrium points exist, we will need to study the stability of each by appropriately shifting the origin.

Definition 4.1. Stability in the sense of Lyapunov

The equilibrium point $x^* = 0$ of (4.31) is *stable (in the sense of Lyapunov)* at $t = t_0$ if for any $\epsilon > 0$ there exists a $\delta(t_0, \epsilon) > 0$ such that

$$\|x(t_0)\| < \delta \implies \|x(t)\| < \epsilon, \quad \forall t \geq t_0. \quad (4.32)$$

Lyapunov stability is a very mild requirement on equilibrium points. In particular, it does not require that trajectories starting close to the origin tend to the origin asymptotically. Also, stability is defined at a time instant t_0 . *Uniform stability* is a concept which guarantees that the equilibrium point is not losing stability. We insist that for a uniformly stable equilibrium point x^* , δ in the Definition 4.1 not be a function of t_0 , so that equation (4.32) may hold for all t_0 . Asymptotic stability is made precise in the following definition:

Definition 4.2. Asymptotic stability

An equilibrium point $x^* = 0$ of (4.31) is *asymptotically stable* at $t = t_0$ if

local stability

1. $x^* = 0$ is stable, and
2. $x^* = 0$ is locally attractive; i.e., there exists $\delta(t_0)$ such that

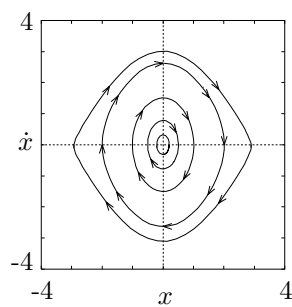
$$\|x(t_0)\| < \delta \implies \lim_{t \rightarrow \infty} x(t) = 0. \quad (4.33)$$

As in the previous definition, asymptotic stability is defined at t_0 . *Uniform asymptotic stability* requires:

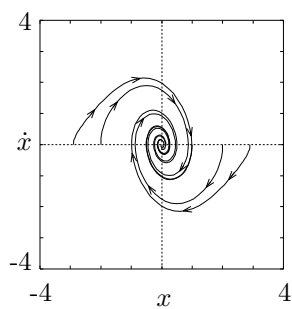
1. $x^* = 0$ is uniformly stable, and
2. $x^* = 0$ is uniformly locally attractive; i.e., there exists δ independent of t_0 for which equation (4.33) holds. Further, it is required that the convergence in equation (4.33) is uniform.

Finally, we say that an equilibrium point is *unstable* if it is not stable. This is less of a tautology than it sounds and the reader should be sure he or she can negate the definition of stability in the sense of Lyapunov to get a definition of instability. In robotics, we are almost always interested in uniformly asymptotically stable equilibria. If we wish to move the robot to a point, we would like to actually converge to that point, not merely remain nearby. Figure 4.7 illustrates the difference between stability in the sense of Lyapunov and asymptotic stability.

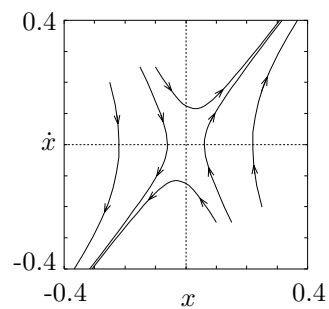
Definitions 4.1 and 4.2 are *local* definitions; they describe the behavior of a system near an equilibrium point. We say an equilibrium point x^* is *globally* stable if it is stable for all initial conditions $x_0 \in \mathbb{R}^n$. Global stability is very desirable, but in many applications it can be difficult to achieve. We will concentrate on local stability theorems and indicate where it is possible to extend the results to the global case. Notions of uniformity are only important for time-varying systems. Thus, for time-invariant systems, stability implies uniform stability and asymptotic stability implies uniform asymptotic stability.



(a) Stable in the sense of Lyapunov



(b) Asymptotically stable



(c) Unstable (saddle)

Figure 4.7: Phase portraits for stable and unstable equilibrium points.

exponential
stability
definitions—)
Lyapunov
stability!direct
method—(
direct method
of Lyapunov
locally positive
definite
functions

It is important to note that the definitions of asymptotic stability do not quantify the rate of convergence. There is a strong form of stability which demands an exponential rate of convergence:

Definition 4.3. Exponential stability, rate of convergence

The equilibrium point $x^* = 0$ is an *exponentially stable* equilibrium point of (4.31) if there exist constants $m, \alpha > 0$ and $\epsilon > 0$ such that

$$\|x(t)\| \leq me^{-\alpha(t-t_0)}\|x(t_0)\| \quad (4.34)$$

for all $\|x(t_0)\| \leq \epsilon$ and $t \geq t_0$. The largest constant α which may be utilized in (4.34) is called the *rate of convergence*.

Exponential stability is a strong form of stability; in particular, it implies uniform, asymptotic stability. Exponential convergence is important in applications because it can be shown to be robust to perturbations and is essential for the consideration of more advanced control algorithms, such as adaptive ones. A system is *globally exponentially stable* if the bound in equation (4.34) holds for all $x_0 \in \mathbb{R}^n$. Whenever possible, we shall strive to prove global, exponential stability.

4.2 The direct method of Lyapunov

Lyapunov's direct method (also called the second method of Lyapunov) allows us to determine the stability of a system without explicitly integrating the differential equation (4.31). The method is a generalization of the idea that if there is some “measure of energy” in a system, then we can study the rate of change of the energy of the system to ascertain stability. To make this precise, we need to define exactly what one means by a “measure of energy.” Let B_ϵ be a ball of size ϵ around the origin, $B_\epsilon = \{x \in \mathbb{R}^n : \|x\| < \epsilon\}$.

Definition 4.4. Locally positive definite functions (lpdf)

A continuous function $V : \mathbb{R}^n \times \mathbb{R}_+ \rightarrow \mathbb{R}$ is a *locally positive definite function* if for

some $\epsilon > 0$ and some continuous, strictly increasing function $\alpha : \mathbb{R}_+ \rightarrow \mathbb{R}$,

$$V(0, t) = 0 \quad \text{and} \quad V(x, t) \geq \alpha(\|x\|) \quad \forall x \in B_\epsilon, \forall t \geq 0. \quad (4.35)$$

positive definite
functions
Lyapunov
stability!basic
theorem

A locally positive definite function is locally like an energy function. Functions which are globally like energy functions are called positive definite functions:

Definition 4.5. Positive definite functions (pdf)

A continuous function $V : \mathbb{R}^n \times \mathbb{R}_+ \rightarrow \mathbb{R}$ is a *positive definite function* if it satisfies the conditions of Definition 4.4 and, additionally, $\alpha(p) \rightarrow \infty$ as $p \rightarrow \infty$.

To bound the energy function from above, we define decrecence as follows:

Definition 4.6. Decrescent functions

A continuous function $V : \mathbb{R}^n \times \mathbb{R}_+ \rightarrow \mathbb{R}$ is *decrecent* if for some $\epsilon > 0$ and some continuous, strictly increasing function $\beta : \mathbb{R}_+ \rightarrow \mathbb{R}$,

$$V(x, t) \leq \beta(\|x\|) \quad \forall x \in B_\epsilon, \forall t \geq 0 \quad (4.36)$$

Using these definitions, the following theorem allows us to determine stability for a system by studying an appropriate energy function. Roughly, this theorem states that when $V(x, t)$ is a locally positive definite function and $\dot{V}(x, t) \leq 0$ then we can conclude stability of the equilibrium point. The time derivative of V is taken along the trajectories of the system:

$$\dot{V} \Big|_{\dot{x}=f(x,t)} = \frac{\partial V}{\partial t} + \frac{\partial V}{\partial x} f.$$

In what follows, by \dot{V} we will mean $\dot{V} \Big|_{\dot{x}=f(x,t)}$.

Theorem 4.4. Basic theorem of Lyapunov

Let $V(x, t)$ be a non-negative function with derivative \dot{V} along the trajectories of the system.

1. If $V(x, t)$ is locally positive definite and $\dot{V}(x, t) \leq 0$ locally in x and for all t , then the origin of the system is locally stable (in the sense of Lyapunov).

Lyapunov
functions!choosing

Table 4.1: Summary of the basic theorem of Lyapunov.

	Conditions on $V(x, t)$	Conditions on $-\dot{V}(x, t)$	Conclusions
1	lpdf	≥ 0 locally	Stable
2	lpdf, decrescent	≥ 0 locally	Uniformly stable
3	lpdf, decrescent	lpdf	Uniformly asymptotically stable
4	pdf, decrescent	pdf	Globally uniformly asymptotically stable

2. If $V(x, t)$ is locally positive definite and decrescent, and $\dot{V}(x, t) \leq 0$ locally in x and for all t , then the origin of the system is uniformly locally stable (in the sense of Lyapunov).
3. If $V(x, t)$ is locally positive definite and decrescent, and $-\dot{V}(x, t)$ is locally positive definite, then the origin of the system is uniformly locally asymptotically stable.
4. If $V(x, t)$ is positive definite and decrescent, and $-\dot{V}(x, t)$ is positive definite, then the origin of the system is globally uniformly asymptotically stable.

The conditions in the theorem are summarized in Table 4.1.

Theorem 4.4 gives sufficient conditions for the stability of the origin of a system. It does not, however, give a prescription for determining the Lyapunov function $V(x, t)$. Since the theorem only gives sufficient conditions, the search for a Lyapunov function establishing stability of an equilibrium point could be arduous. However, it is a remarkable fact that the converse of Theorem 4.4 also exists: if an equilibrium point is stable, then there exists a function $V(x, t)$ satisfying the conditions of the theorem. However, the utility of this and other converse theorems is limited by the lack of a computable technique for generating Lyapunov functions.

Theorem 4.4 also stops short of giving explicit rates of convergence of solutions

to the equilibrium. It may be modified to do so in the case of exponentially stable equilibria.

Lyapunov stability!direct method—)

Theorem 4.5. Exponential stability theorem

Lyapunov stability!indirect method—(

$x^* = 0$ is an exponentially stable equilibrium point of $\dot{x} = f(x, t)$ if and only if there exists an $\epsilon > 0$ and a function $V(x, t)$ which satisfies

indirect method of Lyapunov

$$\alpha_1 \|x\|^2 \leq V(x, t) \leq \alpha_2 \|x\|^2$$

$$\dot{V}|_{\dot{x}=f(x,t)} \leq -\alpha_3 \|x\|^2$$

$$\left\| \frac{\partial V}{\partial x}(x, t) \right\| \leq \alpha_4 \|x\|$$

for some positive constants $\alpha_1, \alpha_2, \alpha_3, \alpha_4$, and $\|x\| \leq \epsilon$.

The rate of convergence for a system satisfying the conditions of Theorem 4.5 can be determined from the proof of the theorem [65]. It can be shown that

$$m \leq \left(\frac{\alpha_2}{\alpha_1} \right)^{1/2} \quad \alpha \geq \frac{\alpha_3}{2\alpha_2}$$

are bounds in equation (4.34). The equilibrium point $x^* = 0$ is globally exponentially stable if the bounds in Theorem 4.5 hold for all x .

4.3 The indirect method of Lyapunov

The indirect method of Lyapunov uses the linearization of a system to determine the local stability of the original system. Consider the system

$$\dot{x} = f(x, t) \tag{4.37}$$

with $f(0, t) = 0$ for all $t \geq 0$. Define

$$A(t) = \left. \frac{\partial f(x, t)}{\partial x} \right|_{x=0} \tag{4.38}$$

to be the Jacobian matrix of $f(x, t)$ with respect to x , evaluated at the origin. It follows that for each fixed t , the remainder

$$f_1(x, t) = f(x, t) - A(t)x$$

stability by
linearization
uniform
stability
local stability

approaches zero as x approaches zero. However, the remainder may not approach zero *uniformly*. For this to be true, we require the stronger condition that

$$\lim_{\|x\| \rightarrow 0} \sup_{t \geq 0} \frac{\|f_1(x, t)\|}{\|x\|} = 0. \quad (4.39)$$

If equation (4.39) holds, then the system

$$\dot{z} = A(t)z \quad (4.40)$$

is referred to as the (uniform) *linearization* of equation (4.31) about the origin. When the linearization exists, its stability determines the local stability of the original nonlinear equation.

Theorem 4.6. Stability by linearization

Consider the system (4.37) and assume

$$\lim_{\|x\| \rightarrow 0} \sup_{t \geq 0} \frac{\|f_1(x, t)\|}{\|x\|} = 0.$$

Further, let $A(\cdot)$ defined in equation (4.38) be bounded. If 0 is a uniformly asymptotically stable equilibrium point of (4.40) then it is a locally uniformly asymptotically stable equilibrium point of (4.37).

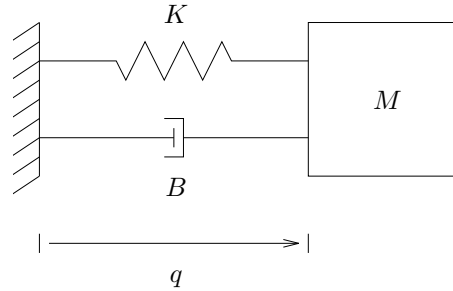
The preceding theorem requires *uniform* asymptotic stability of the linearized system to prove uniform asymptotic stability of the nonlinear system. Counterexamples to the theorem exist if the linearized system is not uniformly asymptotically stable.

If the system (4.37) is time-invariant, then the indirect method says that if the eigenvalues of

$$A = \left. \frac{\partial f(x)}{\partial x} \right|_{x=0}$$

are in the open left half complex plane, then the origin is asymptotically stable.

This theorem proves that *global* uniform asymptotic stability of the linearization implies *local* uniform asymptotic stability of the original nonlinear system. The



Lyapunov sta-
bility!indirect
method—)
harmonic
oscillator
spring mass
system

Figure 4.8: Damped harmonic oscillator.

estimates provided by the proof of the theorem can be used to give a (conservative) bound on the domain of attraction of the origin. Systematic techniques for estimating the bounds on the regions of attraction of equilibrium points of nonlinear systems is an important area of research and involves searching for the “best” Lyapunov functions.

4.4 Examples

We now illustrate the use of the stability theorems given above on a few examples.

Example 4.5. Linear harmonic oscillator

Consider a damped harmonic oscillator, as shown in Figure 4.8. The dynamics of the system are given by the equation

$$M\ddot{q} + B\dot{q} + Kq = 0, \quad (4.41)$$

where M , B , and K are all positive quantities. As a state space equation we rewrite equation (4.41) as

$$\frac{d}{dt} \begin{bmatrix} q \\ \dot{q} \end{bmatrix} = \begin{bmatrix} \dot{q} \\ -(K/M)q - (B/M)\dot{q} \end{bmatrix}. \quad (4.42)$$

Define $x = (q, \dot{q})$ as the state of the system.

Since this system is a linear system, we can determine stability by examining the poles of the system. The Jacobian matrix for the system is

$$A = \begin{bmatrix} 0 & 1 \\ -K/M & -B/M \end{bmatrix},$$

which has a characteristic equation

$$\lambda^2 + (B/M)\lambda + (K/M) = 0.$$

The solutions of the characteristic equation are

$$\lambda = \frac{-B \pm \sqrt{B^2 - 4KM}}{2M},$$

which always have negative real parts, and hence the system is (globally) exponentially stable.

We now try to apply Lyapunov's direct method to determine exponential stability. The "obvious" Lyapunov function to use in this context is the energy of the system,

$$V(x, t) = \frac{1}{2}M\dot{q}^2 + \frac{1}{2}Kq^2. \quad (4.43)$$

Taking the derivative of V along trajectories of the system (4.41) gives

$$\dot{V} = M\dot{q}\ddot{q} + Kq\dot{q} = -B\dot{q}^2. \quad (4.44)$$

The function $-\dot{V}$ is quadratic but not locally positive definite, since it does not depend on q , and hence we cannot conclude exponential stability. It is still possible to conclude *asymptotic* stability using Lasalle's invariance principle (described in the next section), but this is obviously conservative since we already know that the system is exponentially stable.

The reason that Lyapunov's direct method fails is illustrated in Figure 4.9a, which shows the flow of the system superimposed with the level sets of the Lyapunov

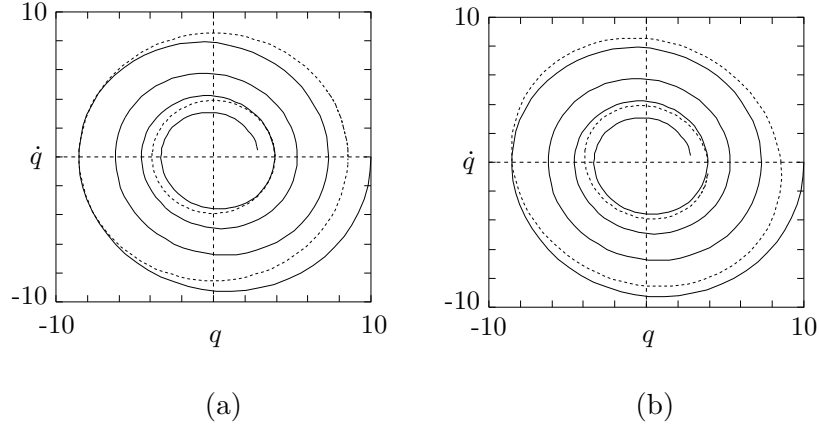


Figure 4.9: Flow of damped harmonic oscillator. The dashed lines are the level sets of the Lyapunov function defined by (a) the total energy and (b) a skewed modification of the energy.

function. The level sets of the Lyapunov function become tangent to the flow when $\dot{q} = 0$, and hence it is not a valid Lyapunov function for determining exponential stability.

To fix this problem, we skew the level sets slightly, so that the flow of the system crosses the level surfaces transversely. Define

$$V(x, t) = \frac{1}{2} \begin{bmatrix} q \\ \dot{q} \end{bmatrix}^T \begin{bmatrix} K & \epsilon M \\ \epsilon M & M \end{bmatrix} \begin{bmatrix} q \\ \dot{q} \end{bmatrix} = \frac{1}{2} \dot{q} M \dot{q} + \frac{1}{2} q K q + \epsilon \dot{q} M q,$$

where ϵ is a small positive constant such that V is still positive definite. The derivative of the Lyapunov function becomes

$$\begin{aligned} \dot{V} &= \dot{q} M \ddot{q} + q K \dot{q} + \epsilon M \dot{q}^2 + \epsilon q M \ddot{q} \\ &= (-B + \epsilon M) \dot{q}^2 + \epsilon (-K q^2 - B q \dot{q}) = - \begin{bmatrix} q \\ \dot{q} \end{bmatrix}^T \begin{bmatrix} \epsilon K & \frac{1}{2} \epsilon B \\ \frac{1}{2} \epsilon B & B - \epsilon M \end{bmatrix} \begin{bmatrix} q \\ \dot{q} \end{bmatrix}. \end{aligned}$$

The function \dot{V} can be made negative definite for ϵ chosen sufficiently small (see Exercise 11) and hence we can conclude *exponential* stability. The level sets of this Lyapunov function are shown in Figure 4.9b.

spring mass
system
passivity
Lasalle's
invariance
principle

This same technique is used in the stability proofs for the robot control laws contained in the next section.

Example 4.6. Nonlinear spring mass system with damper

Consider a mechanical system consisting of a unit mass attached to a *nonlinear* spring with a velocity-dependent damper. If x_1 stands for the position of the mass and x_2 its velocity, then the equations describing the system are:

$$\begin{aligned}\dot{x}_1 &= x_2 \\ \dot{x}_2 &= -f(x_2) - g(x_1).\end{aligned}\tag{4.45}$$

Here f and g are smooth functions modeling the friction in the damper and restoring force of the spring, respectively. We will assume that f, g are both passive; that is,

$$\begin{aligned}\sigma f(\sigma) &\geq 0 \quad \forall \sigma \in [-\sigma_0, \sigma_0] \\ \sigma g(\sigma) &\geq 0 \quad \forall \sigma \in [-\sigma_0, \sigma_0]\end{aligned}$$

and equality is only achieved when $\sigma = 0$. The candidate for the Lyapunov function is

$$V(x) = \frac{x_2^2}{2} + \int_0^{x_1} g(\sigma) d\sigma.$$

The passivity of g guarantees that $V(x)$ is a locally positive definite function. A short calculation verifies that

$$\dot{V}(x) = -x_2 f(x_2) \leq 0 \quad \text{when } |x_2| \leq \sigma_0.$$

This establishes the stability, but not the asymptotic stability of the origin. Actually, the origin is asymptotically stable, but this needs Lasalle's principle, which is discussed in the next section.

4.5 Lasalle's invariance principle

Lasalle's theorem enables one to conclude asymptotic stability of an equilibrium point even when $-\dot{V}(x, t)$ is not locally positive definite. However, it applies only to

autonomous or periodic systems. We will deal with the autonomous case and begin by introducing a few more definitions. We denote the solution trajectories of the autonomous system

$$\dot{x} = f(x) \quad (4.46)$$

as $s(t, x_0, t_0)$, which is the solution of equation (4.46) at time t starting from x_0 at t_0 .

Definition 4.7. ω limit set

The set $S \subset \mathbb{R}^n$ is the ω *limit set* of a trajectory $s(\cdot, x_0, t_0)$ if for every $y \in S$, there exists a strictly increasing sequence of times t_n such that

$$s(t_n, x_0, t_0) \rightarrow y$$

as $t_n \rightarrow \infty$.

Definition 4.8. Invariant set

The set $M \subset \mathbb{R}^n$ is said to be an (positively) *invariant set* if for all $y \in M$ and $t_0 \geq 0$, we have

$$s(t, y, t_0) \in M \quad \forall t \geq t_0.$$

It may be proved that the ω limit set of every trajectory is closed and invariant. We may now state Lasalle's principle.

Theorem 4.7. Lasalle's principle

Let $V : \mathbb{R}^n \rightarrow \mathbb{R}$ be a locally positive definite function such that on the compact set $\Omega_c = \{x \in \mathbb{R}^n : V(x) \leq c\}$ we have $\dot{V}(x) \leq 0$. Define

$$S = \{x \in \Omega_c : \dot{V}(x) = 0\}.$$

As $t \rightarrow \infty$, the trajectory tends to the largest invariant set inside S ; i.e., its ω limit set is contained inside the largest invariant set in S . In particular, if S contains no invariant sets other than $x = 0$, then 0 is asymptotically stable.

spring mass
system
Lyapunov
stability—)

A global version of the preceding theorem may also be stated. An application of Lasalle's principle is as follows:

Example 4.7. Nonlinear spring mass system with damper

Consider the same example as in equation (4.45), where we saw that with

$$V(x) = \frac{x_2^2}{2} + \int_0^{x_1} g(\sigma) d\sigma,$$

we obtained

$$\dot{V}(x) = -x_2 f(x_2).$$

Choosing $c = \min(V(-\sigma_0, 0), V(\sigma_0, 0))$ so as to apply Lasalle's principle, we see that

$$\dot{V}(x) \leq 0 \quad \text{for } x \in \Omega_c := \{x : V(x) \leq c\}.$$

As a consequence of Lasalle's principle, the trajectory enters the largest invariant set in $\Omega_c \cap \{x_1, x_2 : \dot{V} = 0\} = \Omega_c \cap \{x_1, 0\}$. To obtain the largest invariant set in this region, note that

$$x_2(t) \equiv 0 \quad \implies \quad x_1(t) \equiv x_{10} \quad \implies \quad \dot{x}_2(t) = 0 = -f(0) - g(x_{10}),$$

where x_{10} is some constant. Consequently, we have that

$$g(x_{10}) = 0 \quad \implies \quad x_{10} = 0.$$

Thus, the largest invariant set inside $\Omega_c \cap \{x_1, x_2 : \dot{V} = 0\}$ is the origin and, by Lasalle's principle, the origin is locally asymptotically stable.

There is a version of Lasalle's theorem which holds for periodic systems as well. However, there are no significant generalizations for non-periodic systems and this restricts the utility of Lasalle's principle in applications.

5 Position Control and Trajectory Tracking

In this section, we consider the position control problem for robot manipulators: given a desired trajectory, how should the joint torques be chosen so that the manipulator follows that trajectory. We would like to choose a control strategy which is robust with respect to initial condition errors, sensor noise, and modeling errors. We ignore the problems of actuator dynamics, and assume that we can command arbitrary torques which are exerted at the joints.

position
control—(
control!open-
chain@of
open-chain
manipulators—(
robustness of
control laws

5.1 Problem description

We are given a description of the dynamics of a robot manipulator in the form of the equation

$$M(\theta)\ddot{\theta} + C(\theta, \dot{\theta})\dot{\theta} + N(\theta, \dot{\theta}) = \tau, \quad (4.47)$$

where $\theta \in \mathbb{R}^n$ is the set of configuration variables for the robot and $\tau \in \mathbb{R}^n$ denotes the torques applied at the joints. We are also given a joint trajectory $\theta_d(\cdot)$ which we wish to track. For simplicity, we assume that θ_d is specified for all time and that it is at least twice differentiable.

If we have a perfect model of the robot and $\theta(0) = \theta_d(0)$, $\dot{\theta}(0) = \dot{\theta}_d(0)$, then we may solve our problem by choosing

$$\tau = M(\theta_d)\ddot{\theta}_d + C(\theta_d, \dot{\theta}_d)\dot{\theta}_d + N(\theta_d, \dot{\theta}_d).$$

Since both θ and θ_d satisfy the same differential equation and have the same initial conditions, it follows from the uniqueness of the solutions of differential equations that $\theta(t) = \theta_d(t)$ for all $t \geq 0$. This is an example of an *open-loop* control law: the current state of the robot is not used in choosing the control inputs.

Unfortunately, this strategy is not very robust. If $\theta(0) \neq \theta_d(0)$, then the open-loop control law will never correct for this error. This is clearly undesirable, since we

computed
torque—(

almost never know the current position of a robot *exactly*. Furthermore, we have no guarantee that if our starting configuration is near the desired initial configuration that the trajectory of the robot will stay near the desired trajectory for all time. For this reason, we introduce feedback into our control law. This feedback must be chosen such that the actual robot trajectory converges to the desired trajectory. In particular, if our trajectory is a single setpoint, the closed-loop system should be asymptotically stable about the desired setpoint.

There are several approaches for designing stable robot control laws. Using the structural properties of robot dynamics, we will be able to prove stability of these control laws for *all* robots having those properties. Hence, we do not need to design control laws for a specific robot; as long as we show that stability of a particular control algorithm requires only those properties given in Lemma 4.2 on page 209, then our control law will work for general open-chain robot manipulators. Of course, the performance of a given control law depends heavily on the particular manipulator, and hence the control laws presented here should only be used as a starting point for synthesizing a feedback compensator.

5.2 Computed torque

Consider the following refinement of the open-loop control law presented above: given the current position and velocity of the manipulator, cancel all nonlinearities and apply exactly the torque needed to overcome the inertia of the actuator,

$$\tau = M(\theta)\ddot{\theta}_d + C(\theta, \dot{\theta})\dot{\theta} + N(\theta, \dot{\theta}).$$

Substituting this control law into the dynamic equations of the manipulator, we see that

$$M(\theta)\ddot{\theta} = M(\theta)\ddot{\theta}_d,$$

and since $M(\theta)$ is uniformly positive definite in θ , we have

$$\ddot{\theta} = \ddot{\theta}_d. \quad (4.48)$$

Hence, if the initial position and velocity of the manipulator matches the desired position and velocity, the manipulator will follow the desired trajectory. As before, this control law will not correct for any initial condition errors which are present.

The tracking properties of the control law can be improved by adding state feedback. The linearity of equation (4.48) suggests the following control law:

$$\tau = M(\theta) \left(\ddot{\theta}_d - K_v \dot{e} - K_p e \right) + C(\theta, \dot{\theta}) \dot{\theta} + N(\theta, \dot{\theta}) \quad (4.49)$$

where $e = \theta - \theta_d$, and K_v and K_p are constant gain matrices. When substituted into equation (4.47), the error dynamics can be written as:

$$M(\theta) (\ddot{e} + K_v \dot{e} + K_p e) = 0.$$

Since $M(\theta)$ is always positive definite, we have

$$\ddot{e} + K_v \dot{e} + K_p e = 0. \quad (4.50)$$

This is a linear differential equation which governs the error between the actual and desired trajectories. Equation (4.49) is called the *computed torque* control law.

The computed torque control law consists of two components. We can write equation (4.49) as

$$\tau = \underbrace{M(\theta) \ddot{\theta}_d + C \dot{\theta} + N}_{\tau_{ff}} + \underbrace{M(\theta) (-K_v \dot{e} - K_p e)}_{\tau_{fb}}.$$

The term τ_{ff} is the *feedforward* component. It provides the amount of torque necessary to drive the system along its nominal path. The term τ_{fb} is the *feedback* component. It provides correction torques to reduce any errors in the trajectory of the manipulator.

Since the error equation (4.50) is linear, it is easy to choose K_v and K_p so that the overall system is stable and $e \rightarrow 0$ exponentially as $t \rightarrow \infty$. Moreover, we can choose K_v and K_p such that we get independent exponentially stable systems (by choosing K_p and K_v diagonal). The following proposition gives one set of conditions under which the computed torque control law (4.49) results in exponential tracking.

Proposition 4.8. Stability of the computed torque control law

If $K_p, K_v \in \mathbb{R}^{n \times n}$ are positive definite, symmetric matrices, then the control law (4.49) applied to the system (4.47) results in exponential trajectory tracking.

Proof. The error dynamics can be written as a first-order linear system:

$$\frac{d}{dt} \begin{bmatrix} e \\ \dot{e} \end{bmatrix} = \underbrace{\begin{bmatrix} 0 & I \\ -K_p & -K_v \end{bmatrix}}_A \begin{bmatrix} e \\ \dot{e} \end{bmatrix}.$$

It suffices to show that each of the eigenvalues of A has negative real part. Let $\lambda \in \mathbb{C}$ be an eigenvalue of A with corresponding eigenvector $v = (v_1, v_2) \in \mathbb{C}^{2n}$, $v \neq 0$. Then,

$$\lambda \begin{bmatrix} v_1 \\ v_2 \end{bmatrix} = \begin{bmatrix} 0 & I \\ -K_p & -K_v \end{bmatrix} \begin{bmatrix} v_1 \\ v_2 \end{bmatrix} = \begin{bmatrix} v_2 \\ -K_p v_1 - K_v v_2 \end{bmatrix}.$$

It follows that if $\lambda = 0$ then $v = 0$, and hence $\lambda = 0$ is not an eigenvalue of A . Further, if $\lambda \neq 0$, then $v_2 = 0$ implies that $v_1 = 0$. Thus, $v_1, v_2 \neq 0$ and we may assume without loss of generality that $\|v_1\| = 1$. Using this, we write

$$\begin{aligned} \lambda^2 &= v_1^* \lambda^2 v_1 = v_1^* \lambda v_2 \\ &= v_1^* (-K_p v_1 - K_v v_2) = -v_1^* K_p v_1 - \lambda v_1^* K_v v_1, \end{aligned}$$

where $*$ denotes complex conjugate transpose. Since $\alpha = v_1^* K_p v_1 > 0$ and $\beta = v_1^* K_v v_1 > 0$, we have

$$\lambda^2 + \alpha \lambda + \beta = 0 \quad \alpha, \beta > 0$$

and hence the real part of λ is negative. \square

The power of the computed torque control law is that it converts a nonlinear dynamical system into a linear one, allowing the use of any of a number of linear control synthesis tools. This is an example of a more general technique known as *feedback linearization*, where a nonlinear system is rendered linear via full-state nonlinear feedback. One disadvantage of using feedback linearization is that it can be

demanding (in terms of computation time and input magnitudes) to use feedback computed torque— to globally convert a nonlinear system into a single linear system. For robot manip- PD control—(ulators, unboundedness of the inputs is rarely a problem since the inertia matrix of setpoint stabilization the system is bounded and hence the control torques which must be exerted always remain bounded. In addition, experimental results show that the computed torque controller has very good performance characteristics and it is becoming increasingly popular.

5.3 PD control

Another approach to controller synthesis for nonlinear systems is to design a linear controller based on the linearization of the system about an operating point. Since the linearization of a system locally determines the stability of the full system, this class of controllers is guaranteed to be locally stable. In many situations, it is possible to prove global stability for a linear controller by explicit construction of a Lyapunov function.

An example of this design methodology is a proportional plus derivative (PD) control law for a robot manipulator. In its simplest form, a PD control law has the form

$$\tau = -K_v \dot{e} - K_p e, \quad (4.51)$$

where K_v and K_p are positive definite matrices and $e = \theta - \theta_d$. Since this control law has no feedforward term, it can never achieve exact tracking for non-trivial trajectories. A common modification is to add an integral term to eliminate steady-state errors. This introduces additional complications since care must be taken to maintain stability and avoid integrator windup.

Before adding a feedforward term, we first show that the PD controller gives asymptotic setpoint stabilization.

Proposition 4.9. *If $\dot{\theta}_d \equiv 0$ and $K_v, K_p > 0$, the control law (4.51) applied to the system (4.47) renders the equilibrium point $\theta = \theta_d$ globally asymptotically stable.*

Proof. For $\theta_d \equiv 0$, the closed-loop system is

$$M(\theta)\ddot{\theta} + C(\theta, \dot{\theta})\dot{\theta} + K_v\dot{\theta} + K_p(\theta - \theta_d) = 0. \quad (4.52)$$

Without loss of generality, we assume that $\theta_d = 0$ (if not, redefine $\theta' = \theta - \theta_d$). We choose the total energy of the system as our Lyapunov function,

$$V(\theta, \dot{\theta}) = \frac{1}{2}\dot{\theta}^T M(\theta)\dot{\theta} + \frac{1}{2}\theta^T K_p\theta.$$

The function V is (globally) positive definite and decrescent. Evaluating \dot{V} along trajectories of (4.52),

$$\begin{aligned} \dot{V}(\theta, \dot{\theta}) &= \dot{\theta}^T M\ddot{\theta} + \frac{1}{2}\dot{\theta}^T \dot{M}\dot{\theta} + \dot{\theta}^T K_p\theta \\ &= -\dot{\theta}^T K_v\dot{\theta} + \frac{1}{2}\dot{\theta}^T (\dot{M} - 2C)\dot{\theta}, \end{aligned}$$

and since $\dot{M} - 2C$ is skew-symmetric, we have

$$\dot{V} = -\dot{\theta}^T K_v\dot{\theta}.$$

Although K_v is positive definite, the function \dot{V} is only negative *semi*-definite, since $\dot{V} = 0$ for $\dot{\theta} = 0$ and $\theta \neq 0$. Hence from Lyapunov's basic theorem, we can conclude only stability of the equilibrium point.

To check for asymptotic stability, we appeal to Lasalle's principle. The set S for which $\dot{V} \equiv 0$ is given by

$$S = \{(\theta, \dot{\theta}) : \dot{\theta} \equiv 0\}.$$

To find the largest invariant set contained in S , we substitute $\dot{\theta} \equiv 0$ into the closed loop equations 4.52. This gives

$$K_p\theta = 0$$

(recalling that $\theta_d = 0$) and since K_p is positive definite, it follows that the largest invariant set contained within S is the single point $\theta = 0$. Hence, the equilibrium point $\theta = 0$ is asymptotically stable. \square

Since we are primarily interested in tracking, we consider a modified version of the PD control law:

$$\tau = M(\theta)\ddot{\theta}_d + C(\theta, \dot{\theta})\dot{\theta}_d + N(\theta, \dot{\theta}) - K_v\dot{e} - K_p e \quad (4.53)$$

We call this controller the *augmented PD control law*. Note that the second term in equation (4.53) is different from the Coriolis term $C(\theta, \dot{\theta})\dot{\theta}$. The reason for this difference is found in the proof of the following theorem.

Proposition 4.10. Stability of the PD control law

The control law (4.53) applied to the system (4.47) results in exponential trajectory tracking if $K_v, K_p > 0$.

Proof. The closed-loop system is

$$M(\theta)\ddot{e} + C(\theta, \dot{\theta})\dot{e} + K_v\dot{e} + K_p e = 0. \quad (4.54)$$

As in the proof of the previous proposition, using the energy of the system as a Lyapunov function does not allow us to conclude exponential stability because \dot{V} is only negative semi-definite. Furthermore, since the system is time-varying (due to the $\theta_d(\cdot)$ terms), we cannot apply Lasalle's principle.

To show exponential stability, we adopt the same approach as with the spring mass system of the previous section. Namely, we skew the level sets of the energy function by choosing the Lyapunov function candidate

$$V(e, \dot{e}, t) = \frac{1}{2}\dot{e}^T M(\theta)\dot{e} + \frac{1}{2}e^T K_p e + \epsilon e^T M(\theta)\dot{e},$$

PD control—) which is positive definite for ϵ sufficiently small since $M(\theta) > 0$ and $K_p > 0$. Evaluating \dot{V} along trajectories of (4.54):

workspace control—(control!workspace@in workspace coordinates—(

$$\begin{aligned}\dot{V} &= \dot{e}^T M \ddot{e} + \frac{1}{2} \dot{e}^T \dot{M} \dot{e} + \dot{e}^T K_p e + \epsilon \dot{e}^T M \dot{e} + \epsilon e^T (M \ddot{e} + \dot{M} \dot{e}) \\ &= -\dot{e}^T (K_v - \epsilon M) \dot{e} + \frac{1}{2} \dot{e}^T (\dot{M} - 2C) \dot{e} + \epsilon e^T (-K_p e - K_v \dot{e} - C \dot{e} + \dot{M} \dot{e}) \\ &= -\dot{e}^T (K_v - \epsilon M) \dot{e} - \epsilon e^T K_p e + \epsilon e^T (-K_v + \frac{1}{2} \dot{M}) \dot{e}\end{aligned}$$

Choosing $\epsilon > 0$ sufficiently small insures that \dot{V} is negative definite (see Exercise 11) and hence the system is exponentially stable using Theorem 4.5. \square

If $\dot{\theta}_d \equiv 0$, i.e., we wish to stabilize a point, the control law (4.53) simplifies to the original PD control law (4.51). We also note that asymptotic tracking requires exact cancellation of friction and gravity forces and relies on accurate models of these quantities as well as the manipulator inertia matrix. In practice, errors in modeling will result in errors in tracking.

A further difficulty in using the PD control law is choosing the gains K_p and K_v . The linearization of the system about a given operating point θ_0 gives error dynamics of the form

$$M(\theta_0) \ddot{e} + K_v \dot{e} + K_p e = 0.$$

Since this is a linear system, it is possible to choose K_v and K_p to achieve a given performance specification using linear control theory. However, if we are tracking a trajectory, then there is no guarantee that we will remain near θ_0 and the chosen gains may not be appropriate. In practice, one can usually get reasonable results by choosing the gains based on the linearization about an equilibrium point in the middle of the robot's workspace.

5.4 Workspace control

Suppose we are given a path $g_d(t) \in SE(3)$ which represents the desired configuration of the end-effector as a function of time. One way to move the manipulator along

this path is to solve the inverse kinematics problem at each instant in time and generate a desired joint angle trajectory $\theta_d(t) \in Q$ such that $g(\theta_d(t)) = g_d(t)$. The methods of the previous sections can then be used to generate a feedback controller which follows this path.

joint space control!workspace@v
workspace control
workspace control!joint@versus
joint space control

There are several disadvantages to solving the feedback control problem in this manner. Since solving the inverse kinematics problem is a time-consuming task, systems in which g_d is specified in real-time must use powerful computers to compute θ_d at a rate suitable for control. Furthermore, it may be difficult to choose the feedback gains in joint space in a meaningful way, since the original task was given in terms of the end-effector trajectory. For example, a joint-space, computed torque controller with diagonal gain matrices (K_p and K_v) will generate a decoupled response in joint space, resulting in straight line trajectories in θ if the setpoint of the manipulator is changed. However, due to the nonlinear nature of the kinematics, this will *not* generate a straight line trajectory in $SE(3)$. For many tasks, this type of behavior is undesirable.

To overcome these disadvantages, we consider formulating the problem directly in end-effector coordinates. In doing so, we will eliminate the need to solve the inverse kinematics and also generate controllers whose gains have a more direct connection with the task performance. However, in order to use the tools developed in Section 4, we must choose a set of local coordinates for $SE(3)$, such as parameterizing orientation via Euler angles. This limits the usefulness of the technique somewhat, although for many practical applications this limitation is of no consequence. This approach to writing controllers is referred to as *workspace control*, since x represents the configuration of the end-effector in the workspace of the manipulator.

Let $f : Q \rightarrow \mathbb{R}^p$ be a smooth and invertible mapping between the joint variables $\theta \in Q$ and the workspace variables $x \in \mathbb{R}^p$. In particular, this requires that $n = p$ so that the number of degrees of freedom of the robot equals the number of workspace variables x . We allow for the possibility that $p < 6$, in which case the workspace

variables may only give a partial parameterization of $SE(3)$. An example of this situation is the SCARA robot, for which the position of the end-effector and its orientation with respect to the z -axis form a natural set of coordinates for specifying a task.

The dynamics of the manipulator in joint space has the form

$$M(\theta)\ddot{\theta} + C(\theta, \dot{\theta})\dot{\theta} + N(\theta, \dot{\theta}) = \tau,$$

where τ is the vector of joint torques and M , C , and N describe the dynamic parameters of the system, as before.

We can rewrite the dynamics in terms of $x \in \mathbb{R}^p$ by using the Jacobian of the mapping $f : \theta \mapsto x$,

$$\dot{x} = J(\theta)\dot{\theta} \quad J(\theta) = \frac{\partial f}{\partial \theta}.$$

Note that J is the Jacobian of the *mapping* $f : Q \rightarrow \mathbb{R}^p$ and not the manipulator Jacobian. Under the assumption that f is smooth and invertible, we can write

$$\dot{\theta} = J^{-1}\dot{x} \quad \text{and} \quad \ddot{\theta} = J^{-1}\ddot{x} + \frac{d}{dt}(J^{-1})\dot{x}.$$

We can now substitute these expressions into the manipulator dynamics and multiply by $J^{-T} := (J^{-1})^T$ to obtain

$$\begin{aligned} J^{-T}M(\theta)J^{-1}\ddot{x} + \left(J^{-T}C(\theta, \dot{\theta})J^{-1} + J^{-T}M(\theta)\frac{d}{dt}(J^{-1}) \right) \dot{x} \\ + J^{-T}N(\theta, \dot{\theta}) = J^{-T}\tau. \end{aligned}$$

We can write this in a more familiar form by defining

$$\begin{aligned} \tilde{M} &= J^{-T}MJ^{-1} \\ \tilde{C} &= J^{-T} \left(CJ^{-1} + M\frac{d}{dt}(J^{-1}) \right) \\ \tilde{N} &= J^{-T}N \\ F &= J^{-T}\tau, \end{aligned}$$

in which case the dynamics become

$$\tilde{M}(\theta)\ddot{x} + \tilde{C}(\theta, \dot{\theta})\dot{x} + \tilde{N}(\theta, \dot{\theta}) = F. \quad (4.55)$$

workspace
dynamics
structural
properties

This equation represents the dynamics in terms of the workspace coordinates x and the robot configuration θ . We call \tilde{M} , \tilde{C} , and \tilde{N} the *effective* parameters of the system. They represent the dynamics of the system as viewed from the workspace variables. Since f is locally invertible, we can in fact eliminate θ from these equations, and we see that equation (4.55) is nothing more than Lagrange's equations relative to the generalized coordinates x . However, since for most robots we measure θ directly and compute x via the forward kinematics, it is convenient to leave the θ dependence explicit.

Equation (4.55) has the same basic structure as the dynamics for an open-chain manipulator written in joint coordinates. In order to exploit this structure in our control laws, we must verify that some of the properties which we used in proving stability of controllers are also satisfied. The following lemma verifies that this is indeed the case.

Lemma 4.11. Structural properties of the workspace dynamics

Equation (4.55) satisfies the following properties:

1. $\tilde{M}(\theta)$ is symmetric and positive definite.
2. $\dot{\tilde{M}} - 2\tilde{C} \in \mathbb{R}^{n \times n}$ is a skew-symmetric matrix.

Proof. Since J is an invertible matrix, property 1 follows from its definition. To show property 2, we calculate the $\dot{\tilde{M}} - 2\tilde{C}$:

$$\dot{\tilde{M}} - 2\tilde{C} = J^{-T}(\dot{\tilde{M}} - 2\tilde{C})J^{-1} + \frac{d}{dt}(J^{-T})\tilde{M}J^{-1} - J^{-T}\tilde{M}\frac{d}{dt}(J^{-1}).$$

A direct calculation shows that this matrix is indeed skew-symmetric. □

computed
torque

workspace con-
troll!joint@versus
joint space
control

joint space con-
troll!workspace@versus
workspace
control

These two properties allow us to immediately extend the control laws in the previous section to workspace coordinates. For example, the computed torque control law becomes

$$F = \tilde{M}(\theta) (\ddot{x}_d - K_v \dot{e} - K_p e) + C(\theta, \dot{\theta}) \dot{x} + N(\theta, \dot{\theta})$$

$$\tau = J^T F,$$

where x_d is the desired workspace trajectory and $e = x - x_d$ is the workspace error. The proof of stability for this control law is identical to that given previously. Namely, using the fact that $M(\theta)$ is positive definite, we can write the workspace error dynamics as

$$\ddot{e} + K_v \dot{e} + K_p e = 0$$

which is again a linear differential equation whose stability can be verified directly. The PD control law can be similarly extended to workspace coordinates.

The advantage of writing the control law in this fashion is that the matrices K_v and K_p now specify the gains directly in workspace coordinates. This simplifies the task of choosing the gains that are needed to accomplish a specific task. Furthermore, it eliminates the need to solve for the inverse mapping f^{-1} in order to control the robot. Instead, we only have to calculate the Jacobian matrix for f and its (matrix) inverse.

Notice that when the manipulator approaches a singular configuration relative to the coordinates x , the effective inertia \tilde{M} gets very large. This is an indication that it is difficult to move in some directions and hence large forces produce very little motion. It is important to note that this singularity is strictly a function of our choice of parameterization. Such singularities never appear in the joint space of the robot.

Example 4.8. Comparison of joint space and workspace controllers

To illustrate some of the differences between implementing a controller in joint space

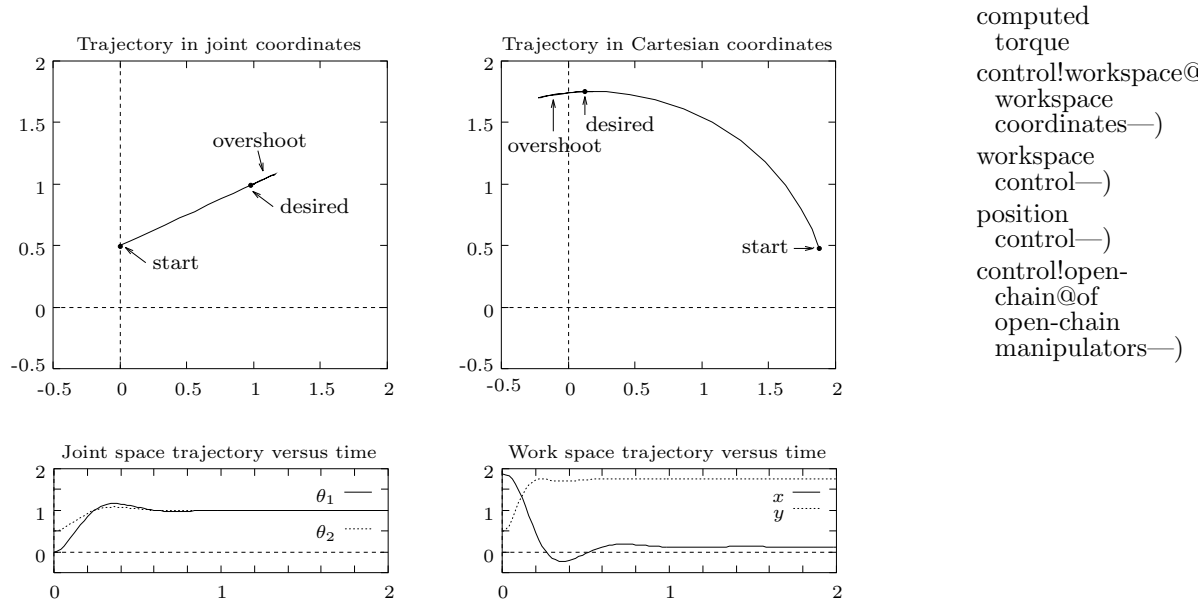


Figure 4.10: Step response of a joint space, computed torque controller.

versus workspace, we consider the control of a planar two degree of freedom robot. We take as our workspace variables the xy position of the end-effector.

Figure 4.10 shows the step response of a computed torque control law written in joint coordinates. Note that the trajectory of the end-effector, shown on the right, follows a curved path. The time response of the joint trajectories is a classical linear response for an underdamped mechanical system.

Figure 4.11 shows the step response of a computed torque control law written in workspace coordinates. Now the trajectory of the end-effector, including the overshoot, follows a straight line in the workspace and a curved line in the joint space.

constrained
manipulators!
dynamics of—(
dynamics!constrained
manipulators—)

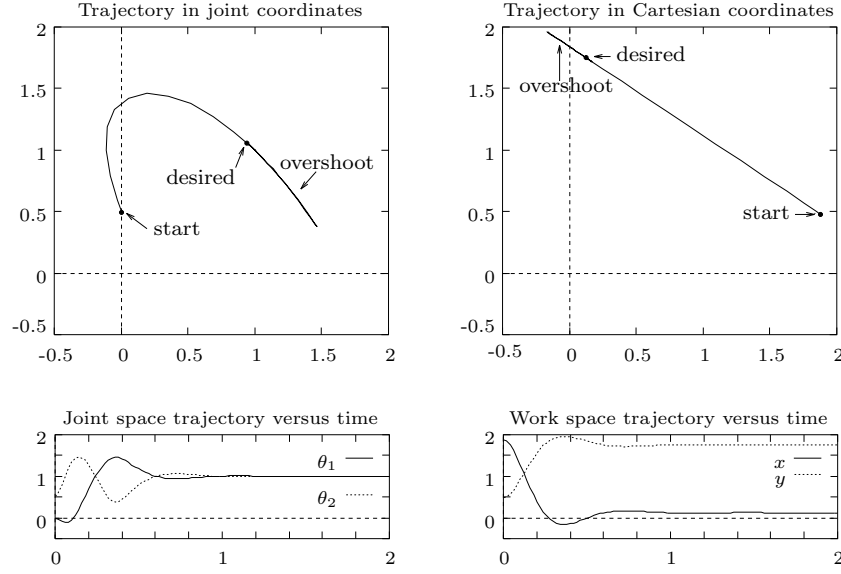


Figure 4.11: Step response of a workspace, computed torque controller.

6 Control of Constrained Manipulators

In this short section, we provide a brief treatment of the control of constrained manipulators. A more thorough development is given in Chapter 6.

6.1 Dynamics of constrained systems

Consider a problem in which we wish to move the tip of a robot along a surface and apply a force against that surface. For simplicity, we assume the surface is frictionless, although the analysis presented here can be readily extended to the more general case. We suppose that the surface we wish to move along can be described by a set of independent, smooth constraints

$$h_j(\theta_1, \dots, \theta_n) = 0 \quad j = 1, \dots, k, \quad (4.56)$$

and that there exists a smooth, injective map $f : \mathbb{R}^{n-k} \rightarrow \mathbb{R}^n$ such that

constraints!forces
of

$$h_j(f_1(\phi), \dots, f_n(\phi)) = 0. \quad (4.57)$$

That is, $\phi \in \mathbb{R}^{n-k}$ parameterizes the allowable motion on the surface and $\theta = f(\phi)$ corresponds to a configuration in which the robot is in contact with the surface.

The control task is to follow a given trajectory $\phi_d(t)$ while applying a force against the surface. Since the surface is represented in joint space as the level set of the map $h(\theta) = 0$, the normal vectors to this surface are given by the span of the gradients of ∇h_i . (Since the surface is $n - k$ dimensional, the dimension of the space of normal vectors is k .) Any torques of the form

$$\tau_N = \sum \lambda_j \nabla h_j(\theta) \quad (4.58)$$

correspond to normal forces applied against the surface. In the absence of friction, the work done by these torques is given by

$$\begin{aligned} \tau_N \cdot \dot{\theta} &= \sum \lambda_i \nabla h_i \cdot \dot{\theta} = \sum \lambda_i \left(\frac{\partial h_i}{\partial \theta} \dot{\theta} \right) \\ &= \sum \lambda_i \frac{d}{dt} (h(\theta)) = 0. \end{aligned}$$

Hence the normal forces do no work on the system and therefore cause no motion in the system. We assume that a desired normal force, specified by $\lambda_1(t), \dots, \lambda_k(t)$, is given as part of the task description.

If the robot remains in contact with the surface, as desired, then the dynamics of the manipulator can be written in terms of ϕ . Differentiating $\theta = f(\phi)$, we have

$$\begin{aligned} \dot{\theta} &= \frac{\partial f}{\partial \phi} \dot{\phi} \\ \ddot{\theta} &= \frac{\partial f}{\partial \phi} \ddot{\phi} + \frac{d}{dt} \left(\frac{\partial f}{\partial \phi} \right) \dot{\phi}. \end{aligned} \quad (4.59)$$

These equations can be substituted into the robot equations of motion,

$$M(\theta)\ddot{\theta} + C(\theta, \dot{\theta})\dot{\theta} + N(\theta, \dot{\theta}) = \tau$$

constrained
manipula-
tors!dynamics
of—)
dynamics!constrained
manipulators—)

to yield

$$M(\theta) \frac{\partial f}{\partial \phi} \ddot{\phi} + \left(C(\theta, \dot{\theta}) \frac{\partial f}{\partial \phi} + M(\theta) \frac{d}{dt} \left(\frac{\partial f}{\partial \phi} \right) \right) \dot{\phi} + N(\theta, \dot{\theta}) = \tau, \quad (4.60)$$

constrained
manipula-
tors!control
of—(
control!constrained
manipulators—)

where we have left M , C , and N in terms of θ to simplify notation.

Equation (4.60) can be made symmetric by multiplying both sides by $\frac{\partial f}{\partial \phi}^T$. Let-

control!constrained
manipulators—)
def $J = \frac{\partial f}{\partial \phi}(\phi)$, we define

$$\begin{aligned} \tilde{M}(\phi) &= J^T M(f(\phi)) J \\ \tilde{C}(\phi, \dot{\phi}) &= J^T \left(C(f(\phi), J\dot{\phi}) J + M(f(\phi)) \dot{J} \right) \\ \tilde{N}(\phi, \dot{\phi}) &= J^T N(f(\phi), J\dot{\phi}) \\ F &= J^T \tau. \end{aligned} \quad (4.61)$$

Using these definitions, the projected equations of motion can be written as

$$\tilde{M}(\phi) \ddot{\phi} + \tilde{C}(\phi, \dot{\phi}) \dot{\phi} + \tilde{N}(\phi, \dot{\phi}) = F. \quad (4.62)$$

This equation has the same form as the equation for an unconstrained manipulator. We shall show in Chapter 6 that equation (4.62) also satisfies the properties in Lemma 4.2. This is not particularly surprising since the coordinates ϕ were chosen to be a set of generalized coordinates under the assumption that the robot maintains contact with the surface.

It is important to keep in mind that equation (4.62) represents the dynamics of the system only along the surface given by the level sets $h(\theta) = 0$. By pre-multiplying by J^T , we have eliminated the information about the forces of constraint. For many applications, we are interested in regulating the forces of constraint and hence we must use the full equations of motion given in equation (4.60).

6.2 Control of constrained manipulators

The control task for a constrained robot system is to simultaneously regulate the position of the system along the constraint surface and regulate the forces of the

system applied against this surface. In terms of analyzing stability, it is enough to analyze only the motion along the surface, since no movement occurs perpendicular to the surface. Of course, implicit in this point of view is that we maintain contact with the surface. If the manipulator is not physically constrained, this may require that we regulate the forces so as to insure that we are always pushing against the surface and never pulling away from it.

In this section we show how to extend the computed torque formalism presented earlier to regulate the position and force of the manipulator. We give only a sketch of the approach, leaving a more detailed discussion until Chapter 6, where we shall see that hybrid position/force control is just one example of the more general problem of controlling single and multiple robots interacting with each other and their environment.

We take as given a path on the constraint surface, specified by $\phi_d(t)$, and a normal force to be applied against the surface, specified by the Lagrange multipliers $\lambda_1(t), \dots, \lambda_k(t)$ as in equation (4.58). Since we are interested in regulating the force applied against the constraint, it is important to insure that the position portion of the controller does not push against the constraint. Define

$$\begin{aligned} \tau_\phi = M(\theta) \frac{\partial f}{\partial \phi} (\ddot{\phi}_d - K_v \dot{e}_\phi - K_p e_\phi) \\ + \left(C(\theta, \dot{\theta}) \frac{\partial f}{\partial \phi} + M(\theta) \frac{d}{dt} \left(\frac{\partial f}{\partial \phi} \right) \right) \dot{\phi} + N(\theta, \dot{\theta}), \end{aligned}$$

where $e_\phi = \phi - \phi_d$. This is the torque required to move the manipulator along the surface while applying no force against the surface. In other words, if we apply $\tau = \tau_\phi$ and remove the constraint completely, the manipulator will follow the correct path, as if the constraint were present.

To apply the appropriate normal forces, we simply add τ_N as defined in equation (4.58) to τ_ϕ . Since τ_N is in the normal direction to the constraint, it does not affect the position portion of the controller. Of course, this requires that the constraint surface actually be present to resist the normal forces applied to it. The

control!constrained@of
 constrained
 manipulators—)
 constrained
 manipula-
 tors!control
 of—)
 constrained
 manipula-
 tors!planar
 example
 two-link planar
 manipula-
 tor!moving in
 a slot
 slider-crank
 mechanism

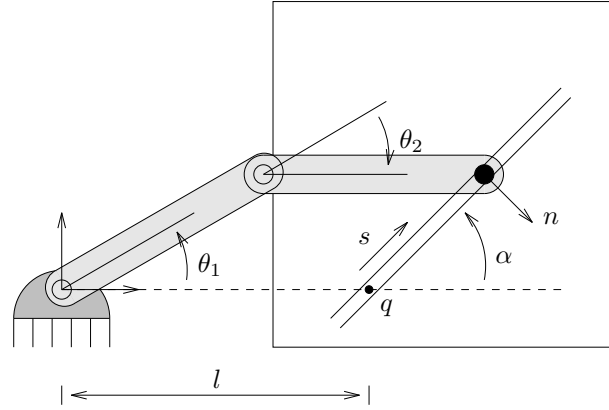


Figure 4.12: Planar manipulator moving in a slot.

complete control law is given by

$$\tau = \tau_\phi + \sum_{i=1}^k \lambda_i(t) \nabla h_i \quad (4.63)$$

where τ_ϕ is given above. We defer the analysis and proof of convergence for this control law until Chapter 6.

As in the previous control laws, the force control law presented here relies on accurate models of the robot and the surface. In particular, we note that the applied normal force does not use feedback to correct for model error, sensor noise, or other non-ideal situations.

6.3 Example: A planar manipulator moving in a slot

As a simple example of a constrained manipulator, consider the control of a two degree of freedom, planar manipulator whose end-effector is forced to lie in a slot, as shown in Figure 4.12. This system resembles a slider-crank mechanism, except that we are allowed to apply torques on both revolute joints, allowing us to control both the motion of the slider as well as the force applied against the slot. This example is easily adapted to a robot pushing against a wall, in which case the forces against the slot must always be pointed in a preferred direction.

We take the slot to be a straight line passing through the point $q = (l, 0)$ and making an angle α with respect to the x -axis of the base frame. The vector normal to the direction of the slot is given by

$$n = \begin{bmatrix} \sin \alpha \\ -\cos \alpha \end{bmatrix},$$

and the slot can be described as the set of all points $p \in \mathbb{R}^2$ such that $(p - q) \cdot n = 0$.

The constraint on the manipulator is obtained by requiring that the position of the end-effector remain in the slot. Letting $p(\theta) \in \mathbb{R}^2$ represent the position of the tool frame, this constraint becomes

$$h(\theta) = \left(p(\theta) - \begin{bmatrix} l \\ 0 \end{bmatrix} \right) \cdot \begin{bmatrix} \sin \alpha \\ -\cos \alpha \end{bmatrix} = 0.$$

Substituting the forward kinematics of the manipulator yields

$$\begin{aligned} h(\theta) &= (l_1 \cos \theta_1 + l_2 \cos(\theta_1 + \theta_2) - l) \sin \alpha \\ &\quad - (l_1 \sin \theta_1 + l_2 \sin(\theta_1 + \theta_2)) \cos \alpha \\ &= -l_1 \sin(\theta_1 - \alpha) - l_2 \sin(\theta_1 + \theta_2 - \alpha) - l \sin \alpha. \end{aligned}$$

The gradient of the constraint, which gives the direction of the normal force, is given by

$$\nabla h(\theta) = \begin{bmatrix} -l_1 \cos(\theta_1 - \alpha) - l_2 \cos(\theta_1 + \theta_2 - \alpha) \\ -l_2 \cos(\theta_1 + \theta_2 - \alpha) \end{bmatrix}.$$

Note that this is the direction of the normal force in *joint coordinates*. That is, joint torques applied in this direction will cause no motion, only forces against the side of the slot.

To parameterize the allowable motion along the slot, we let $s \in \mathbb{R}$ represent the position along the slot, with $s = 0$ denoting the point $q = (l, 0)$. Finding a function $f(s)$ such that $h(f(s)) = 0$ involves solving the inverse kinematics of the manipulator: given the position along the slot, we must find joint angles which achieve that position.

computed
torque

If the end of the manipulator is at a position s along the slot, then the xy coordinates of the end-effector are

$$x(s) = l + s \cos \alpha$$

$$y(s) = s \sin \alpha.$$

Solving the inverse kinematics (see Chapter 3, Section 3) and assuming the elbow down solution, we have

$$f(s) = \begin{bmatrix} \theta_1(s) \\ \theta_2(s) \end{bmatrix} = \begin{bmatrix} \tan^{-1} \left(\frac{s \sin \alpha}{l + s \cos \alpha} \right) + \cos^{-1} \left(\frac{s^2 + 2ls \cos \alpha + l^2 + l_1^2 - l_2^2}{2l_1 \sqrt{s^2 + 2ls \cos \alpha + l^2}} \right) \\ \pi + \cos^{-1} \left(\frac{l_1^2 + l_2^2 - s^2 - 2ls \cos \alpha - l^2}{2l_1 l_2} \right) \end{bmatrix}.$$

The Jacobian of the mapping is given by

$$J = \begin{bmatrix} \frac{-(s + l \cos \alpha)(s^2 + 2ls \cos \alpha + l^2 - l_1^2 + l_2^2)}{2l_1(s^2 + 2ls \cos \alpha + l^2)^{\frac{3}{2}} \sqrt{1 - \frac{(s^2 + 2ls \cos \alpha + l^2 + l_1^2 - l_2^2)}{4l_1^2(s^2 + 2ls \cos \alpha + l^2)}}} + \frac{l \sin \alpha}{s^2 + l^2 + 2ls \cos \alpha} \\ \frac{2(s + l \cos \alpha)}{\sqrt{4l_1^2 l_2^2 - (s^2 + 2ls \cos \alpha + l^2 - l_1^2 - l_2^2)^2}} \end{bmatrix}$$

(after some simplification).

This matrix can now be used to compute the equations of motion and derive an appropriate control law. In particular, the computed torque controller has the form

$$\tau = M(\theta)J(\ddot{s}_d - K_v \dot{e}_s - K_p e_s) + (C(\theta, \dot{\theta})J + M(\theta)\dot{J})\dot{s} + \lambda n,$$

where $e_s = s - s_d$; λ is the desired force against the slot; $K_v, K_p \in \mathbb{R}$ are the gain and damping factors; and M and C are the generalized inertial and Coriolis matrices.

The inertial parameters were calculated in Section 2.3 and are given by

$$M(\theta) = \begin{bmatrix} \alpha + \beta c_2 & \delta + \frac{1}{2}\beta c_2 \\ \delta + \frac{1}{2}\beta c_2 & \delta \end{bmatrix} \quad C(\theta, \dot{\theta}) = \begin{bmatrix} -\frac{1}{2}\beta s_2 \dot{\theta}_2 & -\frac{1}{2}\beta s_2 (\dot{\theta}_1 + \dot{\theta}_2) \\ \frac{1}{2}\beta s_2 \dot{\theta}_1 & 0 \end{bmatrix},$$

where

$$\alpha = \mathcal{I}_{z1} + \mathcal{I}_{z2} + m_1 r_1^2 + m_2 (l_1^2 + r_2^2)$$

$$\beta = m_2 l_1 l_2$$

$$\delta = \mathcal{I}_{z2} + m_2 r_2^2.$$

It is perhaps surprising that such a simple problem can have such an unwieldy solution. The difficulty is that we have cast the entire problem into the joint space of the manipulator, where the constraint $\theta = f(s)$ is a very complex looking curve.

A better way of deriving the equations of motion for this system is to rewrite the dynamics of the system in terms of workspace variables which describe the position of the end-effector (see Exercise 12). Once written in this way, the constraint that the end of the manipulator remain in the slot is a very simple one. This is the basic approach used in Chapter 6, where we present a general framework which incorporates this example and many other constrained manipulation systems.

7 Summary

The following are the key concepts covered in this chapter:

1. The equations of motion for a mechanical system with Lagrangian $L = T(q, \dot{q}) - V(q)$ satisfies *Lagrange's equations*:

$$\frac{d}{dt} \frac{\partial L}{\partial \dot{q}_i} - \frac{\partial L}{\partial q_i} = \Upsilon_i,$$

where $q \in \mathbb{R}^n$ is a set of generalized coordinates for the system and $\Upsilon \in \mathbb{R}^n$ represents the vector of generalized external forces.

2. The equations of motion for a rigid body with configuration $g(t) \in SE(3)$ are given by the *Newton-Euler equations*:

$$\begin{bmatrix} mI & 0 \\ 0 & \mathcal{I} \end{bmatrix} \begin{bmatrix} \dot{v}^b \\ \dot{\omega}^b \end{bmatrix} + \begin{bmatrix} \omega^b \times m v^b \\ \omega^b \times \mathcal{I} \omega^b \end{bmatrix} = F^b,$$

where m is the mass of the body, \mathcal{I} is the inertia tensor, and $V^b = (v^b, \omega^b)$ and F^b represent the instantaneous body velocity and applied body wrench.

3. The equations of motion for an open-chain robot manipulator can be written as

$$M(\theta)\ddot{\theta} + C(\theta, \dot{\theta})\dot{\theta} + N(\theta, \dot{\theta}) = \tau$$

where $\theta \in \mathbb{R}^n$ is the set of joint variables for the robot and $\tau \in \mathbb{R}^n$ is the set of actuator forces applied at the joints. The dynamics of a robot manipulator satisfy the following properties:

- (a) $M(\theta)$ is symmetric and positive definite.
 - (b) $\dot{M} - 2C \in \mathbb{R}^{n \times n}$ is a skew-symmetric matrix.
4. An equilibrium point x^* for the system $\dot{x} = f(x, t)$ is *locally asymptotically stable* if all solutions which start near x^* approach x^* as $t \rightarrow \infty$. Stability can be checked using the *direct method of Lyapunov*, by finding a locally

positive definite function $V(x, t) \geq 0$ such that $-\dot{V}(x, t)$ is a locally positive definite function along trajectories of the system. In situations in which $-\dot{V}$ is only positive semi-definite, *Lasalle's invariance principle* can be used to check asymptotic stability. Alternatively, the *indirect method of Lyapunov* can be employed by examining the linearization of the system, if it exists. Global exponential stability of the linearization implies local exponential stability of the full nonlinear system.

5. Using the form and structure of the robot dynamics, several control laws can be shown to track arbitrary trajectories. Two of the most common are the *computed torque control law*,

$$\tau = M(\theta)(\ddot{\theta}_d + K_v\dot{e} + K_pe) + C(\theta, \dot{\theta})\dot{\theta} + N(\theta, \dot{\theta}),$$

and an *augmented PD control law*,

$$\tau = M(\theta)\ddot{\theta}_d + C(\theta, \dot{\theta})\dot{\theta}_d + N(\theta, \dot{\theta}) + K_v\dot{e} + K_pe.$$

Both of these controllers result in exponential trajectory tracking of a given joint space trajectory. Workspace versions of these control laws can also be derived, allowing end-effector trajectories to be tracked without solving the inverse kinematics problem. Stability of these controllers can be verified using Lyapunov stability.

8 Bibliography

The Lagrangian formulation of dynamics is classical; a good treatment can be found in Rosenberg [62] or Pars [54]. Its application to the dynamics of a robot manipulator can be found in most standard textbooks on robotics, for example [2, 13, 21, 34, 69].

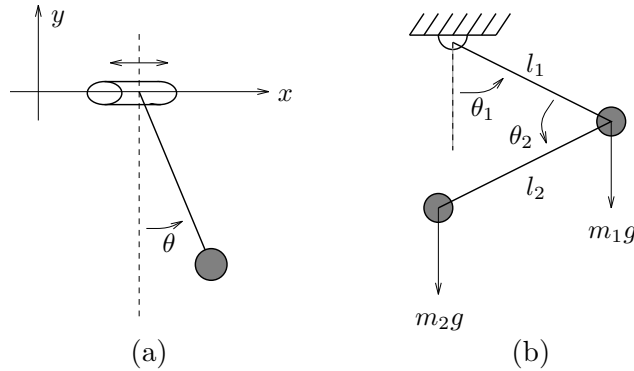
The geometric formulation of the equations of motion for kinematic chains presented in Section 3.3 is based on the recent work of Brockett, Stokes, and Park [9, 52].

This is closely related to the spatial operator algebra formulation of Rodriguez, Jain, and Kreutz-Delgado [30, 61], in which the tree-like nature of the system is more fully exploited in computing inertial properties of the system.

The literature on control of robot manipulators is vast. An excellent treatment, covering many of the different approaches to robot control, is given by Spong and Vidyasagar [69]. The collection [71] also provides a good survey of recent research in this area. The modified PD control law presented in Section 5 was originally formulated by Koditschek [33]. For a survey of manipulator control using exact linearization techniques, see Kreutz [35]. The use of skew terms in Lyapunov functions to prove exponential stability for PD controllers has been pointed out, for example, by Wen and Bayard [75].

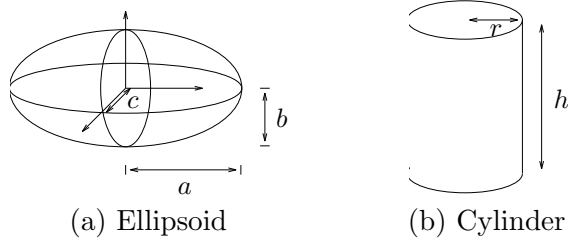
9 Exercises

1. Derive the equations of motion for the systems shown below.



- (a) Pendulum on a wire: an idealized planar pendulum whose pivot is free to slide along a horizontal wire. Assume that the top of the pendulum can move freely on the wire (no friction).
- (b) Double pendulum: two masses connected together by massless links and revolute joints.

2. Compute the inertia tensor for the objects shown below.



(a) Ellipsoid

(b) Cylinder

3. Transformation of the generalized inertia matrix

Show that under a change of body coordinate frame from B to C , the generalized inertia matrix for a rigid body is given by

$$\mathcal{M}_c = \text{Ad}_{g_{bc}}^T \mathcal{M}_b \text{Ad}_{g_{bc}} = \begin{bmatrix} mI & mR_{bc}^T \hat{p}_{bc} R_{bc} \\ -mR_{bc}^T \hat{p}_{bc} R_{bc} & R_{bc}^T (\mathcal{I} - m\hat{p}_{bc}^2) R_{bc} \end{bmatrix},$$

coordinate
transforma-
tions! inertia@on
inertia matrix
inertia ma-
trix! rigid@for
rigid bodies
inertia
matrix! effect
of coordinate
transformation

passivity
dynamics!passivity
property

where g_{bc} denotes the rigid motion taking C to B , and \mathcal{M}_b and \mathcal{M}_c are the generalized inertia matrices expressed in frame B and frame C .

4. Show that Euler's equation written in spatial coordinates is given by

$$\mathcal{I}'\dot{\omega}^f + \omega^f \times \mathcal{I}'\omega^f = \tau,$$

where $\mathcal{I}' = \mathcal{R}\mathcal{I}\mathcal{R}^T$ and τ is the torque applied to the center of mass of the rigid body, written in spatial coordinates.

5. Calculate the Newton-Euler equations in spatial coordinates.
6. Show that it is possible to choose M and C such that the Newton-Euler equations can be written as

$$M\dot{V}^b + C(g, \dot{g})V^b = F^b,$$

where $M > 0$ and $\dot{M} - 2C$ is a skew-symmetric matrix.

7. Verify that the equations of motion for a planar, two-link manipulator, as given in equation (4.11), satisfy the properties of Lemma 4.2.
8. *Passivity of robot dynamics*

Let $H = T + V$ be the total energy for a rigid robot. Show that if $\dot{M} - 2C$ is skew-symmetric, then energy is conserved, i.e., $\dot{H} = \dot{\theta} \cdot \tau$.

9. Show that the workspace version of the PD control law results in exponential trajectory tracking.
10. Show that the control law

$$\tau = M(\theta)(\ddot{\theta}_d + \lambda\dot{e}) + C(\theta, \dot{\theta})(\dot{\theta}_d + \lambda e) + N(\theta, \dot{\theta}) + K_v\dot{e} + K_p e$$

results in exponential trajectory tracking when $\lambda \in \mathbb{R}$ is positive and $K_v, K_p \in \mathbb{R}^{n \times n}$ are positive definite [68].

11. Show that the matrix

$$\begin{bmatrix} \epsilon A & \epsilon B \\ \epsilon B^T & C + \epsilon D \end{bmatrix}$$

is positive definite if A and C are symmetric, positive definite, and $\epsilon > 0$ is chosen sufficiently small.

workspace
control
constrained
manipulators
constrained
manipula-
tors!
control
of

12. *Hybrid control using workspace coordinates*

Consider the constrained manipulation problem described in Section 6.3. Let $p_{st}(\theta) \in \mathbb{R}^2$ be the coordinates of the end-effector and let $w = p(\theta)$ represent a set of workspace coordinates for the system.

- (a) Compute the matrix $J(\theta)$ which is used to convert the joint space dynamics into workspace dynamics (as in Section 5.4).
- (b) Compute the constraint function in terms of the workspace variables and find a parameterization $f : \mathbb{R} \rightarrow \mathbb{R}^2$ which maps the slot position to the workspace coordinates. Let $K(s)$ represent the Jacobian of the mapping $w = f(s)$.
- (c) Write the dynamics of the constrained system in terms of ω and its derivatives, the dynamic parameters of the unconstrained system, and the matrices $J(\theta)$ and $K(s)$.
- (d) Verify that the equations of motion derived in step (c) are the same as the equations of motion derived in Section 6.3. In particular, show that τ_N and the inertia matrix $\tilde{M}(s)$ are the same in both cases.

Bibliography

- [1] J. Angeles. *Rational Kinematics*. Springer-Verlag, 1988.
- [2] H. Asada and J. J. Slotine. *Robot Analysis and Control*. John Wiley, 1986.
- [3] R. S. Ball. *A Treatise on the Theory of Screws*. Cambridge University Press, 1900.
- [4] J. Beckers, J. Patera, M. Perroud, and P. Winternitz. Subgroups of the Euclidean group and symmetry breaking in nonrelativistic quantum mechanics. *Journal of Math. Physics*, 18(1):72–83, 1977.
- [5] W. M. Boothby. *An Introduction to Differentiable Manifolds and Riemannian Geometry*. Academic Press, second edition, 1986.
- [6] O. Bottema and B. Roth. *Theoretical Kinematics*. North-Holland, 1979.
- [7] R. W. Brockett. Robotic manipulators and the product of exponentials formula. In P. A. Fuhrman, editor, *Mathematical Theory of Networks and Systems*, pages 120–129. Springer-Verlag, 1984.
- [8] R. W. Brockett, editor. *Robotics: Proceedings of Symposia in Applied Mathematics, Volume 41*. American Mathematical Society, 1990.
- [9] R. W. Brockett, A. Stokes, and F. Park. A geometrical formulation of the dynamical equations describing kinematic chains. In *IEEE International Conference on Robotics and Automation*, pages 637–642, 1993.
- [10] M. Chasles. Note sur les propriétés generales du systeme de deux corps... *Bull. Sci. Math. Ferrusac*, pages 321–326, 1830.
- [11] D. S. Childress. Artificial hand mechanisms. In *Mechanisms Conference and International Symposium on Gearing and Transmissions*, San Francisco, CA, October 1972.
- [12] P. Coiffet et al. *Robot Technology*. McGraw-Hill, 1983. Translation from the French, *Les Robots* (8 volumes).
- [13] J. J. Craig. *Introduction to Robotics: Mechanics and Control*. Addison-Wesley, third edition, 2005.
- [14] M. R. Cutkosky. *Robotic Grasping and Fine Manipulation*. Kluwer, 1985.

- [15] J. Demmel, G. Lafferriere, J. Schwartz, and M. Sharir. Theoretical and experimental studies using a multifinger planar manipulator. In *IEEE International Conference on Robotics and Automation*, pages 390–395, 1988.
- [16] J. Denavit and R. S. Hartenberg. A kinematic notation for lower-pair mechanisms based on matrices. *Journal of Applied Mechanics*, pages 215–221, June 1955.
- [17] J. Duffy. *Analysis of Mechanisms and Robot Manipulators*. Edward Arnold Ltd., London, 1980.
- [18] J. Duffy and C. Crane. A displacement analysis of the general spatial 7R mechanism. *Mechanisms and Machine Theory*, 15:153–169, 1980.
- [19] A. G. Erdman and G. N. Sandor. *Mechanism Design: Analysis and Synthesis*. Prentice-Hall, 1984.
- [20] L. Euler. Nova methodus motum corporum rigidorum determinandi. *Novii comentarii academie Scientiarum Petropolitane*, 20:208–238, 1776.
- [21] K. S. Fu, R. C. Gonzalez, and C. S. G. Lee. *Robotics: Control, Sensing, Vision and Intelligence*. McGraw Hill, 1987.
- [22] H. Goldstein. *Classical Mechanics*. Addison-Wesley, 2 edition, 1980.
- [23] B. Gorla and M. Renaud. *Modeles des Robots Manipulateurs: applications á leur commande*. Cepadues-Éditions, 1984.
- [24] K.C. Gupta and B. Roth. Design considerations for manipulator workspace. *ASME Journal of Mechanical Design*, 104(4):704–712, 1982.
- [25] H. Hanafusa and H. Asada. A robotic hand with elastic fingers and its application to assembly process. In M. Brady et al., editor, *Robot Motion: Planning and Control*, pages 337–360. MIT Press, 1982.
- [26] J. Herve. Uncoupled actuation of pan-tilt wrists. *IEEE Transactions on Robotics*, 22(1):56–64, 2006.
- [27] J.M. Herve. The planar spherical kinematic bond: Implementation in parallel mechanisms. In www.parallelmic.org/Reviews/Review013.html, pages 1–19, 2003.
- [28] K. H. Hunt. *Kinematic Geometry of Mechanisms*. Oxford University Press, 1978.
- [29] S. Jacobsen, J. Wood, K. Bigger, and E. Iverson. The Utah/MIT hand: Work in progress. *International Journal of Robotics Research*, 4(3):21–50, 1984.
- [30] A. Jain and G. Rodriguez. Recursive flexible multibody system dynamics using spatial operators. *Journal of Guidance, Control, and Dynamics*, 15(6):1453–1466, 1992.
- [31] W. Kahan. Lectures on computational aspects of geometry. Department of Electrical Engineering and Computer Sciences, University of California, Berkeley. Unpublished, July 1983.
- [32] H. K. Khalil. *Nonlinear Systems*. Macmillan, 1992.

- [33] D. Koditschek. Natural motion for robot arms. In *IEEE Control and Decision Conference*, pages 733–735, 1984.
- [34] A. J. Koivo. *Fundamentals for Control of Robotic Manipulators*. Wiley, 1989.
- [35] K. Kreutz. On manipulator control by exact linearization. *IEEE Transactions on Automatic Control*, 34(7):763–767, 1989.
- [36] A. Kumar and K.J. Waldron. The workspace of a mechanical manipulators. *ASME Journal of Mechanical Design*, 103(3):665–672, 1981.
- [37] C.C. Lee and J.M. Herve. Translational parallel manipulator with doubly planar limbs. *Mechanism and Machine Theory*, 41(4):359–486, 2006.
- [38] H. Y. Lee and C. G. Liang. A new vector theory for the analysis of spatial mechanisms. *Mechanisms and Machine Theory*, 23(3):209–217, 1988.
- [39] T.W. Lee and D.C. Yang. On the evaluation of manipulator workspace. *ASME Journal of Mechanisms, Transmissions, and Automation in Design*, 105.
- [40] Q.C. Li, Z. Huang, and J.M. Herve. Type synthesis of 3r2t 5-dof parallel mechanisms using the lie group of displacements. *IEEE Transactions on Robotics and Automation*, 20(2):181–190, 2004.
- [41] Z. Li and J. F. Canny, editors. *Nonholonomic Motion Planning*. Kluwer, 1992.
- [42] J. Loncaric. *Geometric analysis of compliant mechanisms in robotics*. PhD thesis, The Division of Applied Sciences, Harvard University, 1985.
- [43] D. Manocha and J. F. Canny. Real time inverse kinematics for general 6R manipulators. Technical Report ESRC 92-2, University of California, Berkeley, 1992.
- [44] R. Manseur and K. L. Doty. A robot manipulator with 16 real inverse kinematic solutions. *International Journal of Robotics Research*, 8(5):75–79, 1989.
- [45] M. T. Mason and J. K. Salisbury. *Robot Hands and the Mechanics of Manipulation*. MIT Press, 1985.
- [46] J. M. McCarthy. *An Introduction to Theoretical Kinematics*. MIT Press, 1990.
- [47] J. Meng, G.F. Liu, and Z.X. Li. A geometric theory for analysis and synthesis of sub-6 dof parallel manipulators. *IEEE Transactions on Robotics*, 23(X):XX, 2007.
- [48] R. M. Murray and S. S. Sastry. Control experiments in planar manipulation and grasping. In *IEEE International Conference on Robotics and Automation*, pages 624–629, 1989.
- [49] Y. Nakamura. *Advanced Robotics: Redundancy and Optimization*. Addison-Wesley, 1991.
- [50] T. Okada. Computer control of multijointed finger system for precise object-handling. *IEEE Transactions on Systems, Man and Cybernetics*, SMC-12(3):289–299, 1982.

- [51] B. Paden. *Kinematics and Control Robot Manipulators*. PhD thesis, Department of Electrical Engineering and Computer Sciences, University of California, Berkeley, 1986.
- [52] F. C. Park, J. E. Bobrow, and S. R. Ploen. A Lie group formulation of robot dynamics. UCI Mechanical Systems Technical Report, Department of Mechanical Engineering, University of California, Irvine, April 1993.
- [53] F.C. Park and B. Ravani. Smooth invariant interpolation of rotations. *ACM Trans. on Graphics*, 16:277–295, 1997.
- [54] L. A. Pars. *A Treatise on Analytical Dynamics*. Wiley, 1965.
- [55] R. P. Paul. *Robot Manipulators: Mathematics, Programming and Control*. MIT Press, 1981.
- [56] L. Poinsot. Sur la composition des moments et la composition des aires. *J. Éc. Polyt. Paris*, 6:182–205, 1806.
- [57] E. J. F. Primrose. On the input-output equation of the general 7R mechanism. *Mechanisms and Machine Theory*, 21:509–510, 1986.
- [58] M. Raghavan. Manipulator kinematics. In R. W. Brockett, editor, *Robotics: Proceedings of Symposia in Applied Mathematics, Volume 41*, pages 21–48. American Mathematical Society, 1990.
- [59] M. Raghavan and B. Roth. Inverse kinematics of the general 6R manipulator and related linkages. *Journal of Mechanical Design*, 115:502–508, 1993.
- [60] O. Rodrigues. Des lois géométriques qui régissent les déplacements d’un système solide dans l’espace et de la variation des coordonnées provenant de ces déplacements considérés indépendamment des causes qui peuvent les produire. *Liouville’s Journal Math.*, v:380–440, 1840.
- [61] G. Rodriguez, A. Jain, and K. Kreutz-Delgado. A spatial operator algebra for manipulator modeling and control. *International Journal of Robotics Research*, 10(4):371–381, 1991.
- [62] R. M. Rosenberg. *Analytical Dynamics of Discrete Systems*. Plenum Press, New York, 1977.
- [63] B. Roth. Performance evaluation of manipulators from a kinematic viewpoint. Technical Report 39-61, NBS Special publication, 1975.
- [64] B. Roth, J. Rastegar, and V. Scheinman. On the design of computer controlled manipulators. *On the Theory and Practice of Robots and Manipulators, Proceedings of the First CISM-IFTOMM Symposium*, pages 93–113, 1973.
- [65] S. S. Sastry and M. Bodson. *Adaptive Control: Stability, Convergence, and Robustness*. Prentice-Hall, 1989.
- [66] J. M. Selig. *Geometrical methods in robotics*. Springer, 1996.

- [67] F. Skinner. Designing a multiple prehension manipulator. *Journal of Mechanical Engineering*, 97(9):30–37, 1975.
- [68] J. E. Slotine and W. Li. On the adaptive control of robot manipulators. *International Journal of Robotics Research*, 6:49–59, 1987.
- [69] M. W. Spong, S Hutchinson, and M. Vidyasagar. *Robot modeling and control*. John Wiley, 2006.
- [70] M. W. Spong, S Hutchinson, and M. Vidyasagar. *Robot modeling and control*. John Wiley, 2006.
- [71] M. W. Spong, F. L. Lewis, and C. T. Abdallah, editors. *Robot Control: Dynamics, Motion Planning and Analysis*. IEEE Press, 1991.
- [72] D. Stewart. A platform with six degrees of freedom. *Proceedings of the Institute of Mechanical Engineering*, 180, part I(5):371–186, 1954. 1965–66.
- [73] R. Tomović and G. Boni. An adaptive artificial hand. *IRE Transactions on Automatic Control*, 7(3):3–10, 1962.
- [74] M. Vidyasagar. *Nonlinear Systems Analysis*. Prentice-Hall, second edition, 1993.
- [75] J. T. Wen and D. S. Bayard. New class of control laws for robot manipulators. Part 1: Non-adaptive case. *International Journal of Control*, 47(5):1361–1385, 1988.
- [76] T. Yoshikawa. *Foundations of Robotics: Analysis and Control*. MIT Press, 1990.

